

AD-A067 843

AIR FORCE GEOPHYSICS LAB HANSCOM AFB MASS
MODELING OF THE GEOSYNCHRONOUS ORBIT PLASMA ENVIRONMENT. PART 3--ETC(U)
JAN 79 H B GARRETT, R E MCINERNEY
AFGL-TR-79-0015

F/G 4/1

UNCLASSIFIED

NL

1 of 3
AD
A067843



LEVEL IV

APOL-TR-79-0013

ENVIRONMENTAL RESEARCH TOWER, 20-00

12
nu



AD A067843

Modeling of the Geosynchronous
Orbit Plasma Environment—Part 3.
ATS-5 and ATS-6 Pictorial Data Atlas

FRANK E. GARDNER, Capt. USAF
U.S. AIR FORCE
AFSC/AFM
AFM/AFM



10 January 1979

DDC FILE COPY

Unclassified

SECURITY CLASSIFICATION OF THIS PAGE (When Data Entered)

REPORT DOCUMENTATION PAGE		READ INSTRUCTIONS BEFORE COMPLETING FORM	
1. REPORT NUMBER	2. GOVT ACCESSION NO.	3. REPORT'S CATALOG NUMBER	
AFGL-TR-79-0015	AFGL-ERP-653		
4. TITLE (and Subtitle)	5. TYPE OF REPORT & PERIOD COVERED		
MODELING OF THE GEOSYNCHRONOUS ORBIT PLASMA ENVIRONMENT, PART 3. ATS-5 AND ATS-6 PICTORIAL DATA ATLAS.	Scientific. Interim.		
6. AUTHOR(s)	7. PERFORMING ORG. REPORT NUMBER		
Henry B. Garrett, Capt. USAF R. E. McInerney, B. Johnson S. E. DeForest	ERP No. 653		
8. PERFORMING ORGANIZATION NAME AND ADDRESS	9. CONTRACT OR GRANT NUMBER(s)		
Air Force Geophysics Laboratory (PHG) Hanscom AFB Massachusetts 01731			
10. CONTROLLING OFFICE NAME AND ADDRESS	11. PROGRAM ELEMENT, PROJECT, TASK AREA & WORK UNIT NUMBERS		
Air Force Geophysics Laboratory (PHG) Hanscom AFB Massachusetts 01731	62101F 76610803		
12. MONITORING AGENCY NAME & ADDRESS (if different from Controlling Office)	13. REPORT DATE		
Interim rept's	15 January 1979		
	14. NUMBER OF PAGES		
	268		
	15. SECURITY CLASS. (of this report)		
	Unclassified		
	15a. DECLASSIFICATION/DOWNGRADING SCHEDULE		
16. DISTRIBUTION STATEMENT (of this Report)			
Approved for public release; distribution unlimited.			
17. DISTRIBUTION STATEMENT (of the abstract entered in Block 20, if different from Report)			
266 p.			
18. SUPPLEMENTARY NOTES			
19. KEY WORDS (Continue on reverse side if necessary and identify by block number)			
Geosynchronous environment Space charging Plasma environment			
20. ABSTRACT (Continue on reverse side if necessary and identify by block number)			
Data on the geosynchronous plasma environment derived from the UCSD plasma detectors on the ATS-5 and ATS-6 satellites have been carefully compiled into a pictorial atlas. The atlas consists of 12 days of data from 1969 (ATS-5), 38 days from 1970 (ATS-5), 37 days from 1974 (ATS-6), and 8 days from 1976 (ATS-6). The data are 10-min averages of the first four moments of the plasma distribution function for the electrons and ions. The data are presented in the form of spectrograms and line plots along with detailed ephemeris and geophysical information. Two computer tapes are available, the			

DD FORM 1 JAN 75 1473 EDITION OF 1 NOV 65 IS OBSOLETE

Unclassified

SECURITY CLASSIFICATION OF THIS PAGE (When Data Entered)

409 578

over

Unclassified

SECURITY CLASSIFICATION OF THIS PAGE(When Data Entered)

20. (Cont)

formats of which are given in an appendix.

Unclassified

SECURITY CLASSIFICATION OF THIS PAGE(When Data Entered)

Preface

The work accomplished by the University of California at San Diego was performed under AF Contract F19628-77-C-0014. Many people contributed to this study. In particular, programming at AFGL was provided by A. Lacroix and E. Ziemba (originally of ASEC). At UCSD, C. McPhadden was responsible for providing tapes and spectrograms. Valuable assistance was also rendered by the AFGL photographic laboratory. C. Pike was, undoubtedly, the prime moving force behind this document and it is to him we dedicate the results. E. Robinson (AFGL/SUA) kindly provided the orbital data.

ACCESSION for	
NTIS	Write Section <input checked="" type="checkbox"/>
DOC	Buff Section <input type="checkbox"/>
UNANNOUNCED	<input type="checkbox"/>
JST ICAION	
DISTRIBUTION/AVAILABILITY CODES	
SPECIAL	
A	

Contents

1. INTRODUCTION	7
2. INSTRUMENTS	8
3. MOMENT CALCULATIONS	9
4. PROBLEM AREAS	13
5. CONCLUSIONS	16
REFERENCES	19
APPENDIX A: ATS-5 and ATS-6 Spectrograms and Line Plots	21
APPENDIX B: Orbital Elements of ATS-5 and ATS-6	215
APPENDIX C: K_p Indices	259
APPENDIX D: ATS Data Tape Formats	265

Illustrations

1. Spectrogram of ATS-6 Particle Fluxes for Day 178 of 1974 (Local Midnight is ~0600 UT)	14
---	----

Tables

1. Days Used in AFGL Statistical Analysis	9
D1. ATS Data Tape Formats	266

Modeling of the Geosynchronous Orbit Plasma Environment - Part 3. ATS-5 and ATS-6 Pictorial Data Atlas

1. INTRODUCTION

A basic difficulty in studying the low-energy geosynchronous environment has been the lack of readily available data (see review by Garrett¹). The University of California at San Diego (USCD) has been a chief source of such data owing to the unique plasma experiments they flew on the ATS-5 and ATS-6 geosynchronous satellites. This report seeks to provide random selections of that data that have been carefully reviewed and, as far as possible, put in a form readily accessible to the scientific and engineering community interested in studying the geosynchronous environment.

The report is arranged in four sections. The first section will deal with the general characteristics of the ATS-5 and ATS-6 detectors. Subsequent sections will in turn deal with the conversion of the data into the four moments and other useful quantities, assumptions made in preparing the data, and finally with the availability and use of the data. The text is supplemented with four appendices that consist of the daily spectrograms and line plots of the four moments, the orbital elements, geophysical parameters, and the tape formats for the two ATS-5 and ATS-6 data tapes.

(Received for publication 12 January 1979)

1. Garrett, H. B. (1979) Review of quantitative models of the 0 to 100 keV near-earth plasma. To appear in Rev. of Geophys.

2. INSTRUMENTS

Two satellites served as data sources for the study. These were the ATS-5 and ATS-6 geosynchronous satellites. Although we shall briefly describe each of these satellites, the reader is referred to DeForest and McIlwain² for details of the ATS-5 instrument, and Mauk and McIlwain³ for details of the ATS-6 instrument.

The ATS-5 and ATS-6 satellites are in low inclination, geosynchronous orbits. The ATS-5 satellite is cylindrical (1.8 m long by 1.5 m in diameter). It spins at 1.27 rps with its axis parallel to the earth's rotation axis. The ATS-6, in contrast, is essentially a large (10 m) spin-stabilized dish antenna. The plasma data were obtained from the University of California at San Diego (UCSD) plasma experiments on ATS-5 and ATS-6. Both instruments consist of electrostatic analyzers designed to measure the positive ion and electron populations between 51 eV and 51 keV for ATS-5 and between 0 and 80 keV for ATS-6.

The ATS-5 and ATS-6 instruments measure the particle flux in 64 channels (2 background channels and 62 energy channels), returning a complete energy spectrum in 20 and 15 sec, respectively. For ATS-5, the center energy for a channel is 112 percent of the center energy of the previous channel. For ATS-6 this value is ~113 percent. This results in an uncertainty of about ± 5 percent in the energy (or potential) determination.

The ATS-5 and ATS-6 instruments return count rate data which are converted to differential energy spectra. From the differential energy spectra, the ambient currents and distribution functions necessary in estimating the ambient environment are determined. The satellite spectra also indicate the spacecraft potential. Briefly, the low energy ion (electron) population is accelerated if the satellite has a negative (positive) potential relative to the ambient plasma. This acceleration produces a pronounced peak in the low energy ion (electron) channels at an energy in electron volts (eV) corresponding to the satellite potential in volts (V) (see Figure 1). Thus, ATS-5 and ATS-6 provide information on both the ambient plasma and the spacecraft potential. Table 1 lists the days for which continuous data were available. In actuality, there was approximately 80 percent data coverage for these days.

2. DeForest, S. E., and McIlwain, C. E. (1971) Plasma clouds in the magnetosphere, J. Geophys. Res. 76(No. 16):3587-3611.

3. Mauk, B. H., and McIlwain, C. E. (1975) ATS-6 UCSD auroral particles experiment, IEEE Trans. Aerospace and Electronic Systems, AEA-11(No. 6):1125-1130.

Table 1. Days Used in AFGL Statistical Analysis

ATS-5 (Year/Day)				
1969/312	1969/ 326	1970/ 37	1970/ 109	1970/ 319
313	327	38	110	320
318	1970/ 25	39	111	321
319	26	40	112	322
320	27	41	113	323
321	28	42	114	324
322	29	43	271	325
323	30	44	272	326
324	31	107	273	327
325	32	108	274	328
ATS-6 (Year/Day)				
1974/186	1974/ 196	1974/ 266	1974/ 299	1976/ 44
187	197	267	300	45
188	198	268	301	46
189	199	269	302	47
190	200	270	303	48
191	201	271	304	
192	202	272	305	
193	203	274	1976/ 41	
194	204	296	42	
195	205	297	43	

3. MOMENT CALCULATIONS

The ATS-5 and ATS-6 return count rates in selected energy channels. These count rates, for electrostatic analyzers, are converted directly to the differential energy flux by multiplication by a fixed constant (this constant varies slightly at the lower energies for ATS-6). The differential energy flux is then converted to the distribution function for the plasma—that is, the function (usually referred to as f) which when integrated over all velocity directions and positions in a volume gives the total number of particles in the volume. As will be outlined in this section, the distribution functions were employed to estimate 10-min values of the first four plasma moments. It is these values that are presented in the study.

A commonly encountered distribution function is the so-called Maxwellian distribution for an isotropic plasma

$$f(v_i) = n_i \left(\frac{m_i}{2\pi kT_i} \right)^{3/2} e^{-m_i v_i^2 / 2kT_i} \quad (1)$$

where

- n_i = number density of species i ,
 m_i = mass of species i ,
 T_i = temperature of species i ,
 v_i = velocity of i species,
 k = Boltzmann constant,
 f = distribution function in sec^3/km^6 .

Although most plasma distributions in space are neither Maxwellian nor isotropic, these assumptions are commonly made in characterizing a plasma in order to reduce the number of parameters necessary for description. Further, Eq. (1) can be used in the calculation of the first four plasma moments that will generate the model. For a Maxwellian particle distribution, they are

$$\langle n_i \rangle = 4\pi \int_0^\infty (v_i^0) f_i v_i^2 dv_i = n_i, \quad (2)$$

$$\langle NF_i \rangle = \int_0^\infty (v_i^1) f_i v_i^2 dv_i = \frac{n_i}{2\pi} \left(\frac{2kT_i}{\pi m_i} \right)^{1/2}, \quad (3)$$

$$\langle E_i \rangle = 4\pi \int_0^\infty \frac{1}{2} m_i (v_i^2) f_i v_i^2 dv_i = \frac{3}{2} n_i k T_i, \quad (4)$$

$$\langle EF_i \rangle = \int_0^\infty \frac{1}{2} m_i (v_i^3) f_i v_i^2 dv_i = \frac{m_i n_i}{2} \left(\frac{2kT_i}{\pi m_i} \right)^{3/2} \quad (5)$$

where

$$\langle n_i \rangle = \text{number density for species } i \text{ (number/cm}^3\text{)},$$

$$\langle NF_i \rangle = \text{number flux for species } i \text{ (number/cm}^2\text{-sec-sr)},$$

$$\langle E_i \rangle = \text{energy density for species } i \text{ (eV/cm}^3\text{)},$$

$$\langle EF_i \rangle = \text{energy flux for species } i \text{ (eV/cm}^2\text{-sec-sr)}.$$

The use of moments is similar to expanding a function in a Taylor series. The moments are, in statistical terms, the expectation values of a variable (that is, the average value, the standard deviation, and so on). For a plasma, the moments of the velocity are taken as follows: $\langle v^0 \rangle$, $\langle v^1 \rangle$, $\langle v^2 \rangle$, and $\langle v^3 \rangle$. In Eqs. (2) to (5),

these moments have been multiplied by constants to give physically meaningful quantities. For example, the $\langle v^2 \rangle$ moment has been multiplied by 4π and $1/2 m_i$ to give the isotropic energy density $4\pi \langle 1/2 m_i v^2 \rangle$.

As previously discussed, the count rates are directly proportional to the differential energy flux $\frac{d\langle EF \rangle}{dE}$ (where E is energy). The differential energy flux is converted to the distribution function by the simple relation

$$f_i(E) = \frac{d\langle EF_i \rangle}{dE} \frac{1}{E^2} \frac{m_i^2}{2} \quad (6)$$

where

$$E = 1/2 m_i v^2.$$

The distribution function thus determined is, however, the distribution function at the detector and hence is not representative of the true ambient environment. In Section 4 we will cover the corrections necessary. Here we merely note that they are carried out and the moments calculated for 10-min intervals employing Eqs. (2) to (6). Applications of these moments will be discussed in the following.

The four moments of the distribution function are of value in their own right. Assuming, for example, an isotropic flux, the number flux is equal to the current striking the spacecraft (if $\langle NF_i \rangle$ is multiplied by $\pi q = 5 \times 10^{-10}$, where q is the charge, the results are in $n A/cm^2$). Several other quantities can, however, also be derived—namely the distribution function of Eq. (1). As we know the density from Eq. (2) we only need derive the temperature T . According to Eqs. (2) to (5), T is given by

$$T(\text{AVG}) = \frac{2}{3} \frac{\langle E_i \rangle}{\langle n_i \rangle}, \quad (7)$$

or by

$$T(\text{RMS}) = \frac{\langle EF_i \rangle}{2 \langle NF_i \rangle}. \quad (8)$$

If the plasma is Maxwellian (and isotropic) then $T(\text{AVG}) = T(\text{RMS})$. Unfortunately, in general $T(\text{AVG}) \neq T(\text{RMS})$ (see Garrett et al.⁴) at geosynchronous orbit. Observation reveals that in reality the distribution function is much more complex and can better be represented by sums of two or more Maxwellian components.

4. Garrett, H. B., Mullen, E. G., Ziemba, E., and DeForest, S. E. (1978) Modeling of the Geosynchronous Orbit Plasma Environment—Part 2. ATS-5 and ATS-6 Statistical Atlas, AFGL-TR-78-0304.

From the four moments of the distribution function, it is possible to derive a two-Maxwellian fit to the plasma distribution. That is, if f_2 is given by:

$$f_2(v_i) = \left(\frac{m_i}{2\pi k} \right)^{3/2} \left[\frac{N1_i}{T1_i^{3/2}} e^{-\frac{m_i v_i^2}{2kT1_i}} + \frac{N2_i}{T2_i^{3/2}} e^{-\frac{m_i v_i^2}{2kT2_i}} \right] . \quad (9)$$

the expressions for $N1_i$, $T1_i$, $N2_i$, and $T2_i$ are easily derived from the 4 moments. Inserting Eq. (9) into Eqs. (2) to (5), we get

$$N1_i + N2_i = \langle n_i \rangle = C_1 , \quad (10)$$

$$N1_i T1_i^{1/2} + N2_i T2_i^{1/2} = \langle NF_i \rangle \left(\frac{\pi m_i}{2k} \right)^{1/2} 2\pi = C_2 , \quad (11)$$

$$N1_i T1_i + N2_i T2_i = \frac{2}{3} \frac{\langle E_i \rangle}{k} = C_3 , \quad (12)$$

$$N1_i T1_i^{3/2} + N2_i T2_i^{3/2} = \langle EF_i \rangle \left(\frac{\pi m_i}{2k} \right)^{3/2} \frac{2}{m_i} = C_4 . \quad (13)$$

These four equations can be reduced to a quadratic expression in terms of $T1_i^{1/2}$. If we define three new variables

$$A = C_2^2 - C_1 C_3 , \quad (14)$$

$$B = C_1 C_4 - C_2 C_3 , \quad (15)$$

$$C = C_3^2 - C_2 C_4 , \quad (16)$$

then it can be shown that

$$T1_i^{1/2} = \frac{-B + \sqrt{B^2 - 4AC}}{2A} \quad (17)$$

$$T2_i^{1/2} = \frac{-B - \sqrt{B^2 - 4AC}}{2A} \quad (18)$$

$$N2_i = \frac{C_2 - T1_i^{1/2} C_1}{T2_i^{1/2} - T1_i^{1/2}} , \quad (19)$$

$$N1_i = \langle n_i \rangle - N2_i . \quad (20)$$

It is simple to prove the uniqueness of this solution and, in general, no ambiguities exist. Occasionally (for example if the distribution function is actually a single Maxwellian) $T_{1i}^{1/2}$, $T_{2i}^{1/2}$, N_{1i} , or N_{2i} may be negative or imaginary. Thus a certain amount of care must be exercised in computing these parameters.

4. PROBLEM AREAS

In Figure 1 we present a spectrogram for Day 178 of 1974. The spectrogram is a 3-dimensional plot developed by UCSD (see DeForest and McIlwain²), in which the X-axis is time, the Y-axis is energy, and the third dimension, represented by shading, is the detector count rate (remember this is directly proportional to the differential energy flux). Day 178 happens to be one of the most exceptional days recorded by ATS-6 (it is not, however, included in our study) as the potential between the spacecraft and the ambient environment reached nearly -2000 V while the satellite was in sunlight at ~0415 UT. We have included it here to illustrate some of the problems encountered in interpreting the ATS-5 and ATS-6 data.

The first significant feature to be observed is the absence of data at varying energies below about 10 eV for the electrons and ions (particularly between 0300 UT and 0200 UT and between 1700 UT and 2400 UT—this is not the same as loss of data between 0930 UT and 1100 UT). This is due to a temperature problem affecting the lower energy channels on ATS-6 (note: ATS-5 did not have this problem). Although it is normally possible to accurately correct for this effect, the ion data for 1976 covered in this report are affected as reflected in the sudden increase in the density—in one case rising to $320/\text{cm}^3$ —in conjunction with the temperature change. Thus, any data where a significant change in temperature is observed in the spectrogram (as evidenced by a change in the low energy cut-off), should be considered very carefully. The effect is primarily in the interpretation of the energy of the low energy ions. As the low-energy component is given less and less weight in the moment integrals as we go to higher moments, this effect becomes insignificant for the energy density and energy flux (hence the general reliance on these values and $T(\text{RMS})$ in many studies).

A related problem also visible on Day 178 is the intense electron flux below about 20-50 eV. These fluxes are in general not believed to be true ambient fluxes but a superposition of photoelectrons and secondaries trapped in the fields around the spacecraft. It is very difficult to accurately judge which are true ambients and which are these contaminants. As ATS-5 does not measure below 50 eV, it is impossible to judge whether these effects occur at all. For ATS-6, one of us (B. Johnson) has carefully gone through every spectrogram and, by hand, terminated the moment integrals at the energy (see tape listings) below which the contaminants

began to appear. Although great care was exercised, the absolute electron densities for ATS-6 should be considered somewhat (\sim factor 2) circumspectly. Again, however, this effect damps out quickly with the higher moments, the density appearing to be the only moment significantly affected.

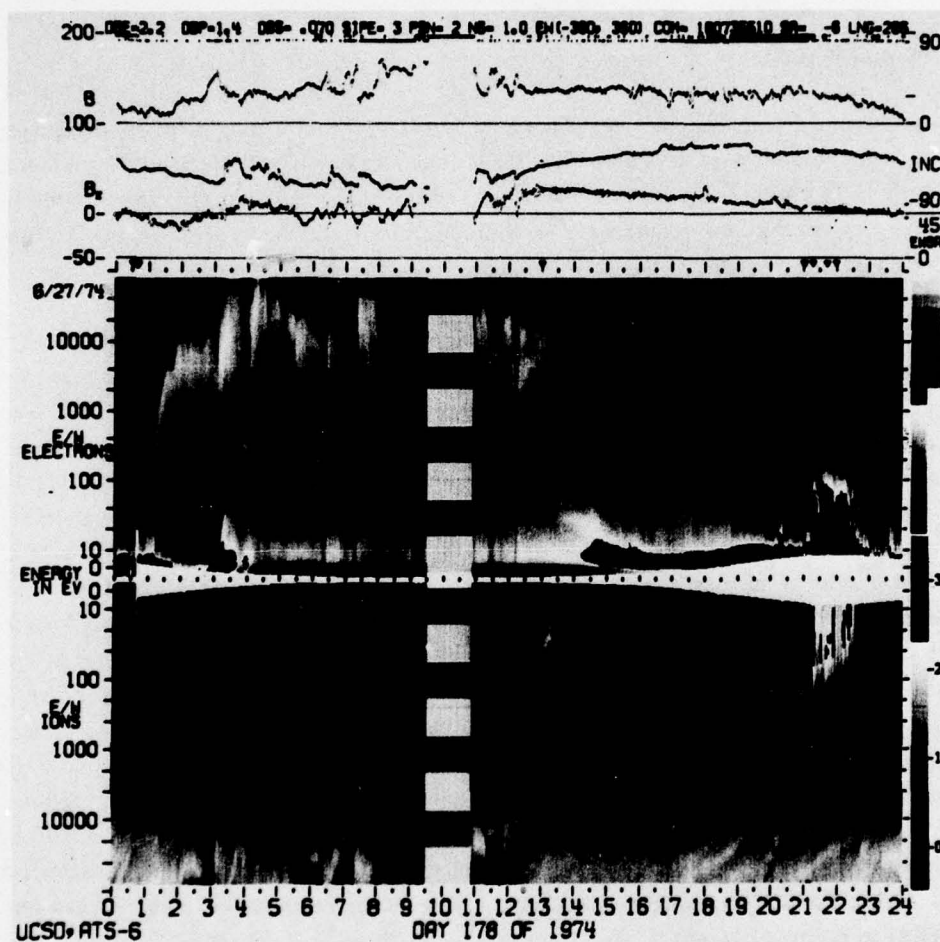


Figure 1. Spectrogram of ATS-6 Particle Fluxes for Day 178 of 1974 (Local Midnight is \sim 0600 UT). Note the high daylight potential near 0415 UT of -2000 V

Charging of the spacecrafts by the ambient plasma, as already mentioned in regards to Day 178, is also a source of significant error in moment determinations. The effect, produced generally by a buildup of negative charge on the whole or portions of the satellite owing to the higher ($\sim 40\times$) velocities of the electrons over the ions,

causes a marked reduction in the electron moments and an increase in the ions. Charging can occur at all times though the highest voltages have been observed only in eclipse. Two types of charging are primarily observed—charging between the satellite and space and charging between portions of the spacecraft. Charging, as described earlier, manifests itself primarily as a dropout of particles having energies below the potential of the spacecraft—usually observable in the low energy ions. DeForest^{5,6} and Garrett et al⁷ carefully review many examples of this phenomena.

For the purpose of this study, B. Johnson has carefully corrected all ATS-6 data for potential variations and the potential has been recorded (see tape formats). For ATS-5, the processing technique and low energy resolution limit of the detector prevented this. Specifically, Days 271, 272, 273, and 274 of 1970 all had eclipses though only the data within ± 30 min 0630 UT on Days 272 and 274 show any effect that might justify removal. Days 313, 324, and 325 of 1969 and Days 322, 325, and 327 exhibit charging but the time periods are short and the effects are not apparent in the moment calculations.

S. DeForest has carefully reviewed the difficulties associated with potential corrections for ATS-5 and ATS-6 and the attendant problem that they in general do not cover the same energy ranges (the ATS-6 energy range in fact being variable at low energies). He finds errors less than 20 percent for uncorrected potentials below -50V. Within the ranges of our data, a factor of 2 error is probably a realistic "worst case". As this is much smaller than the actual variations in the plasma (~ 100) in time periods of tens of minutes, we doubt that such errors are significant in such a large data base as considered here.

Other problems that must be considered but cannot at this time be corrected are the lack of precise data on the extremely low energy environment (≤ 10 eV), ion composition, and anisotropies. In the case of the low energy environment, Lennartsson and Reasoner (1978) have employed ATS-6 data to estimate the low energy ion population and their paper should be consulted for estimates. Direct measurements by the GEOS satellites will appear shortly. G. Wrenn (private communication) has indicated large densities ($\sim 50/\text{cm}^3$) below 50 eV, disappearing, however, with increased geomagnetic activity. In any case, the electron and ion densities are in general very close to each other (varying only by a factor of 2 to 3 at the most) for the data presented here indicating that, for the approximate range of accuracy of

5. DeForest, S. E. (1972) Spacecraft charging at synchronous orbit, J. Geophys. Res. 77(No. 4):651.
6. DeForest, S. E. (1973) Electrostatic Potentials Developed by ATS-5, Photon and Particle Interactions with Surfaces in Space, R. J. C. Grand (ed.) D. Reidel Publishing Co., Dordrecht, Holland, pp 263-276.
7. Garrett, H. B., Pavel, A. L., and Hardy, D. A. (1977) Rapid Variations in Spacecraft Potential, AFGL-TR-77-0312.

measurements (~ 50 eV to 50 keV), the results are an adequate if not an accurate reflection of the true density. Again the higher moments are little affected by errors in the low energy density. As regards the ion composition the reader is referred to the review by Young.⁸ The distribution of field-aligned fluxes are almost totally unknown — the SCATHA program and GEOS will hopefully provide answers. Some estimate can be made, however, by comparing the ATS-5 perpendicular and parallel (to the satellite spin axis) detector data. As is revealed in the data anisotropy clearly exists and can at times be quite pronounced. For analysis purposes we normally average the two detectors in order to better estimate the omnidirectional fluxes. As the ATS-6 data are only for the North-South (relative to the earth's axis) detector, directional effects cannot be estimated.

5. CONCLUSIONS

In the preceding sections we have briefly discussed the data sources, how the data were used to calculate the moments, how to calculate other useful quantities, and problems associated with the data and their interpretation. In this section, we will describe the general form in which the data are available and suggest possible uses.

Several sets of information have been provided in this pictorial atlas. The first of these are daily spectrograms of ATS-5 and ATS-6 data such as presented in Figure 1. The energy scales are slightly different for ATS-5 and ATS-6 (see Appendix A) but otherwise the spectrograms are identical in their presentation. Accompanying each spectrogram are daily line plots of the 10-min averages of the four moments of the distribution functions for the electrons and ions. In the case of ATS-5 the solid lines are the perpendicular components and the dashed lines are the parallel components. The units are defined in the Appendix.

In Appendix B we have included the orbital elements of ATS-5 and ATS-6. These consist of 2 types of plots. The first of these is the geographic longitude of the satellite vs the geographic latitude. The start and stop times in Universal Time (UT) are given at the top of the page. Along the orbital track is listed the local time at various locations. Also indicated is the time of minimum latitude or start and stop time. The second type of plot consists of the radial position (in geographic coordinates) of the satellite as a function of UT (Jan 1 ~ Day 1).

The final two Appendices contain the harmonic plots of the K_p index (Solar-Geophysical Data - Prompt Reports, 1970, 1971, 1975, 1977) and listings of the formats of the 2 CDC 6600 tapes available with this report.

The details of these formats are explained in the appendix.

8. Young, D. T. (1979) Ion composition measurements in magnetospheric modeling, Quantitative Modeling of the Magnetospheric Processes, Geophys. Monogr. Ser., 21, W. P. Olson (ed.) AGU, Washington, D. C.

The four appendices and the two computer tapes are useful in a variety of geophysical and engineering applications. In various reports (DeForest and McIlwain,² Su and Konradi,⁹ Garrett,¹⁰ Garrett et al,⁴ DeForest,¹¹ and Garrett and DeForest¹²), the ATS-5 and ATS-6 data have been extensively exploited in order to model the geosynchronous environment. The reader is referred to these reports and the review by Garrett¹ for details.

The data presented here have been and are being carefully analyzed in order to establish the baseline low-energy geosynchronous plasma environment observed by ATS-5 and ATS-6. The documented results have already revealed many new features. The data are readily useable as they are in order to simulate actual geophysical variations likely to be encountered at geosynchronous orbit. Further, they can be analyzed to provide detailed information on variations at various local times and under varying geophysical conditions. Cross-correlations between various parameters including the solar wind and DMSP photos are hoped for in the future. In all, it is felt that the data base presented in this report represents, at present, the most readily accessible data for general use on the geosynchronous environment.

9. Sy, S. -Y, and Knoradi, A. (1977) Description of the Plasma Environment at Geosynchronous Altitude, NASA Johnson Technical Note P-10.
10. Garrett, H. B. (1977) Modeling of the Geosynchronous Orbit Plasma Environment - Part I, AFGL-TR-77-0288.
11. DeForest, S. E. (1979) Final Report for Contract F19628-77-C-0014, Atlas of the Geosynchronous Plasma Environment, AFGL-TR-79-0100.
12. Garrett, H. B., and DeForest, S. E. (1979) An analytical simulation of the geosynchronous plasma environment, to appear in Planet. Space. Sci.

References

1. Garrett, H. B. (1979) Review of quantitative models of the 0 to 100 keV near-earth plasma. To appear in Rev. of Geophys.
2. DeForest, S. E., and McIlwain, C. E. (1971) Plasma clouds in the magnetosphere, J. Geophys. Res. 76(No. 16):3587-3611.
3. Mauk, B. H., and McIlwain, C. E. (1975) ATS-6 UCSD auroral particles experiment, IEEE Trans. Aerospace and Electronic Systems, AEA-11(No. 6):1125-1130.
4. Garrett, H. B., Mullen, E. G., Ziemba, E., and DeForest, S. E. (1978) Modeling of the Geosynchronous Orbit Plasma Environment - Part 2. ATS-5 and ATS-6 Statistical Atlas, AFGL-TR-78-0304.
5. DeForest, S. E. (1972) Spacecraft charging at synchronous orbit, J. Geophys. Res. 77(No. 4):651.
6. DeForest, S. E. (1973) Electrostatic Potentials Developed by ATS-5, Photon and Particle Interactions with Surfaces in Space, R. J. C. Grand (ed.) D. Reidel Publishing Co., Dordrecht, Holland, pp 263-276.
7. Garrett, H. B., Pavel, A. L., and Hardy, D. A. (1977) Rapid Variations in Spacecraft Potential, AFGL-TR-77-0312.
8. Young, D. T. (1979) Ion composition measurements in magnetospheric modeling. Quantitative Modeling of the Magnetospheric Processes, Geophys. Monogr. Ser., 21, W. P. Olson (ed.) AGU, Washington, D. C.
9. Su, S. -Y, and Konradi, A. (1977) Description of the Plasma Environment at Geosynchronous Altitude, NASA Johnson Technical Note P-10.
10. Garrett, H. B. (1977) Modeling of the Geosynchronous Orbit Plasma Environment - Part I, AFGL-TR-77-0288.
11. DeForest, S. E. (1979) Final Report for Contract F19628-77-C-0014, Atlas of the Geosynchronous Plasma Environment, AFGL-TR-79-0100.
12. Garrett, H. B., and DeForest, S. E. (1979) An analytical simulation of the geosynchronous plasma environment, to appear in Planet. Space. Sci.

Appendix A

ATS-5 and ATS-6 Spectrograms and Line Plots

This appendix contains spectrograms and line plots for the ATS-5 and ATS-6 days listed in Table 1. As indicated in the text these data have as far as possible been corrected for potential variations, bad data, and temperature effects. Each day consists of a spectrogram and line plot, the spectrogram being for either the parallel (indicated by a "||" on the left hand side) or perpendicular (indicated by an "⊥") detector for ATS-5 and for the North-South detector on ATS-6. The line plots for ATS-5 show the 10-min averages of the four moments of the distribution function for the parallel (--) and perpendicular (—) detectors. The ATS-6 data are only for the North-South detector.

The spectrograms are to be interpreted as follows. For both satellites the local time position of the satellites are given in Appendix B (roughly, local midnight was at ~0630 UT for ATS-5, ~0600 UT for ATS-6 in 1974, and ~2100 UT for ATS-6 in 1976), Universal Time being given along the X-axis. In the case of ATS-5 the Y-axis energy is a logarithmic scale with 50 eV at the bottom (top) for electrons (ions) and a scale proportional to $1/(E+3 \text{ keV})$. The gray scale at the lower right determines the value of G on the scale marked 0 to 3. The differential energy flux in $\text{eV}/\text{cm}^2\text{-sec-ster-eV}$ is given by $(10^G - 1) 10^{b+4.367}$ where b is given by "EL" in the lower left corner for electrons and "PR" for ions. The reader is referred to DeForest and McIlwain² for details of the other parameters plotted. The spectrograms for ATS-6 are practically identical, only with the scale being logarithmic in energy between 10 eV and 80 keV (linear below 10 eV). The values of "EL" and "PL" are not given. UCSD should be contacted directly for these values if desired.

The line plots are scaled so that whatever factors are indicated (either the power of 10 on the side scale or the factor of 2 in the upper right of some plots) should be multiplied by the indicated value to arrive at the final value. As an example, the ion energy density on day 312, 1969 should be multiplied by a factor of 10^3 and a factor of 4.

The units are:

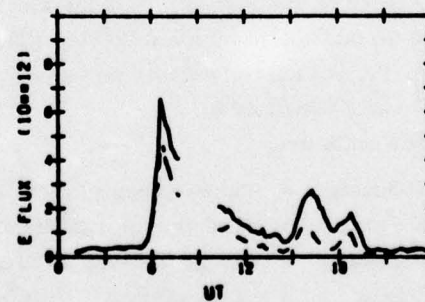
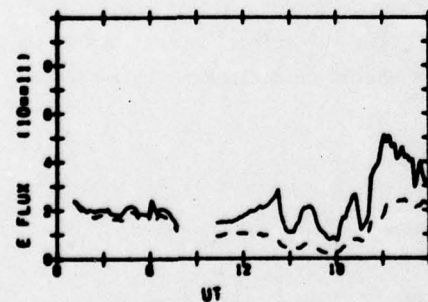
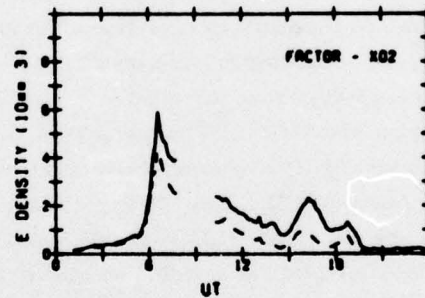
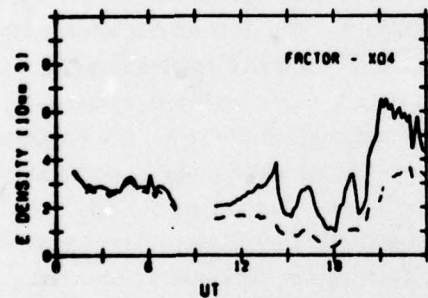
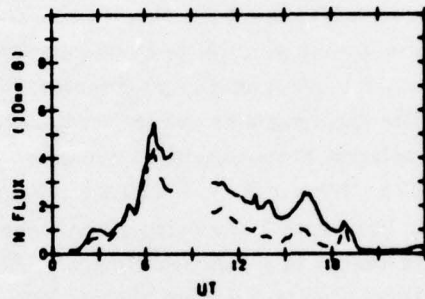
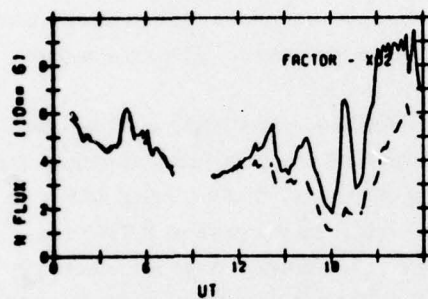
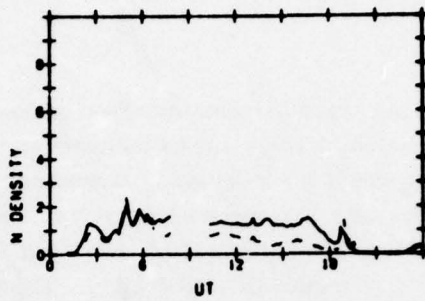
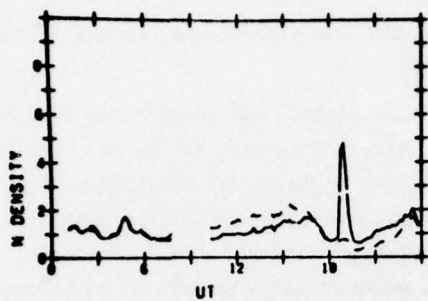
- N Density = number density = $N^\#/\text{cm}^3$
- N Flux = number flux = $N^\#/\text{cm}^2\text{-sec-ster}$
- E Density = energy density = eV/cm^3
- E Flux = energy flux = $\text{eV}/\text{cm}^2\text{-sec-ster}$

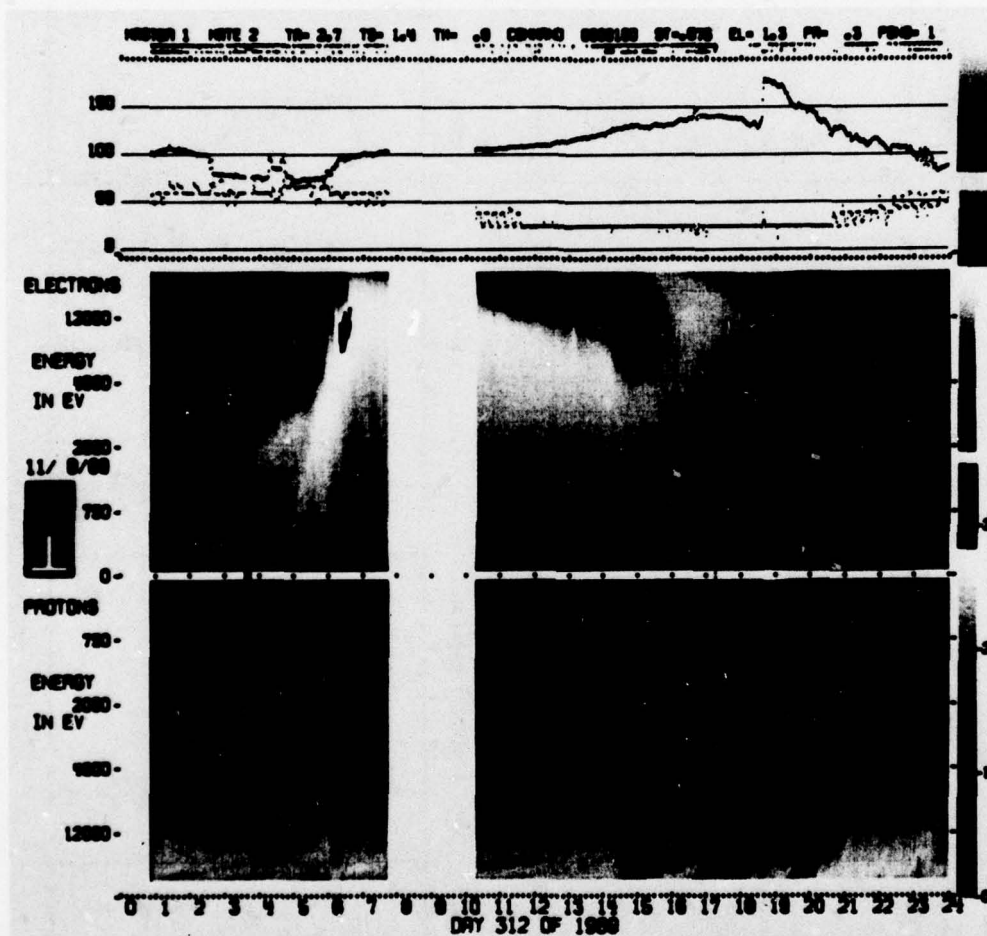
The data are arranged chronologically.

ATS-5
69/312

IONS

ELECTRONS

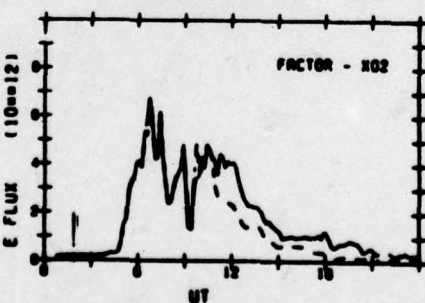
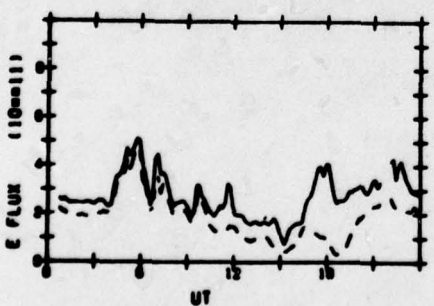
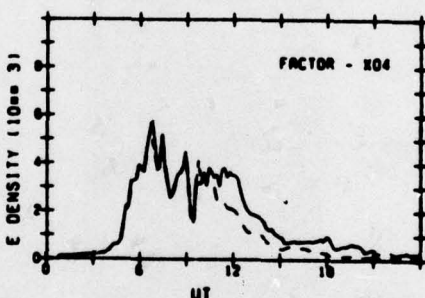
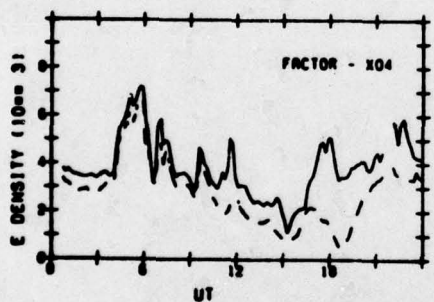
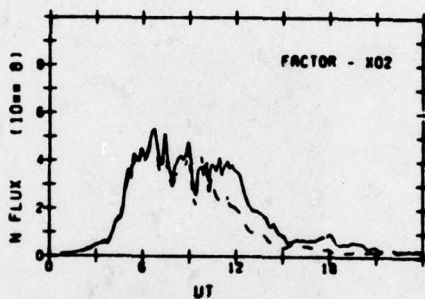
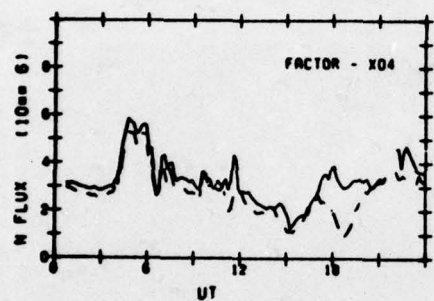
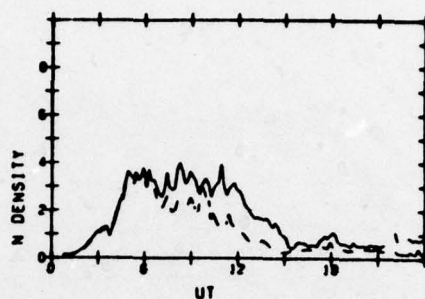
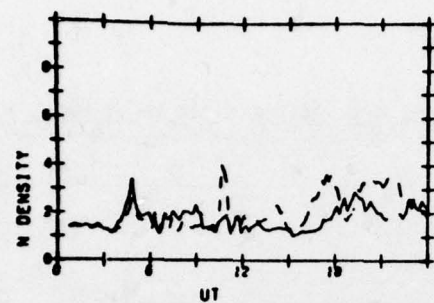


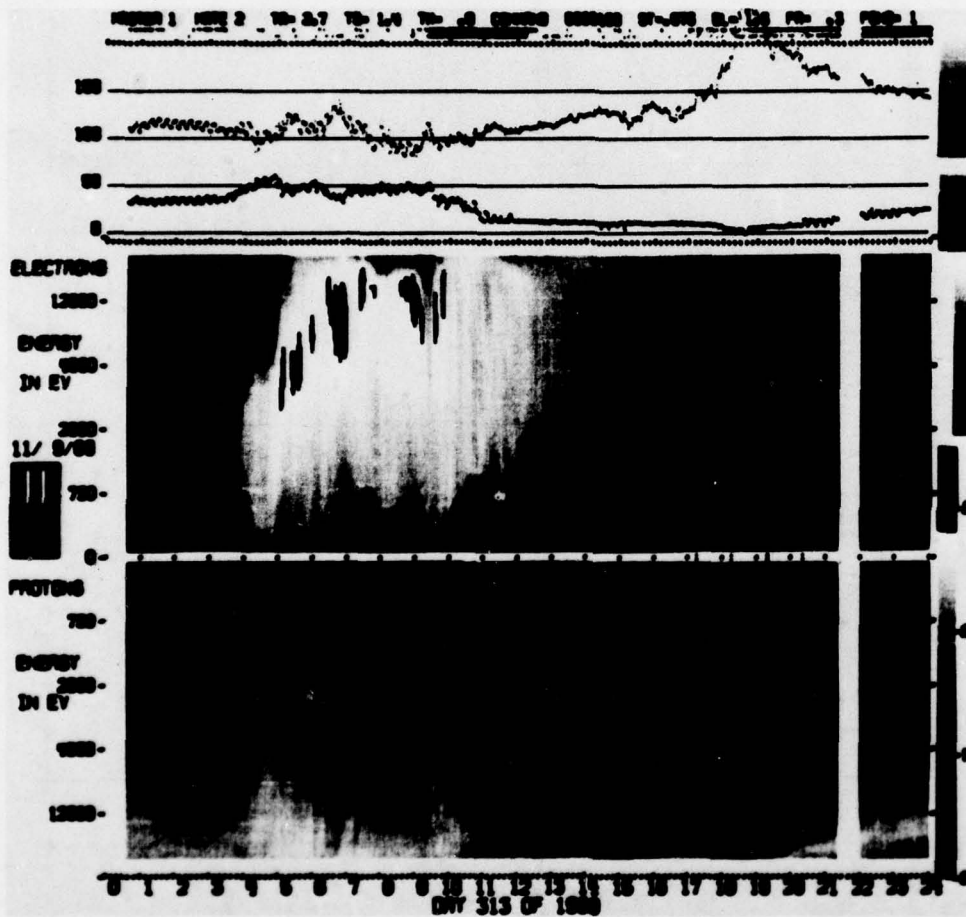


ATS-5
69/313

IONS

ELECTRONS

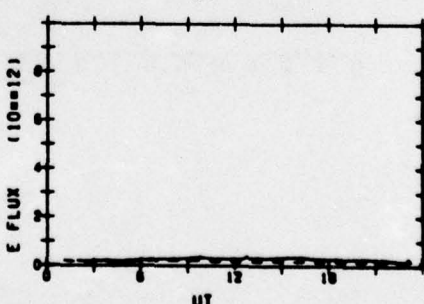
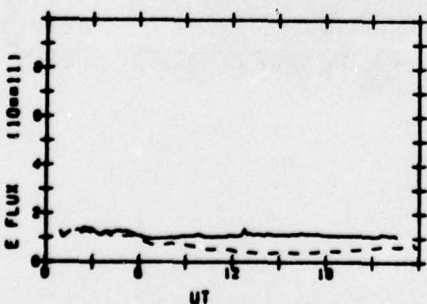
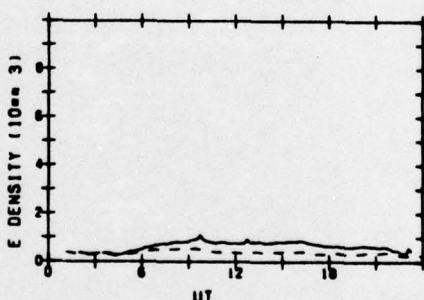
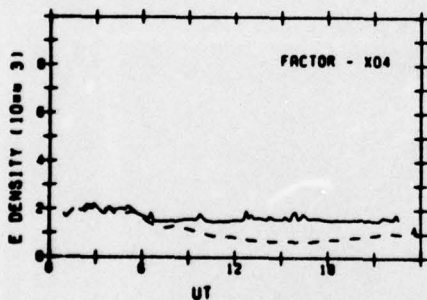
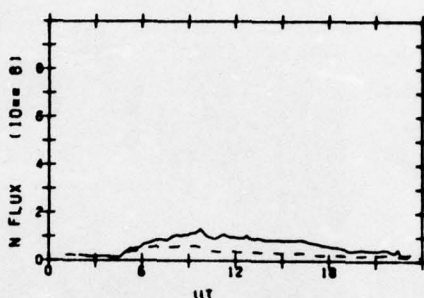
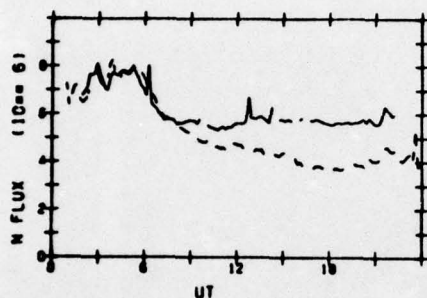
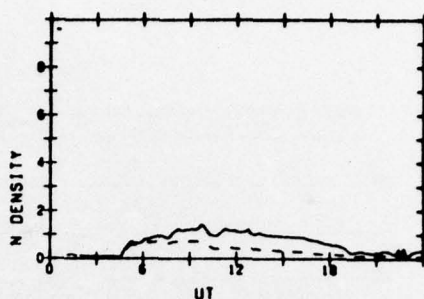
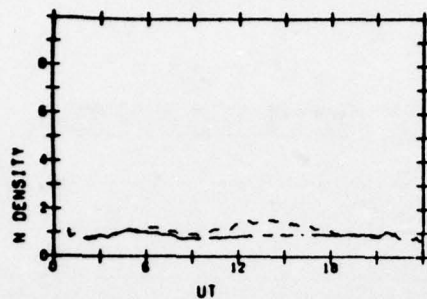




ATS-5
69/318

IONS

ELECTRONS



Q. E. PLX
P. E. PLX
P. E. PLX

FOR INFO
CALL 1-800-451-7243
OR VISIT www.451.com

ELECTRONS

ENERGY
IN EV

11/14/00

PROTEINS

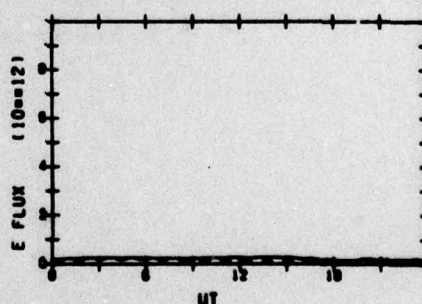
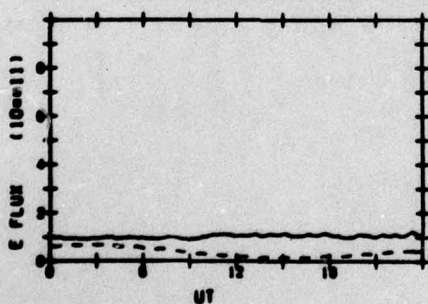
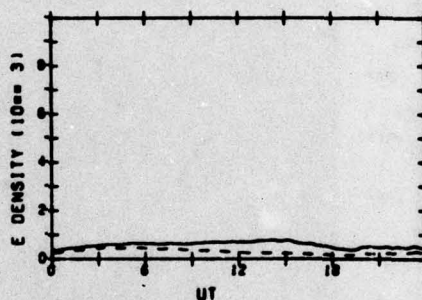
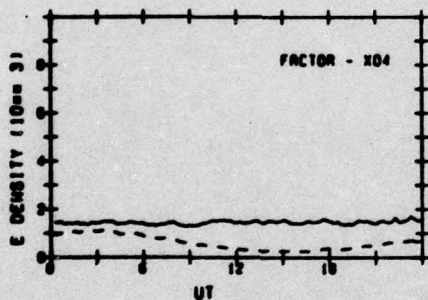
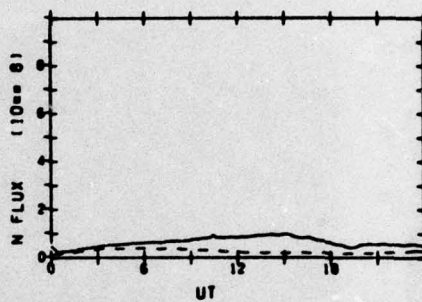
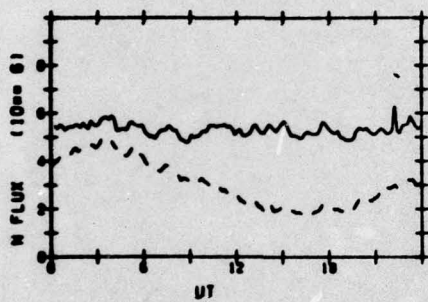
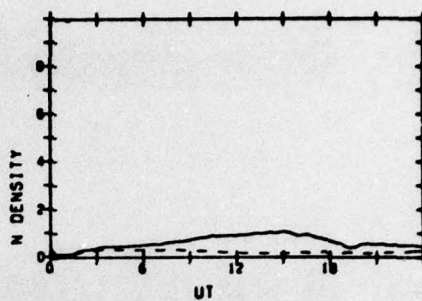
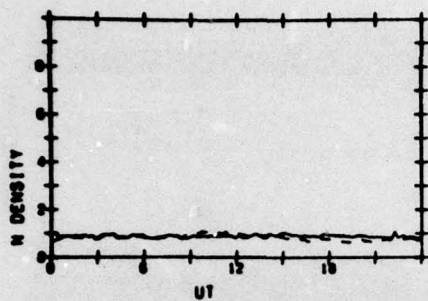
ENERGY
IN EV

— 259 —

ATS-5
69/319

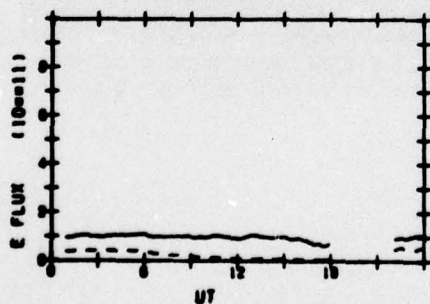
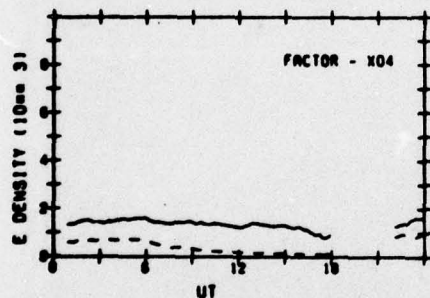
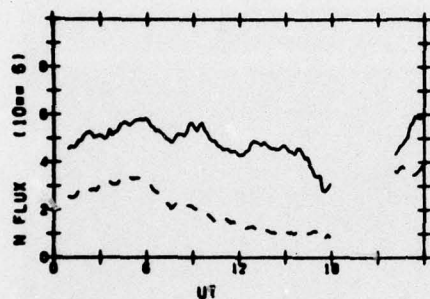
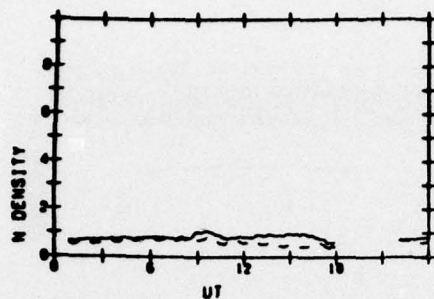
IONS

ELECTRONS

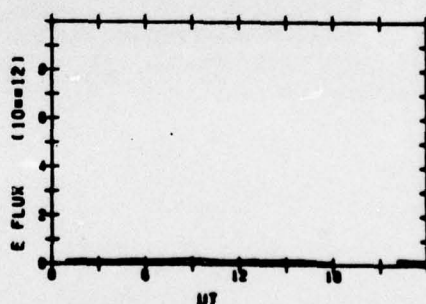
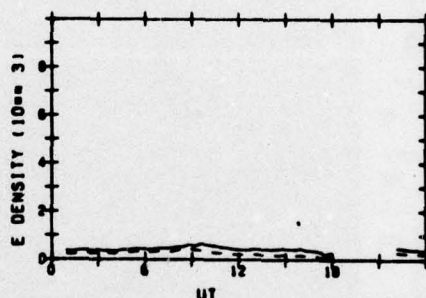
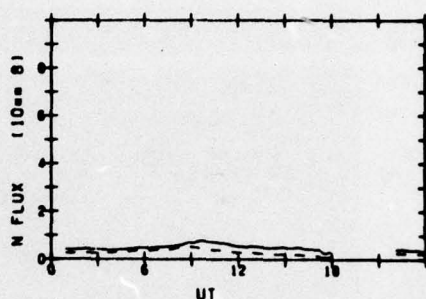
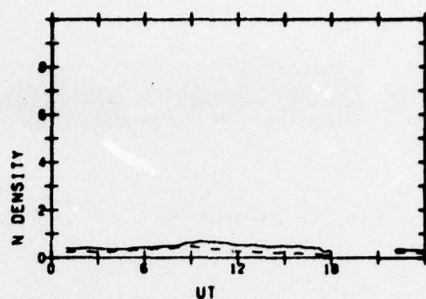


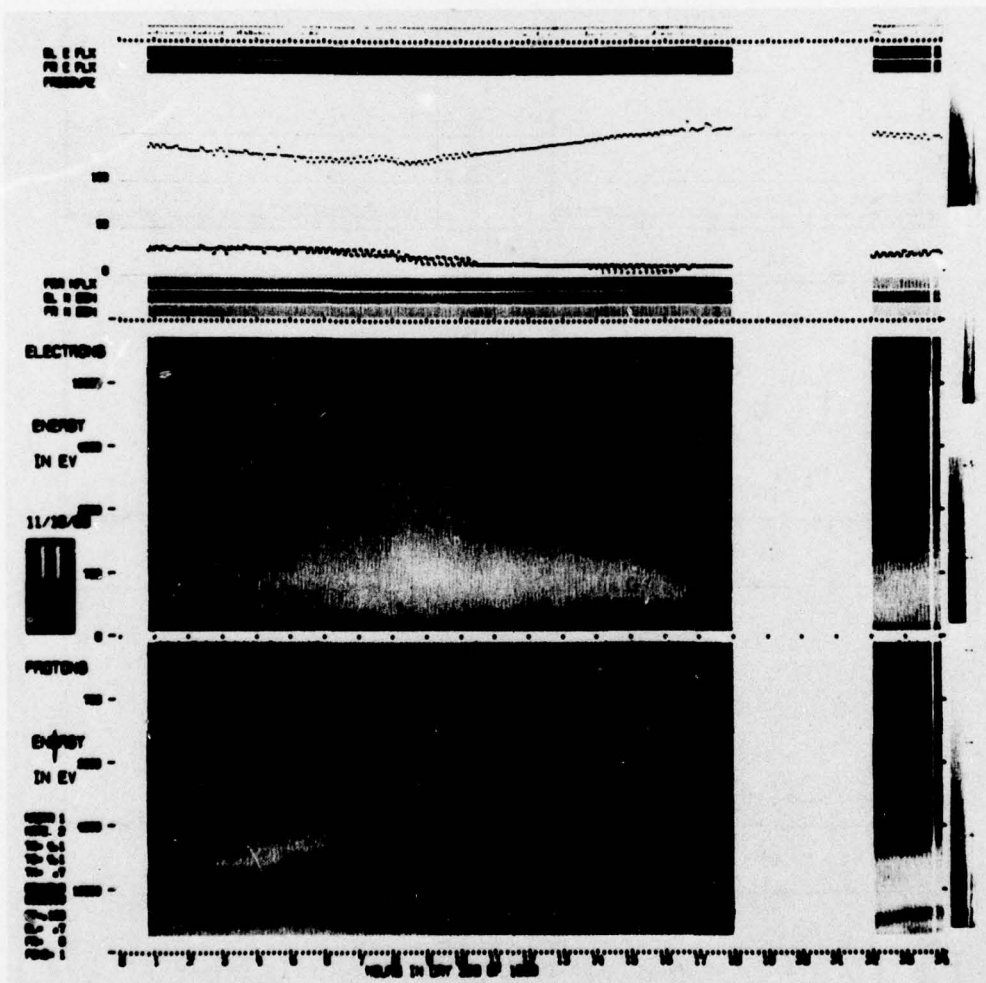
ATS-5
69/320

IONS



ELECTRONS

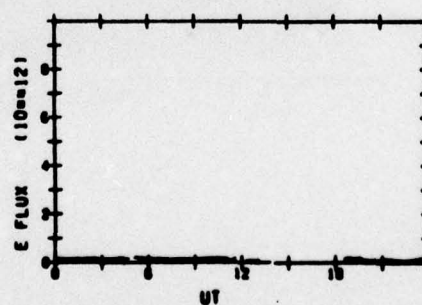
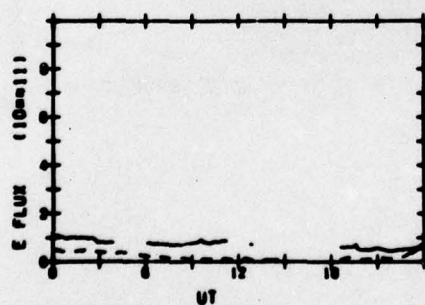
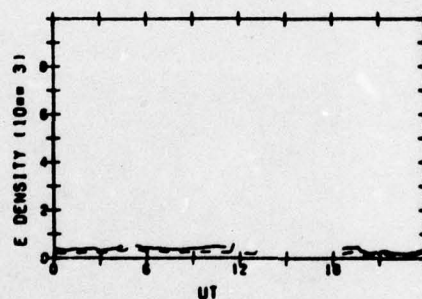
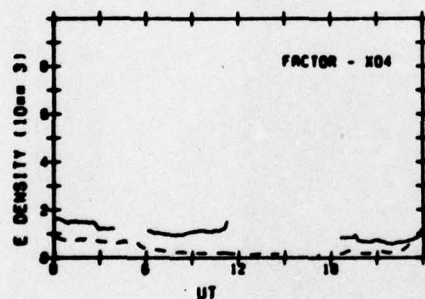
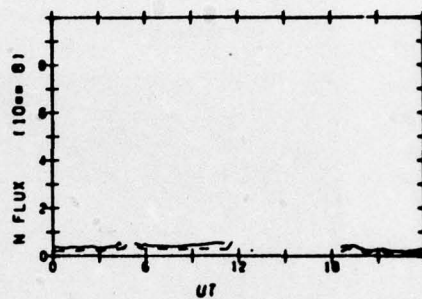
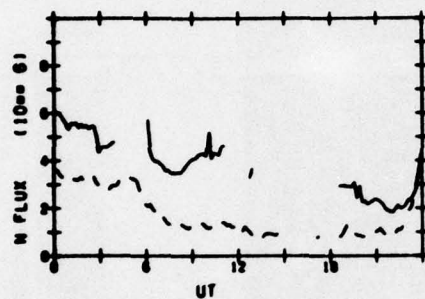
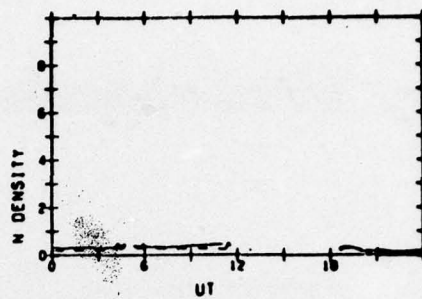
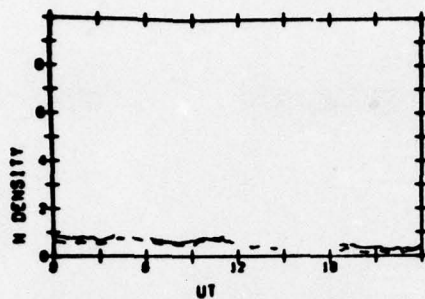


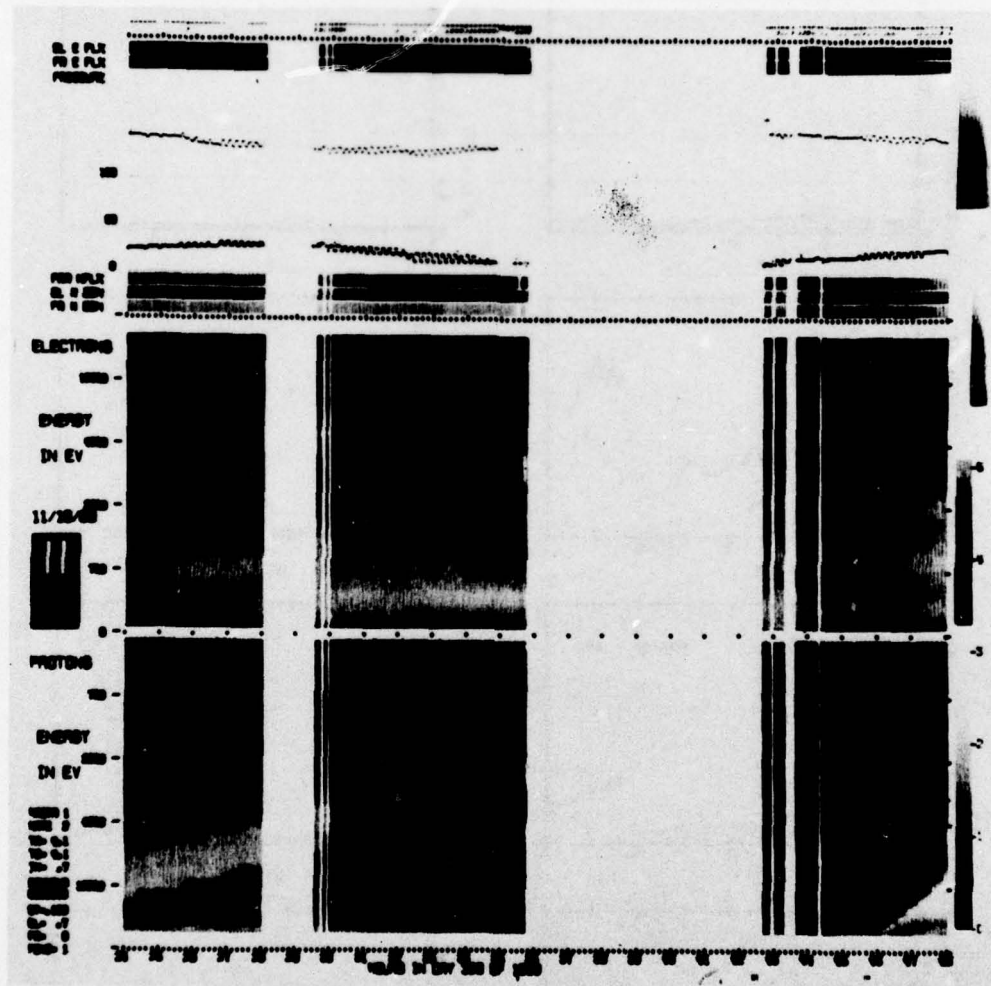


ATS-5
69/321

IONS

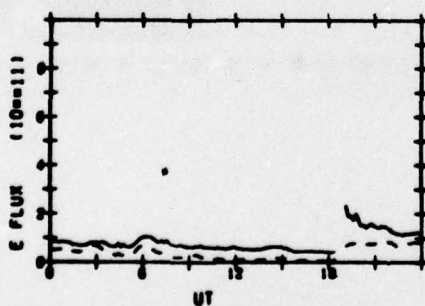
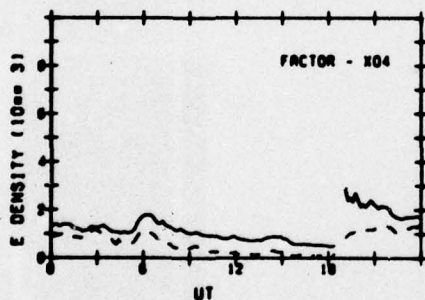
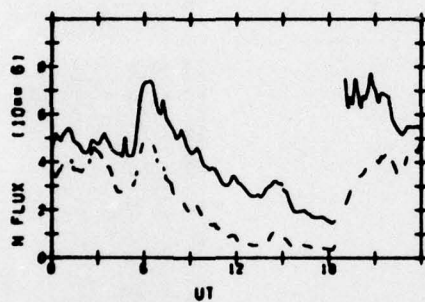
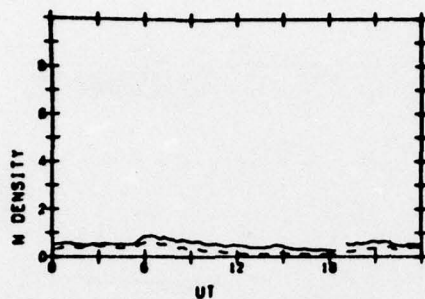
ELECTRONS



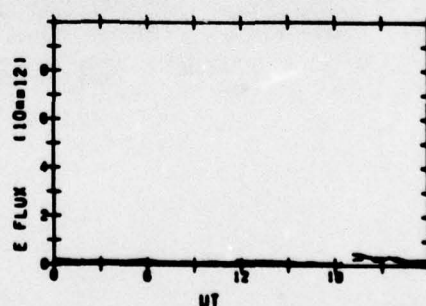
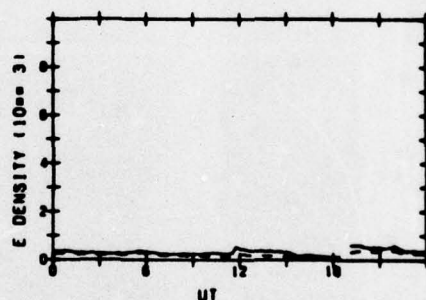
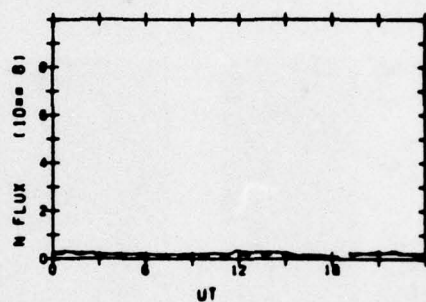
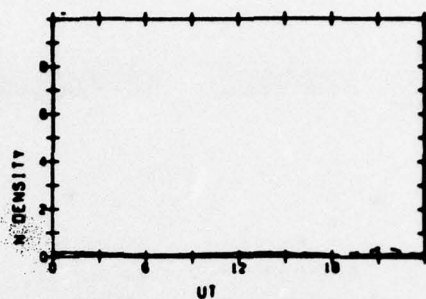


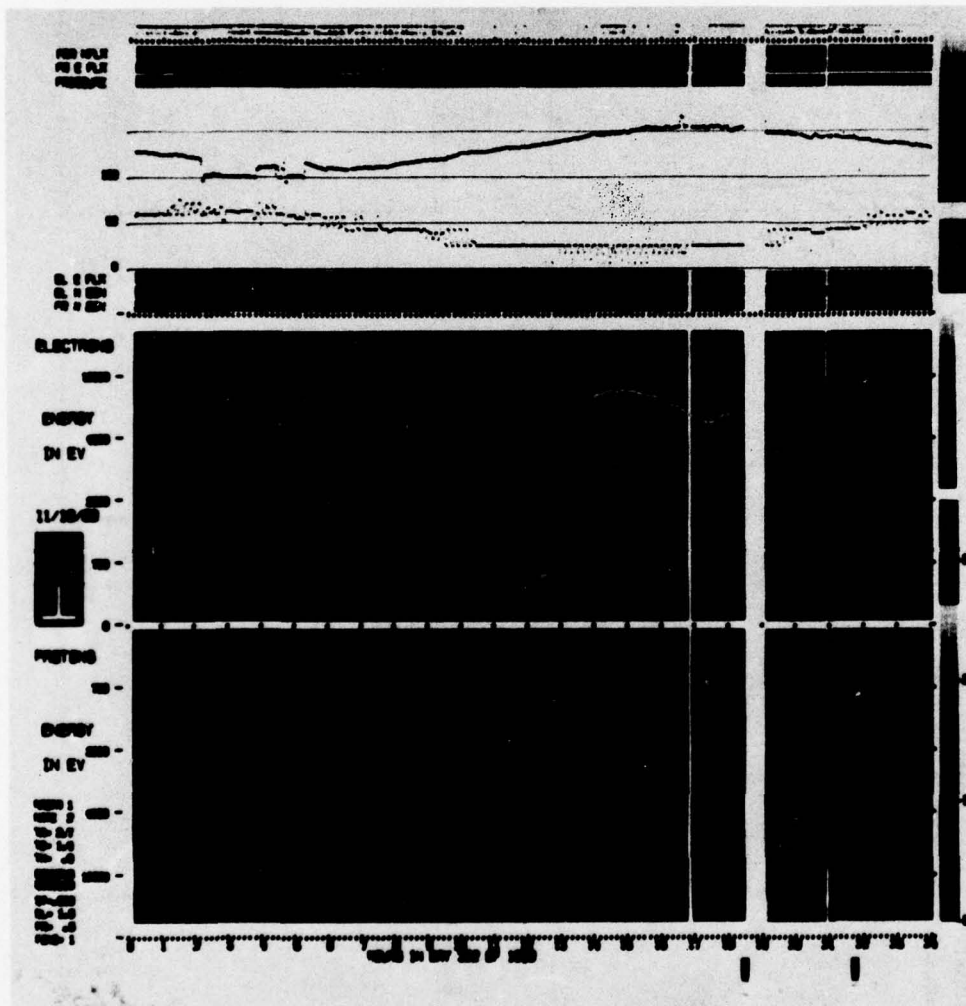
ATS-5
69/322

IONS



ELECTRONS

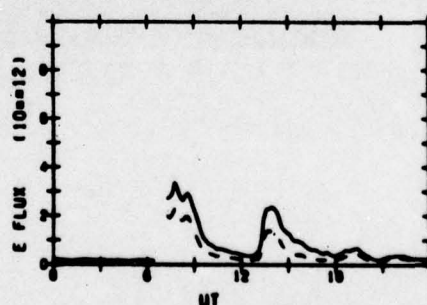
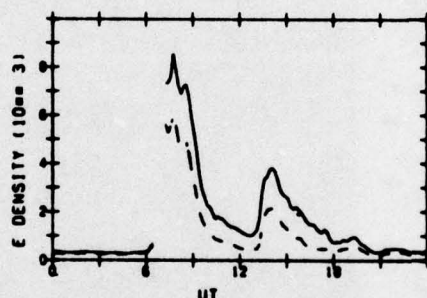
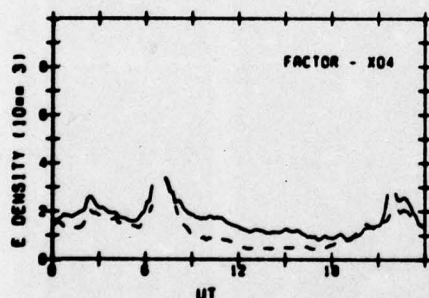
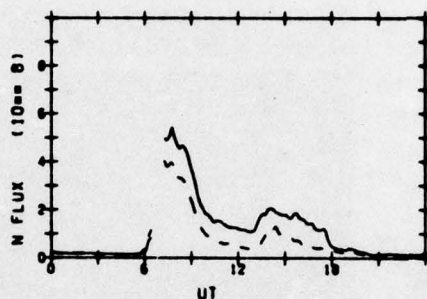
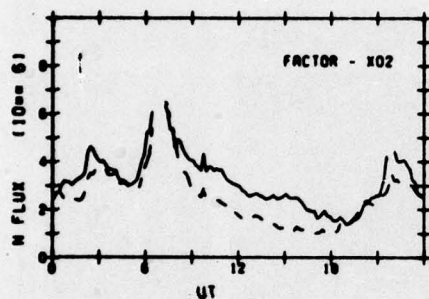
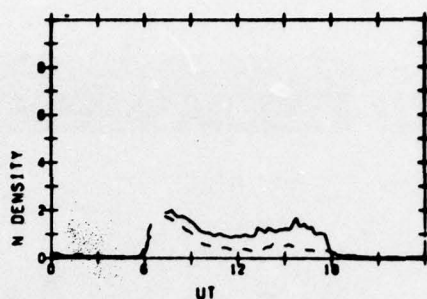
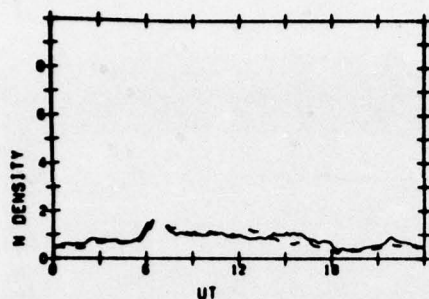


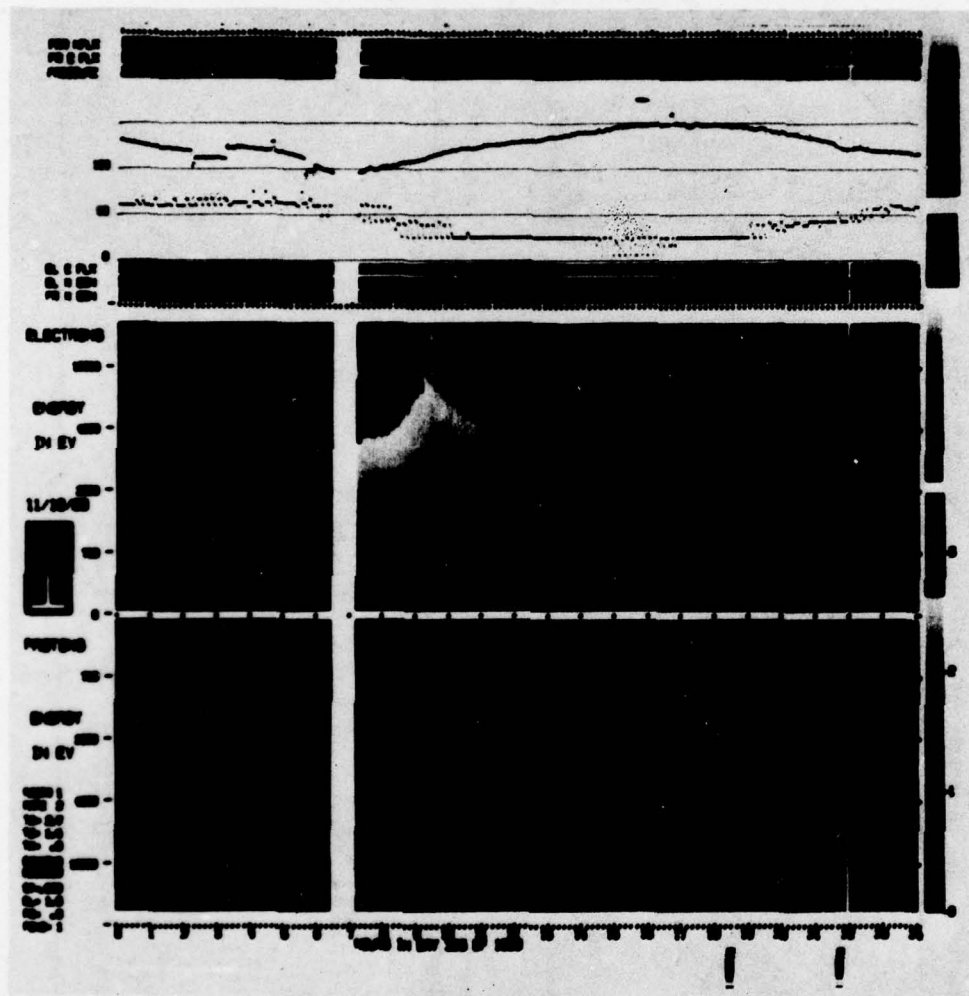


ATS-5
69/323

IONS

ELECTRONS

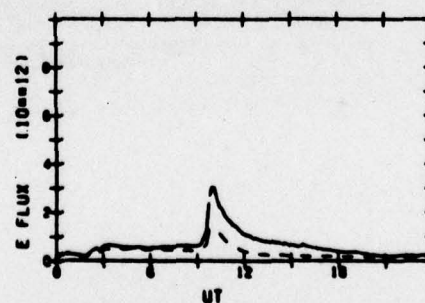
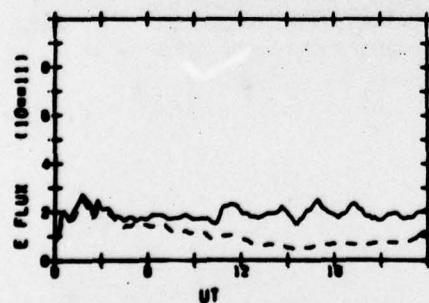
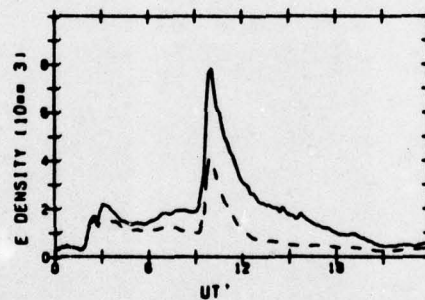
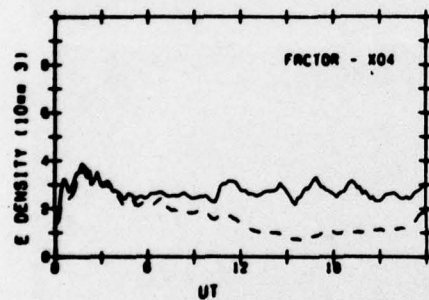
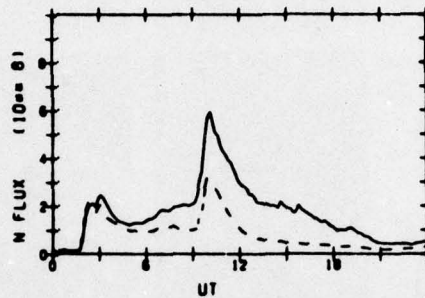
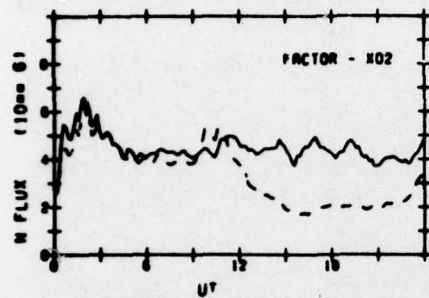
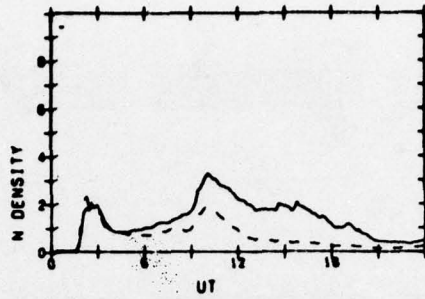
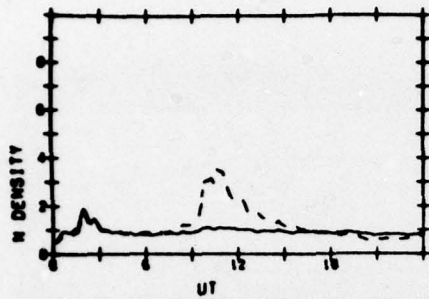


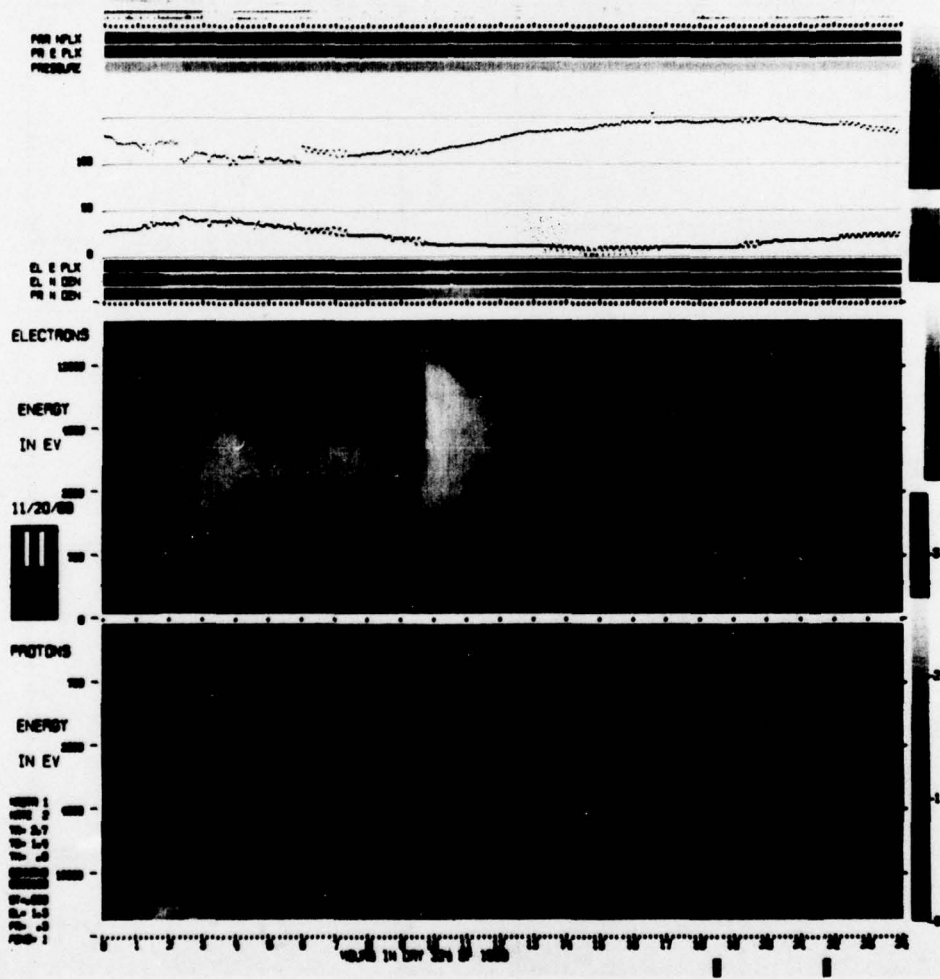


ATS-5
69/324

IONS

ELECTRONS

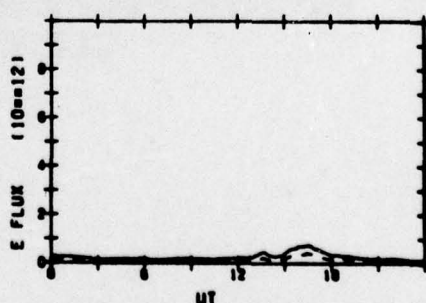
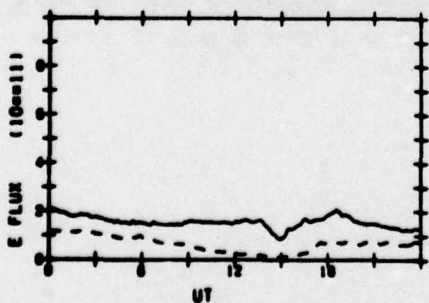
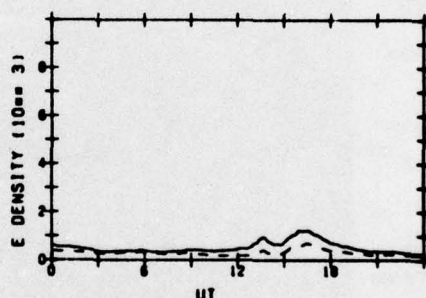
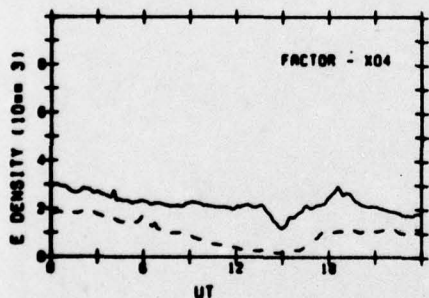
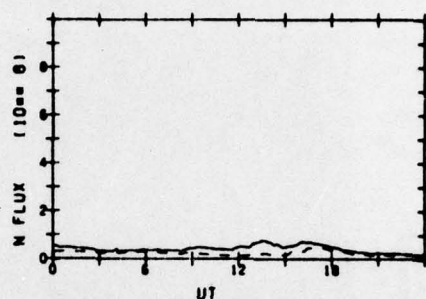
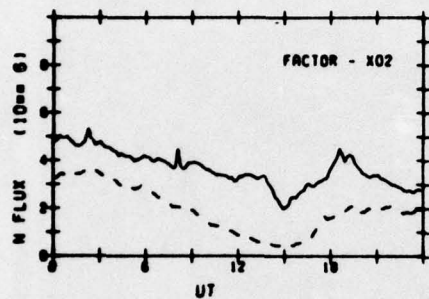
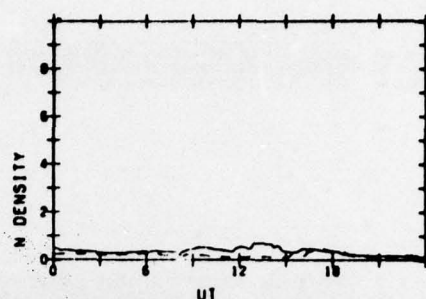
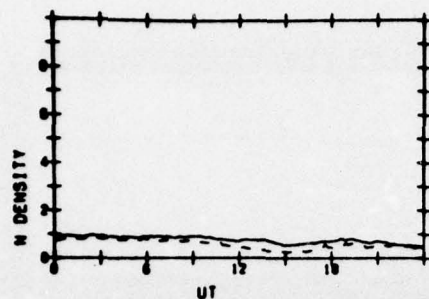




ATS-5
69/325

IONS

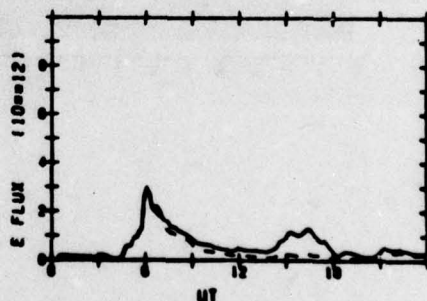
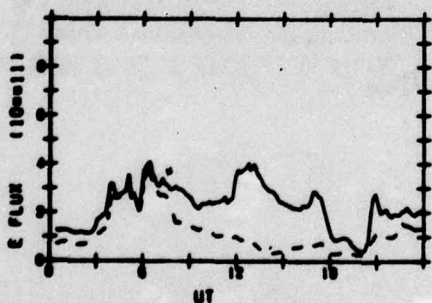
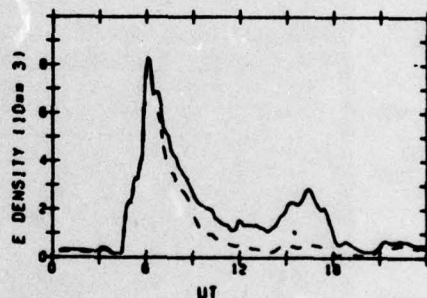
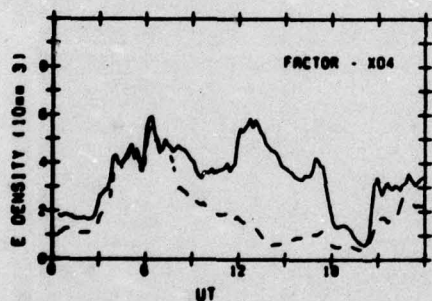
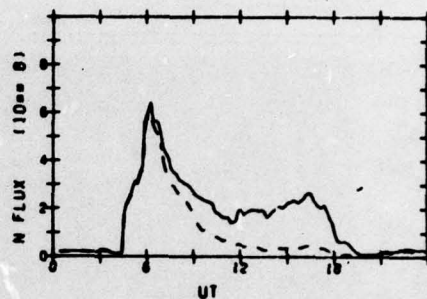
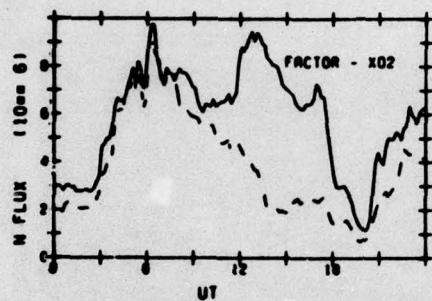
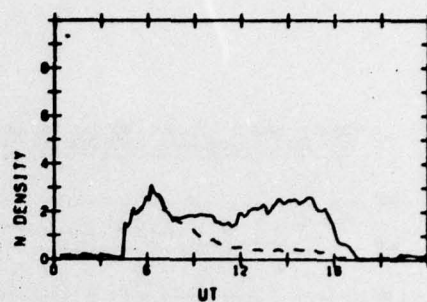
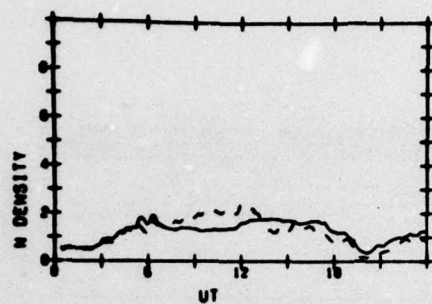
ELECTRONS

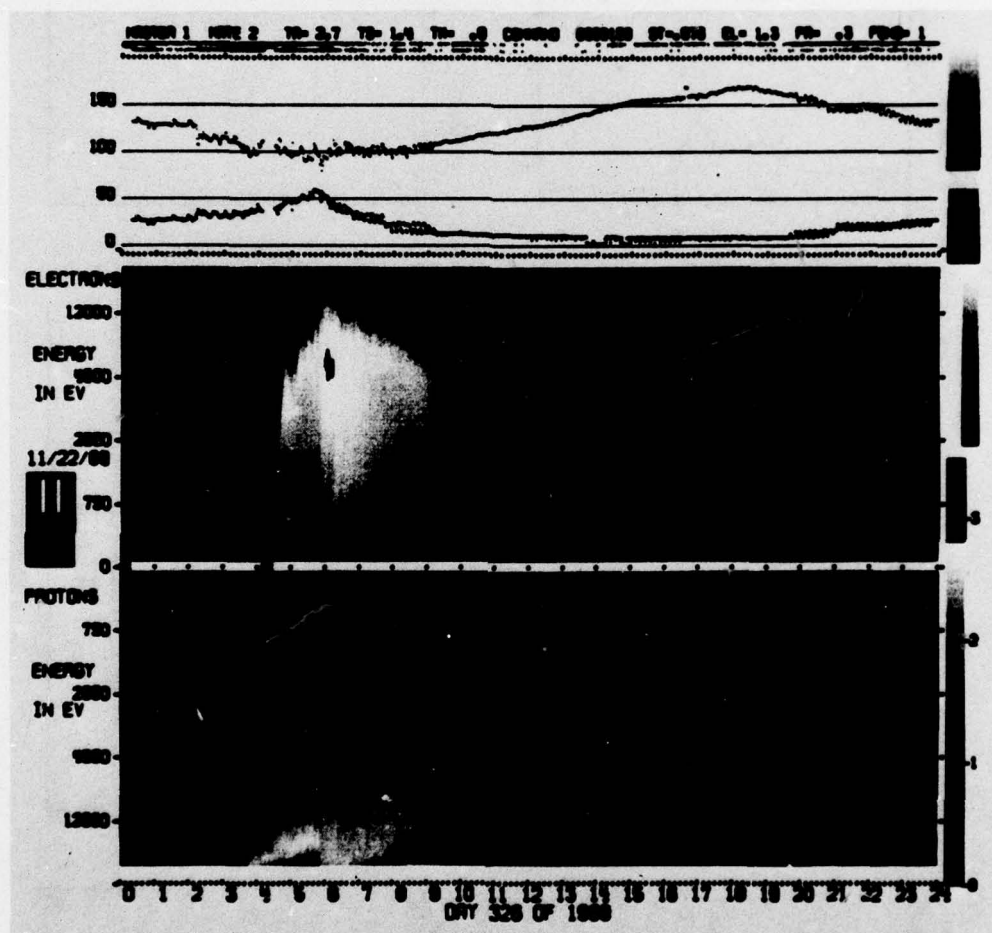


ATS-5
69/326

IONS

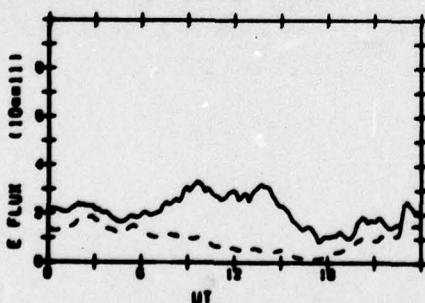
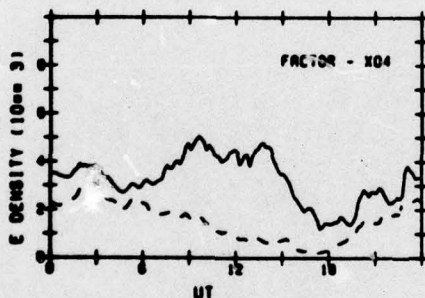
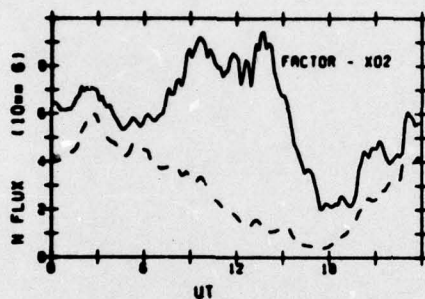
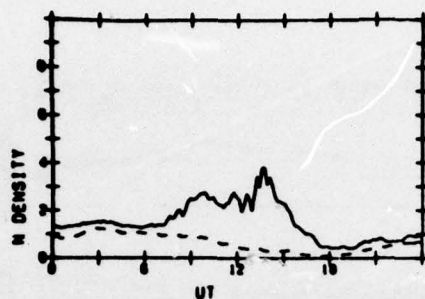
ELECTRONS



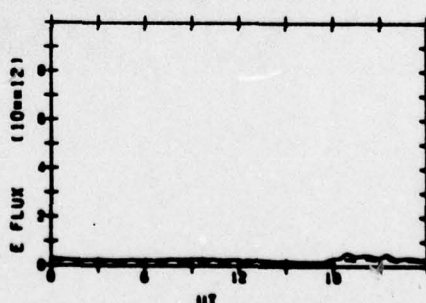
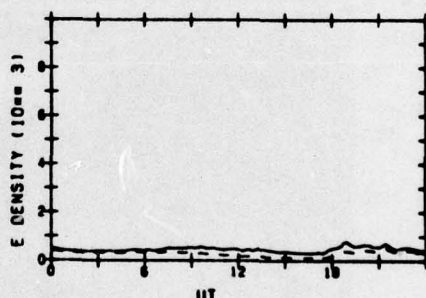
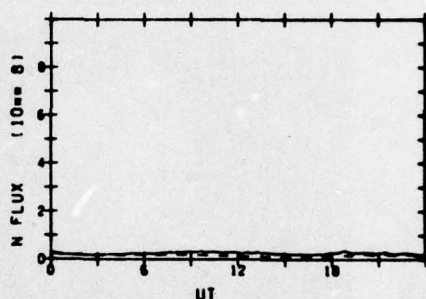
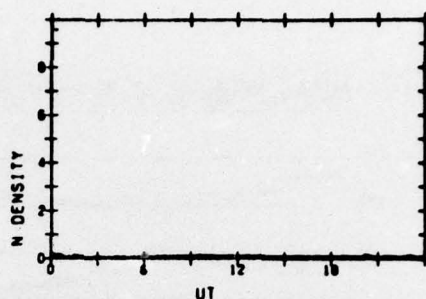


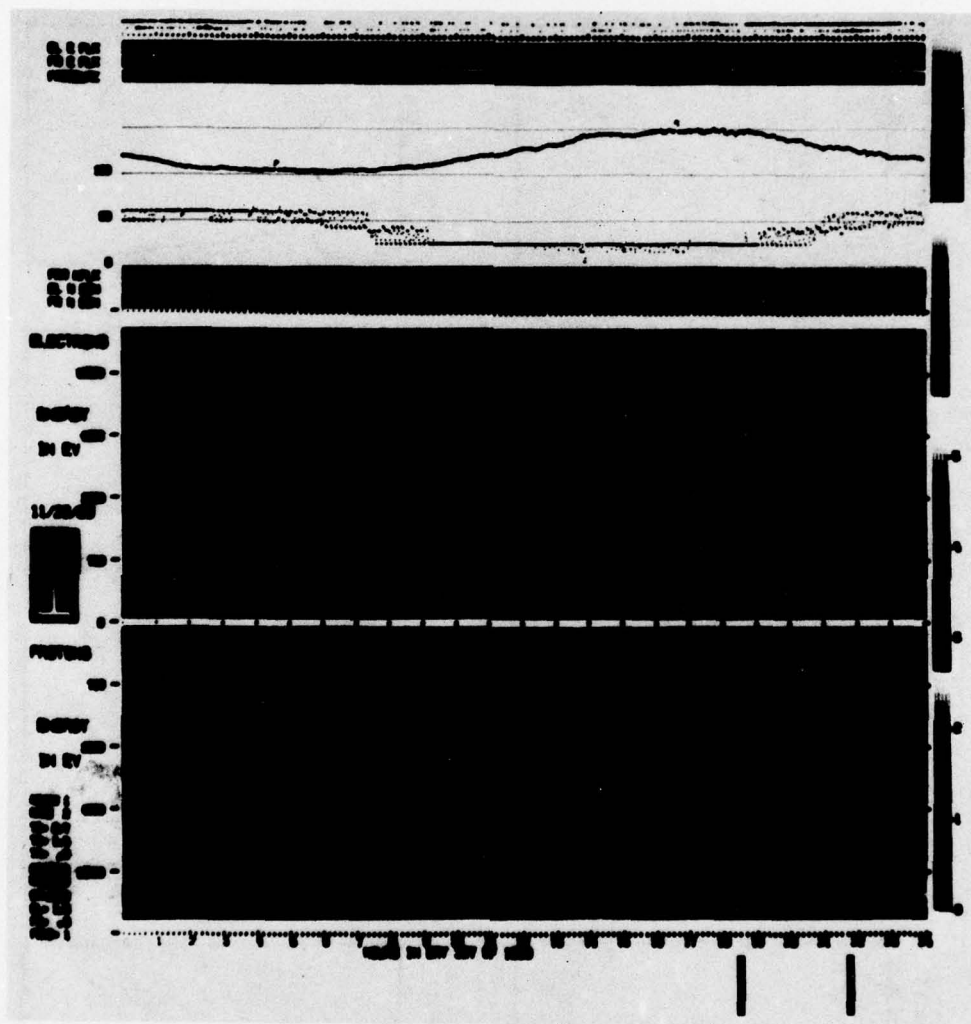
ATS-5
69/327

IONS



ELECTRONS

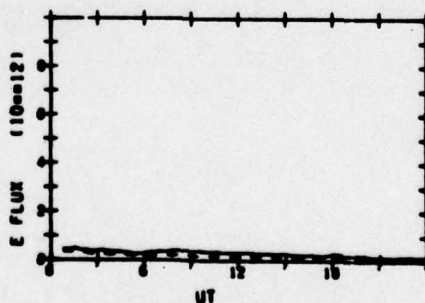
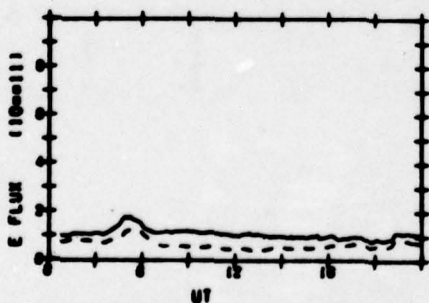
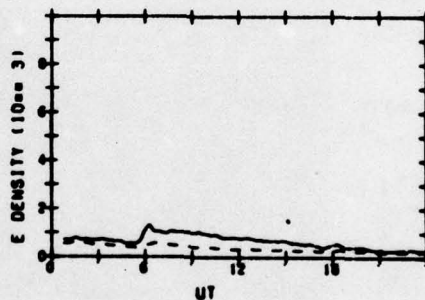
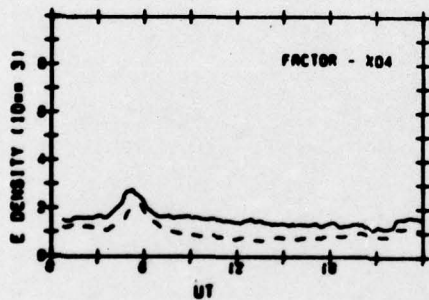
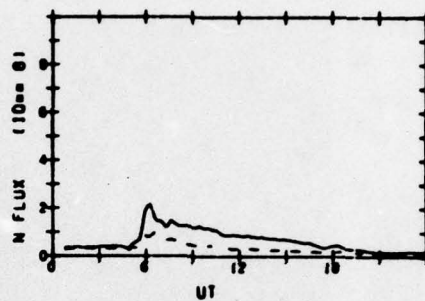
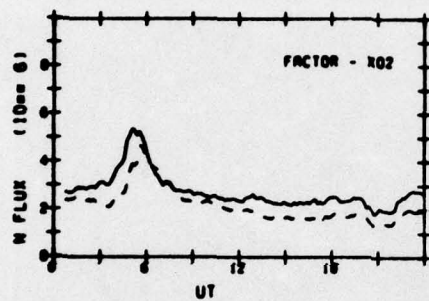
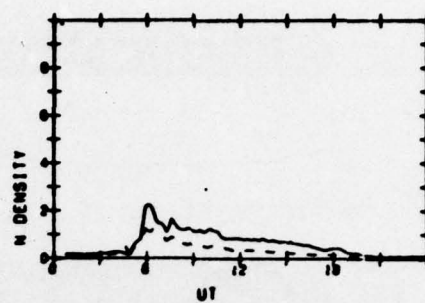
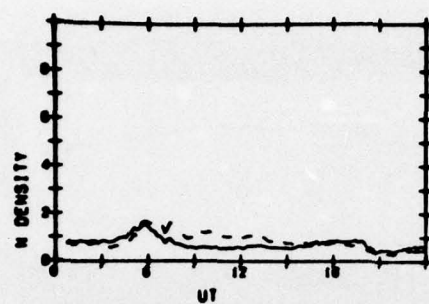


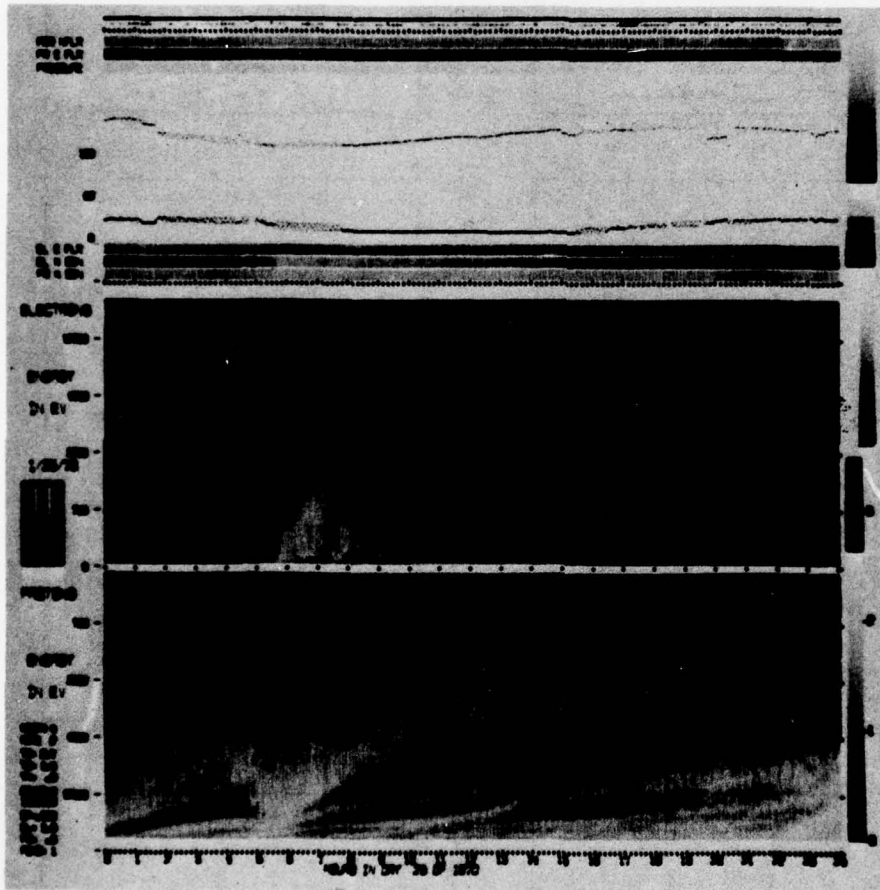


ATS-5
70/025

IONS

ELECTRONS

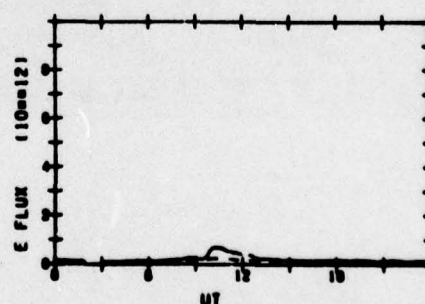
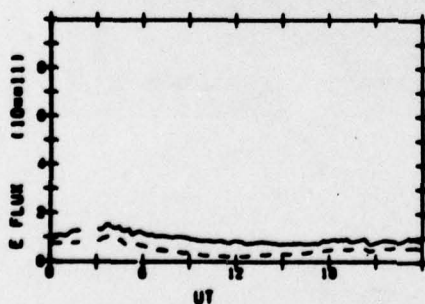
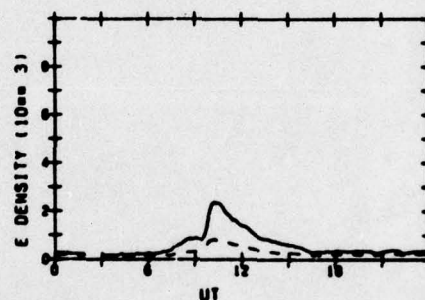
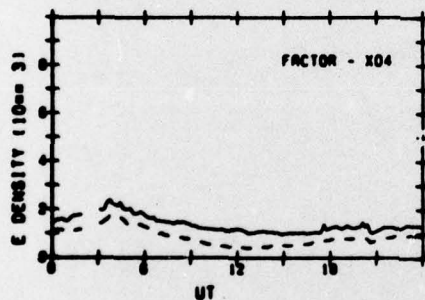
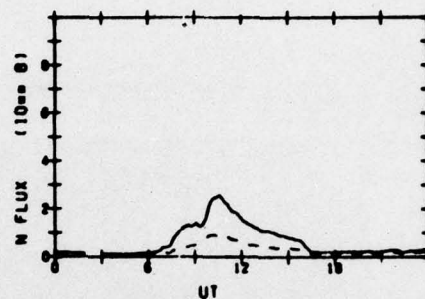
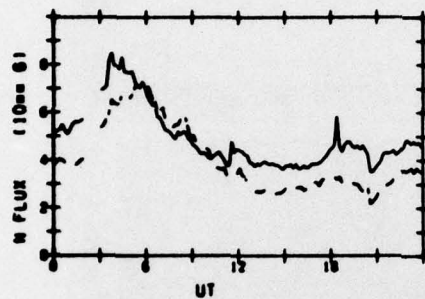
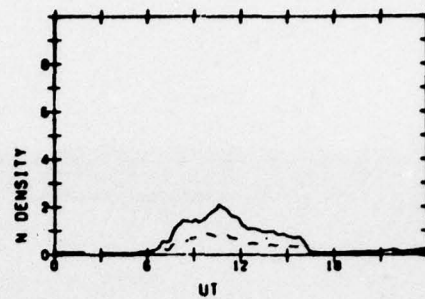
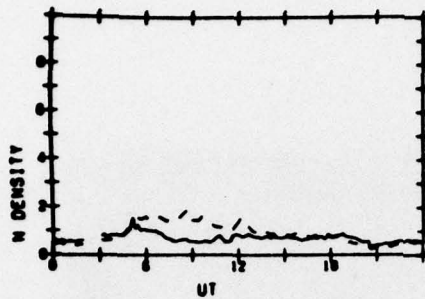




ATS-5
70/02C

IONS

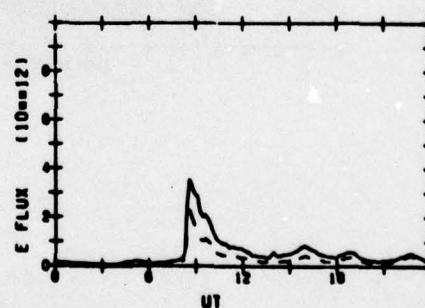
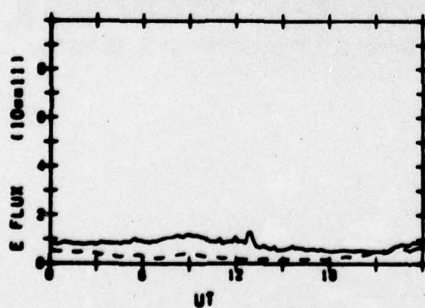
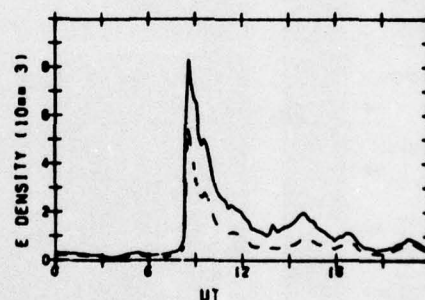
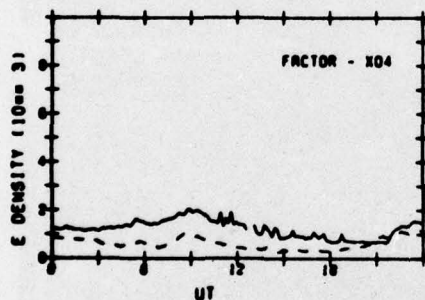
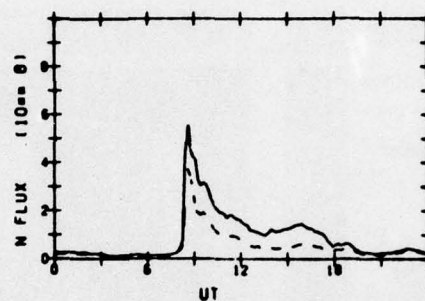
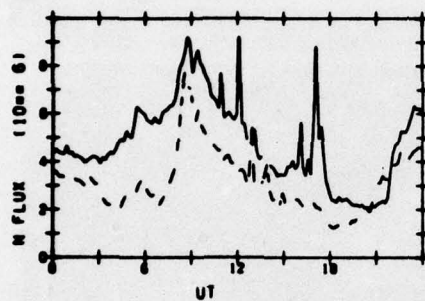
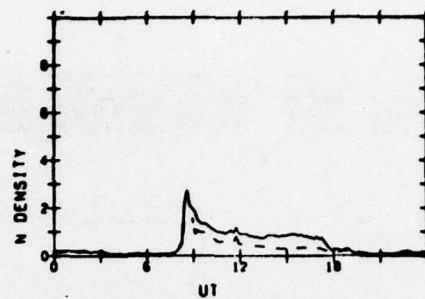
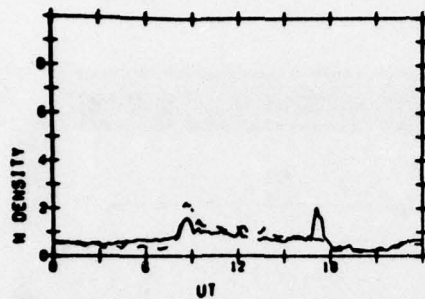
ELECTRONS

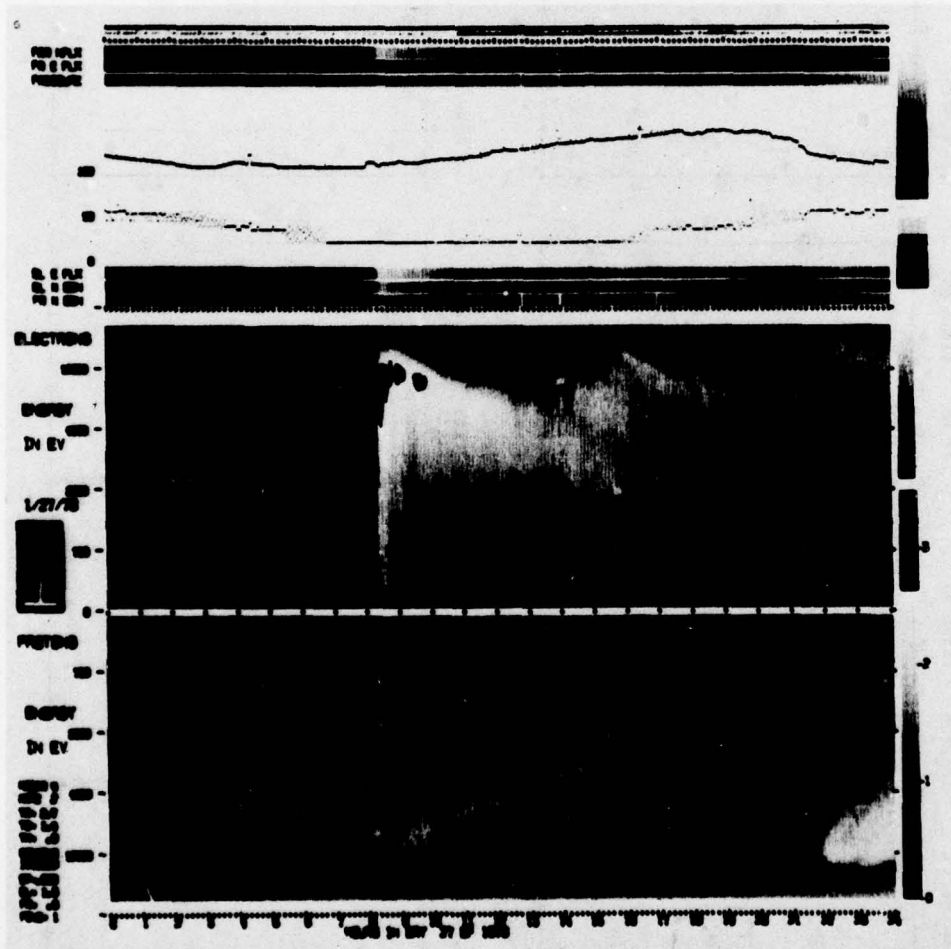


ATS-5
70/027

IONS

ELECTRONS

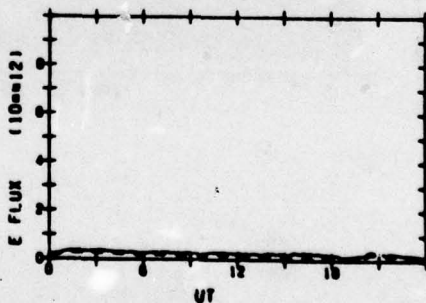
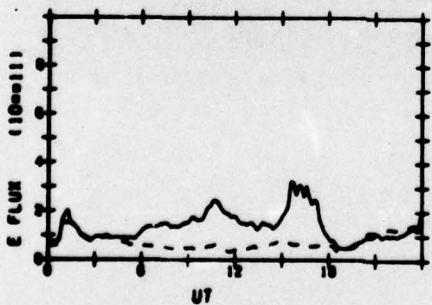
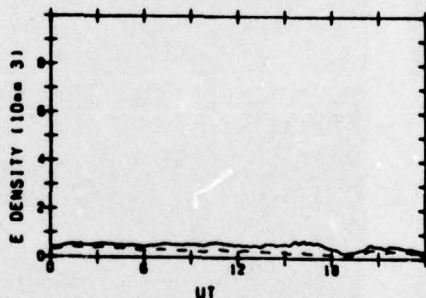
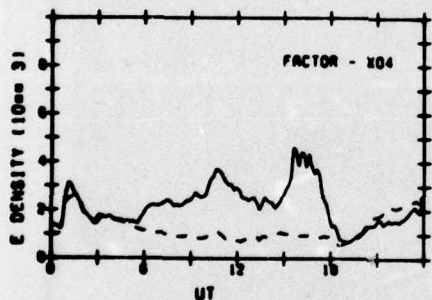
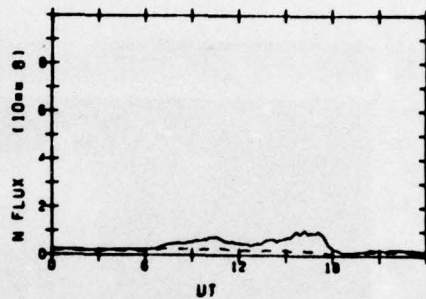
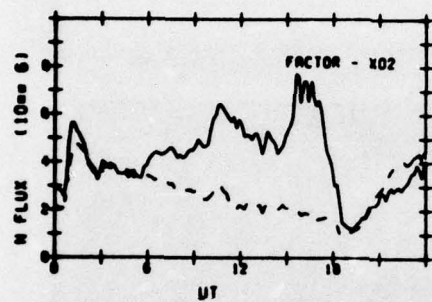
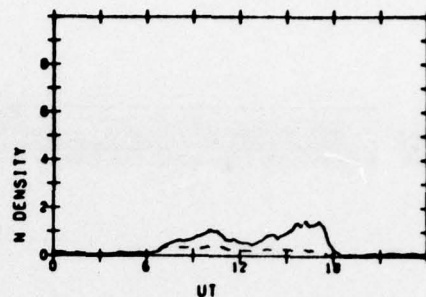
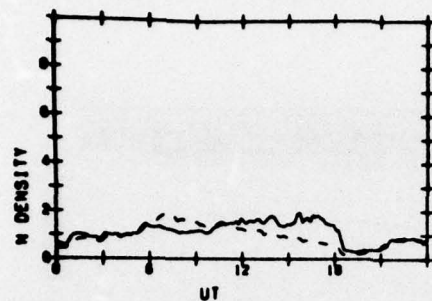


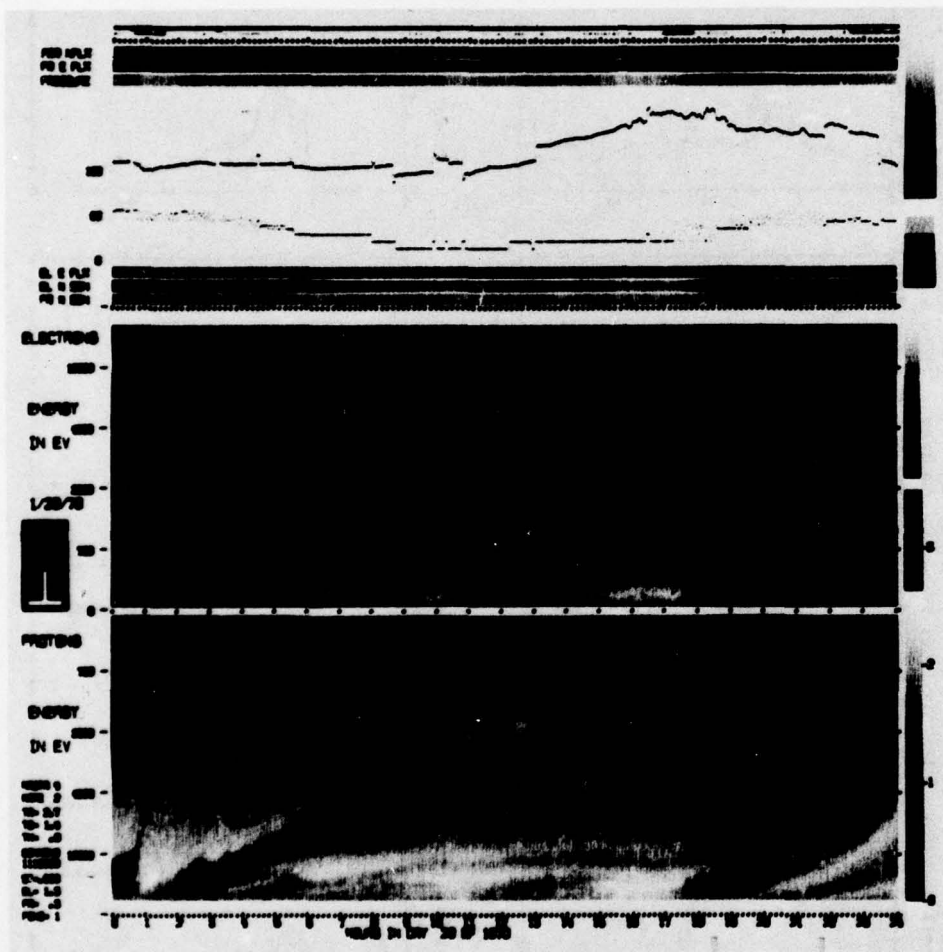


ATS-5
70/028

IONS

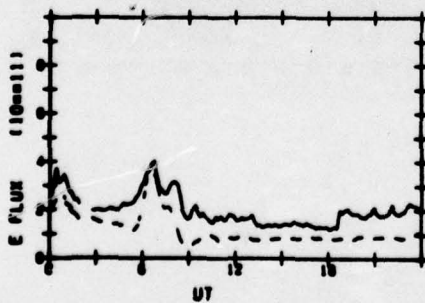
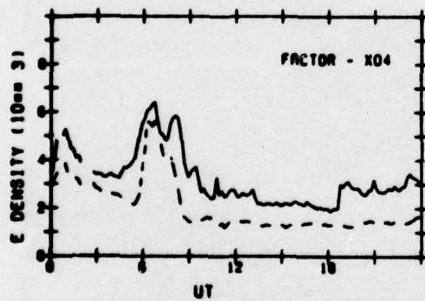
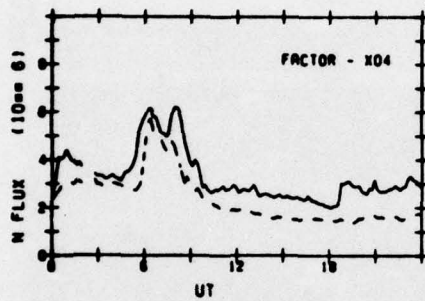
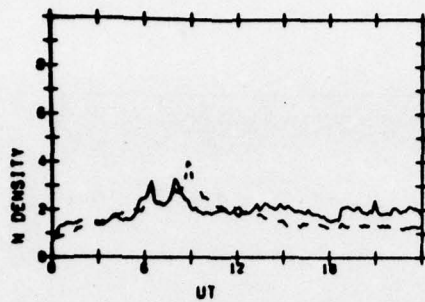
ELECTRONS



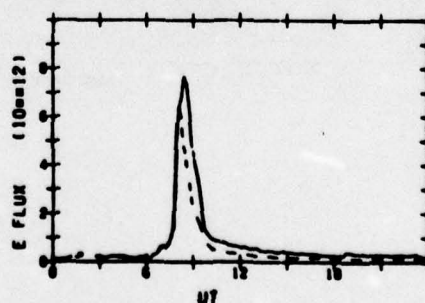
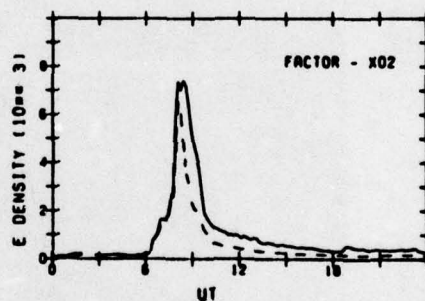
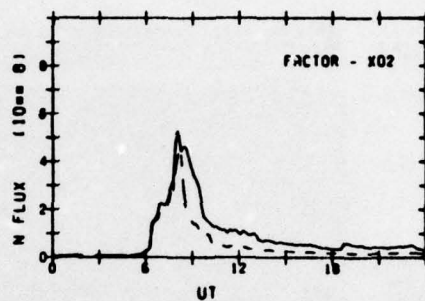
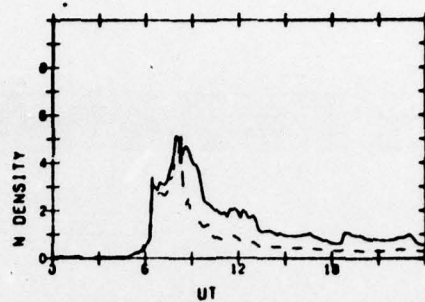


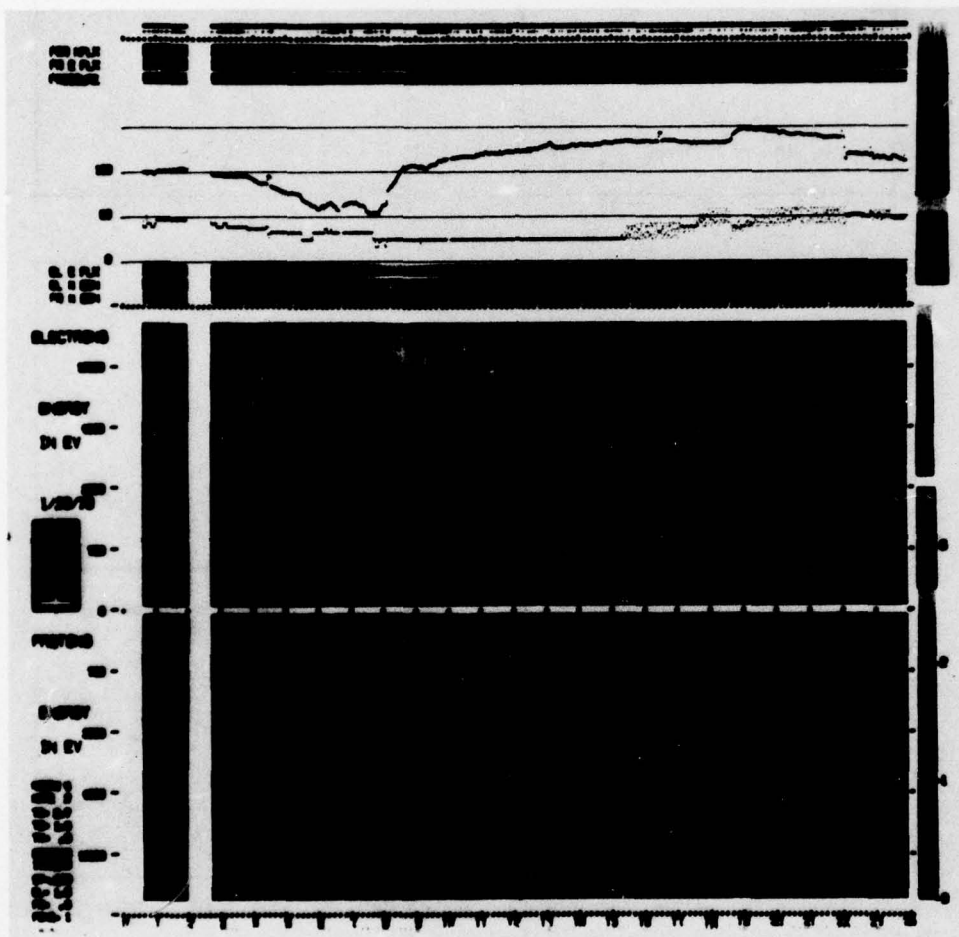
ATS-5
70/029

IONS



ELECTRONS

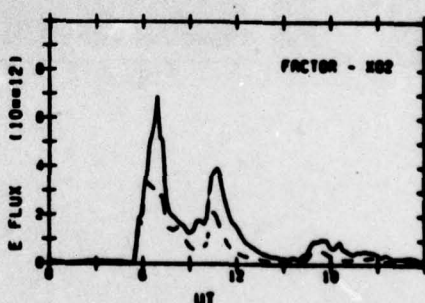
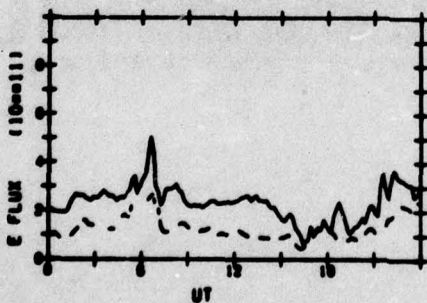
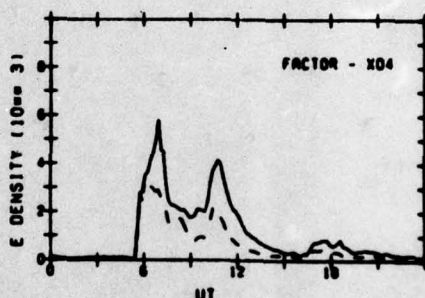
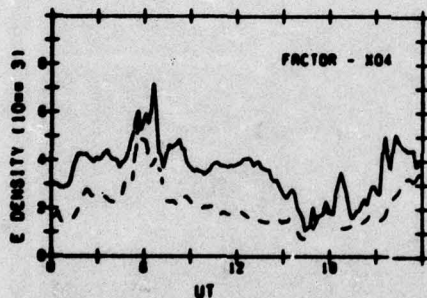
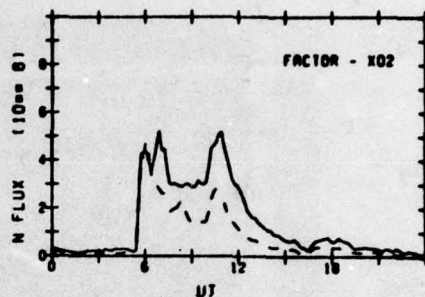
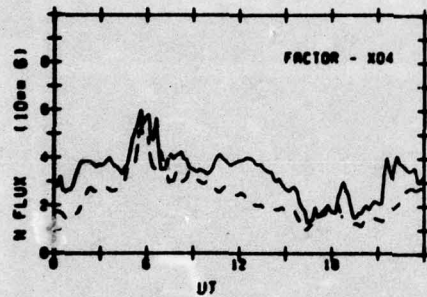
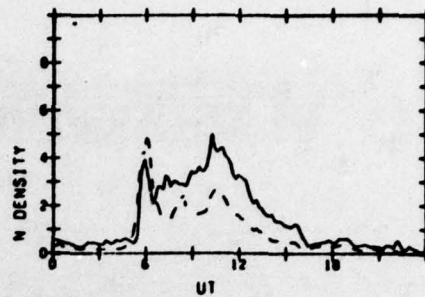
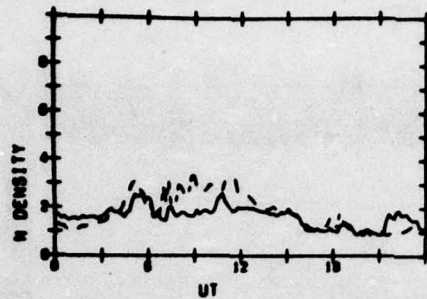


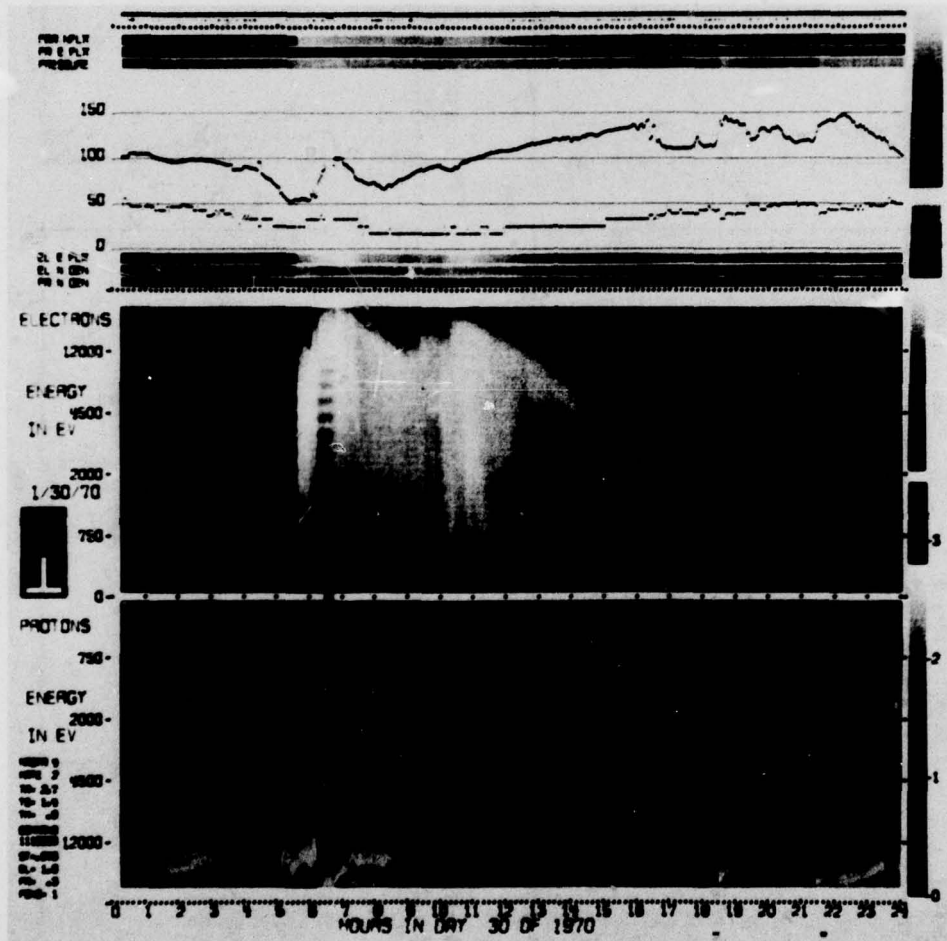


ATS-5
70/030

IONS

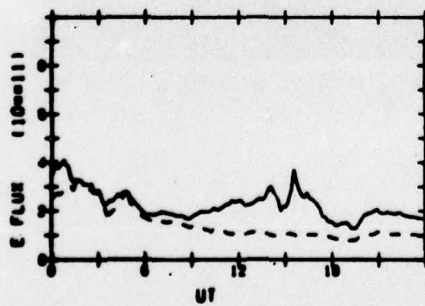
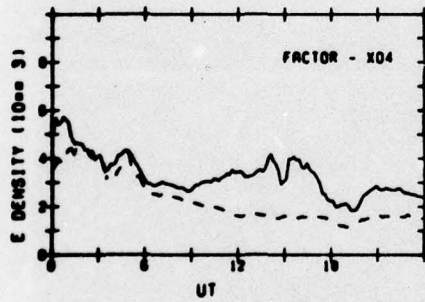
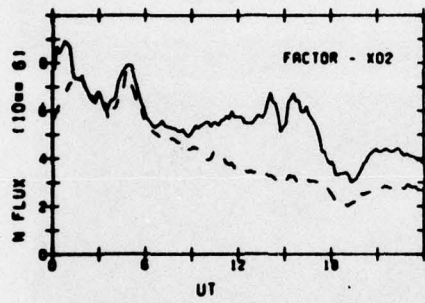
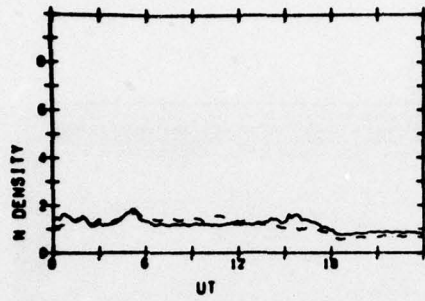
ELECTRONS



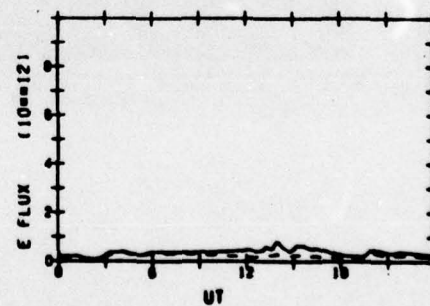
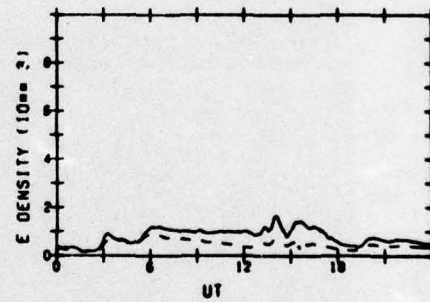
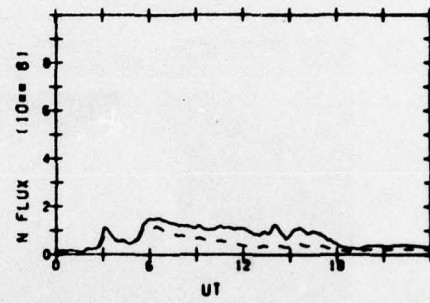
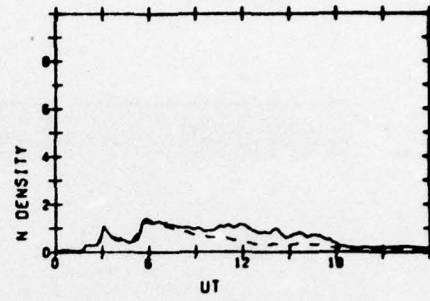


AT6-5
70/031

IONS



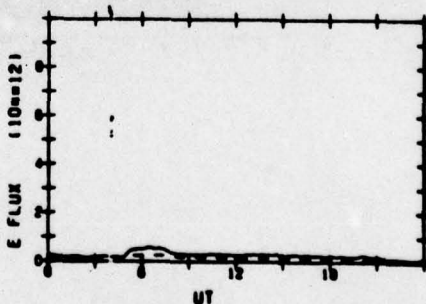
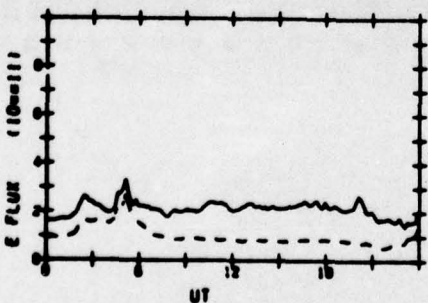
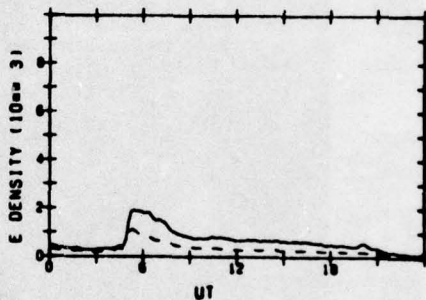
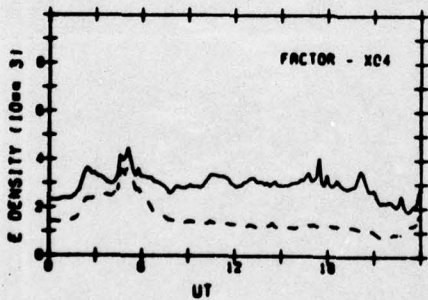
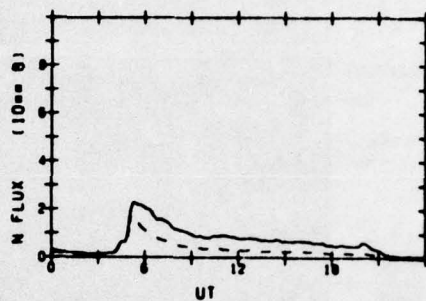
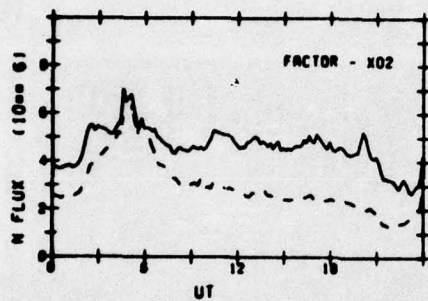
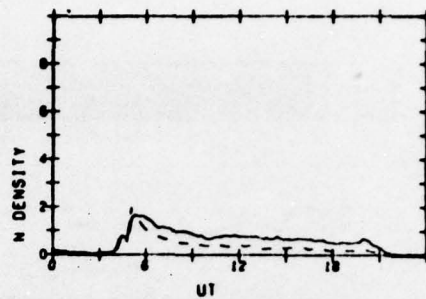
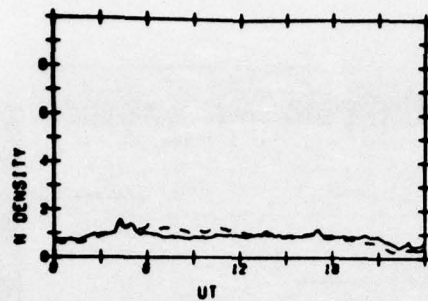
ELECTRONS

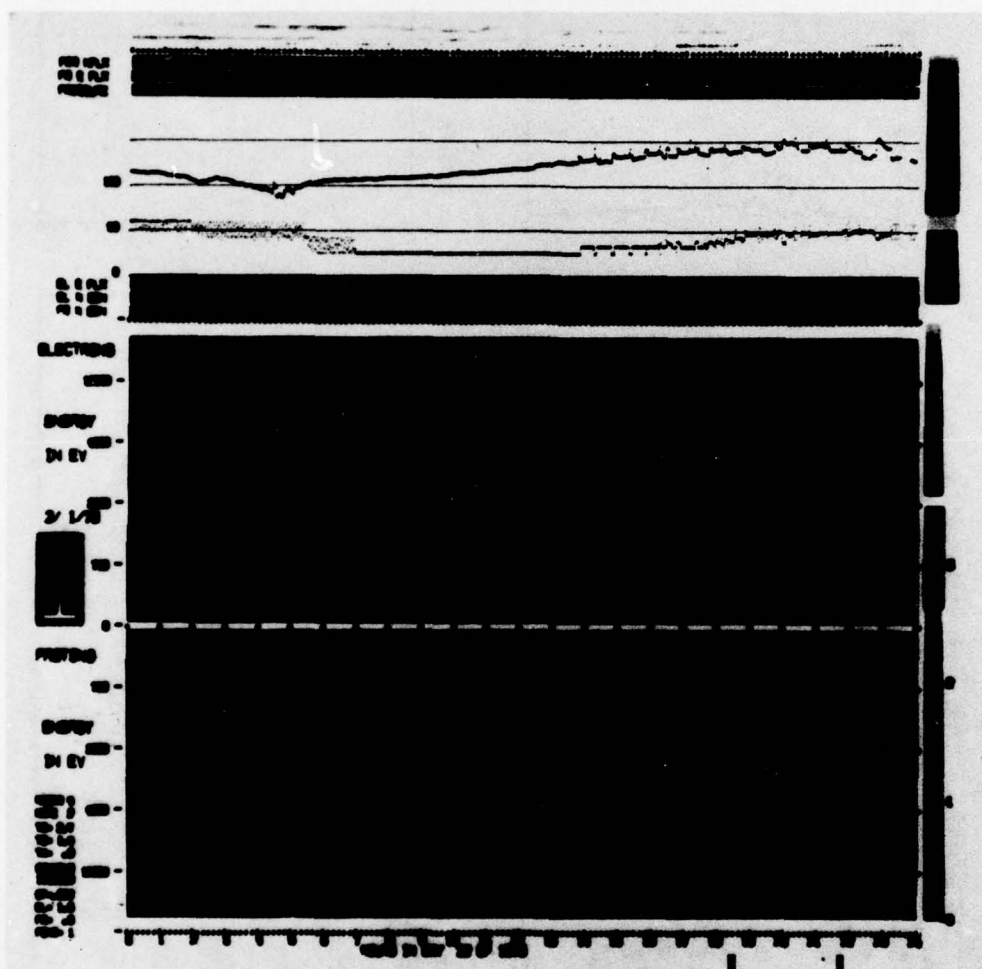


ATS-5
70/032

IONS

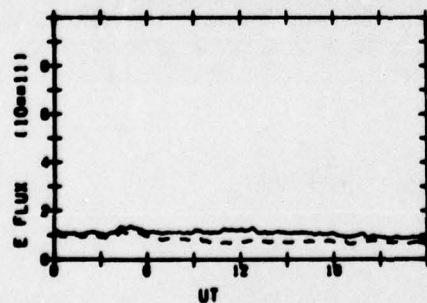
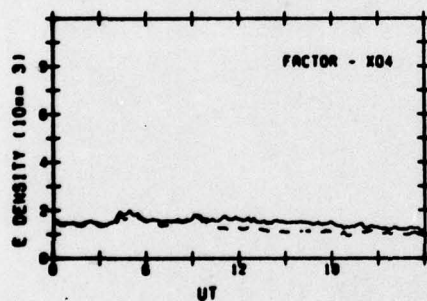
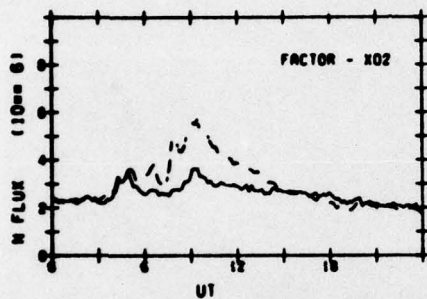
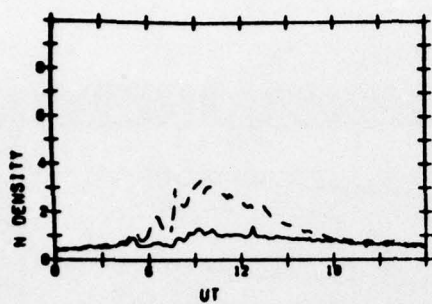
ELECTRONS



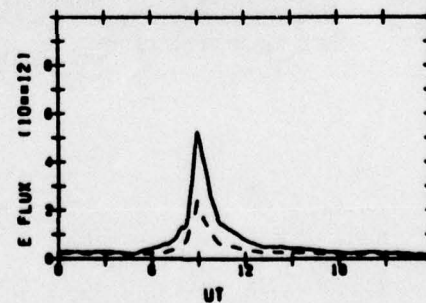
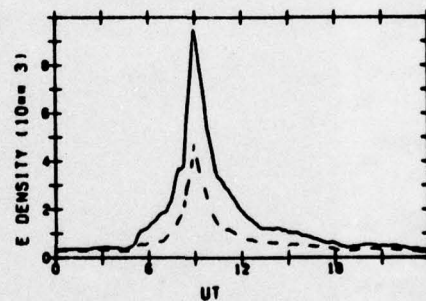
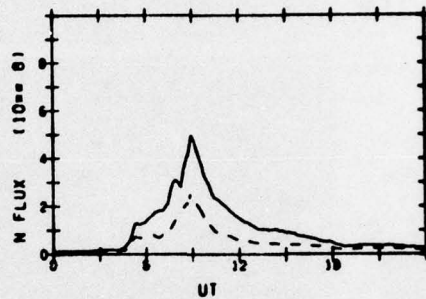
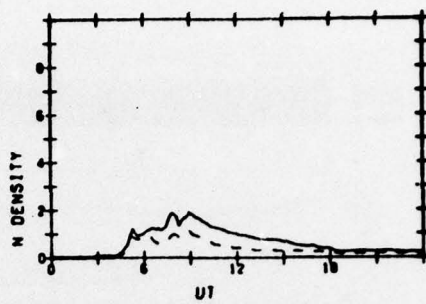


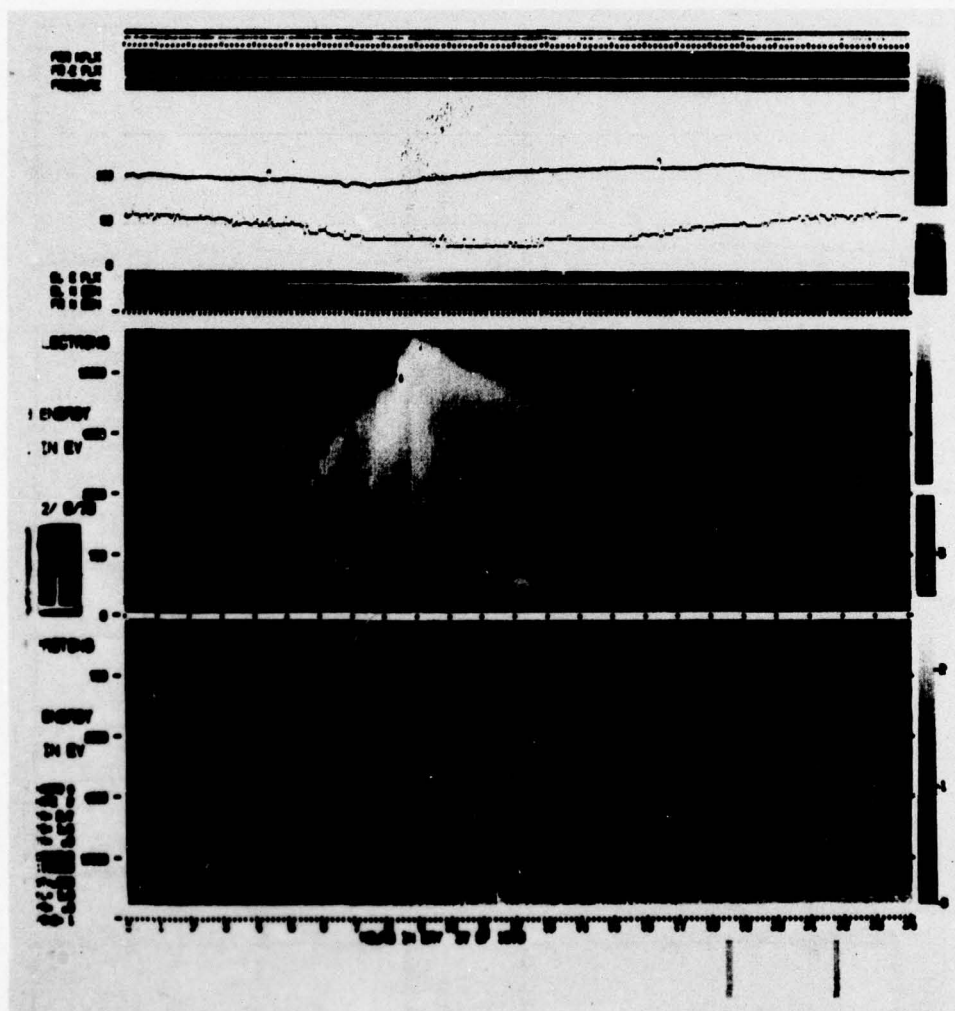
ATS-5
70/037

IONS



ELECTRONS

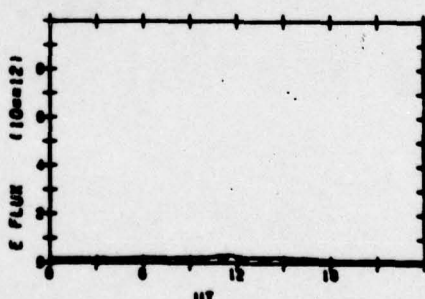
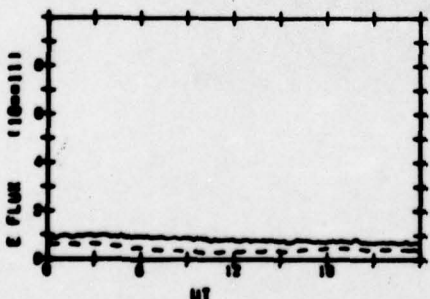
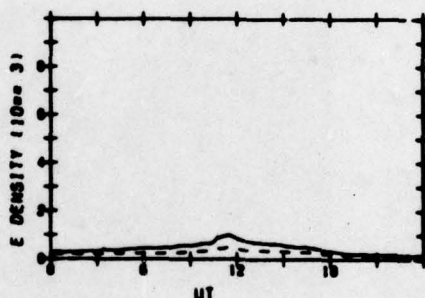
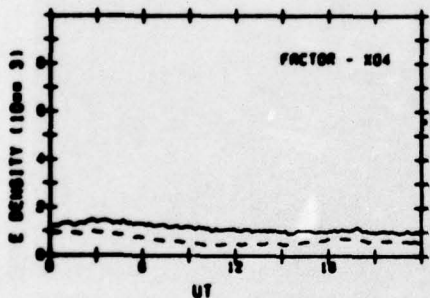
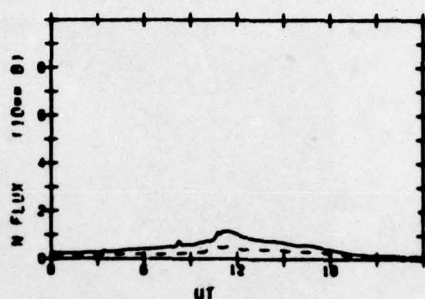
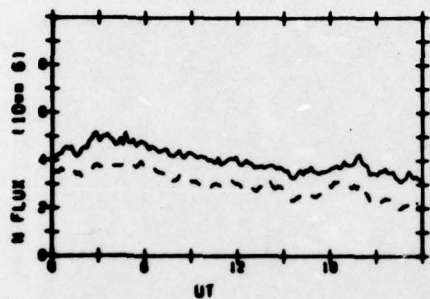
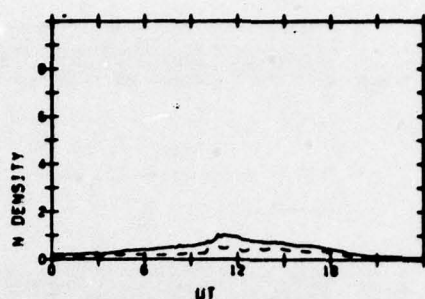
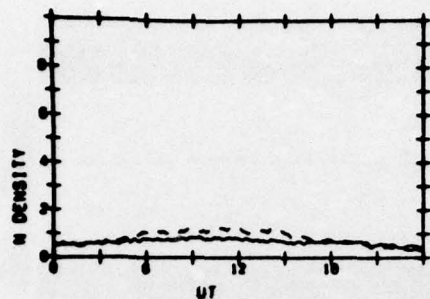




ATS-5
70/030

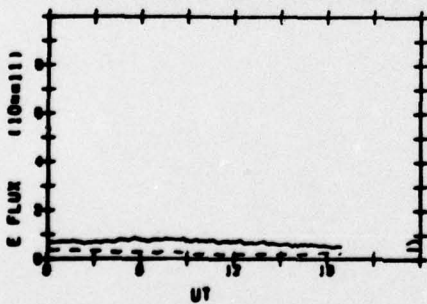
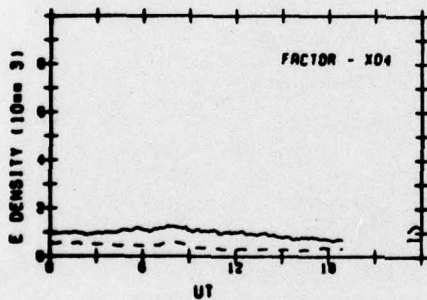
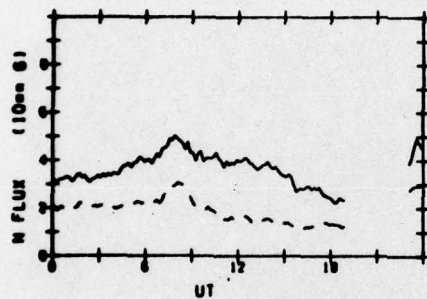
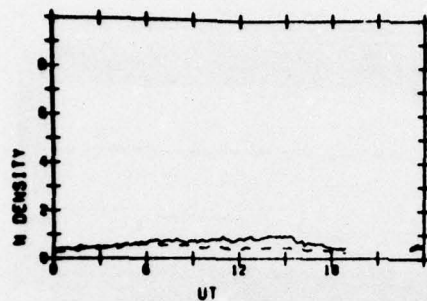
IONS

ELECTRONS

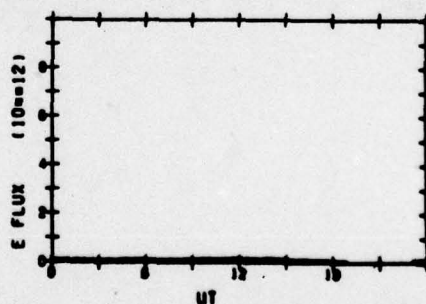
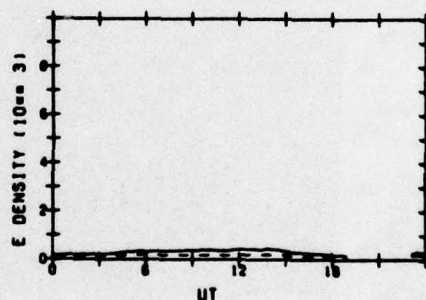
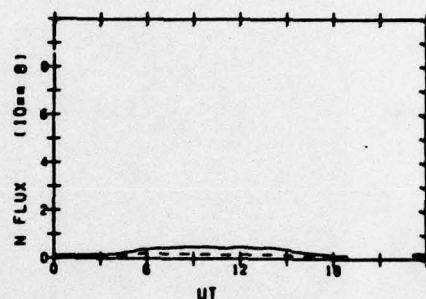
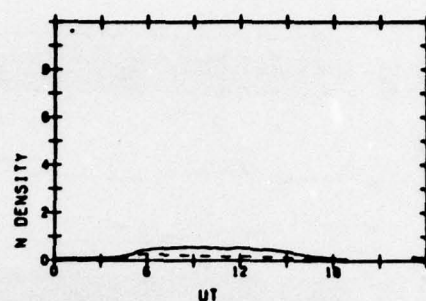


ATS-5
70/039

IONS

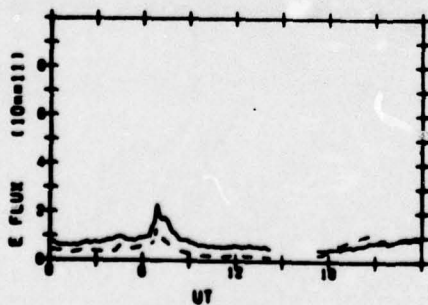
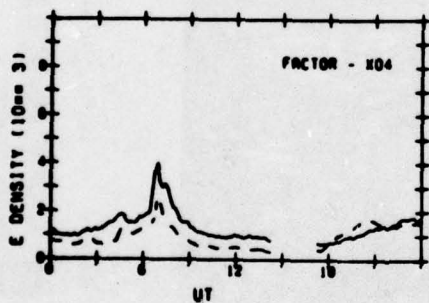
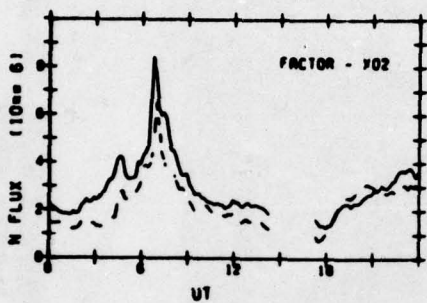
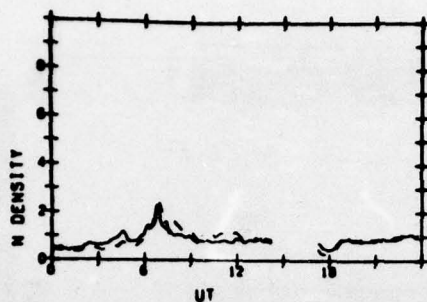


ELECTRONS

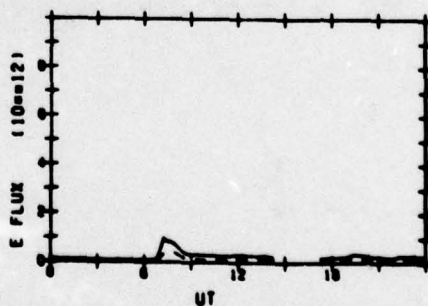
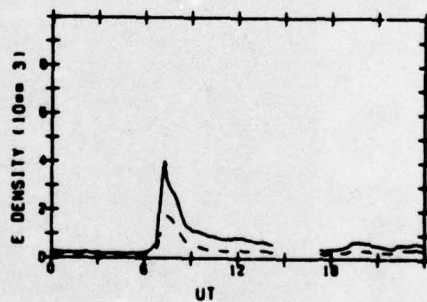
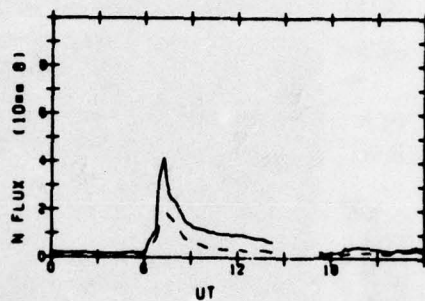
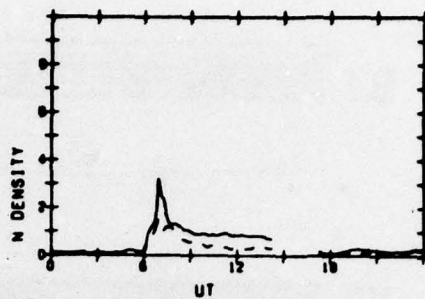


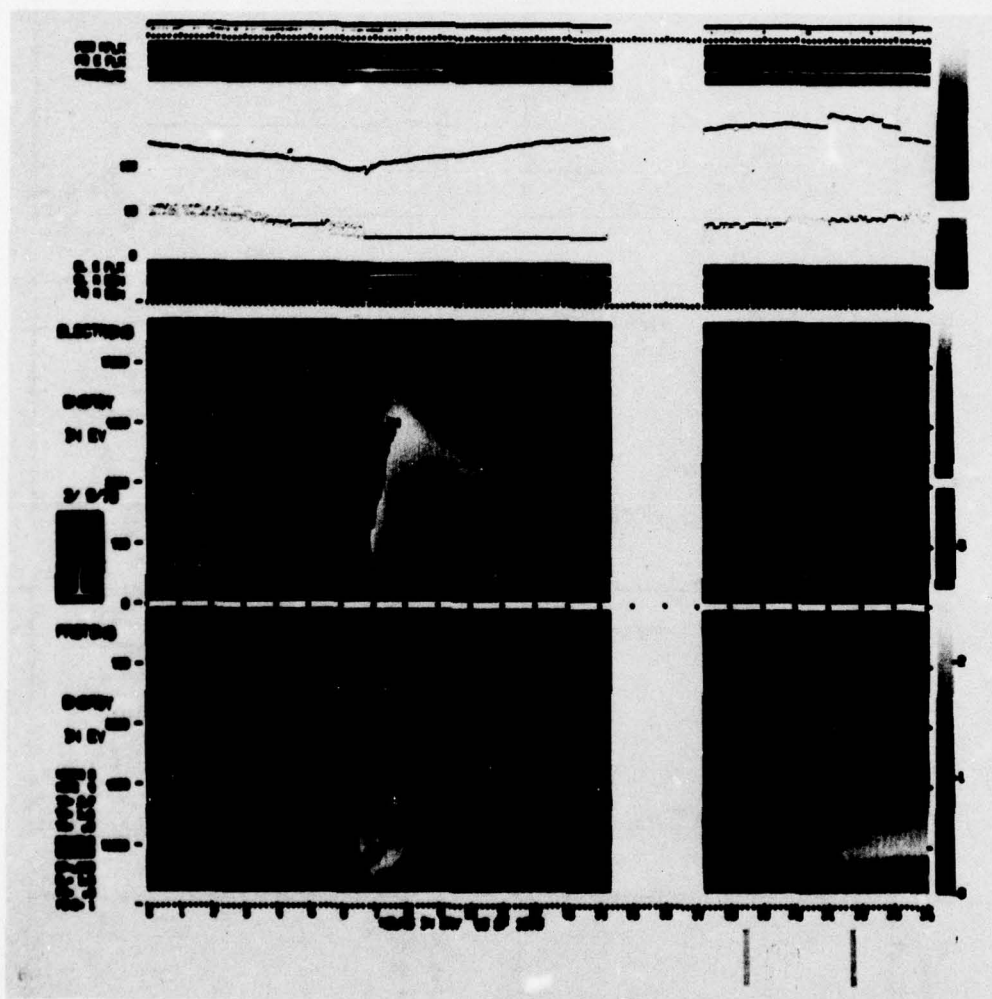
ATS-5
70/040

IONS



ELECTRONS

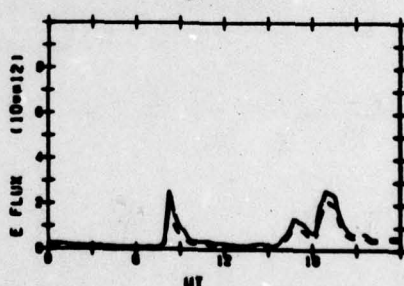
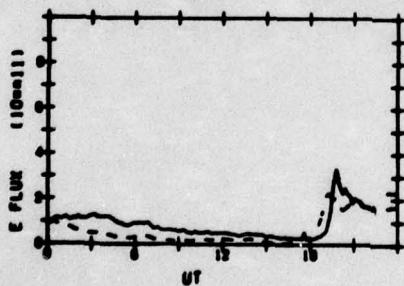
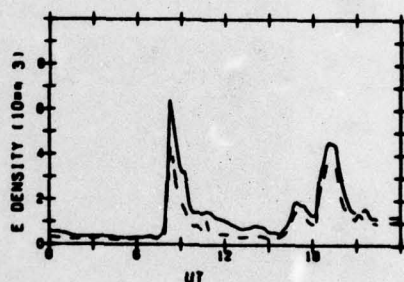
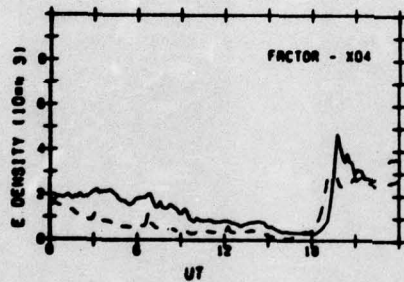
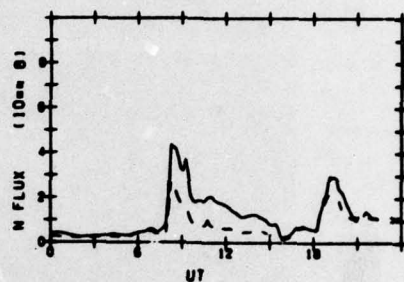
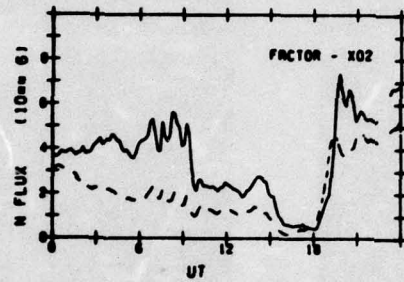
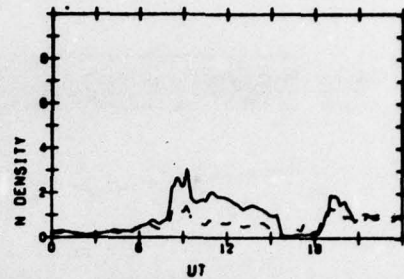
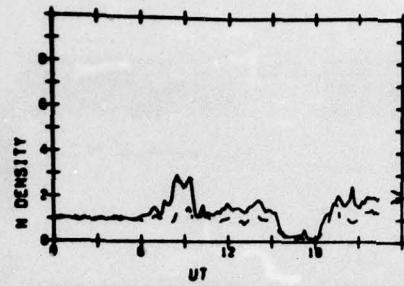


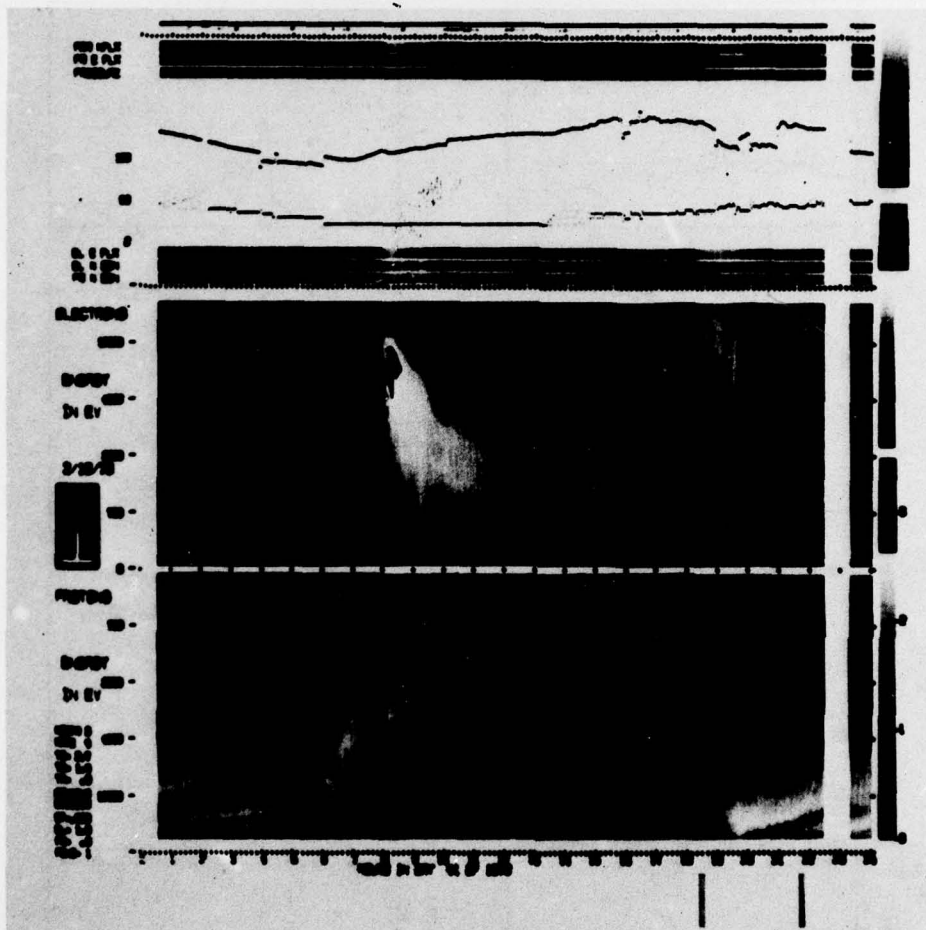


ATS-5
70/041

IONS

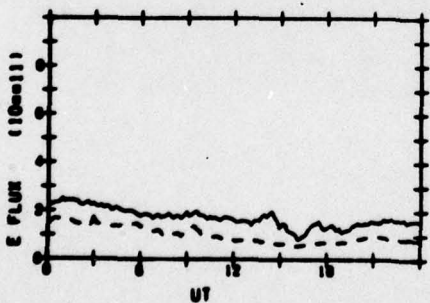
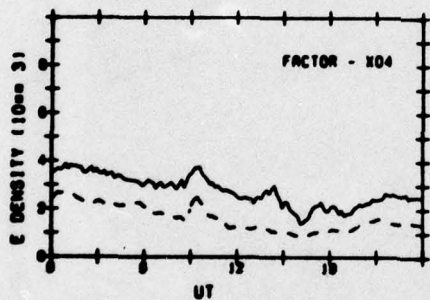
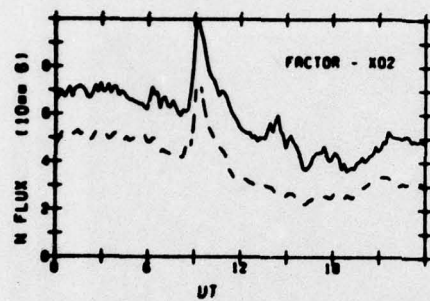
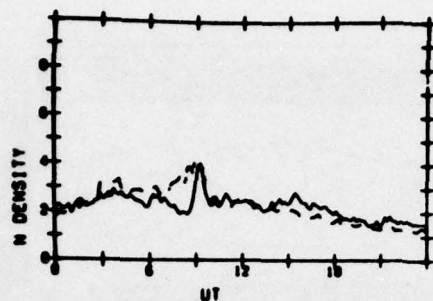
ELECTRONS



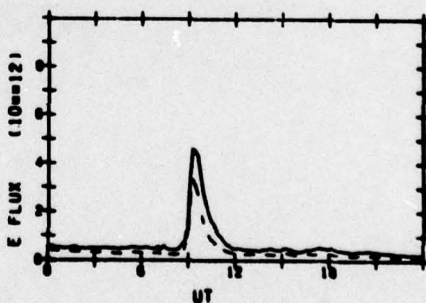
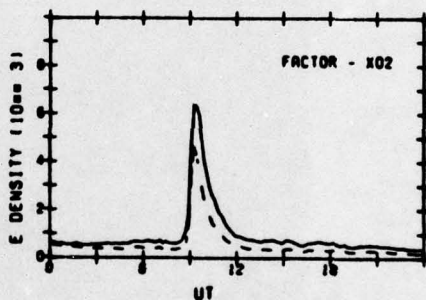
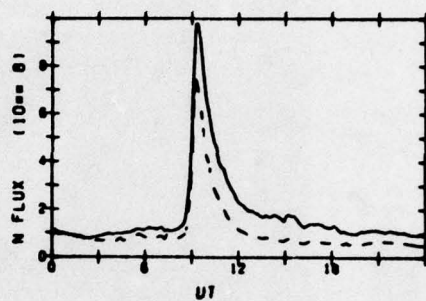
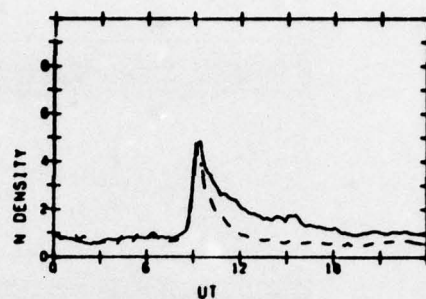


RTS-5
70/042

IONS



ELECTRONS



FOR NUT
PRE E PLT
PREBLUE

E. E PLT
E. N ON
PRE N ON

ELECTRONS

ENERGY
IN EV

2/11/70

PROTONS

ENERGY
IN EV

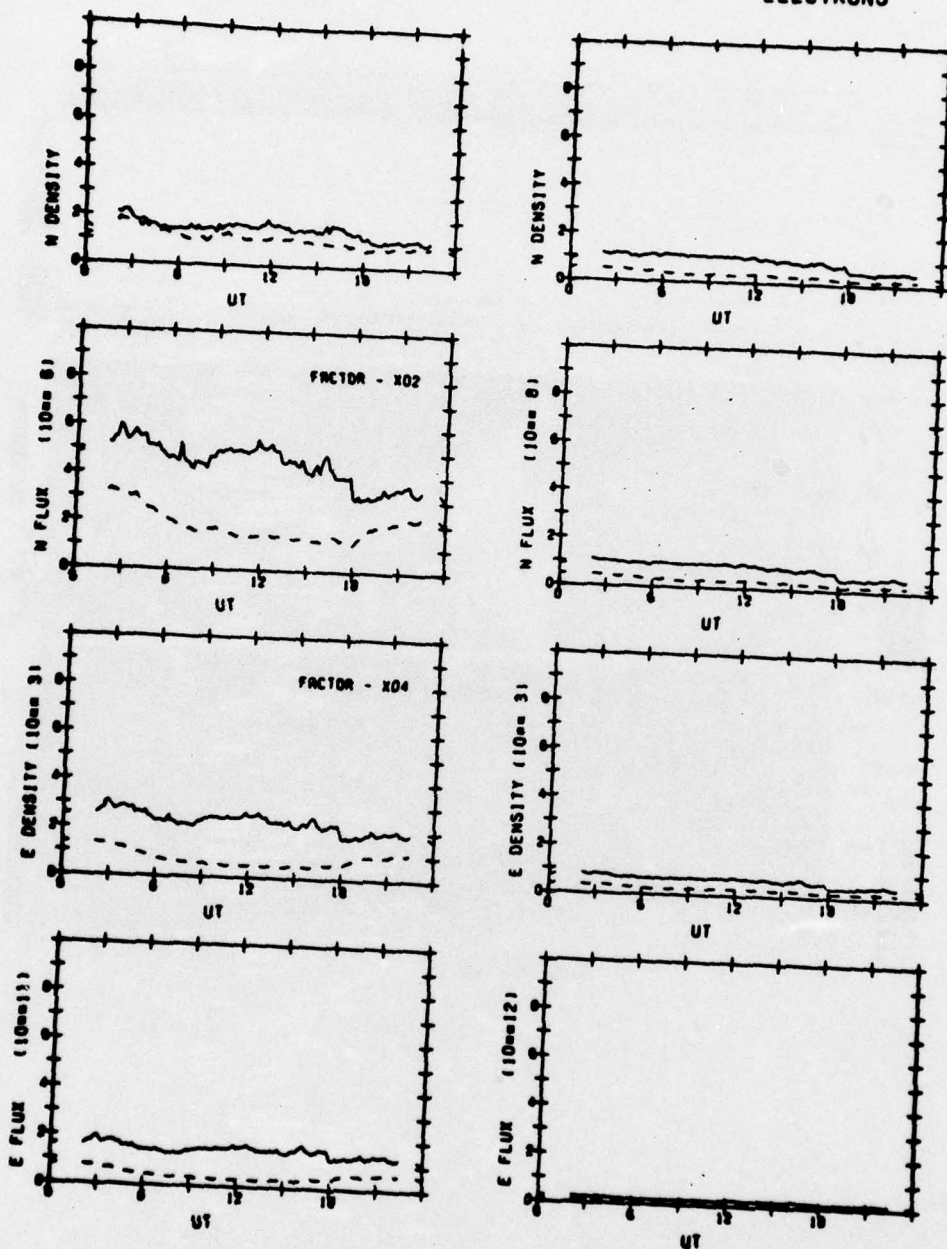
1000
800
600
400
200
0

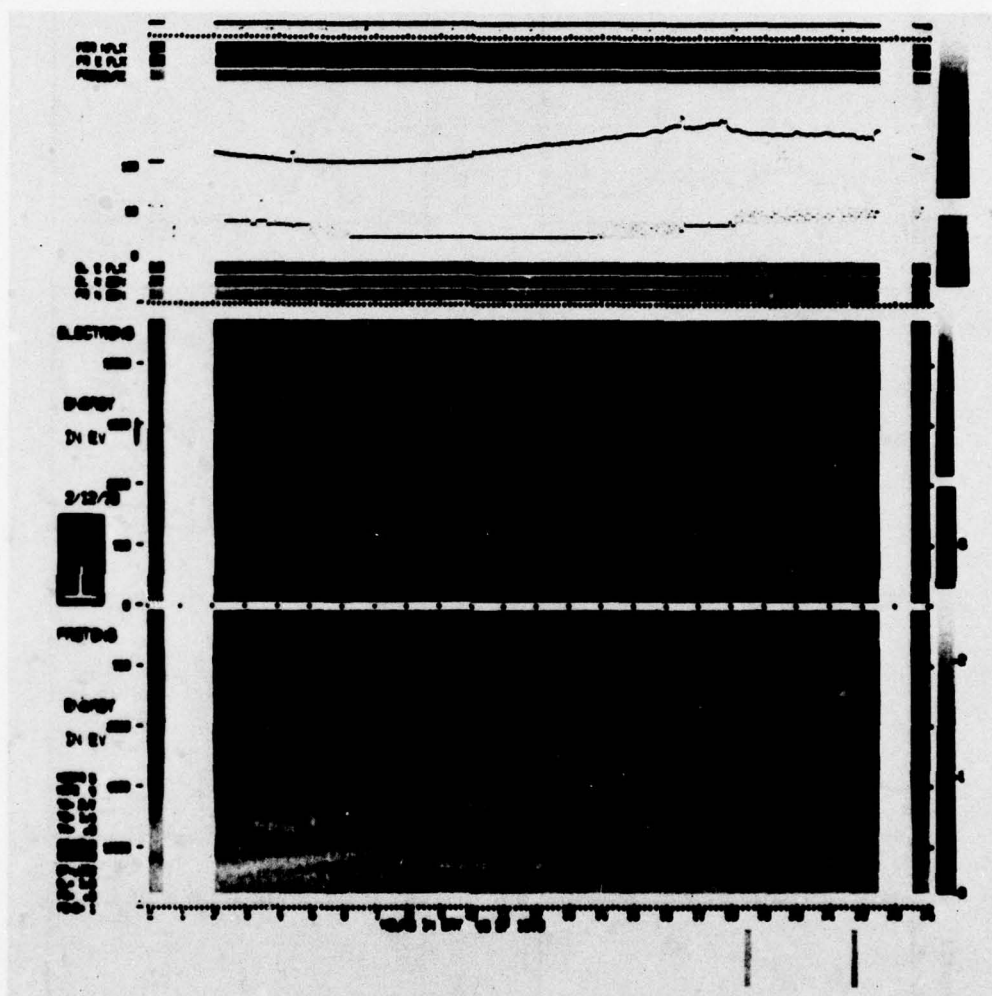
IN DW 1570

ATS-5
70/043

IONS

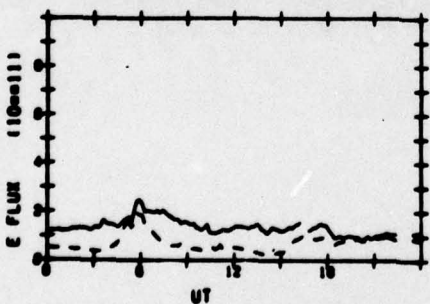
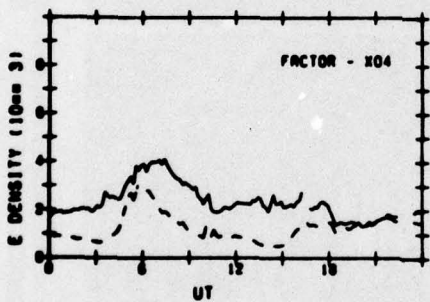
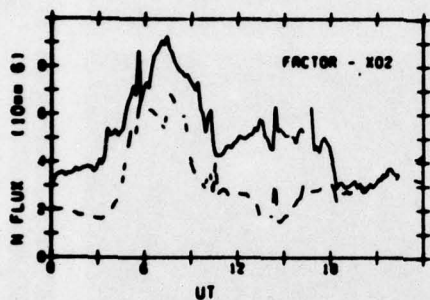
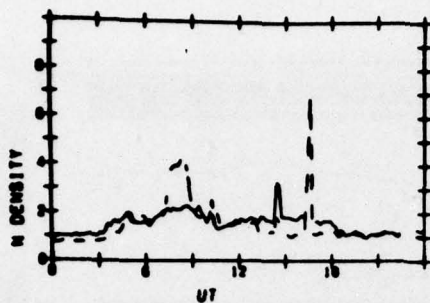
ELECTRONS



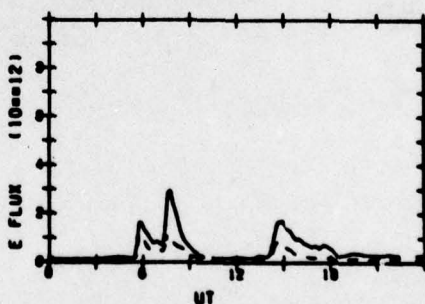
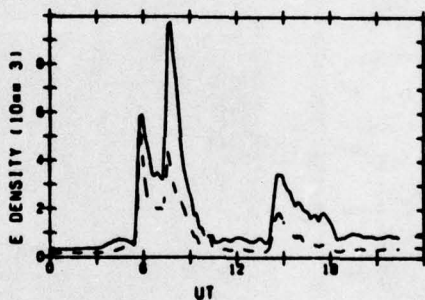
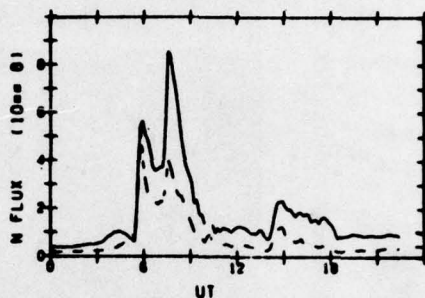
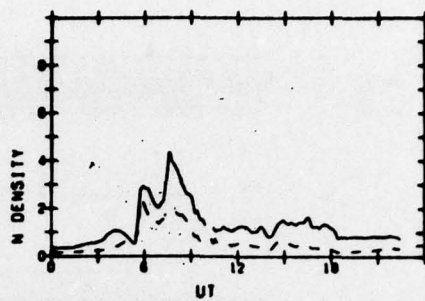


ATS-5
70/044

IONS



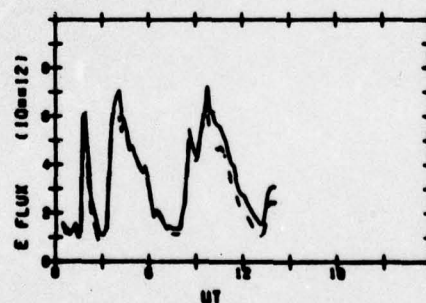
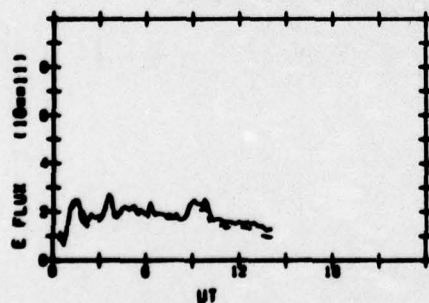
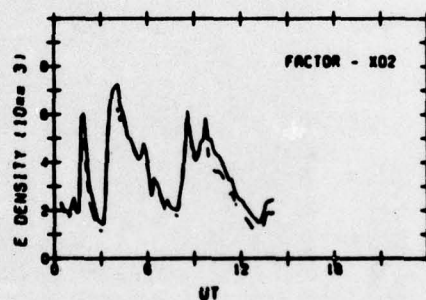
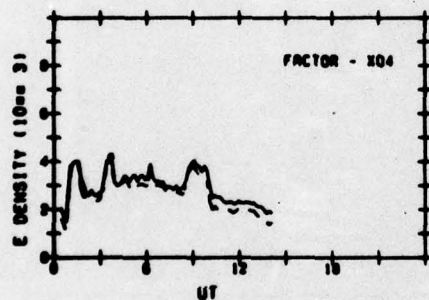
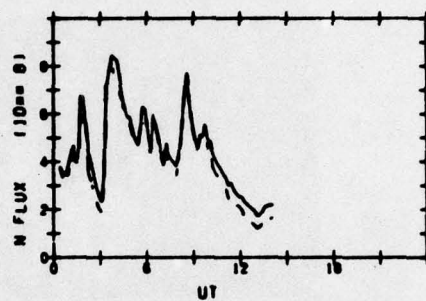
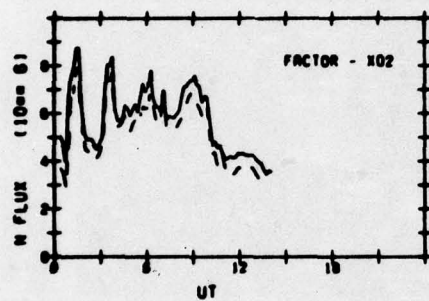
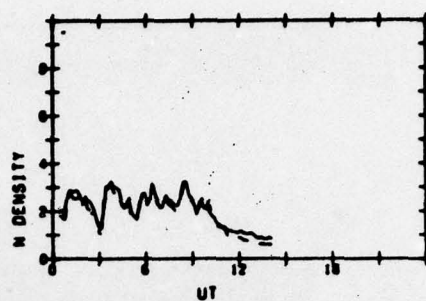
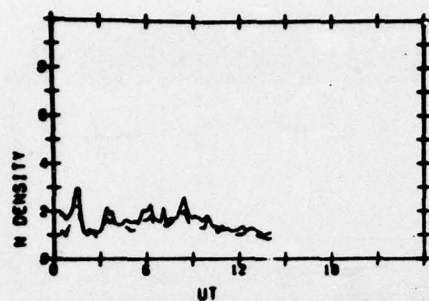
ELECTRONS

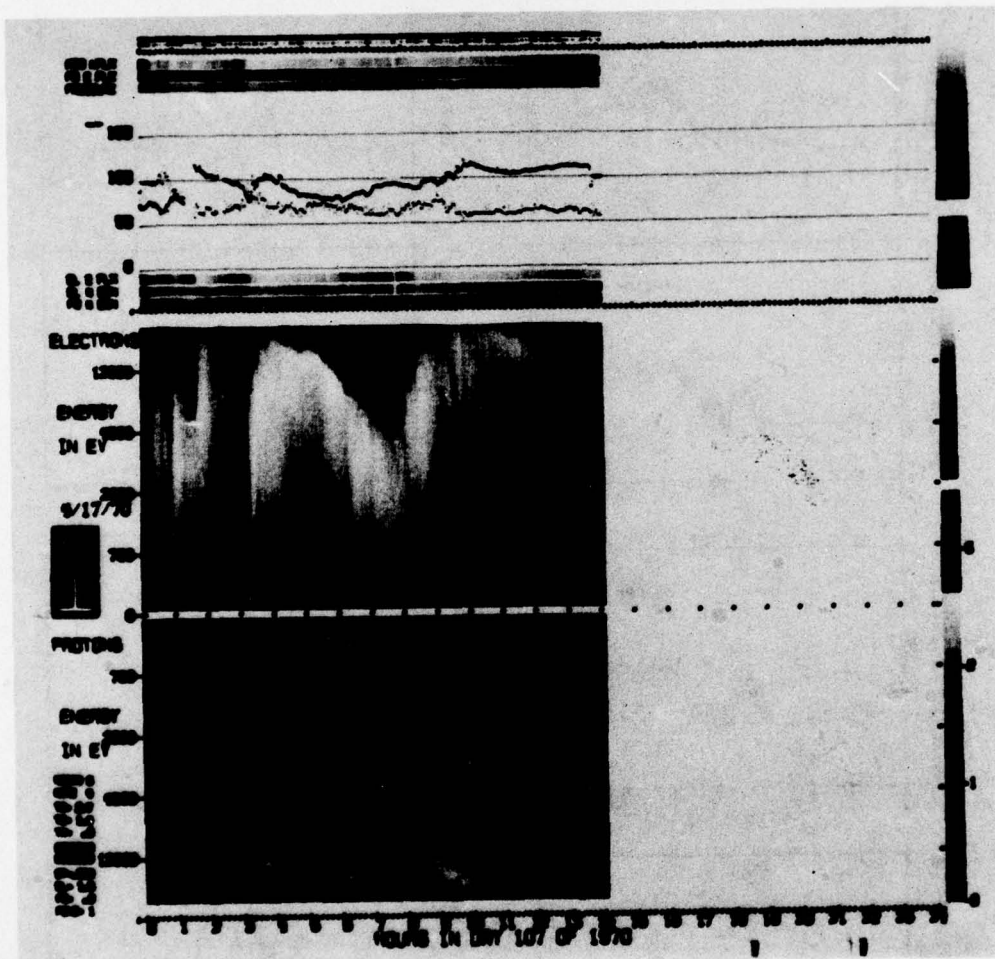


ATS-5
70/107

IONS

ELECTRONS

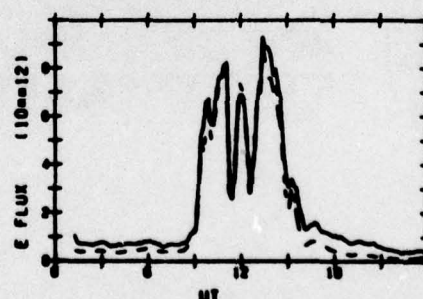
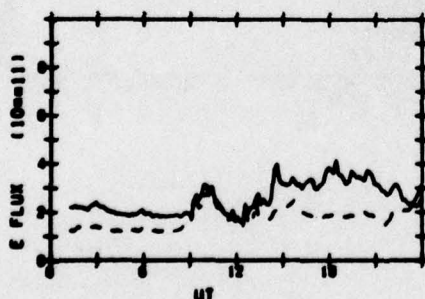
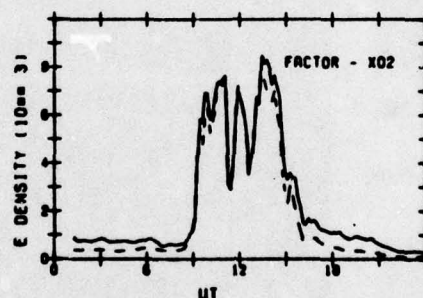
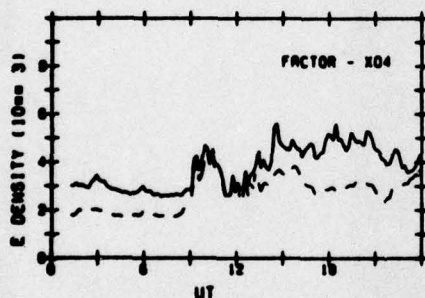
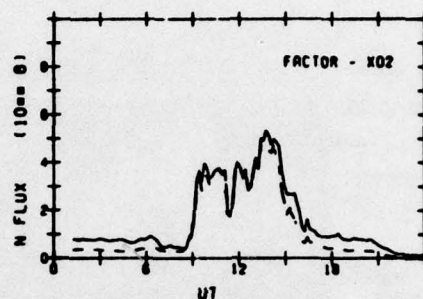
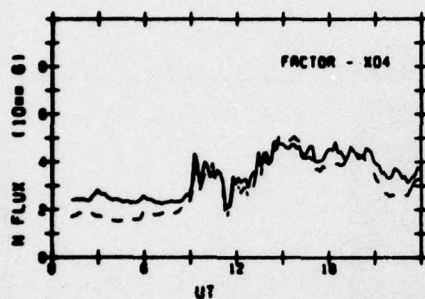
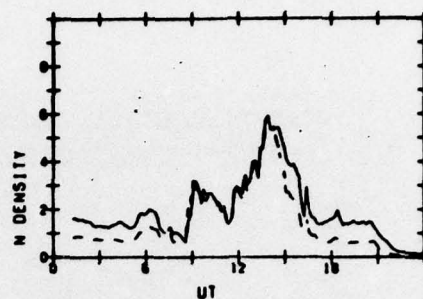
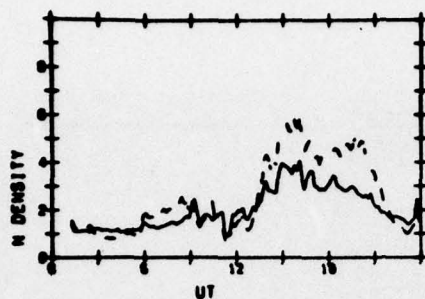


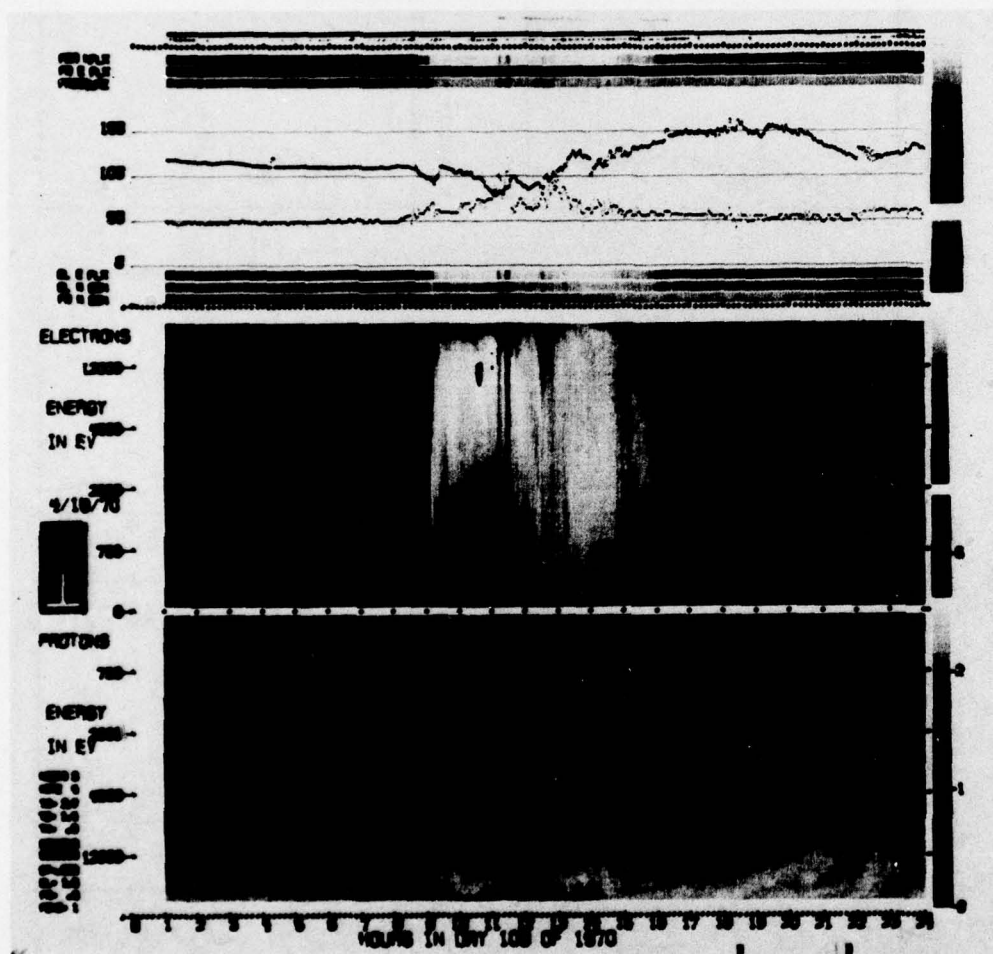


ATS-5
70/108

IONS

ELECTRONS

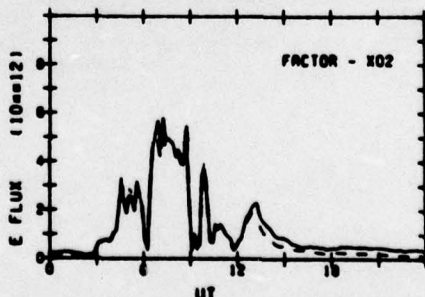
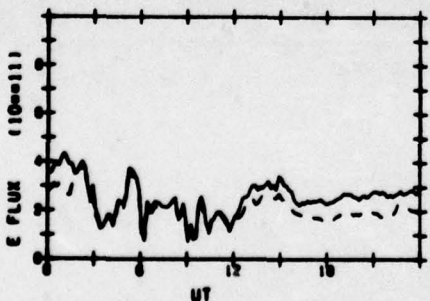
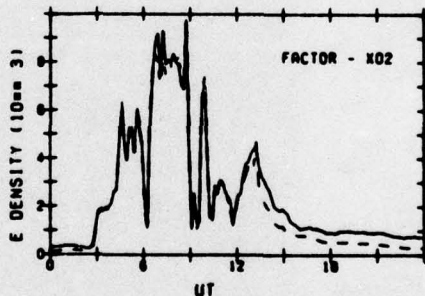
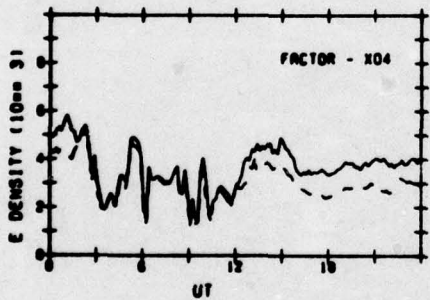
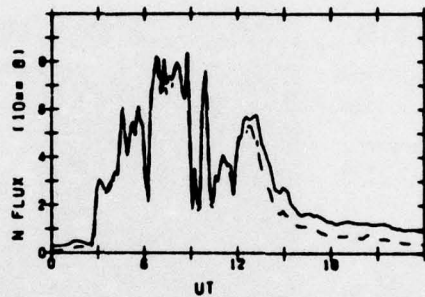
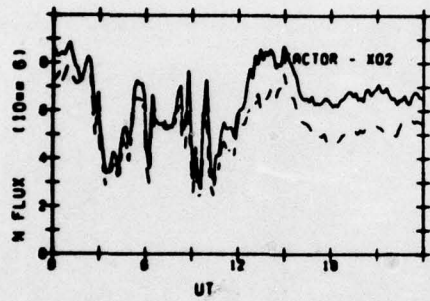
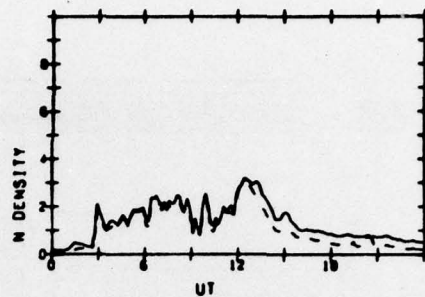
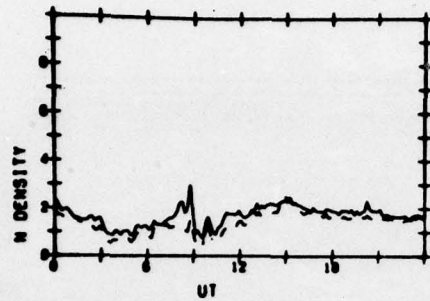


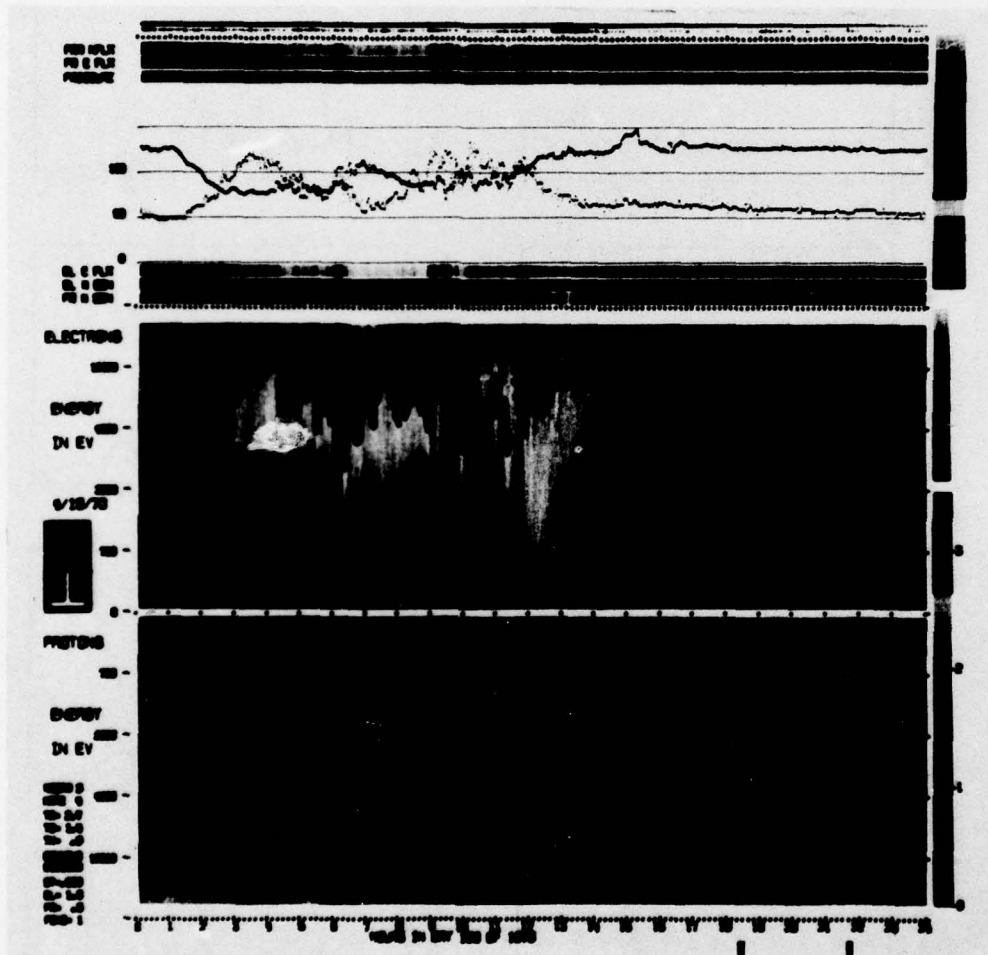


RTS-5
70/109

IONS

ELECTRONS

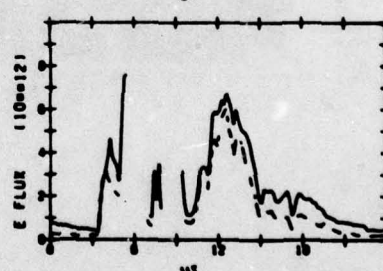
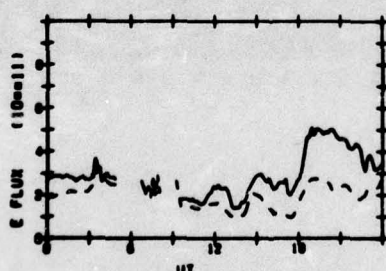
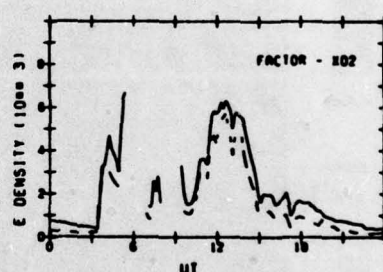
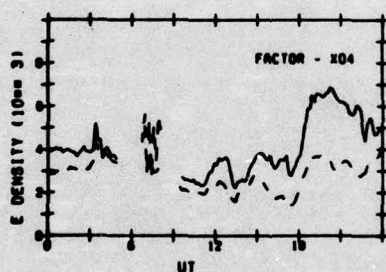
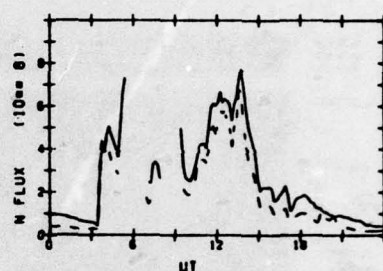
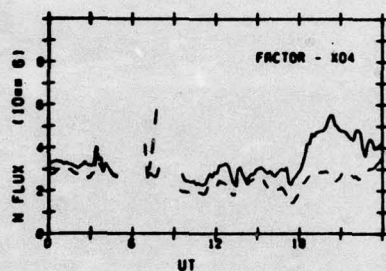
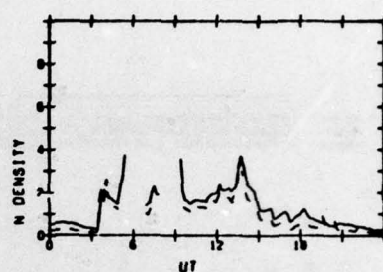
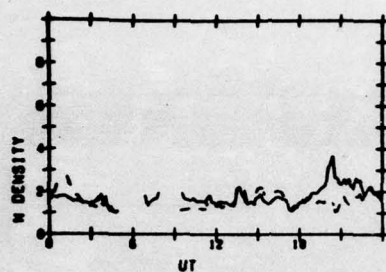


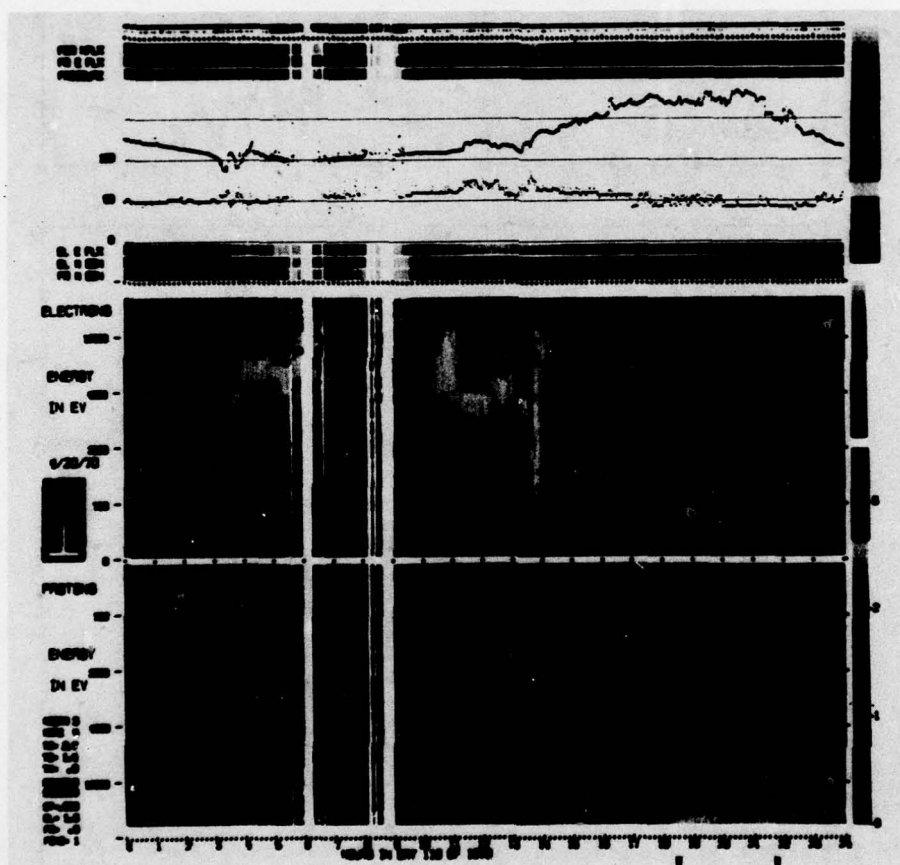


ATS-5
70/110

IONS

ELECTRONS

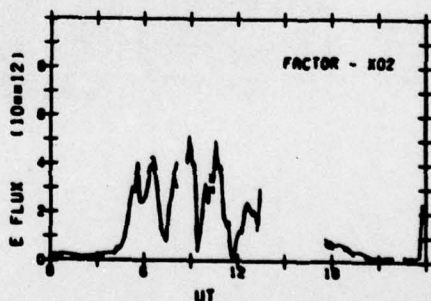
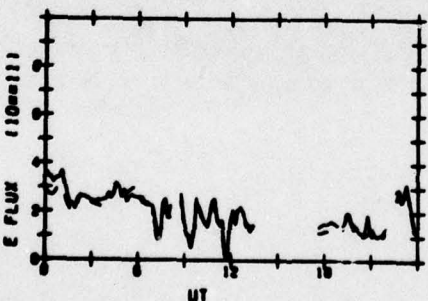
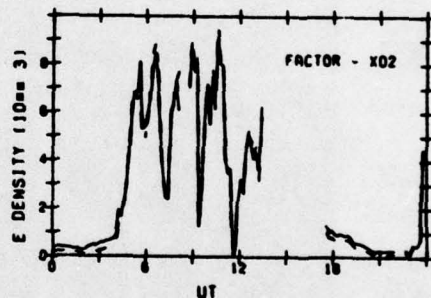
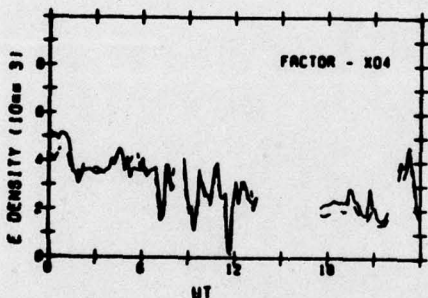
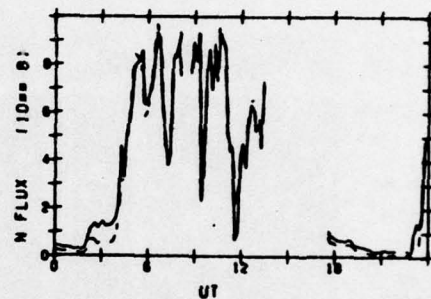
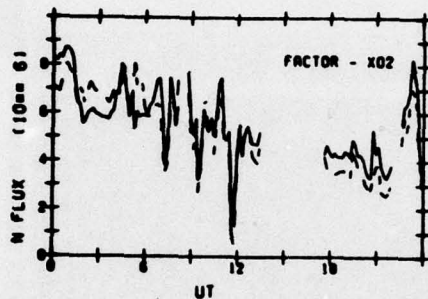
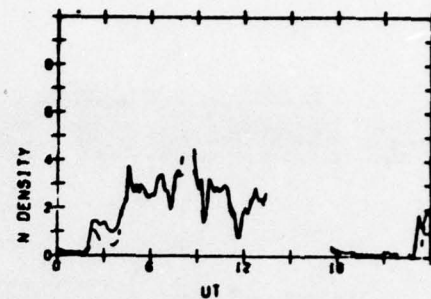
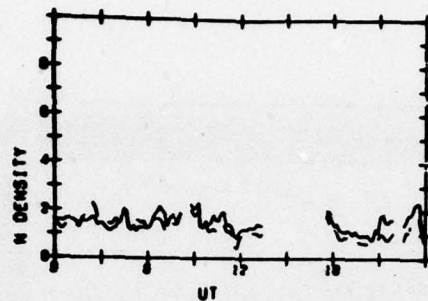


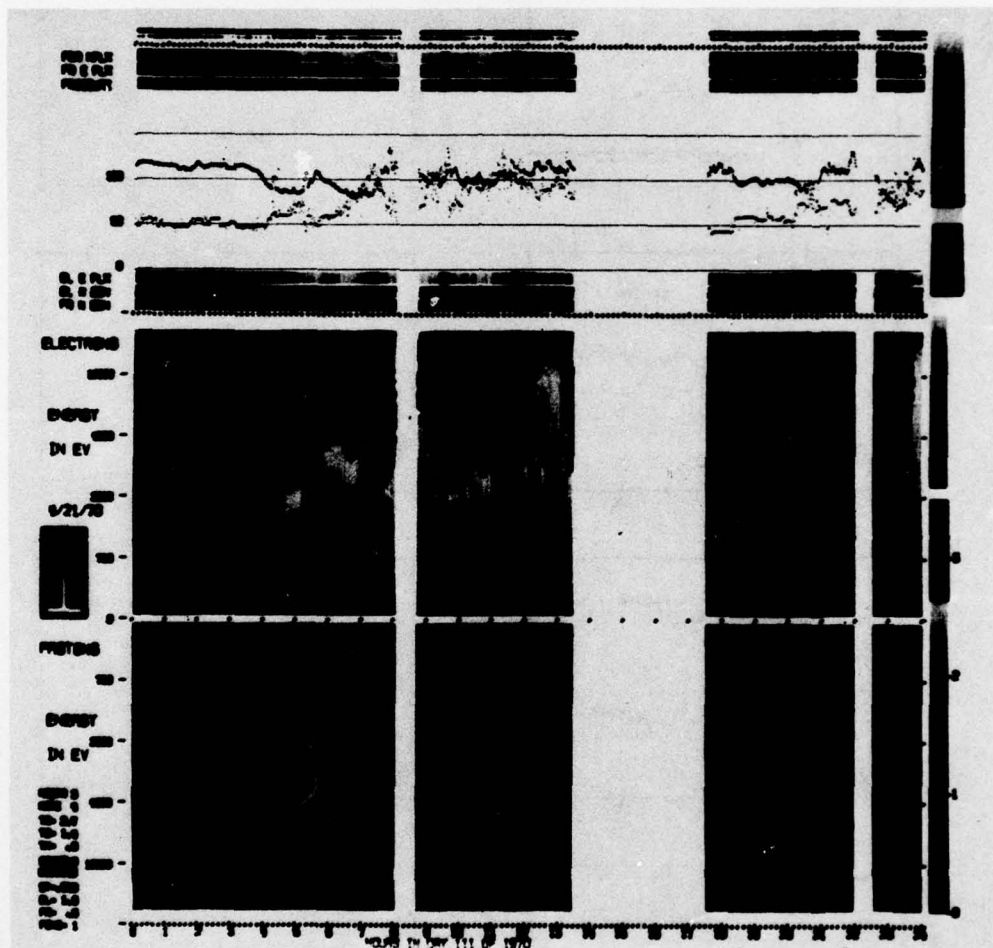


ATS-5
70/111

IONS

ELECTRONS

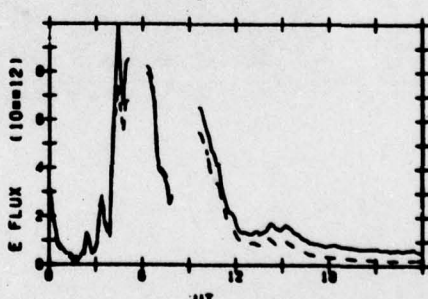
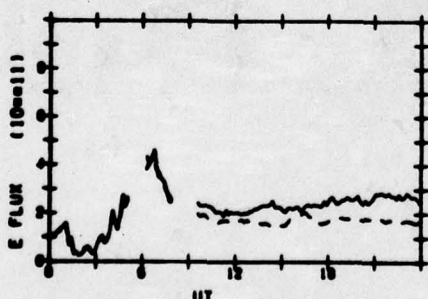
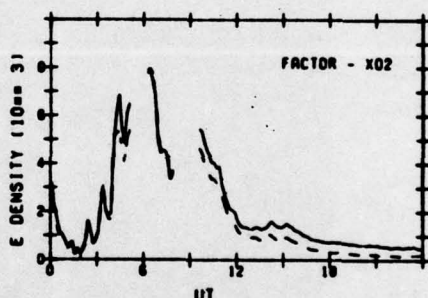
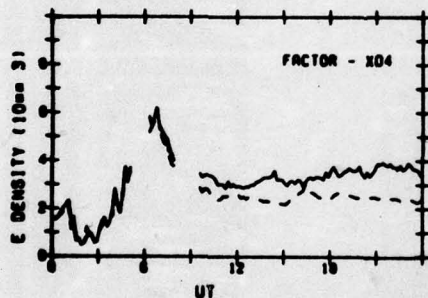
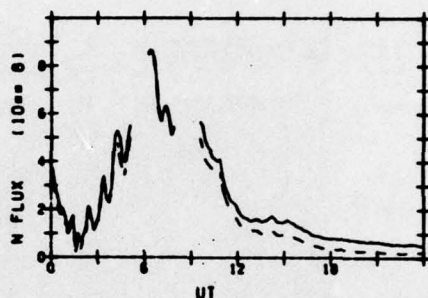
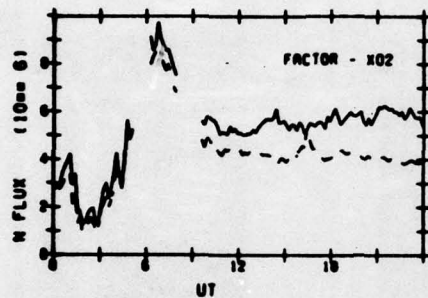
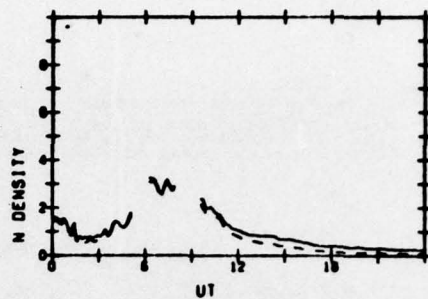
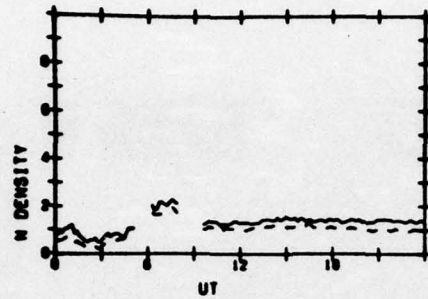




ATS-6
70/112

IONS

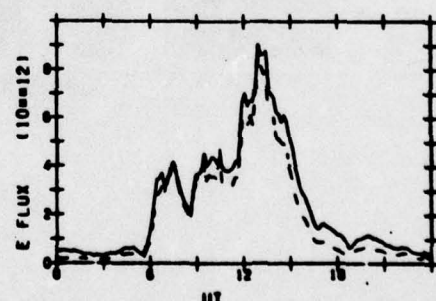
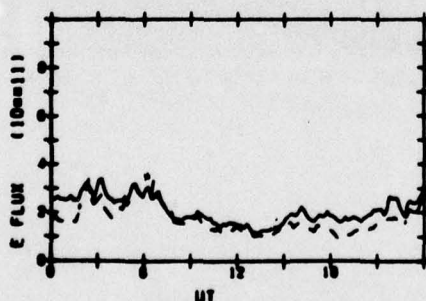
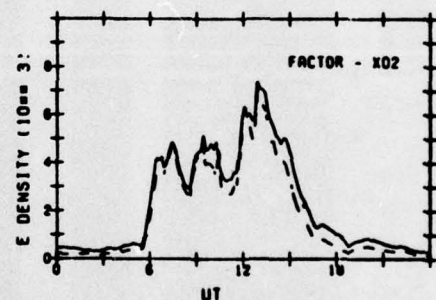
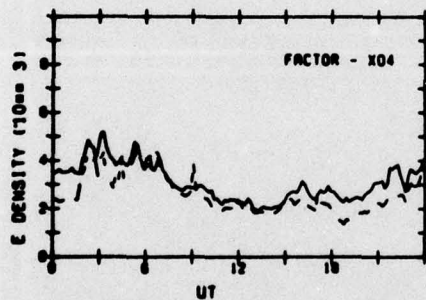
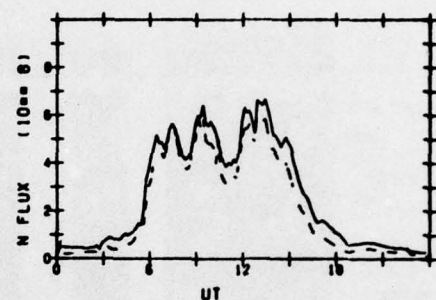
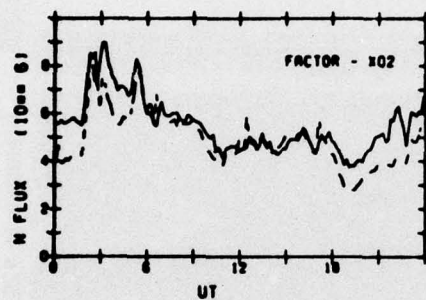
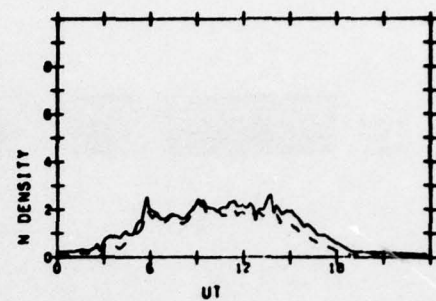
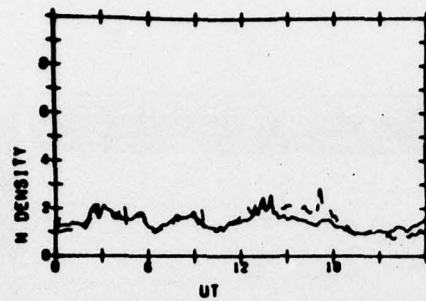
ELECTRONS

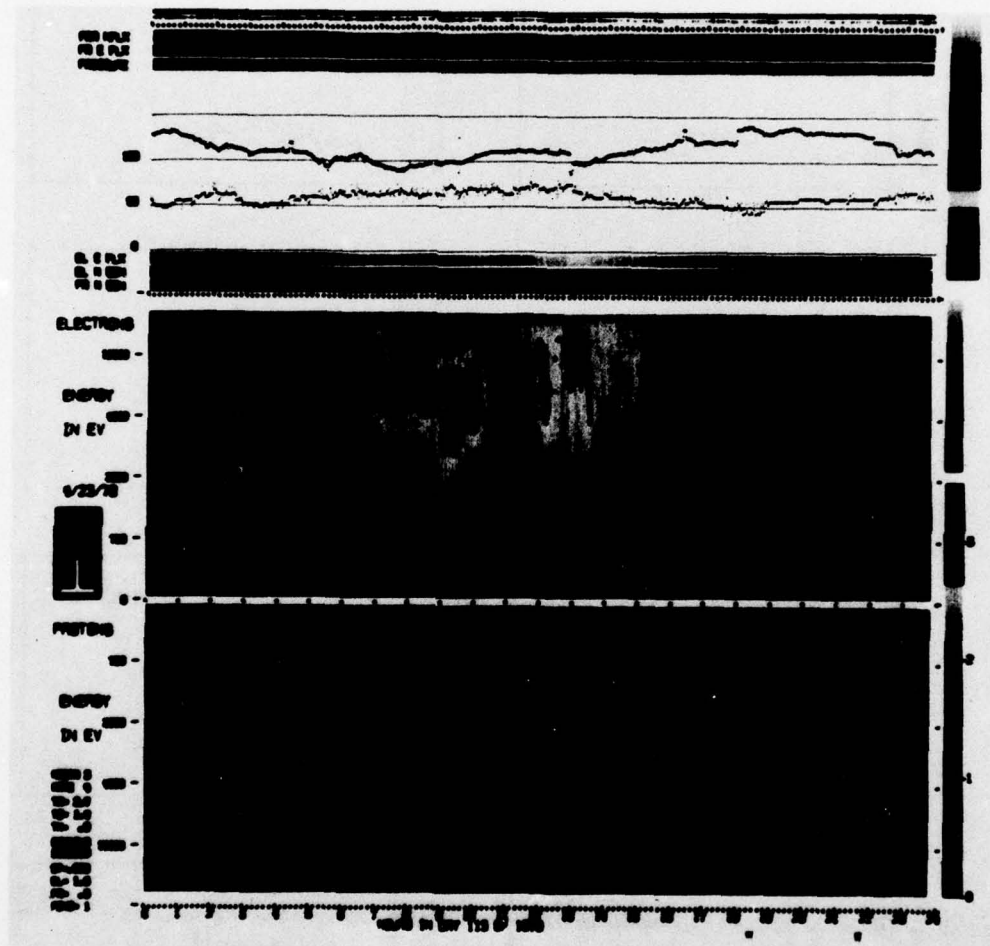


ATS-6
70/113

IONS

ELECTRONS

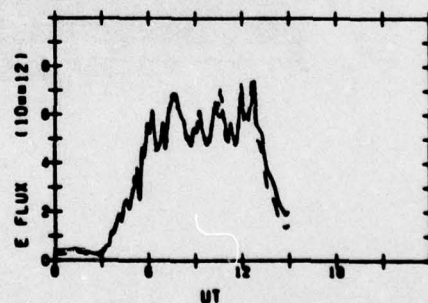
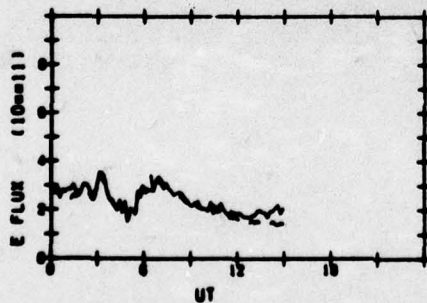
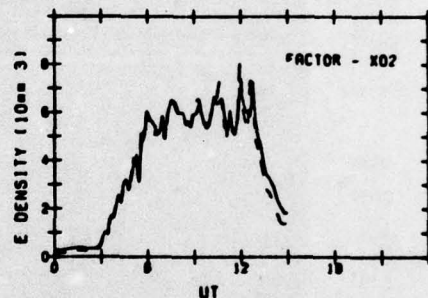
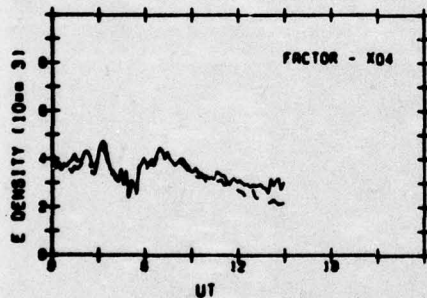
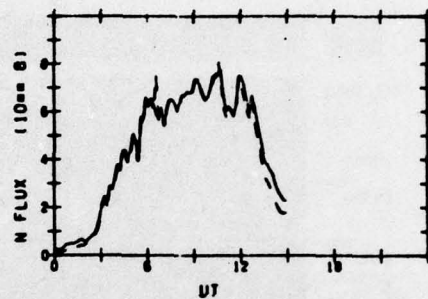
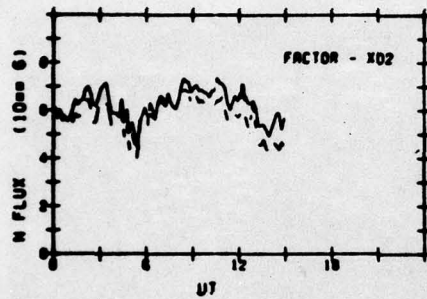
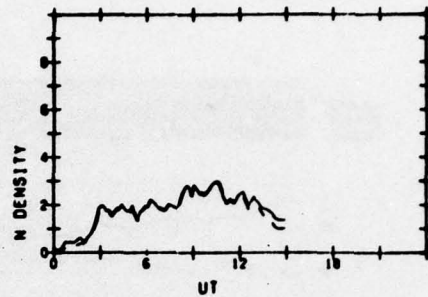
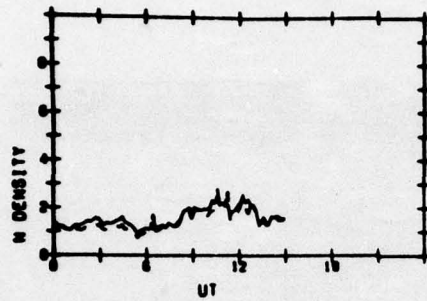


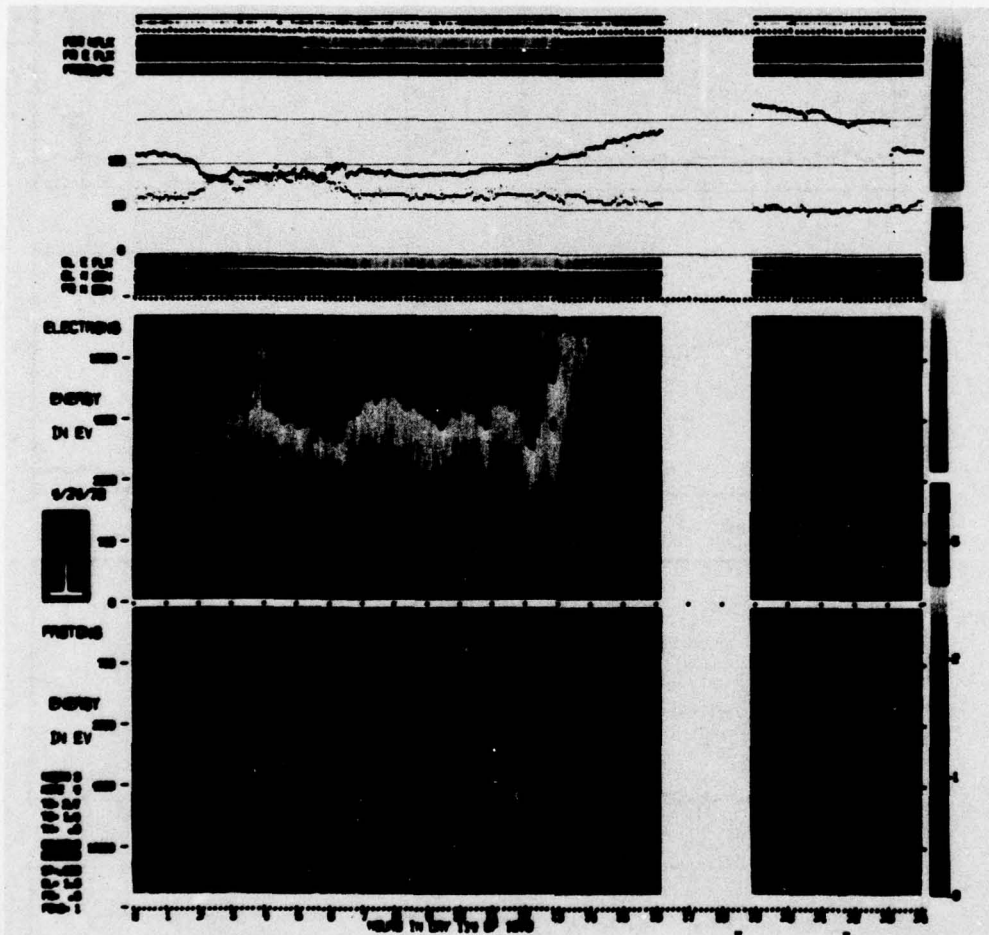


ATS-5
70/114

IONS

ELECTRONS

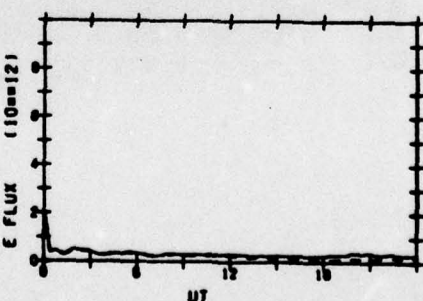
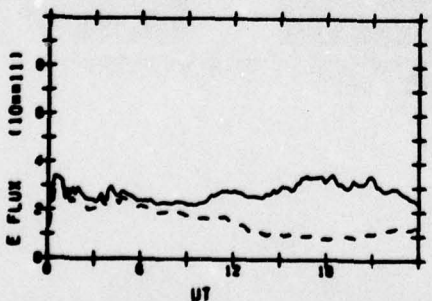
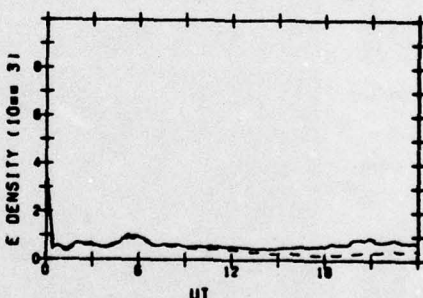
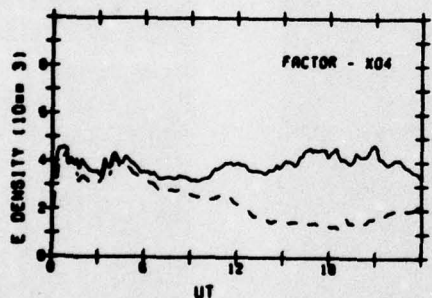
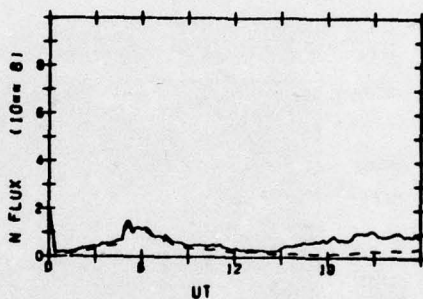
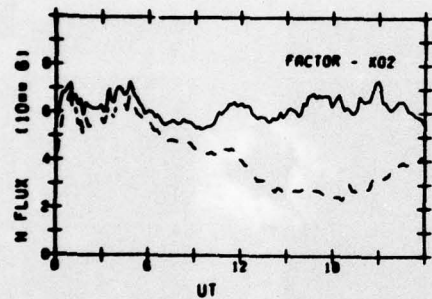
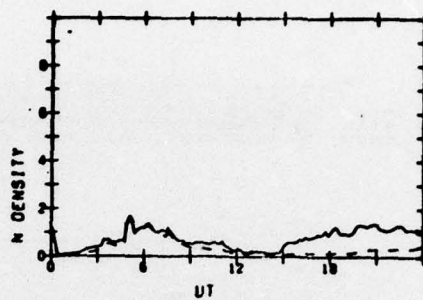
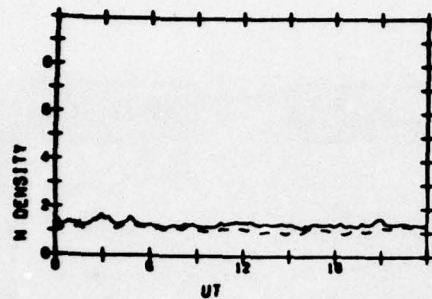


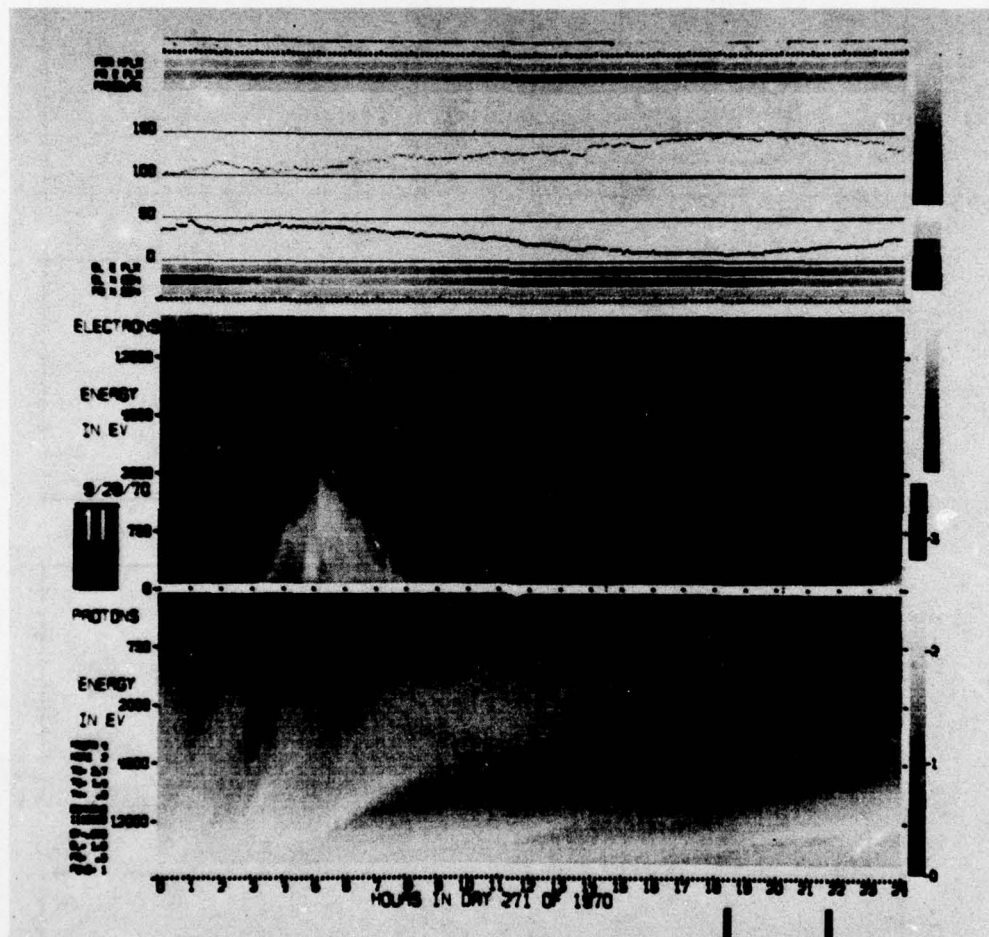


ATS-5
70/271

IONS

ELECTRONS

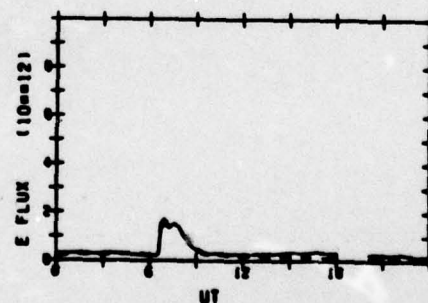
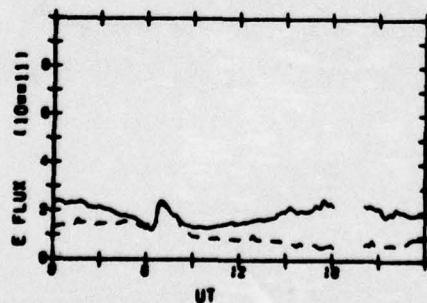
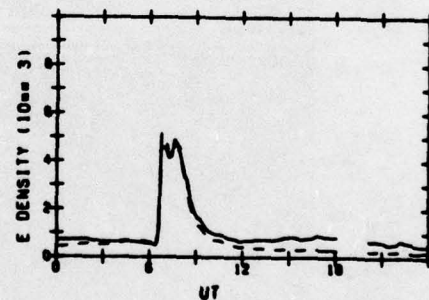
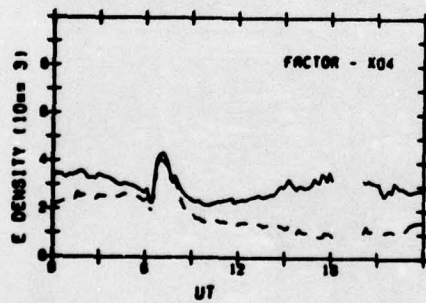
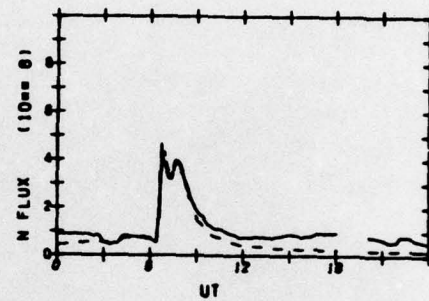
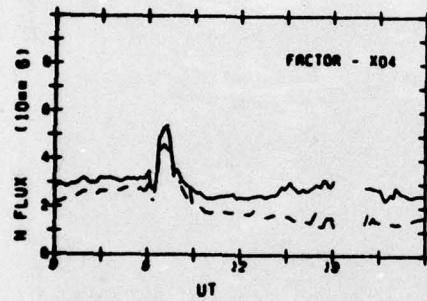
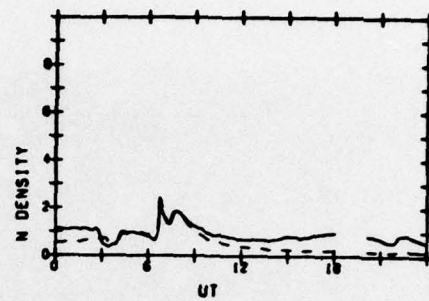
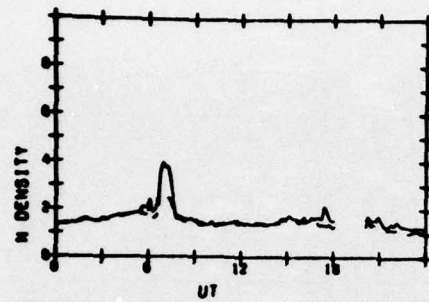


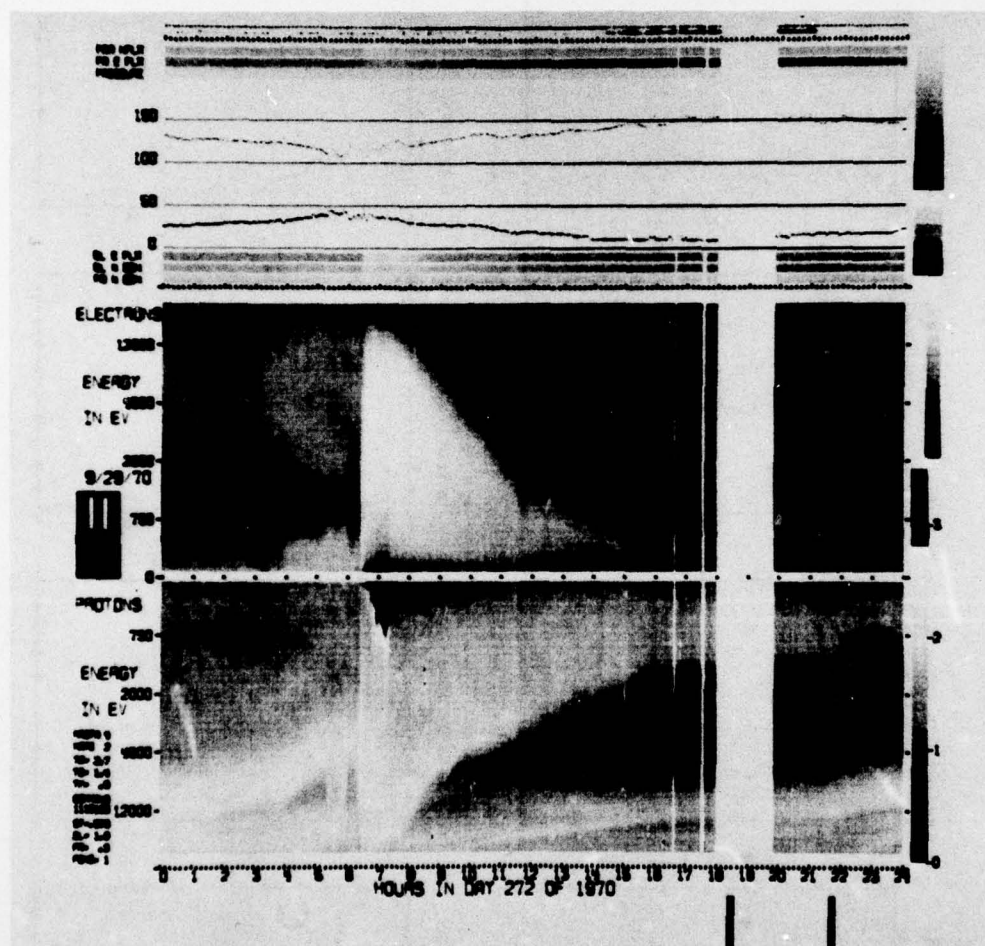


ATS-5
70/272

IONS

ELECTRONS





AD-A067 843

AIR FORCE GEOPHYSICS LAB HANSCOM AFB MASS
MODELING OF THE GEOSYNCHRONOUS ORBIT PLASMA ENVIRONMENT. PART 3--ETC(U)
JAN 79 H B GARRETT, R E MCINERNEY

F/G 4/1

UNCLASSIFIED

AF6L-TR-79-0015

NL

2 OF 3

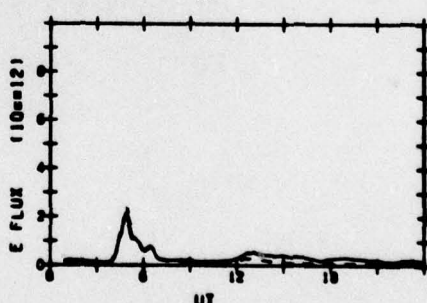
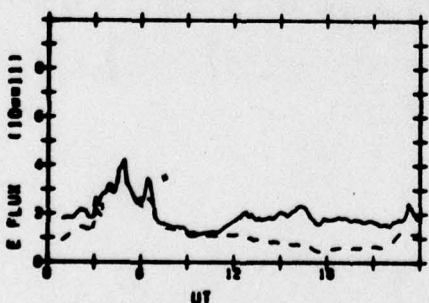
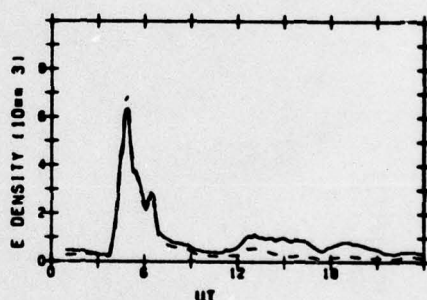
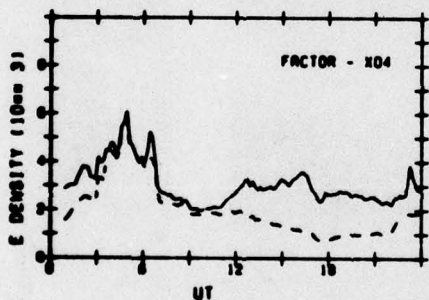
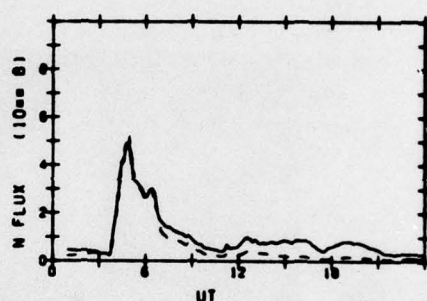
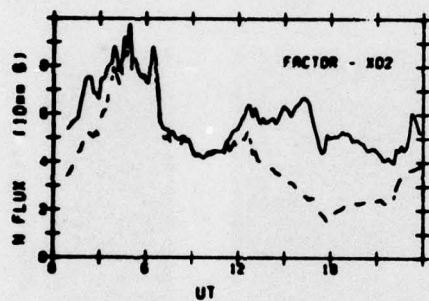
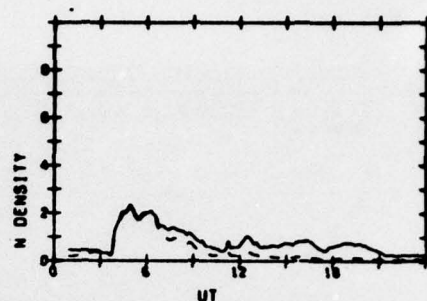
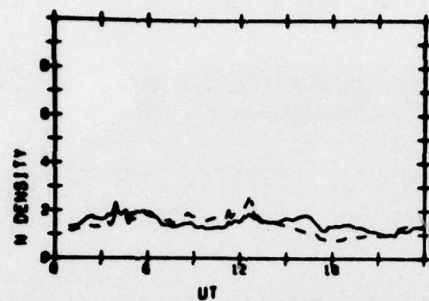
AD
A067843

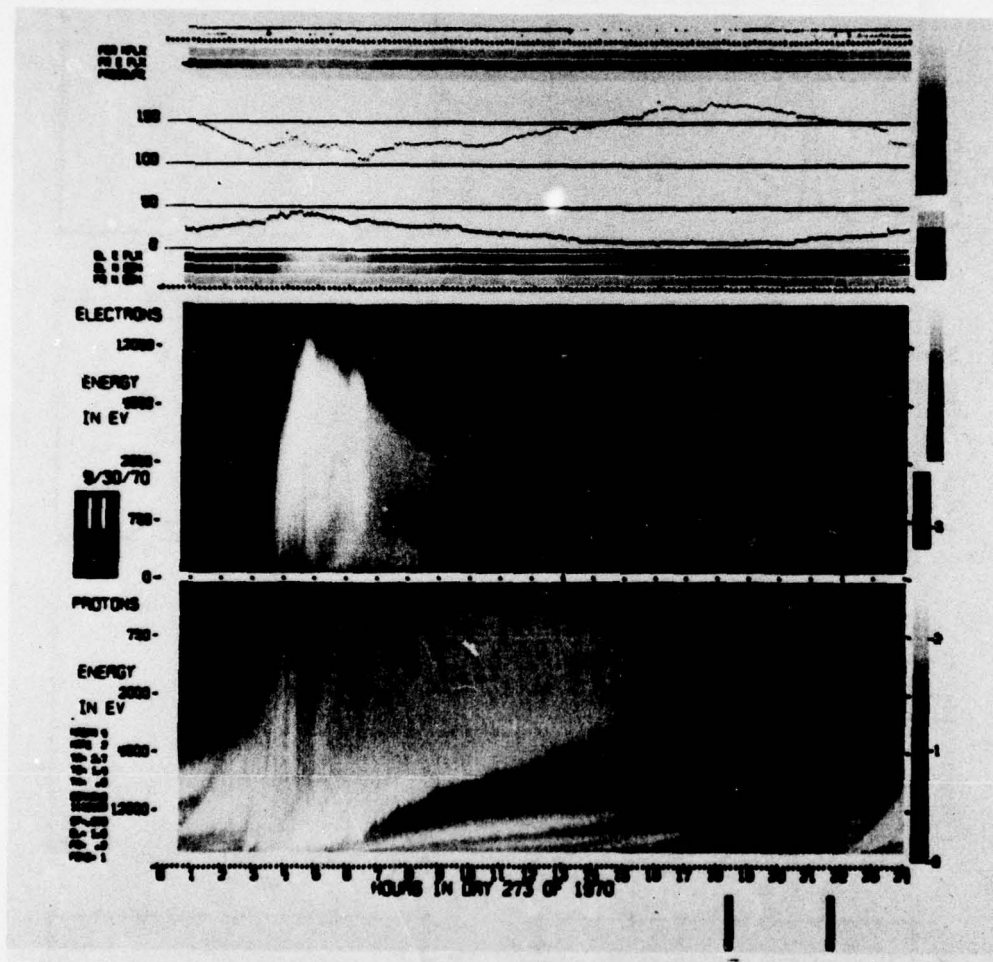


ATS-5
70/273

IONS

ELECTRONS

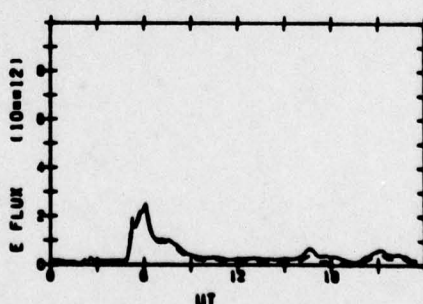
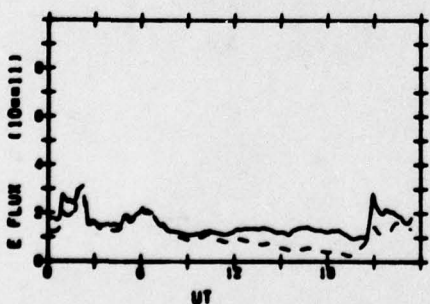
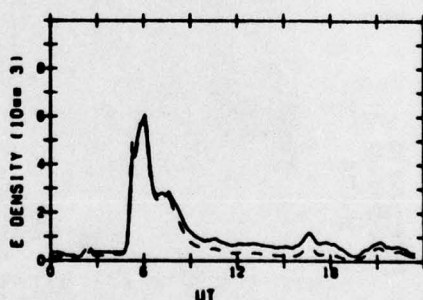
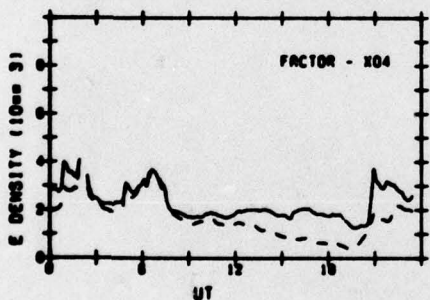
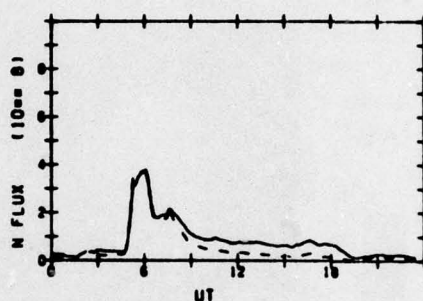
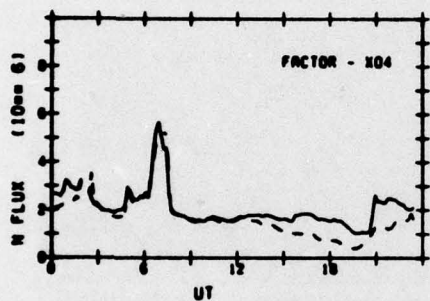
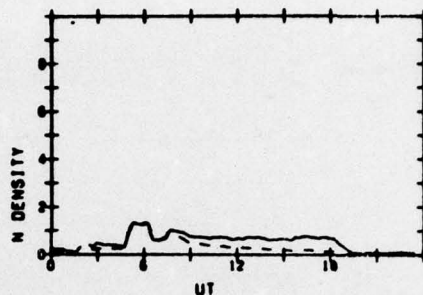
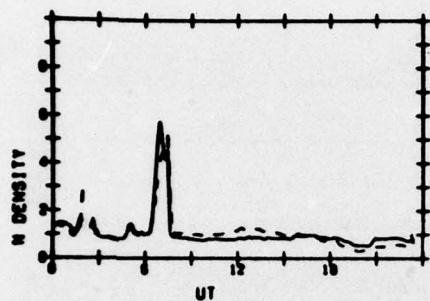


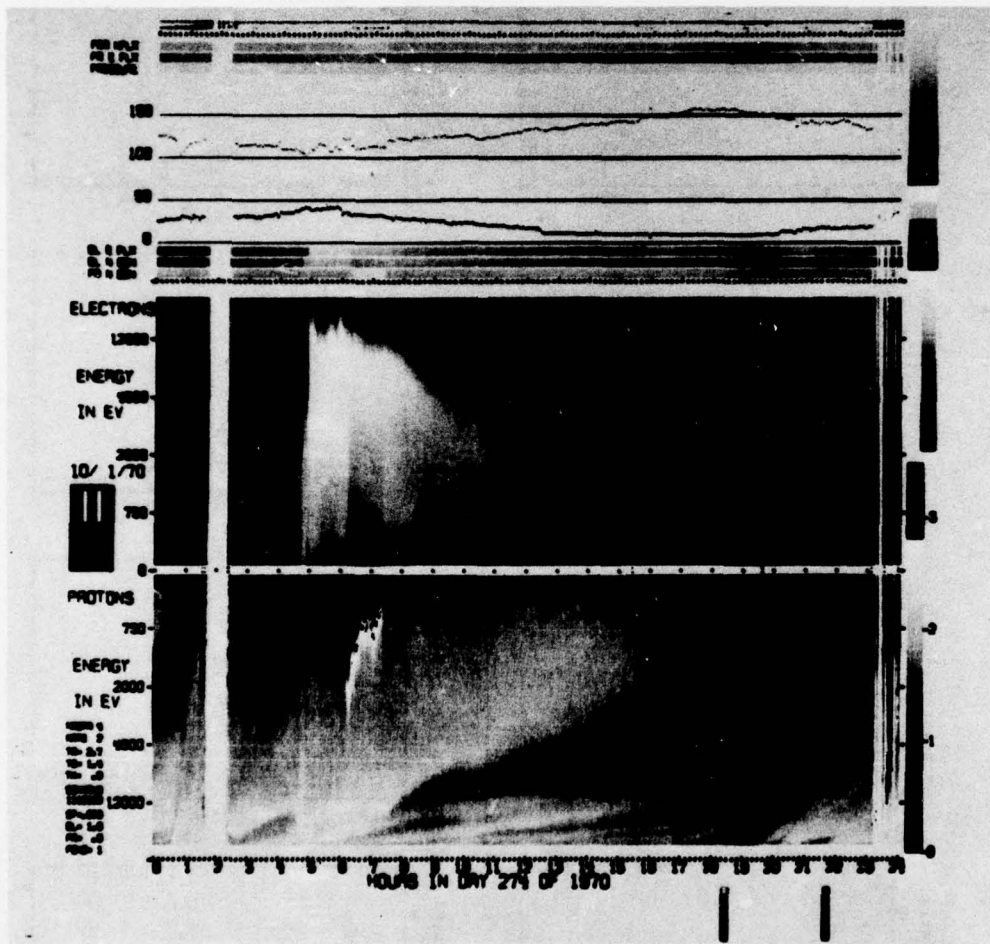


ATS-5
70/274

IONS

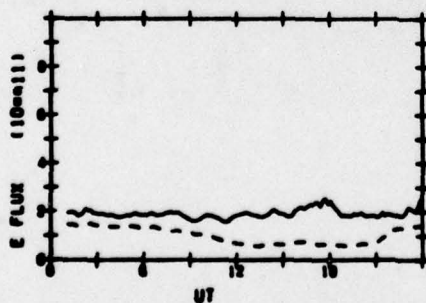
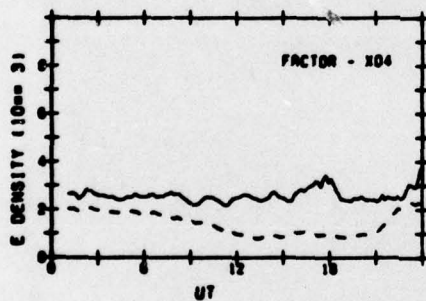
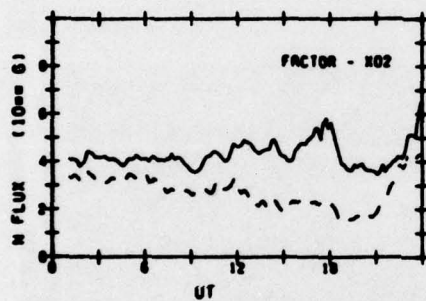
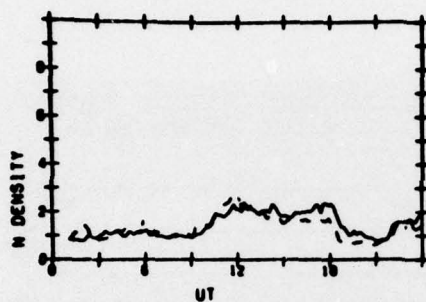
ELECTRONS



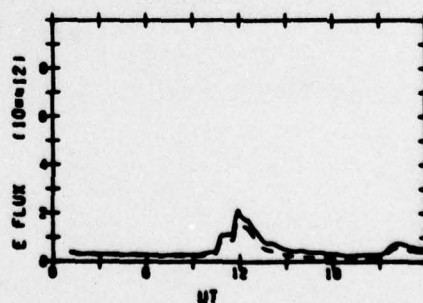
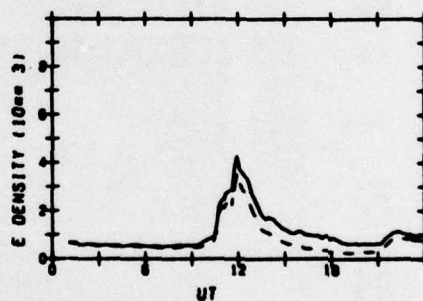
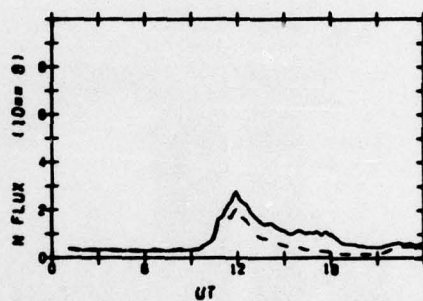
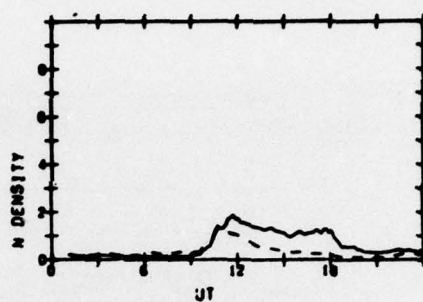


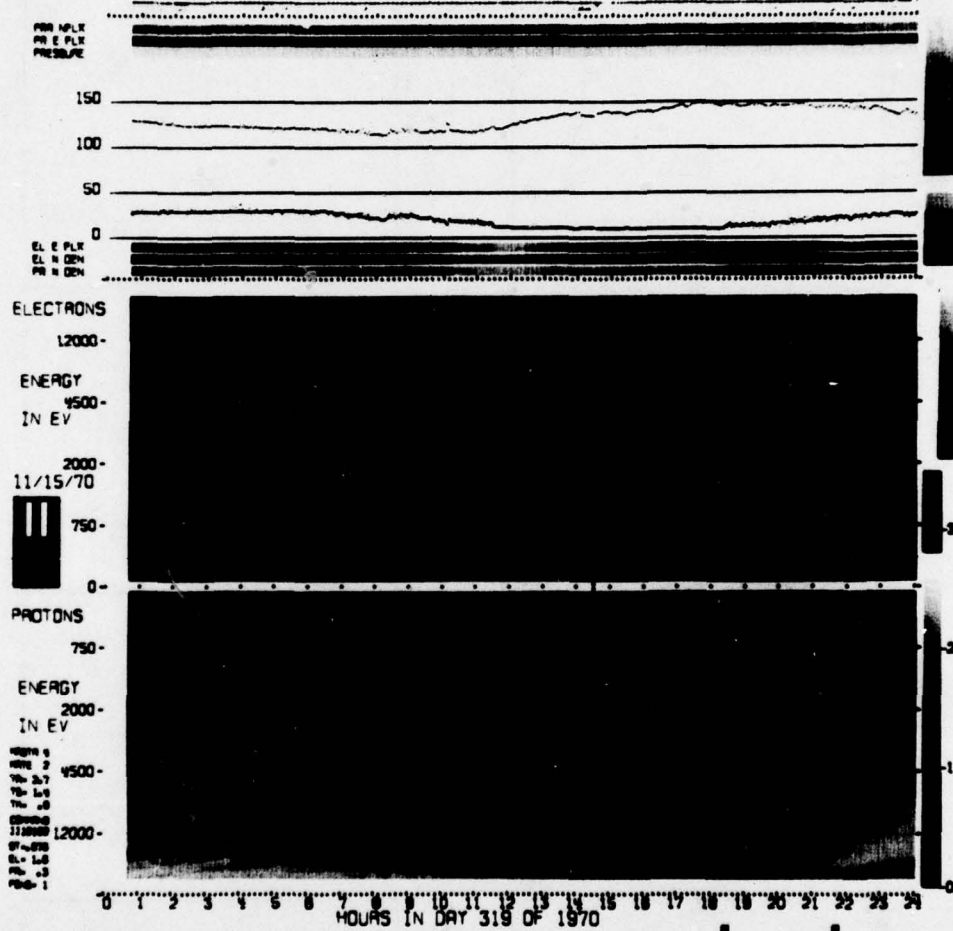
ATS-5
70/319

IONS



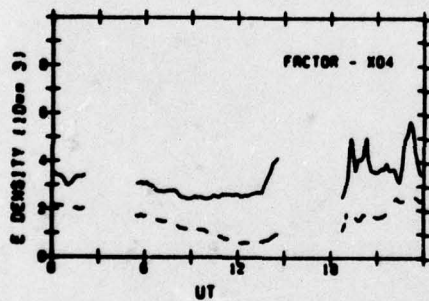
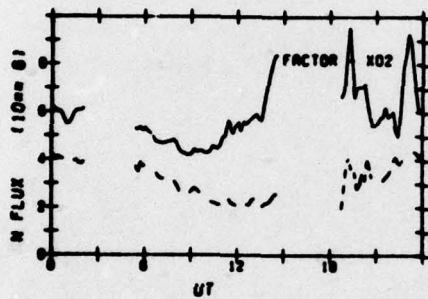
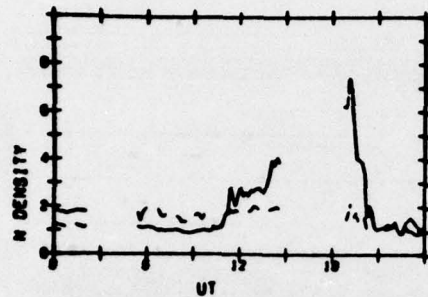
ELECTRONS



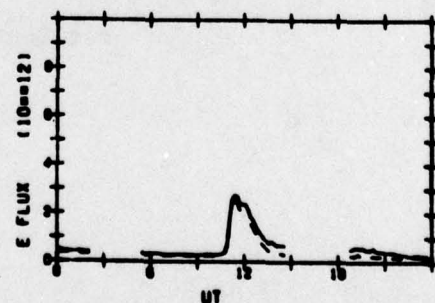
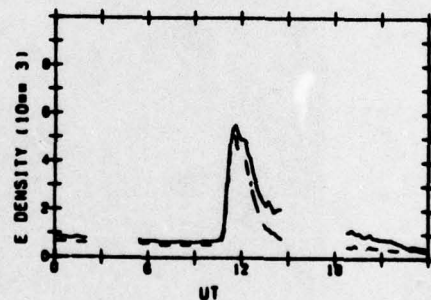
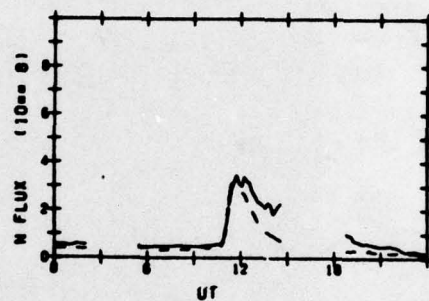
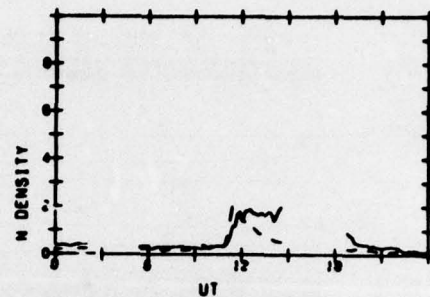


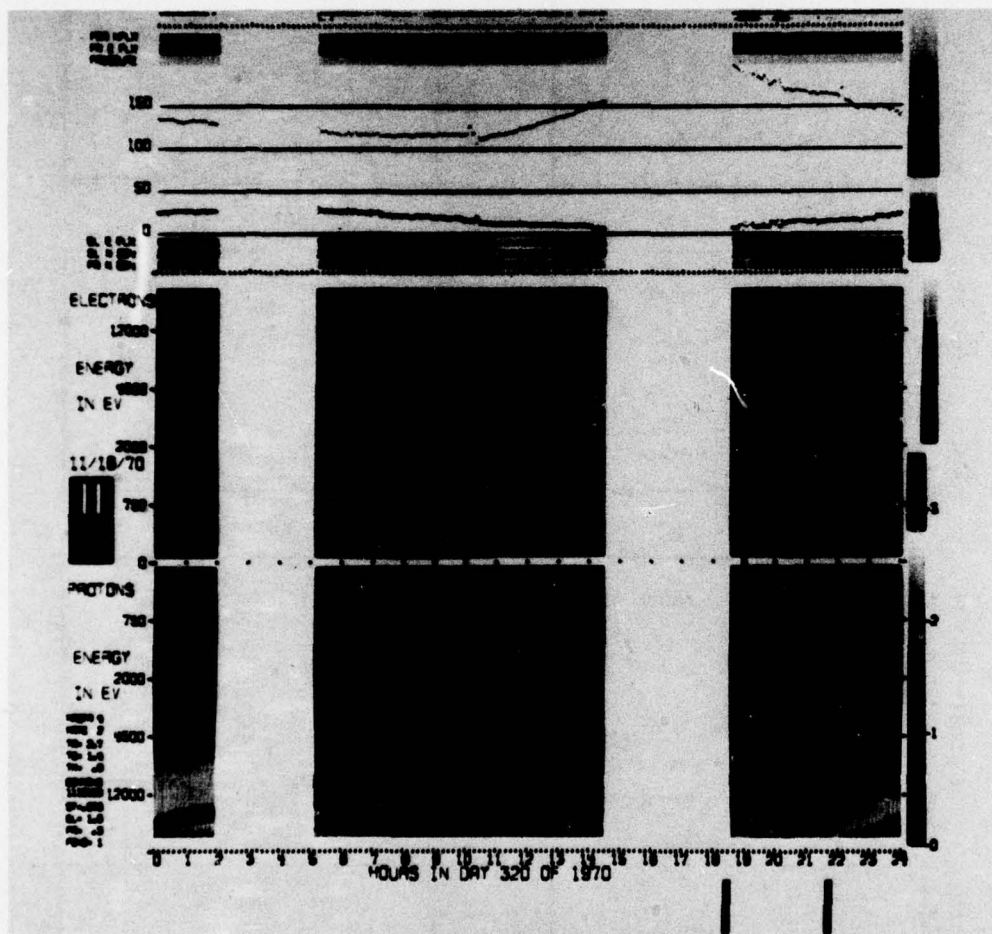
ATS-5
70/320

IONS



ELECTRONS

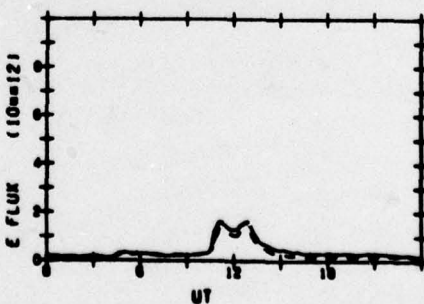
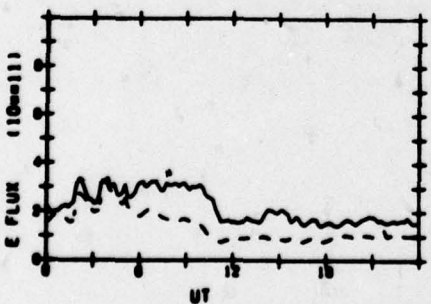
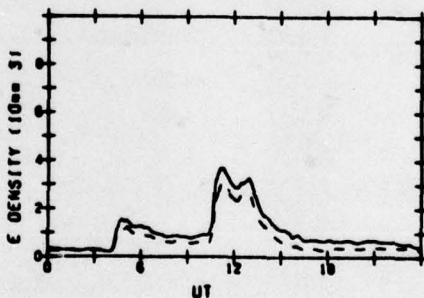
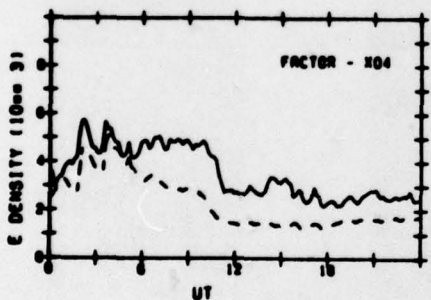
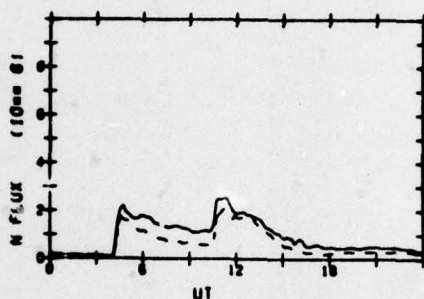
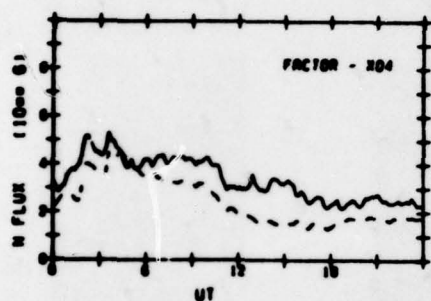
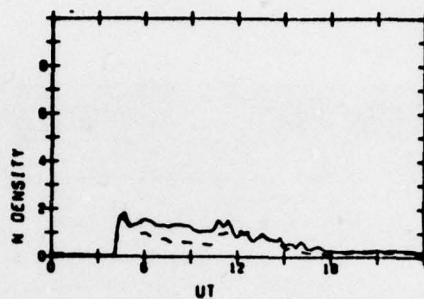


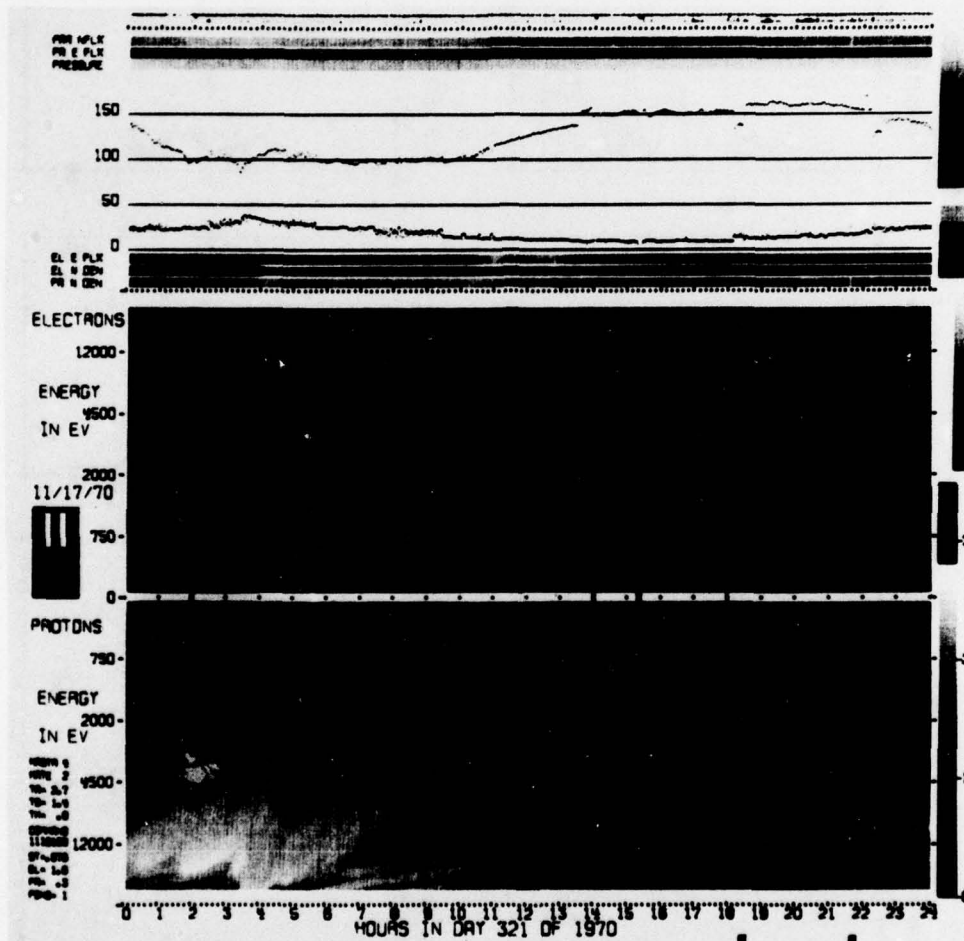


ATS-5
70/321

IONS

ELECTRONS

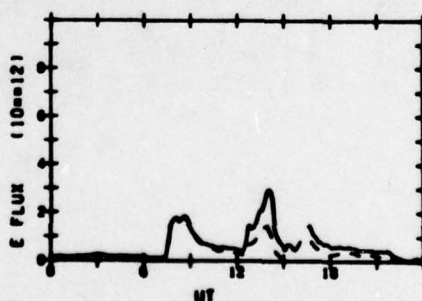
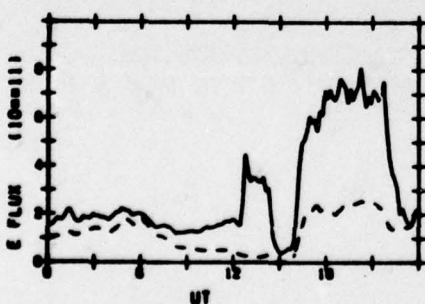
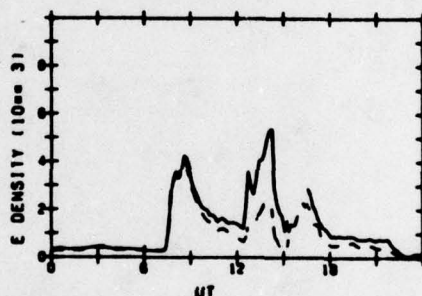
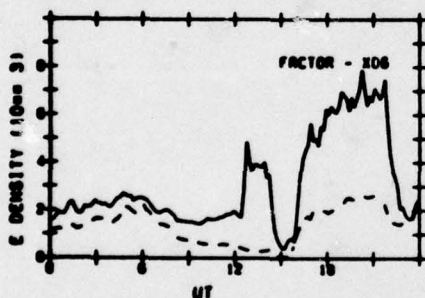
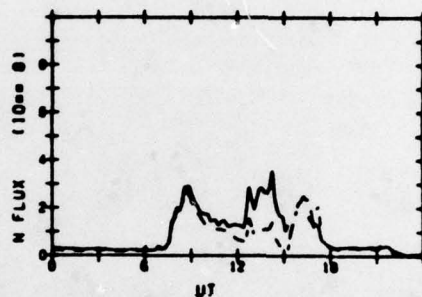
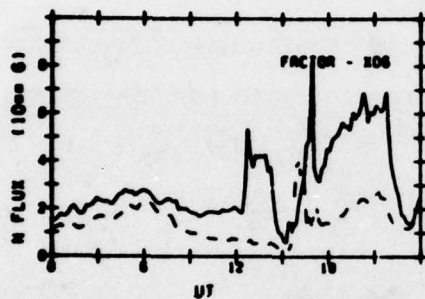
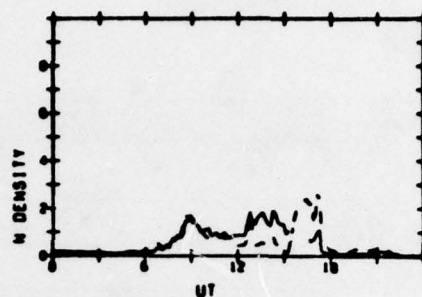
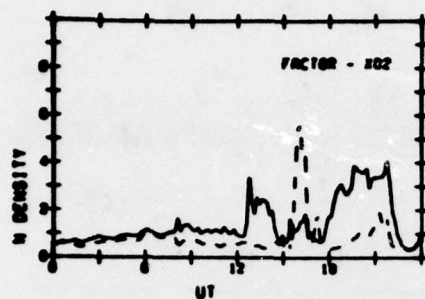


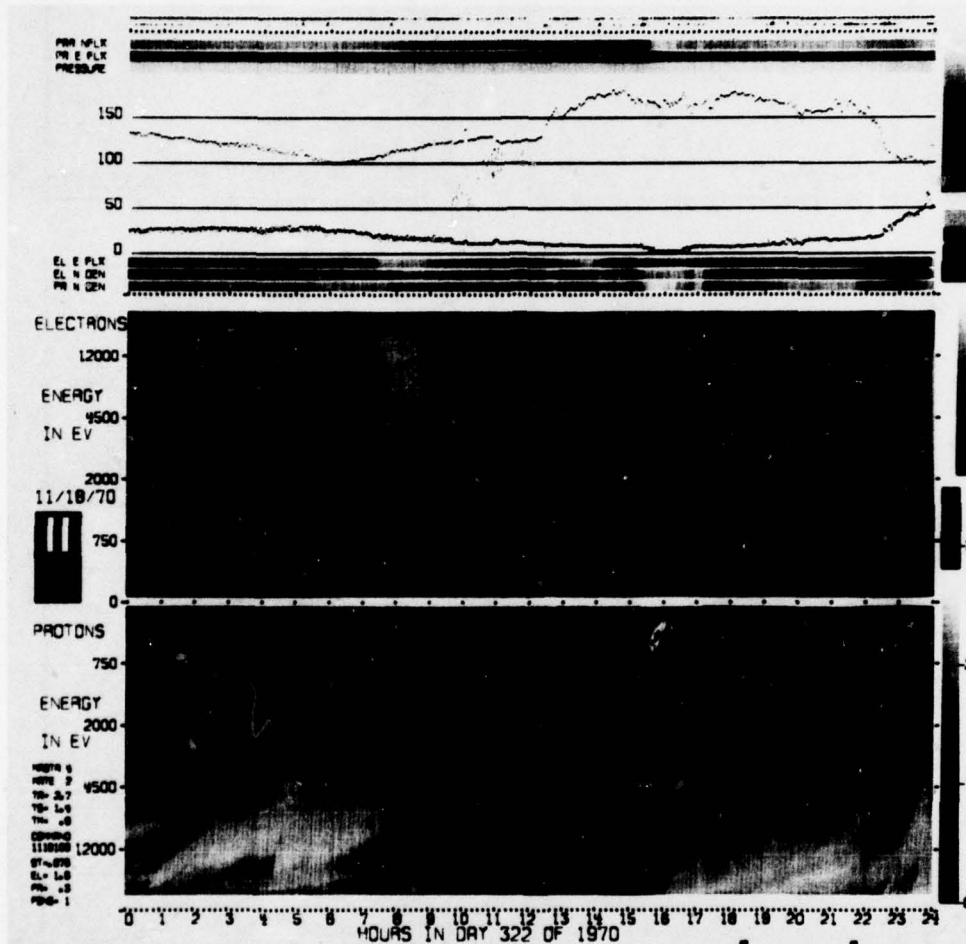


ATS-5
70/322

IONS

ELECTRONS

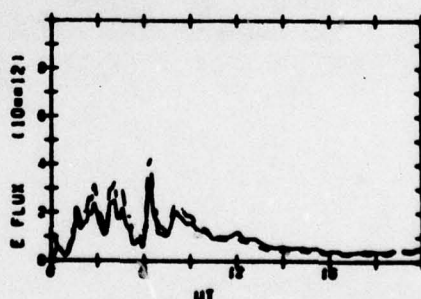
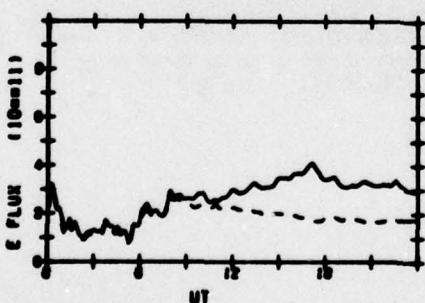
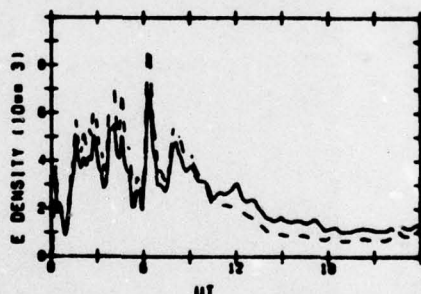
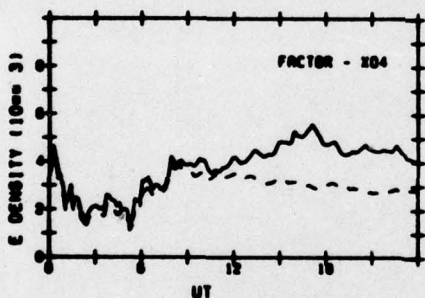
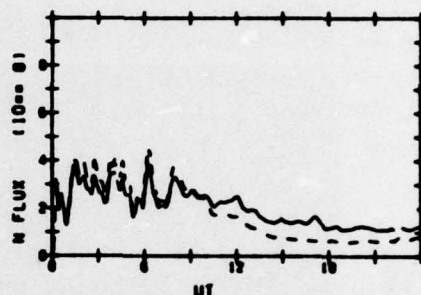
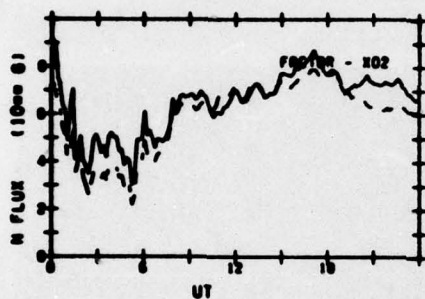
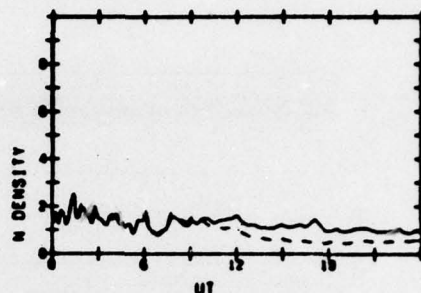
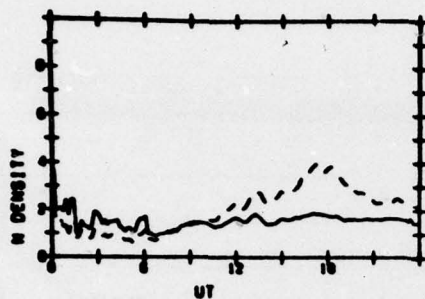


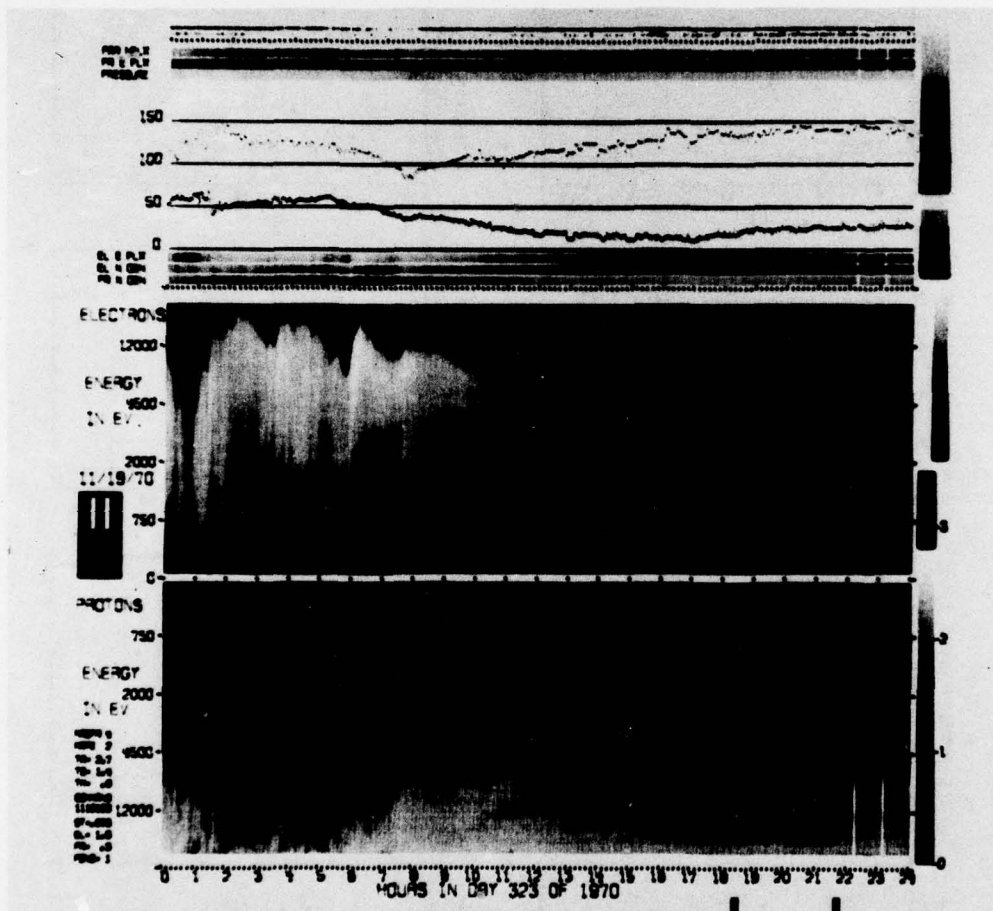


ATS-5
70/323

IONS

ELECTRONS

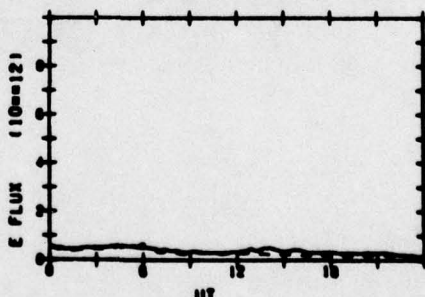
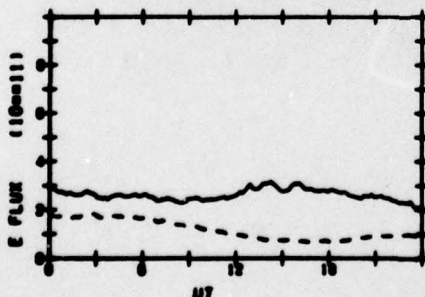
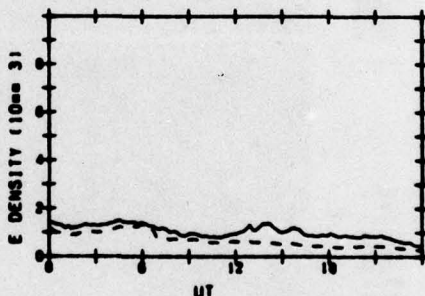
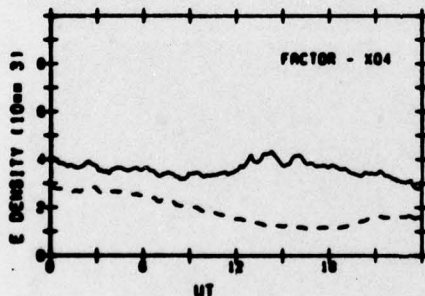
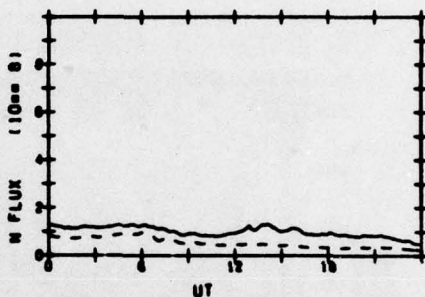
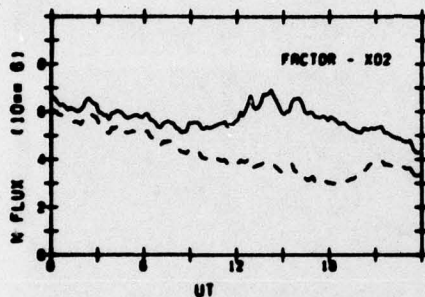
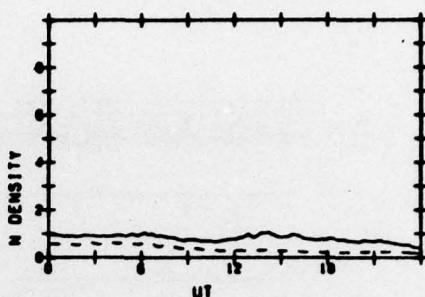
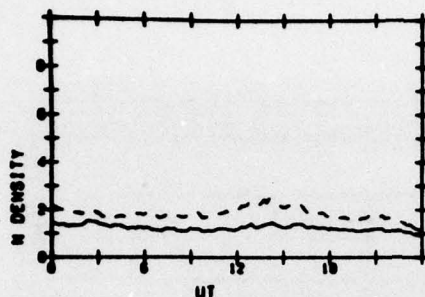


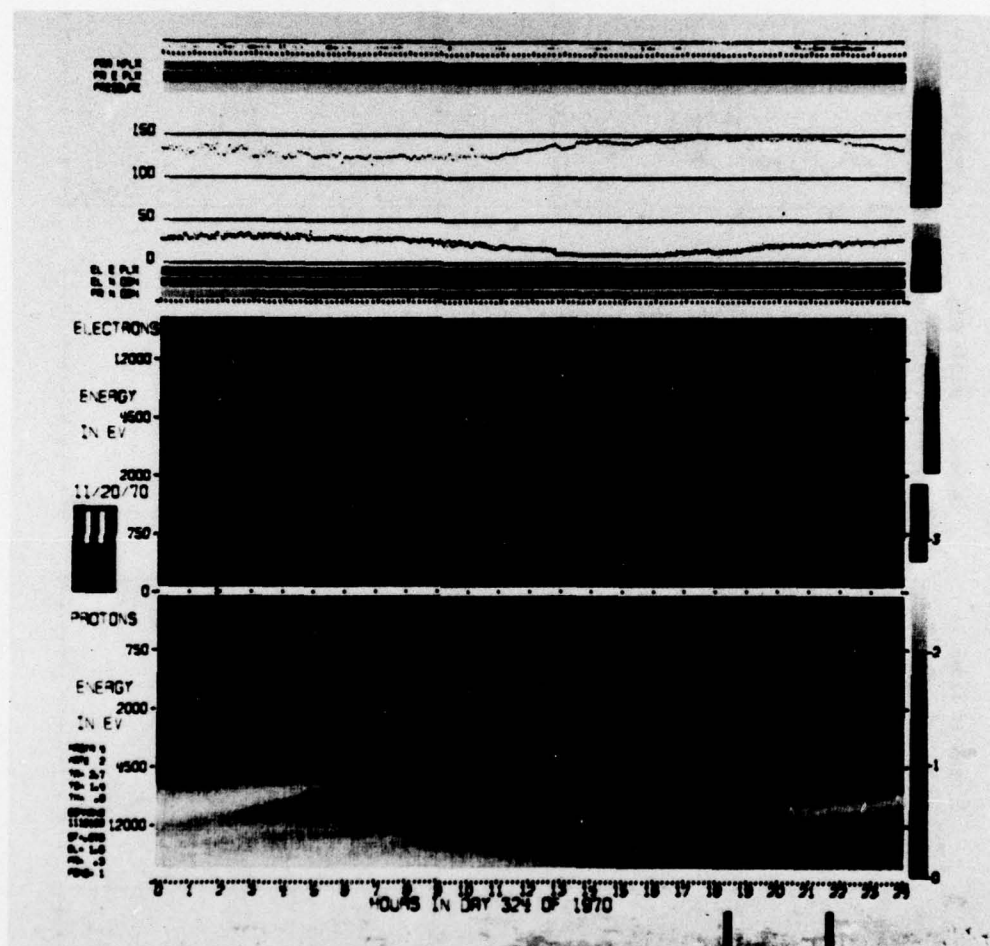


ATS-5
70/324

IONS

ELECTRONS

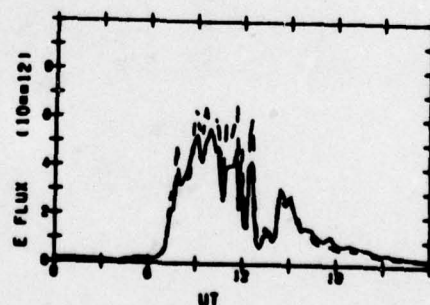
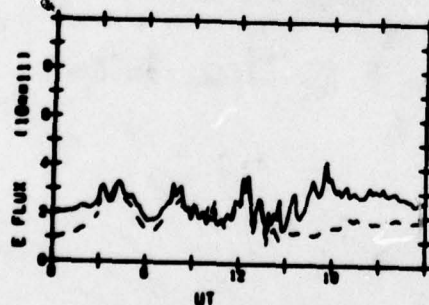
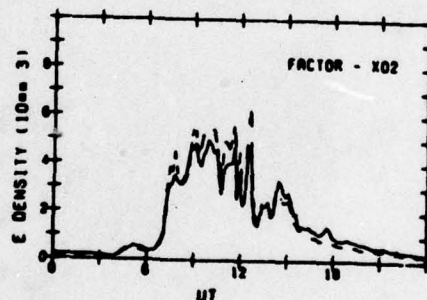
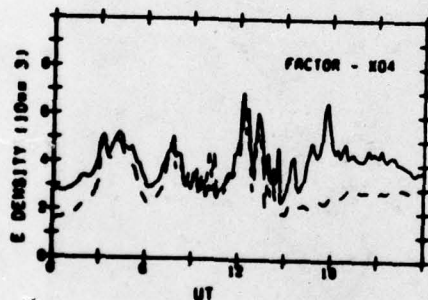
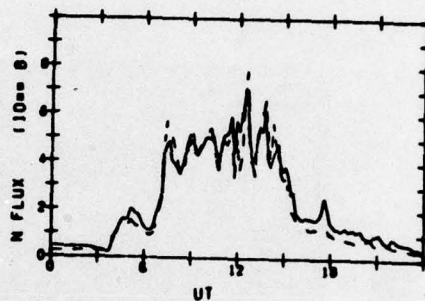
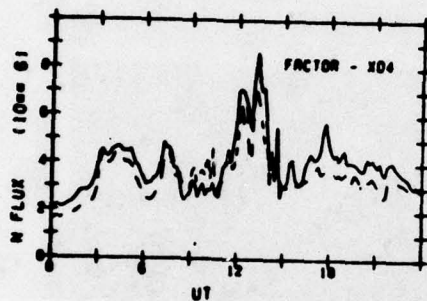
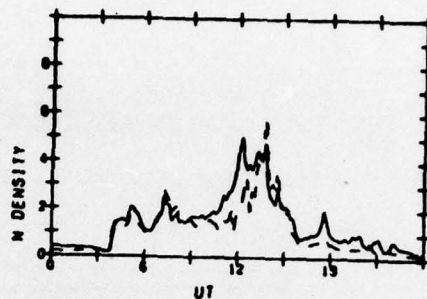
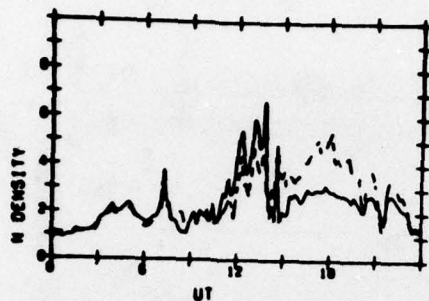


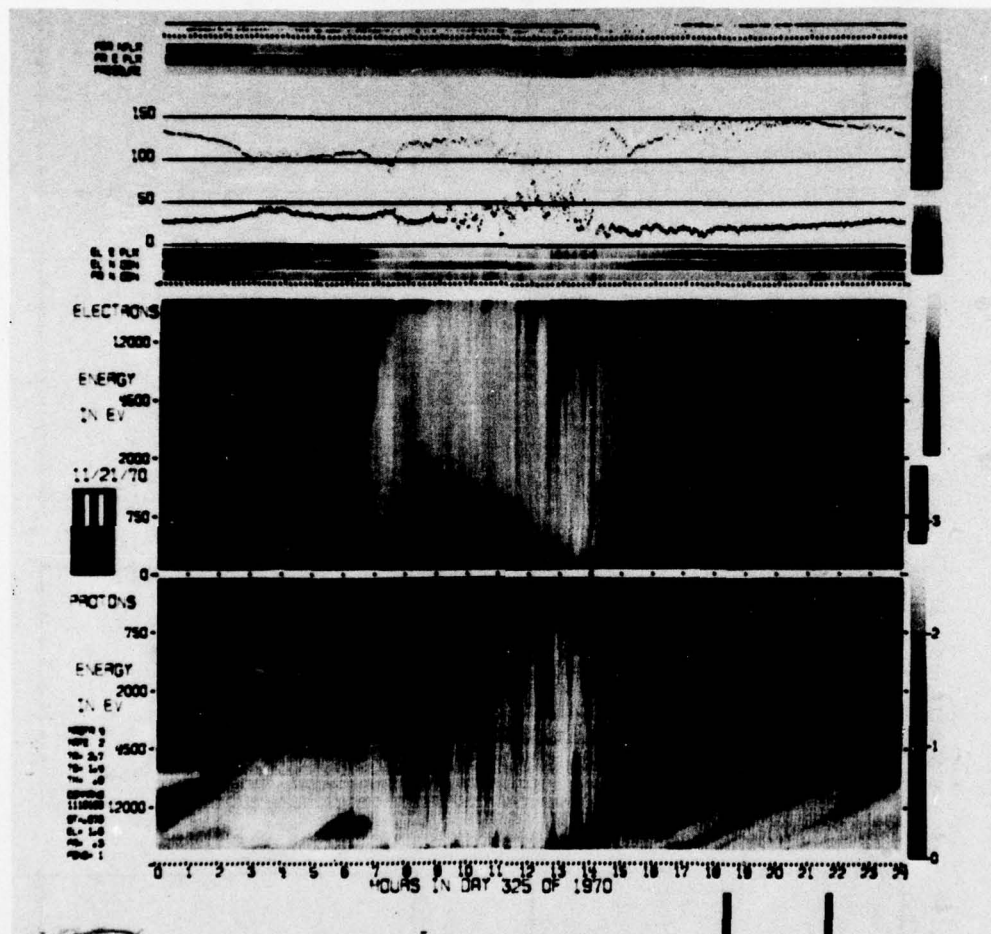


ATS-5
70/325

IONS

ELECTRONS

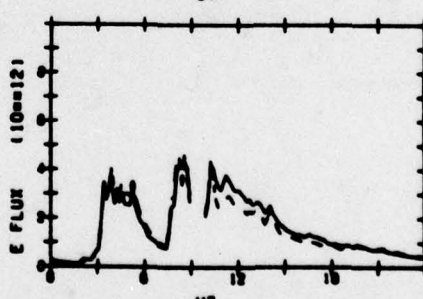
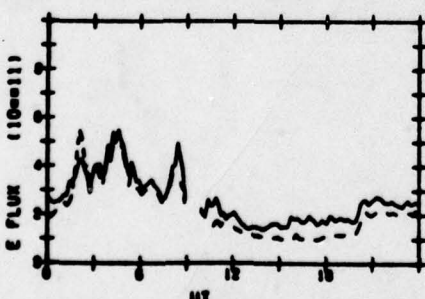
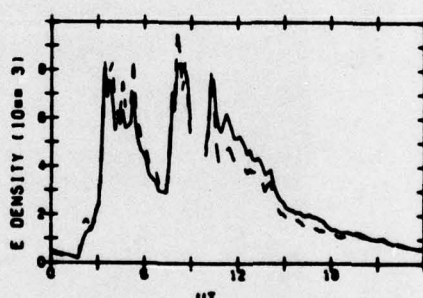
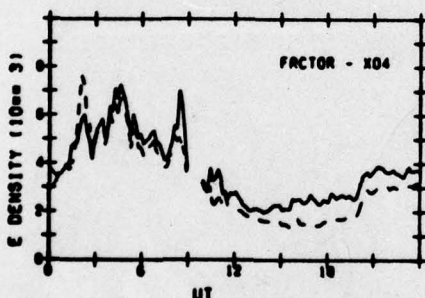
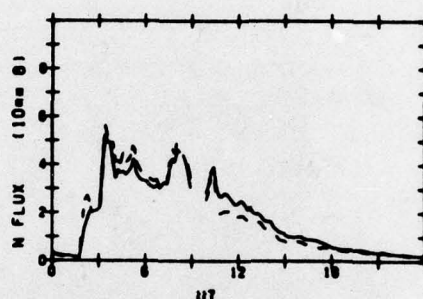
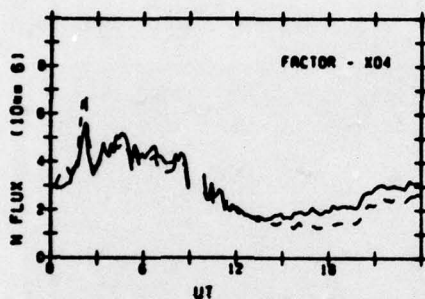
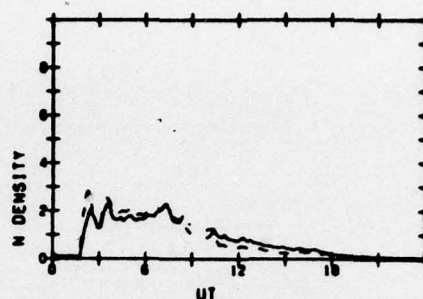
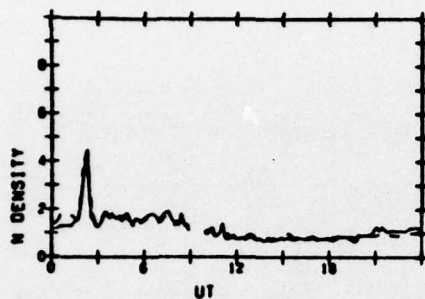


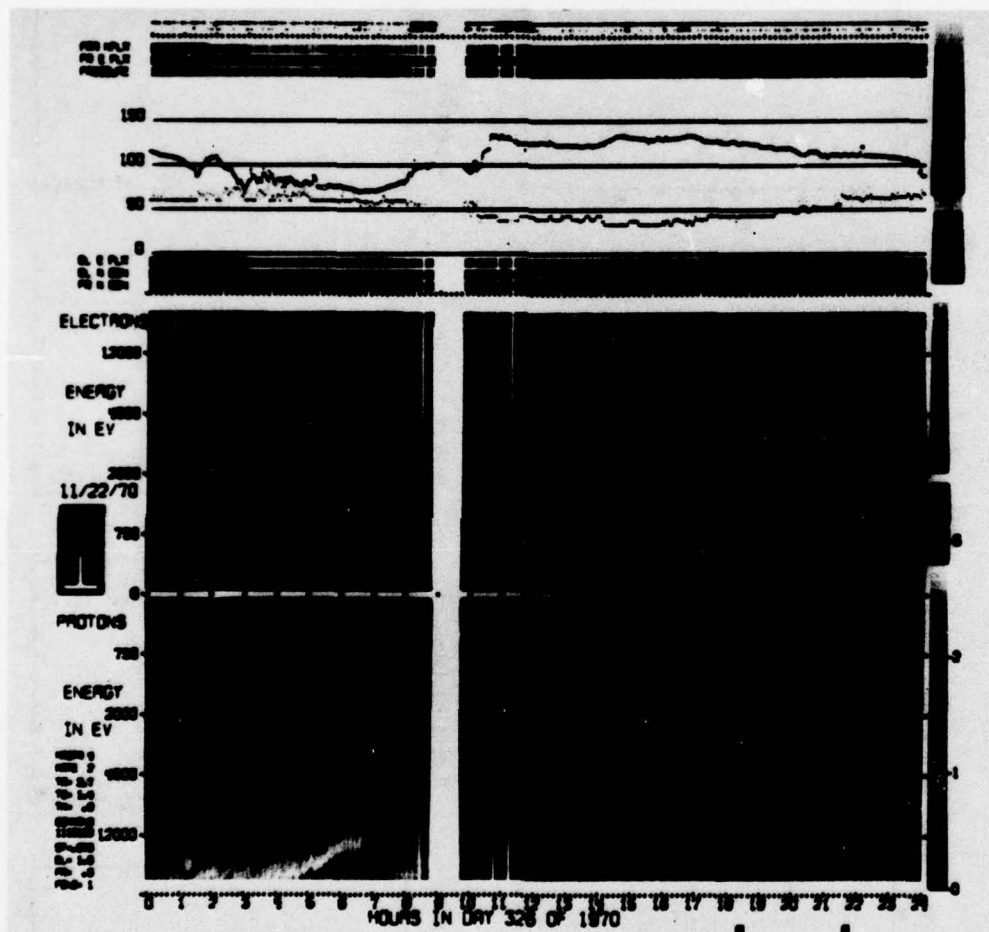


ATS-5
70/326

IONS

ELECTRONS

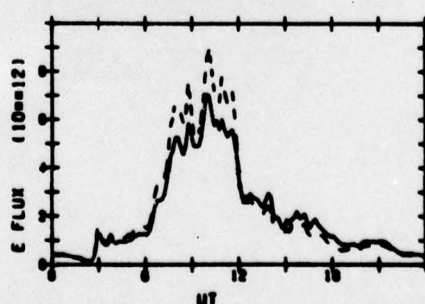
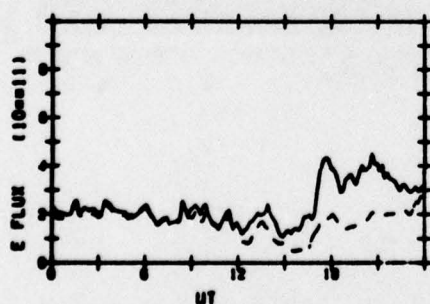
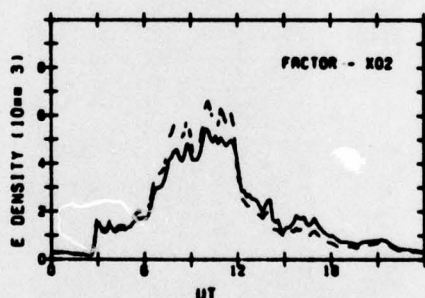
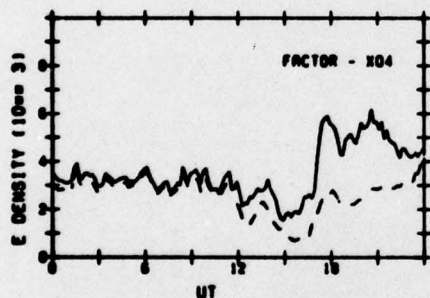
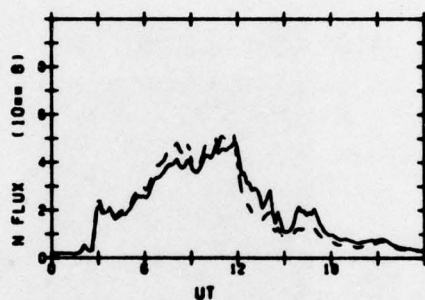
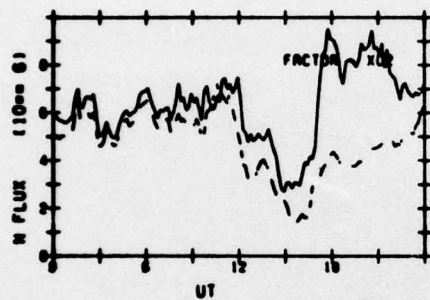
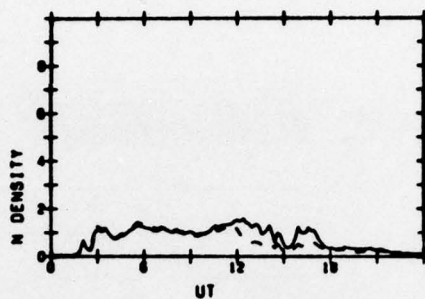
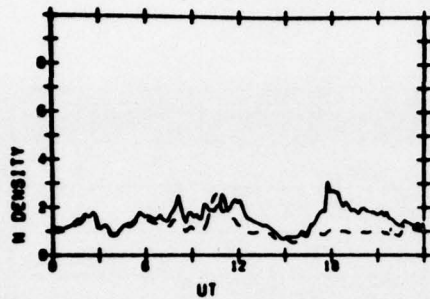


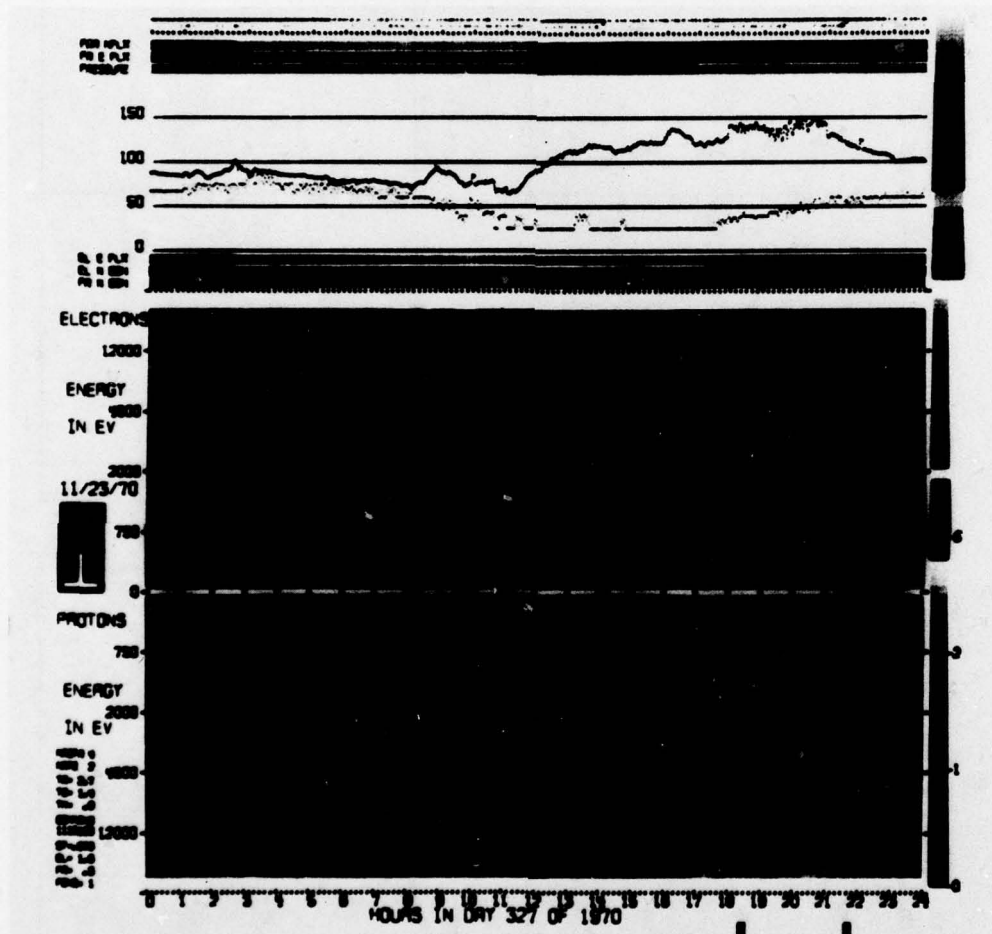


ATS-5
70/327

IONS

ELECTRONS

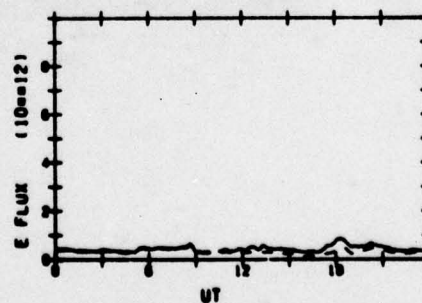
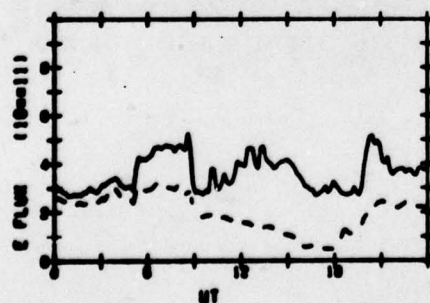
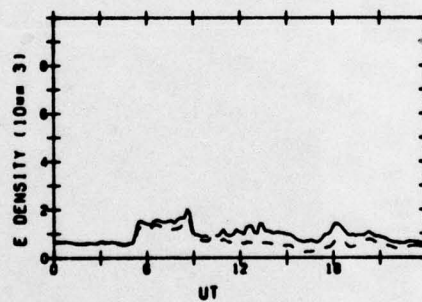
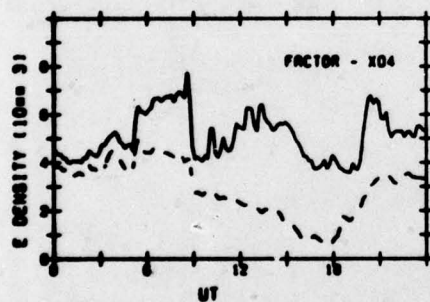
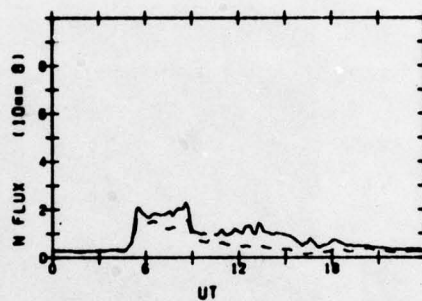
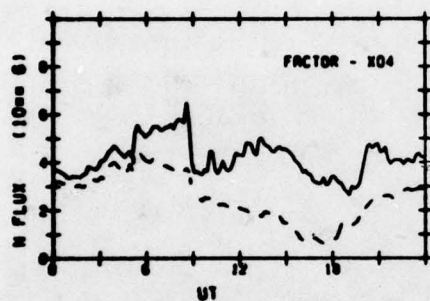
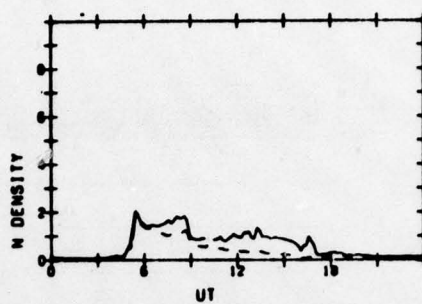
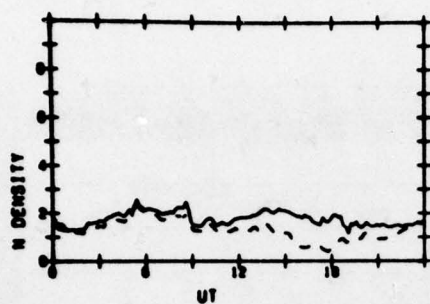


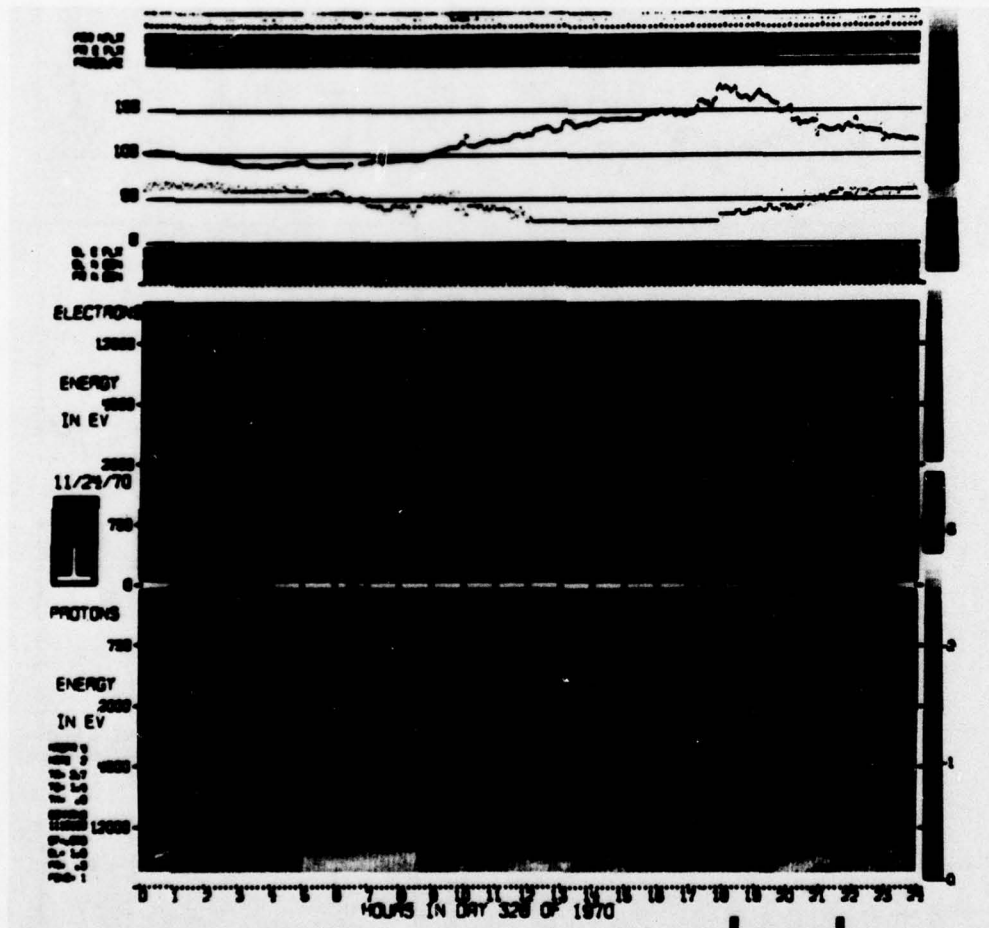


ATS-5
70/328

IONS

ELECTRONS

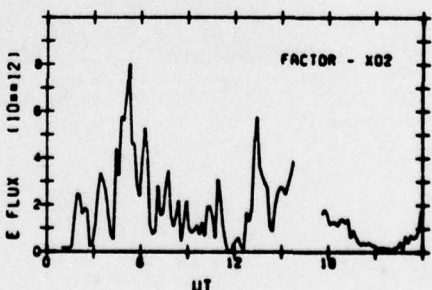
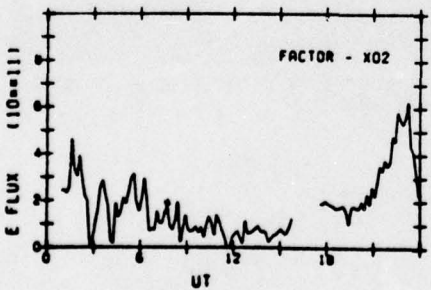
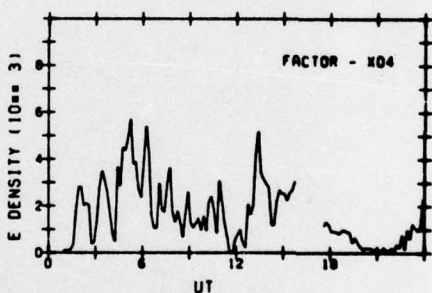
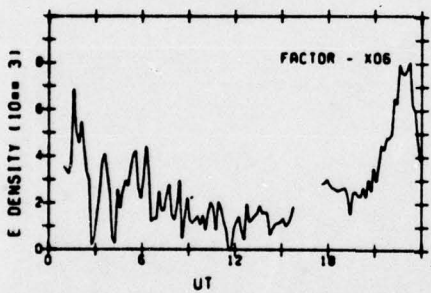
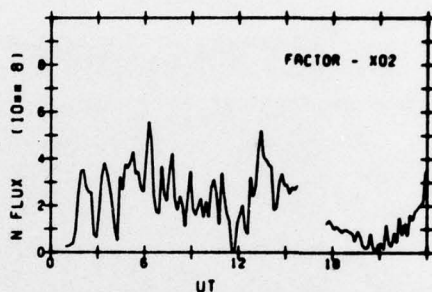
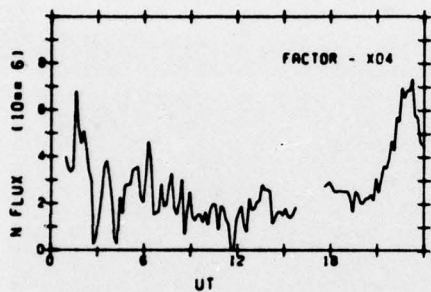
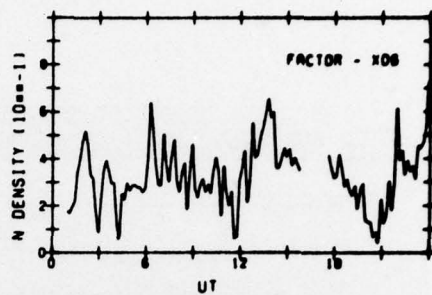
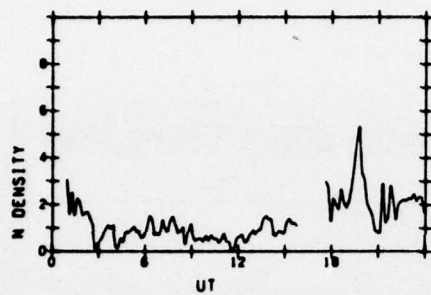


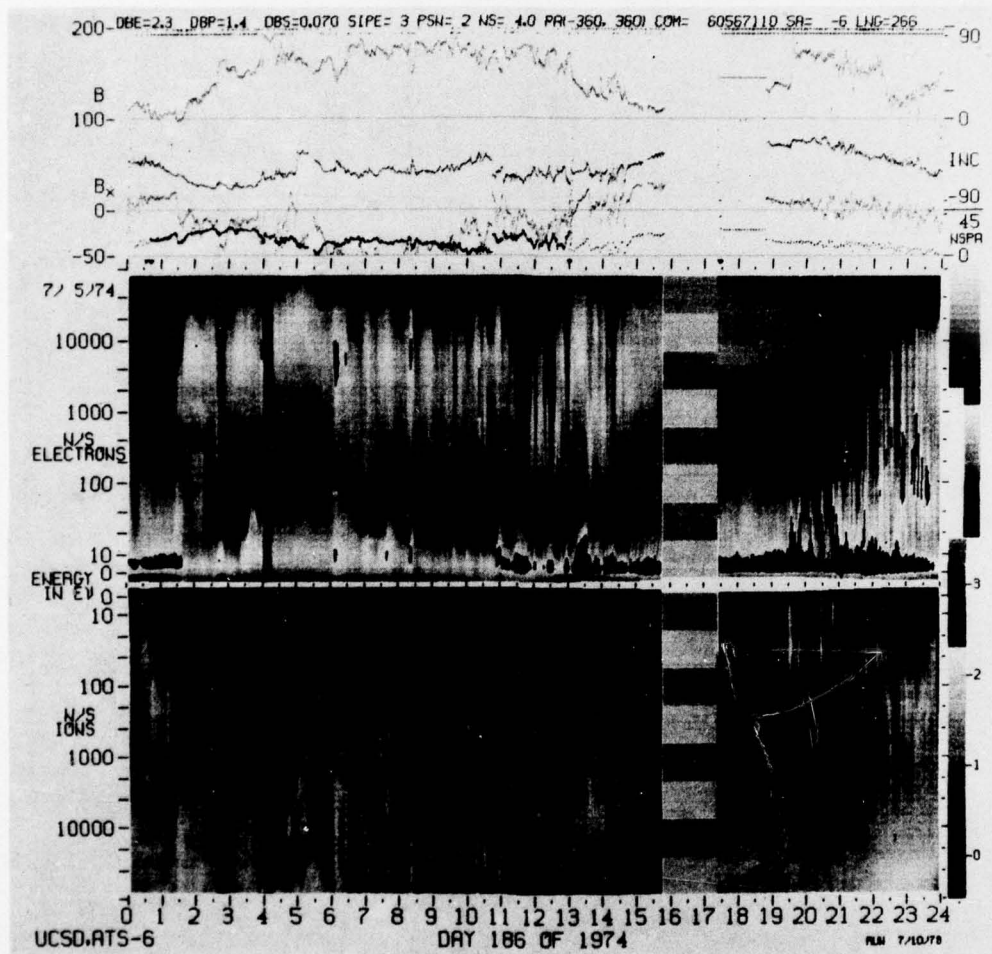


RTS-6 DATA
74/186

IONS

ELECTRONS

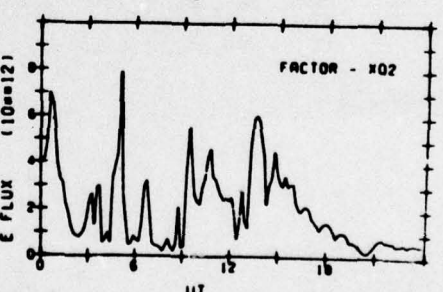
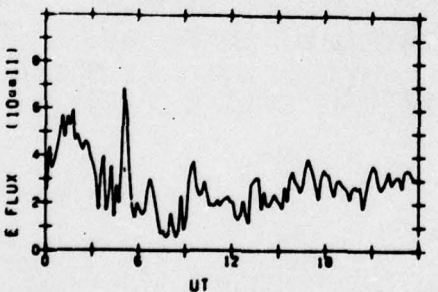
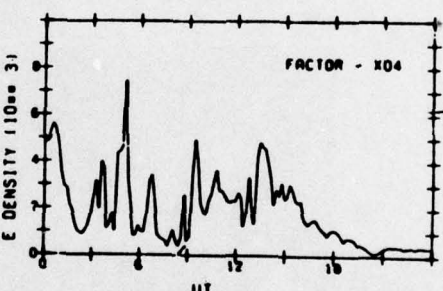
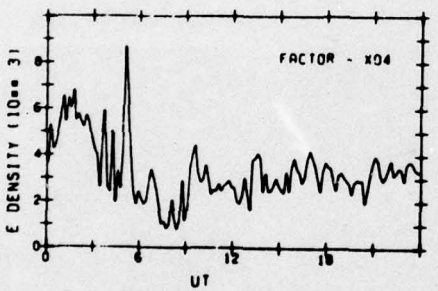
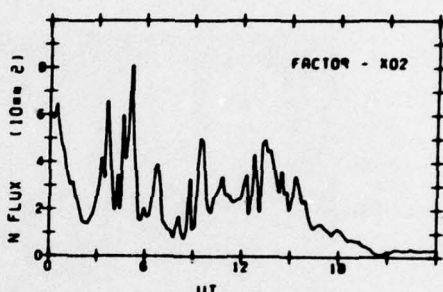
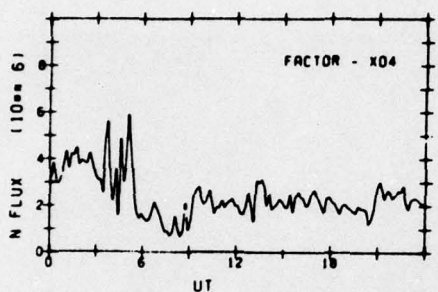
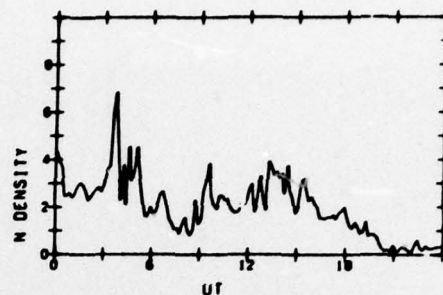
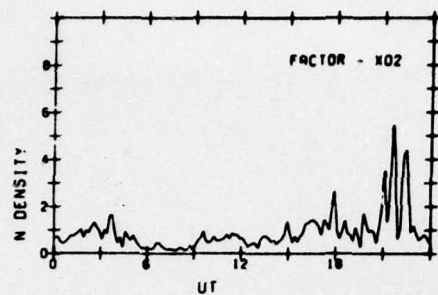


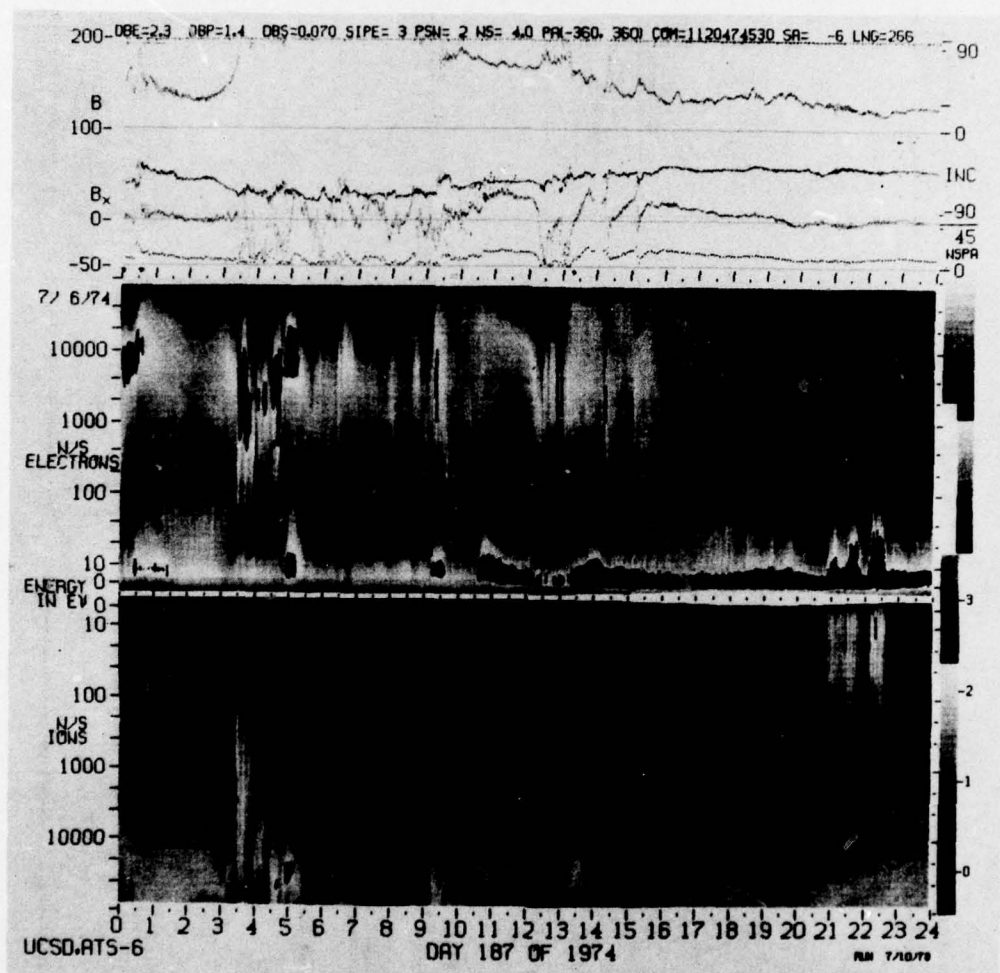


ATS-6 DATA
74/187

IONS

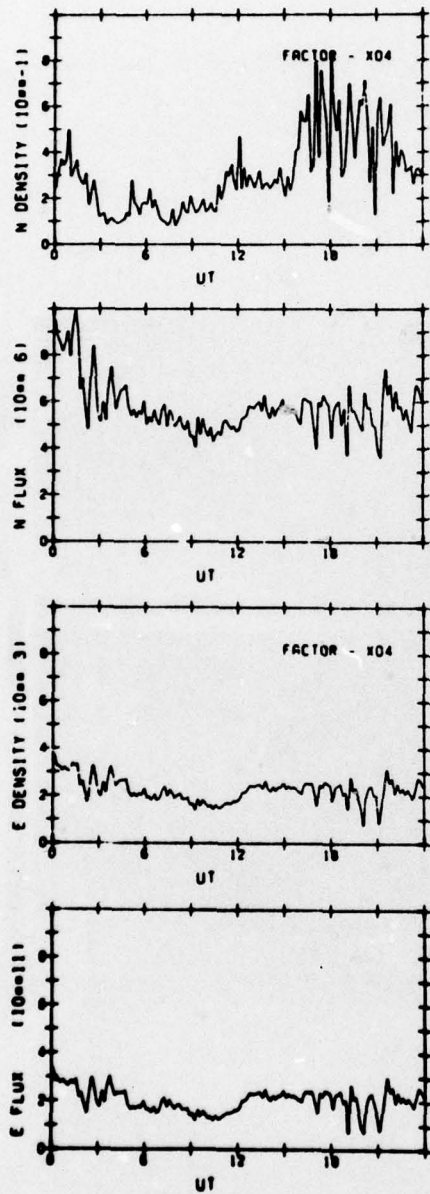
ELECTRONS



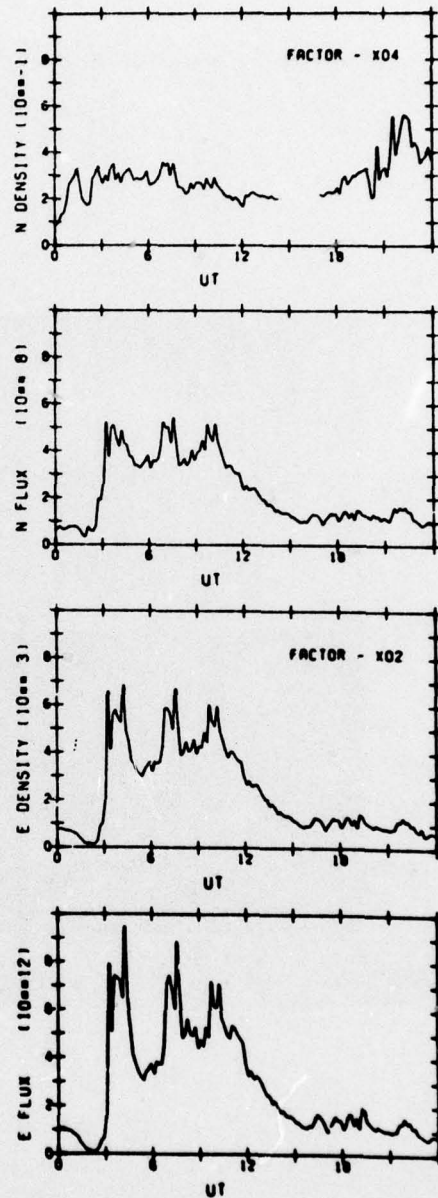


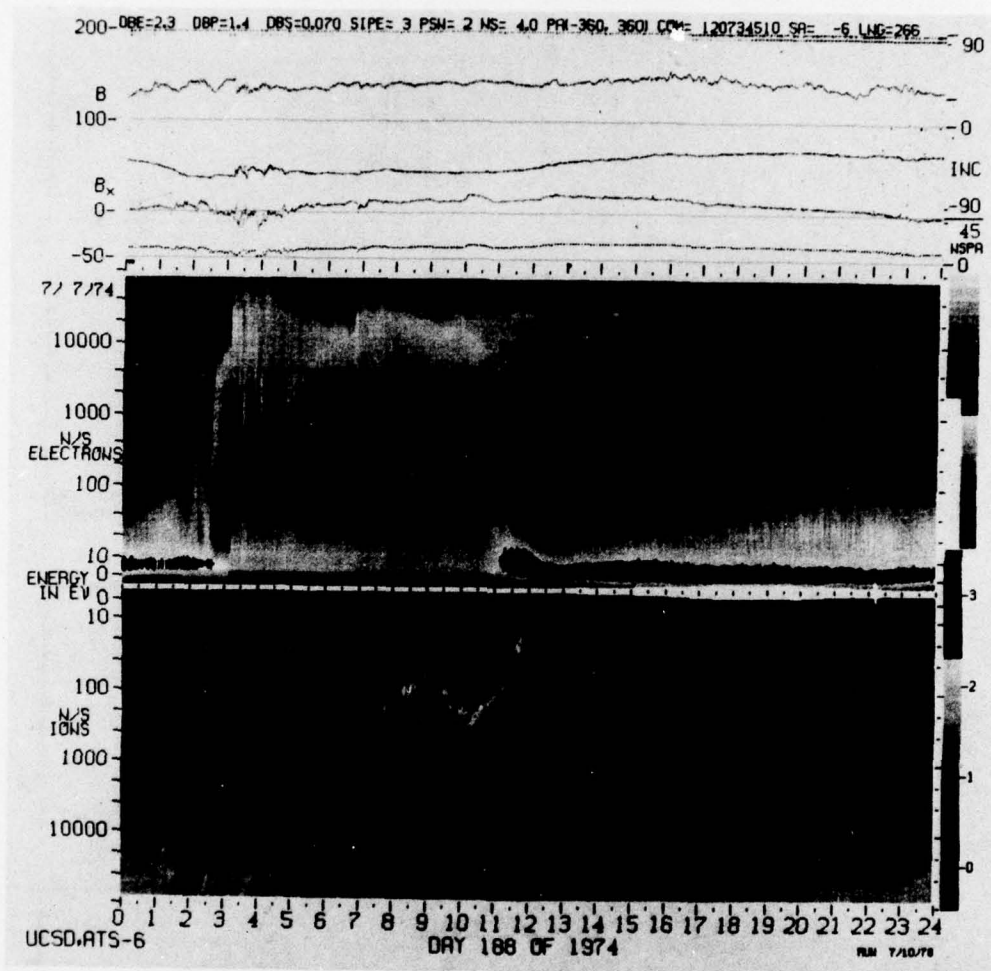
ATS-6 DATA
74/188

IONS



ELECTRONS

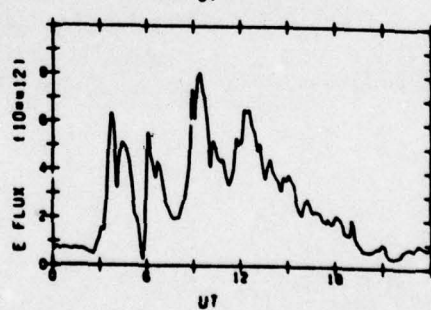
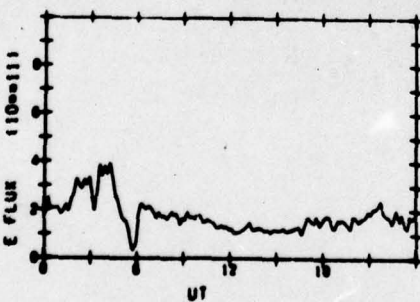
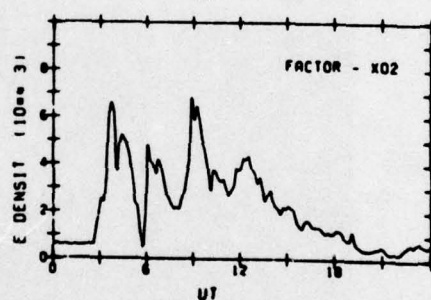
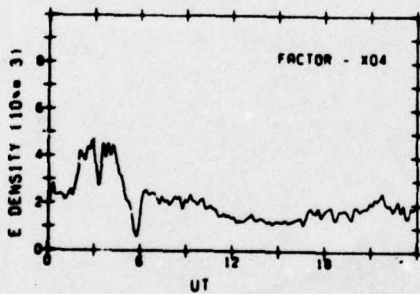
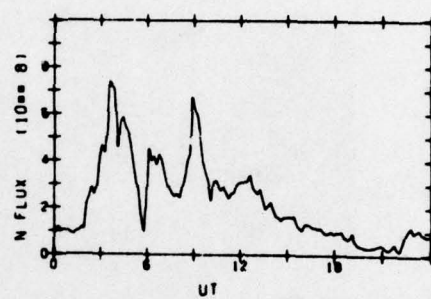
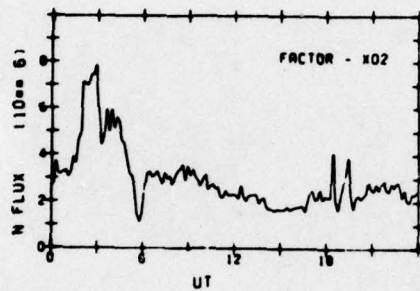
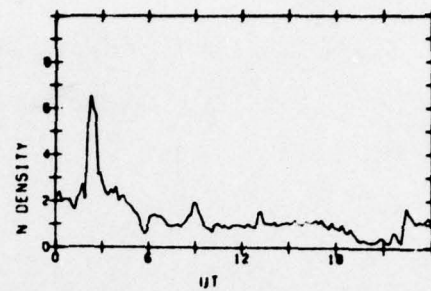
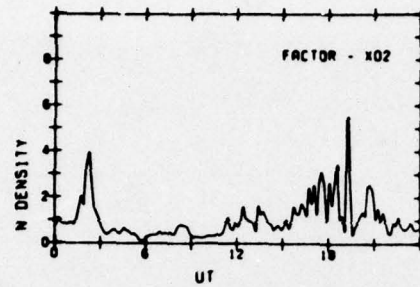


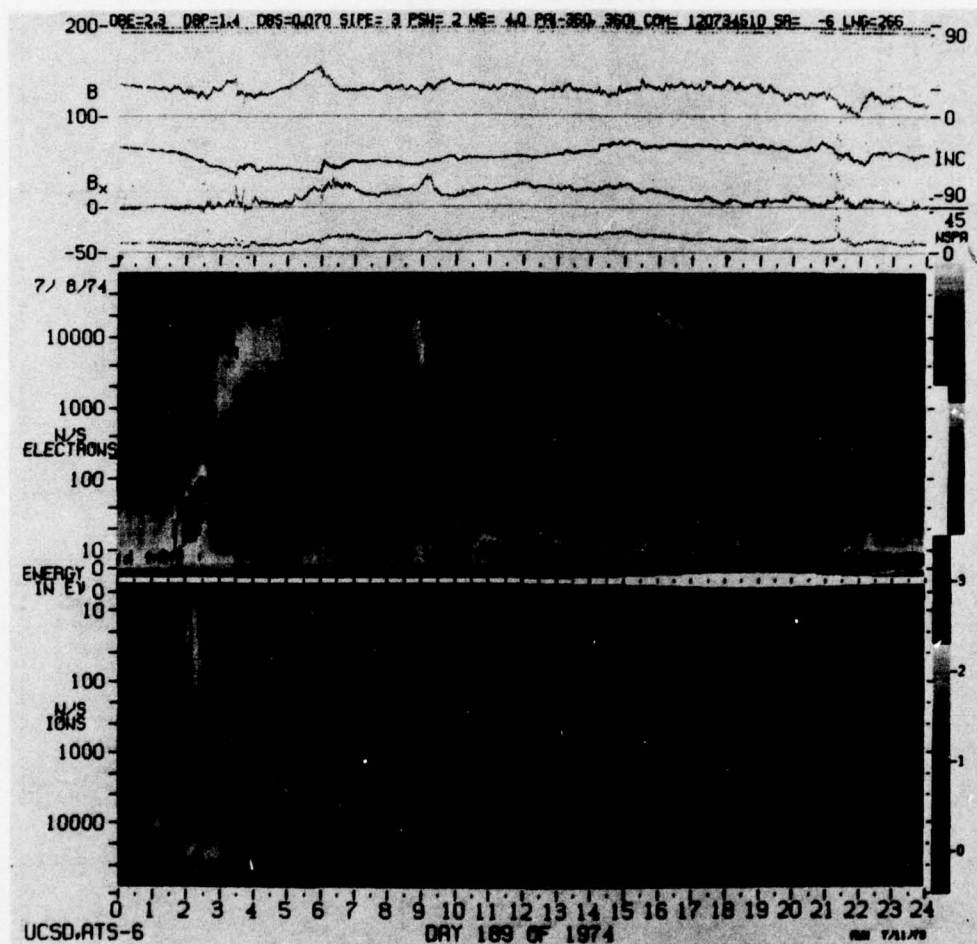


ATS-6 DATA
74/189

IONS

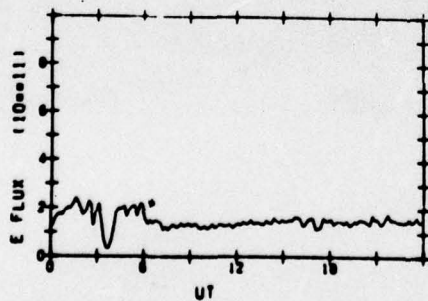
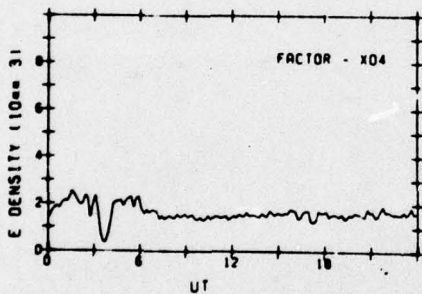
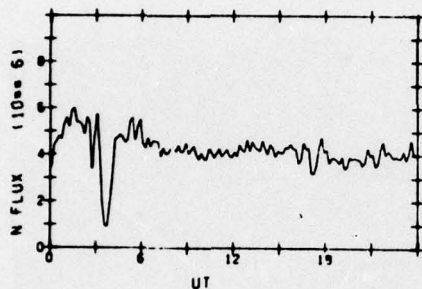
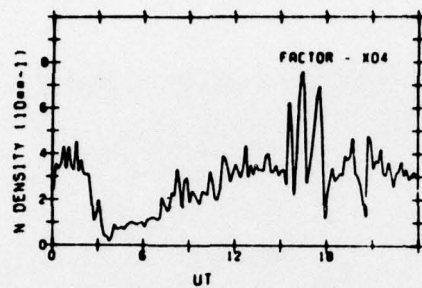
ELECTRONS



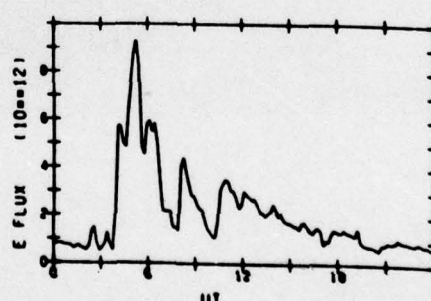
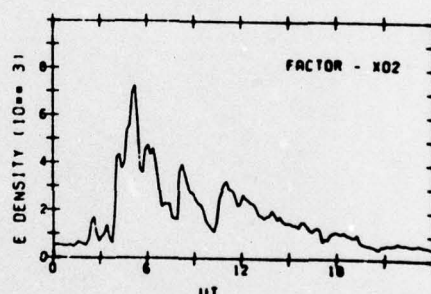
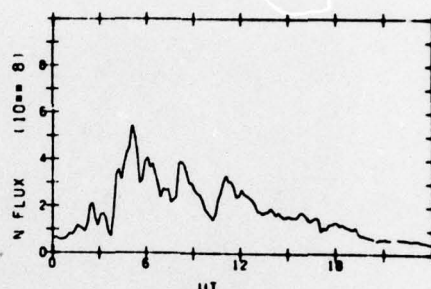
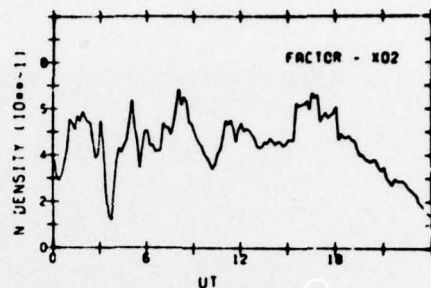


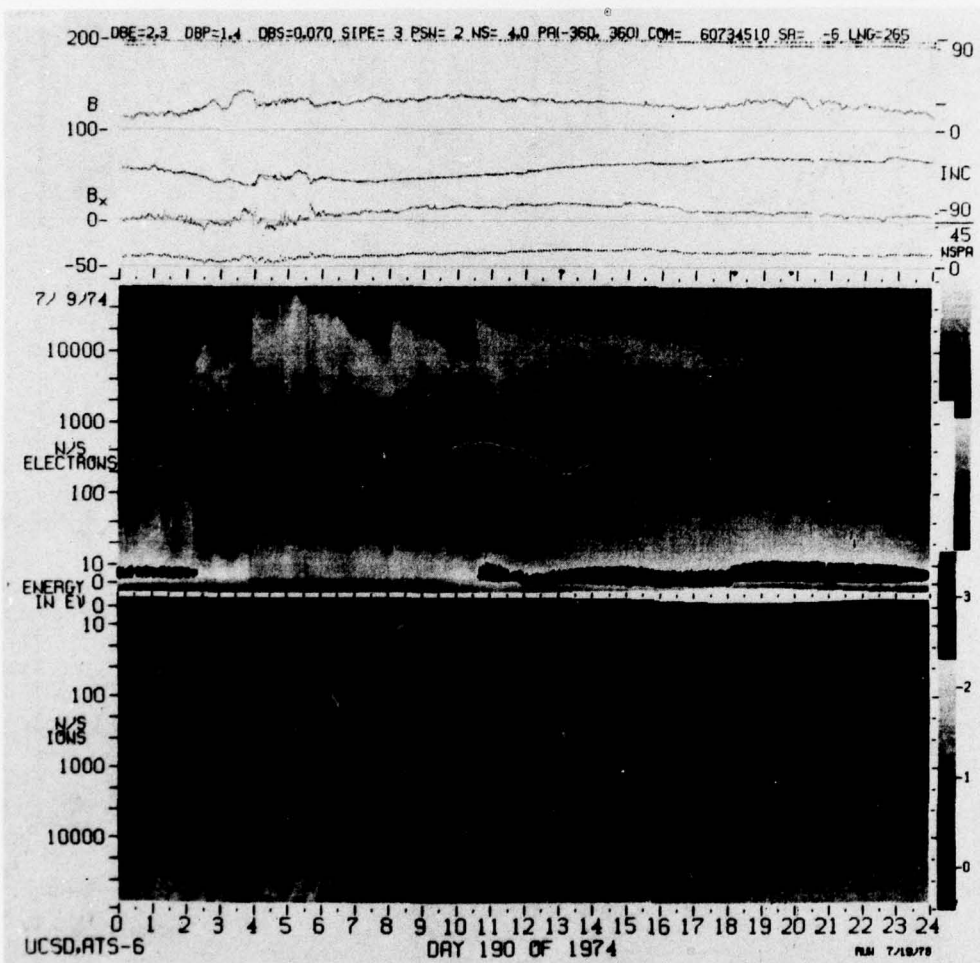
ATS-6 DATA
74/190

IONS



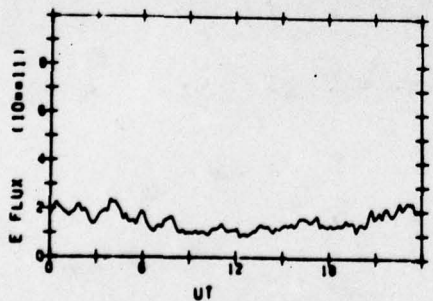
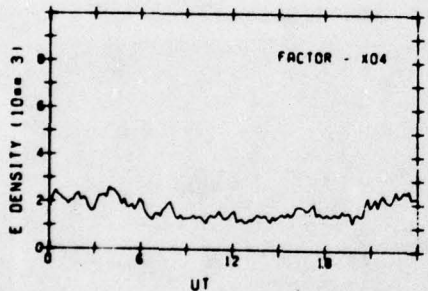
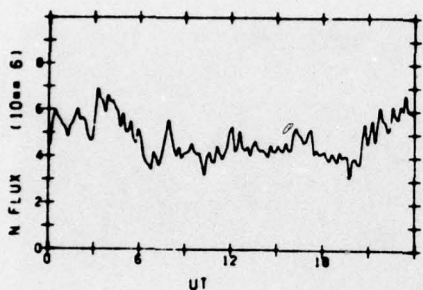
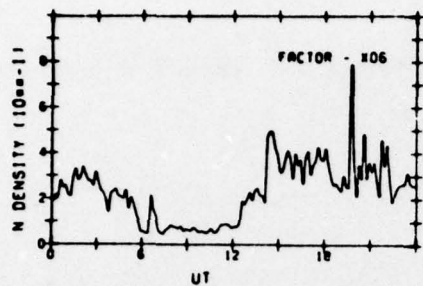
ELECTRONS



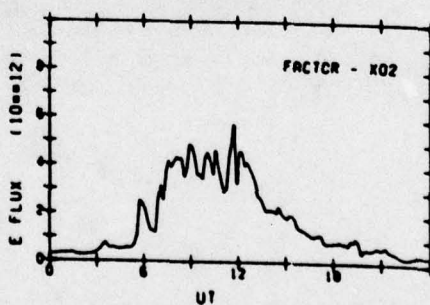
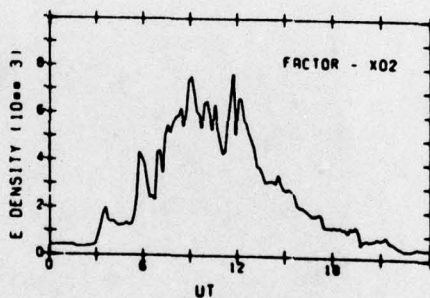
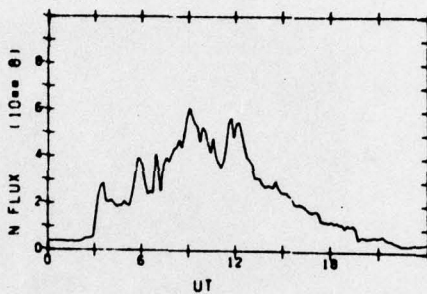
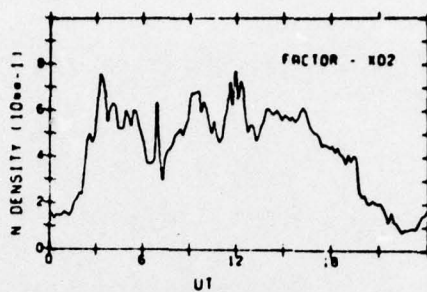


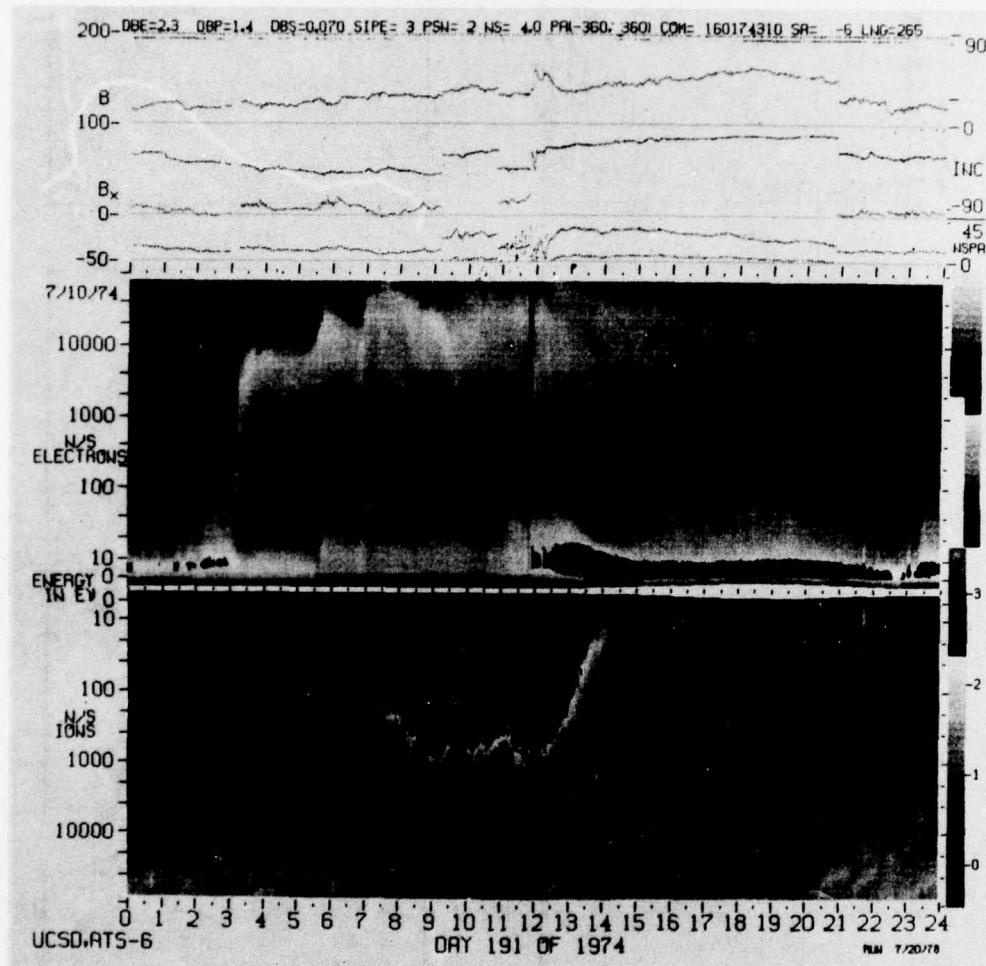
ATS-6 DATA
74/191

IONS



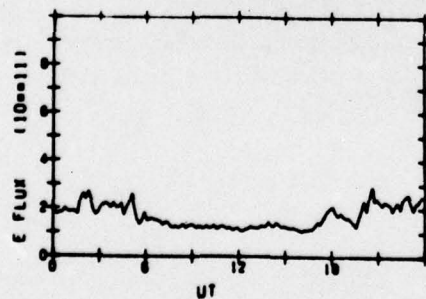
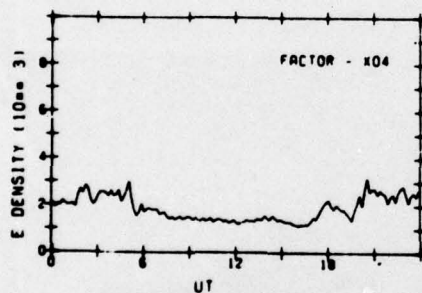
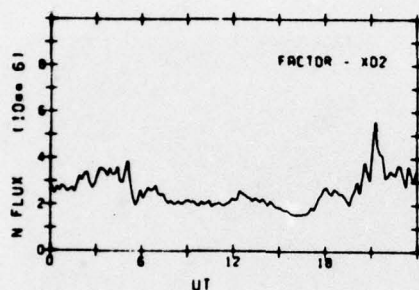
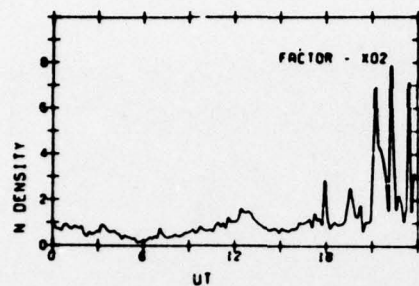
ELECTRONS



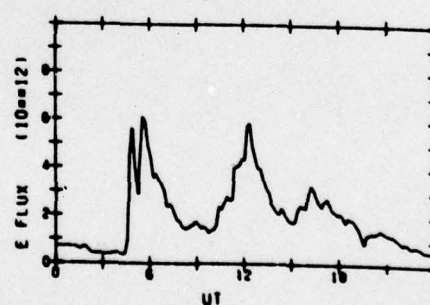
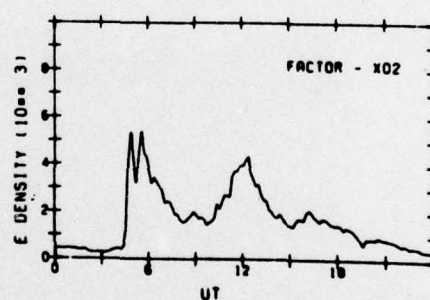
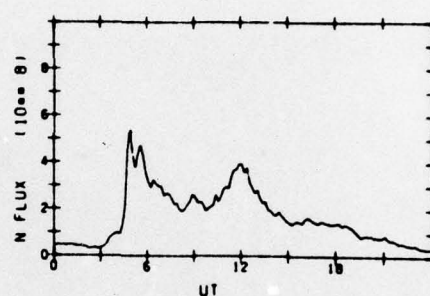
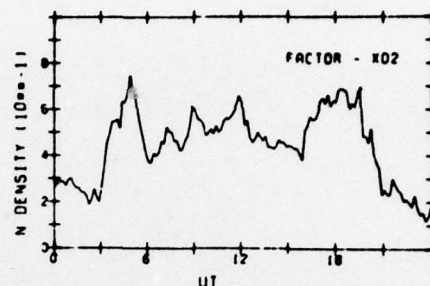


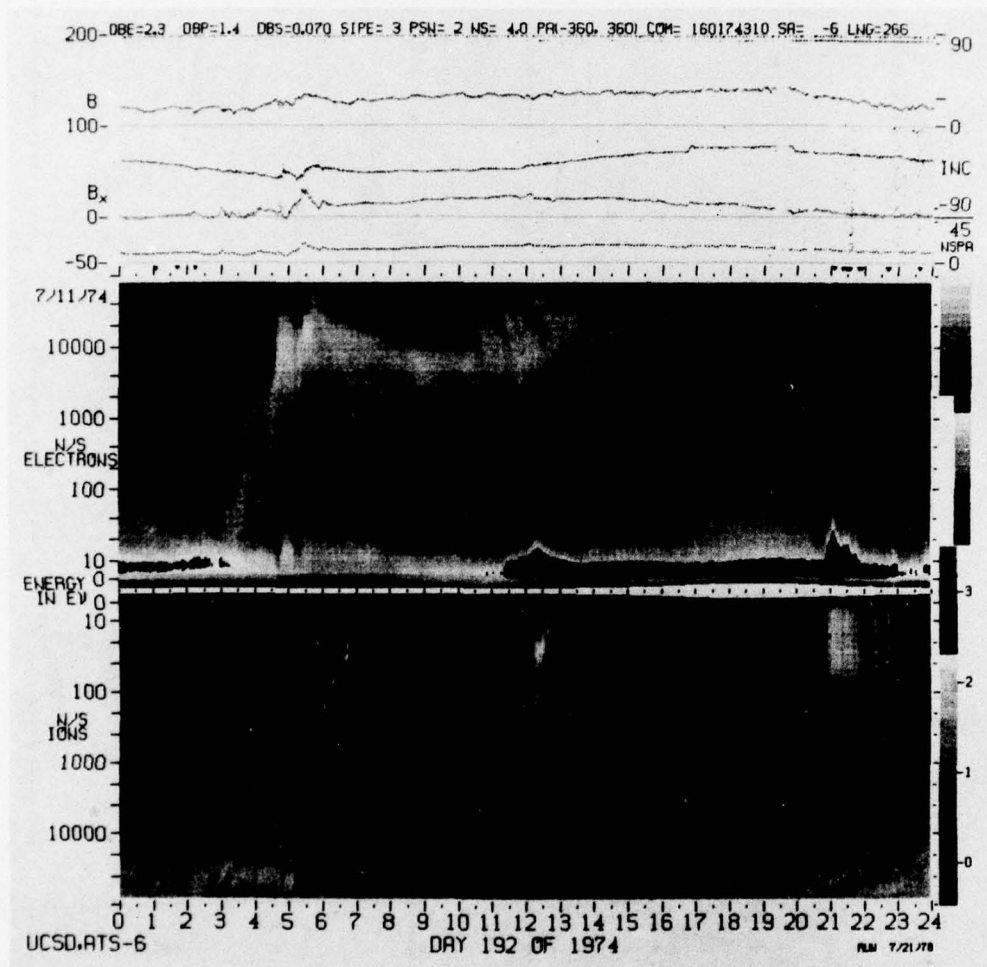
ATS-6 DAT
74/192

IONS



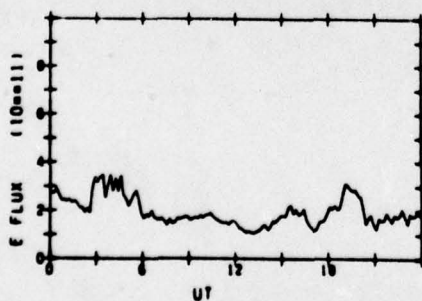
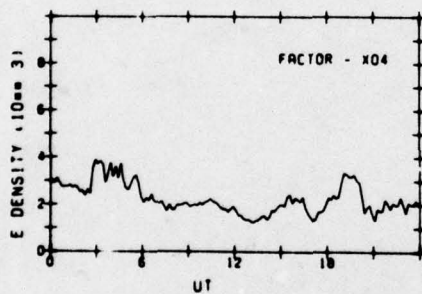
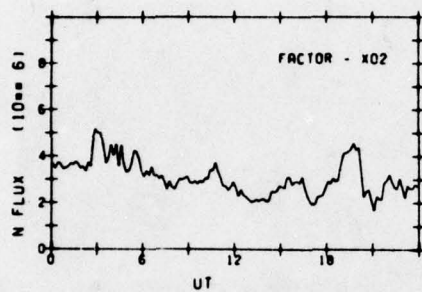
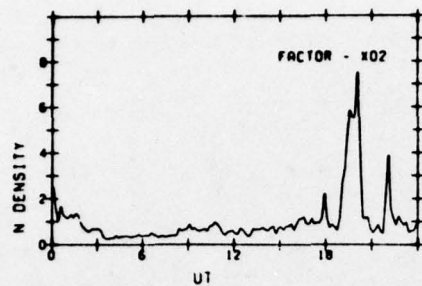
ELECTRONS



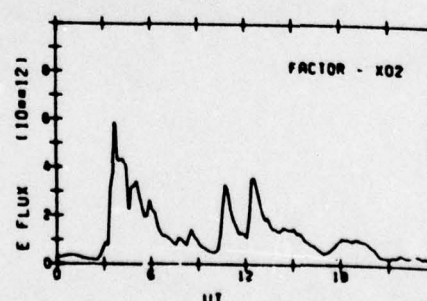
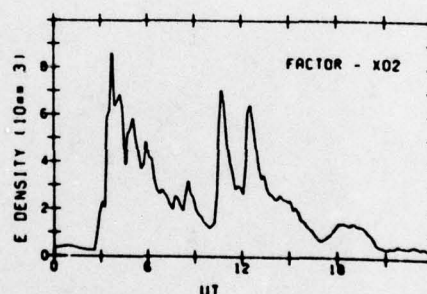
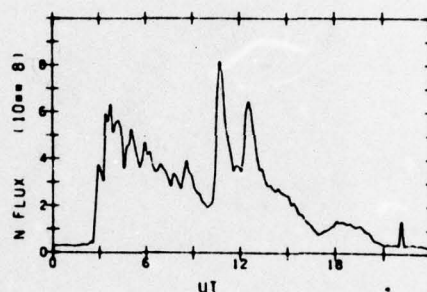
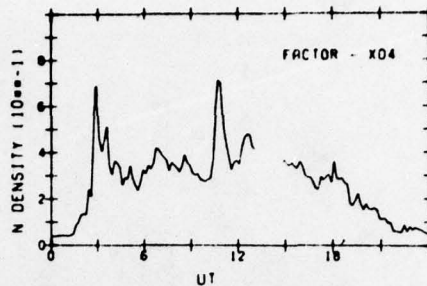


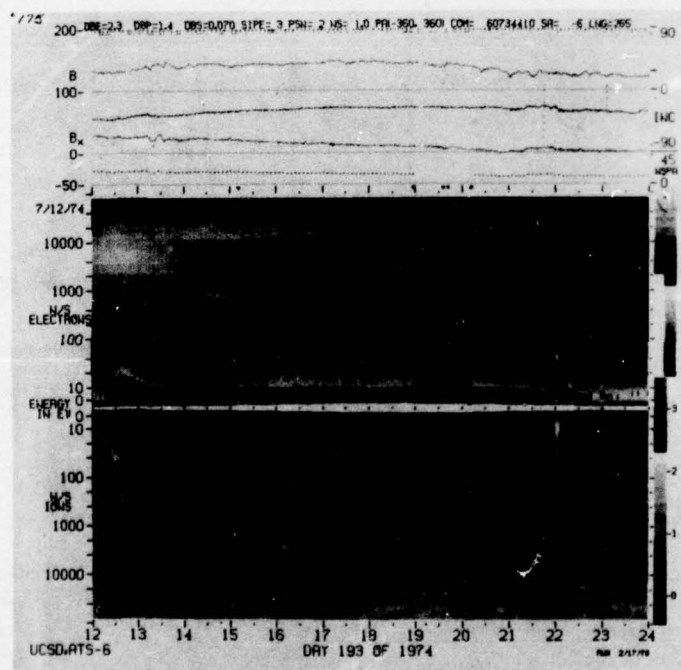
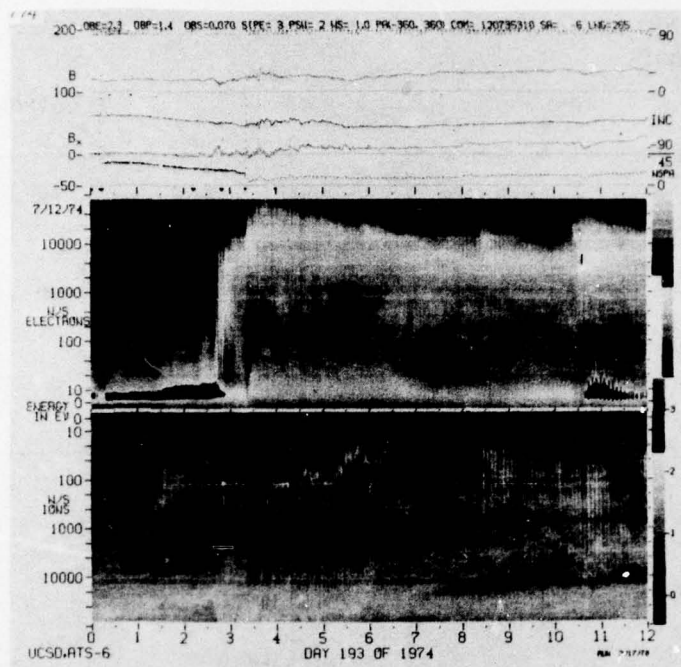
ATS-6 DATA
74/193

IONS



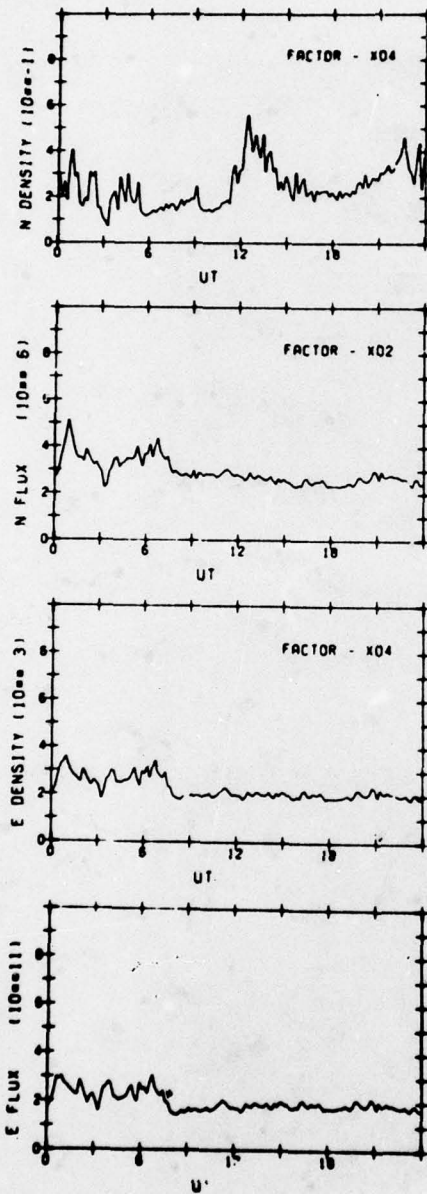
ELECTRONS



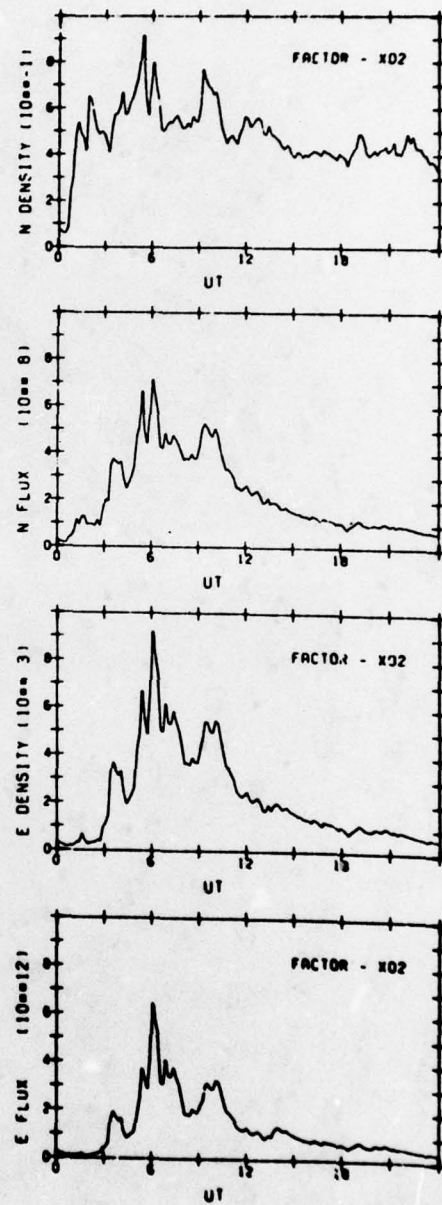


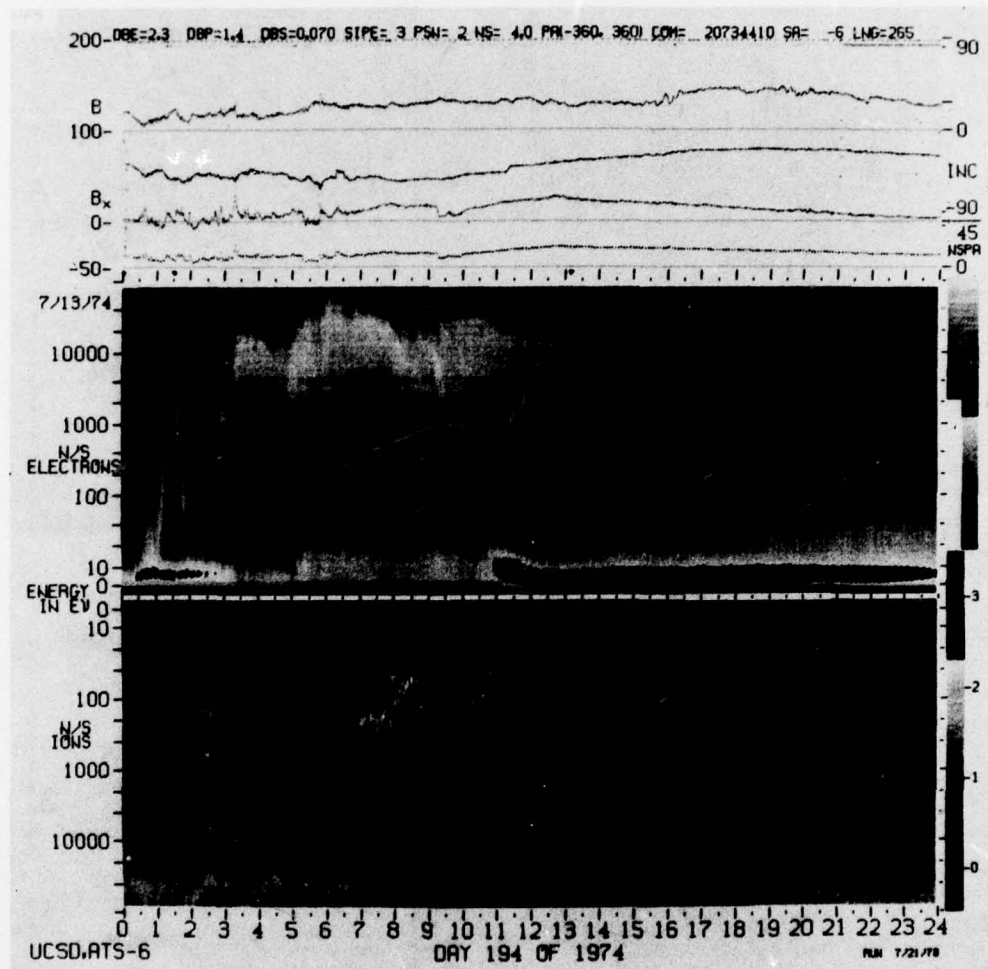
ATS-6 DATA
74/194

IONS



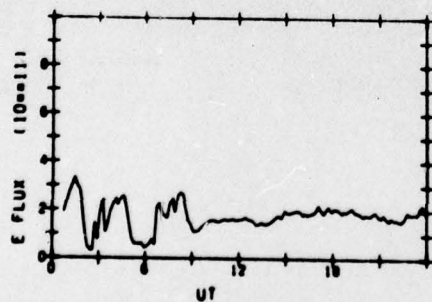
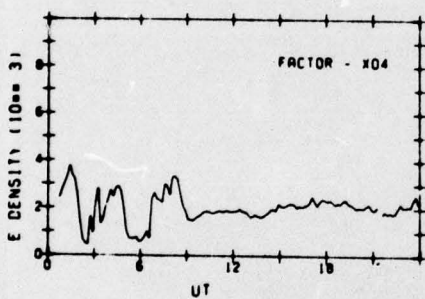
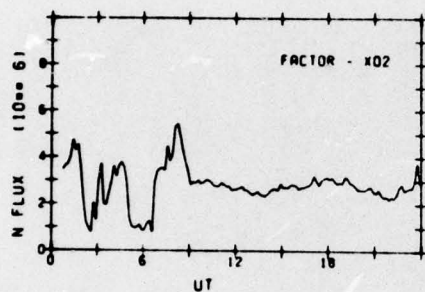
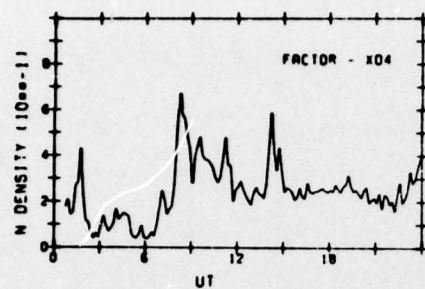
ELECTRONS



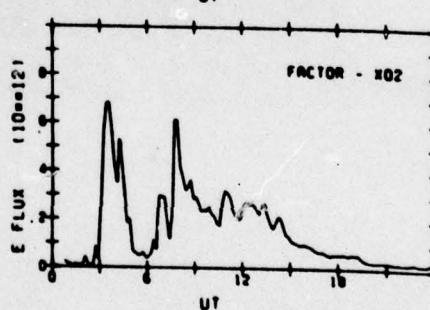
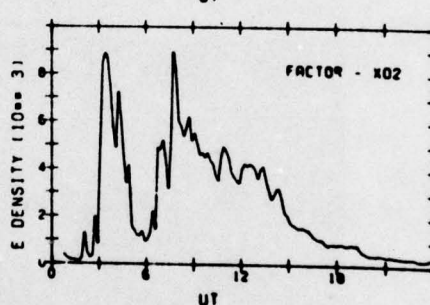
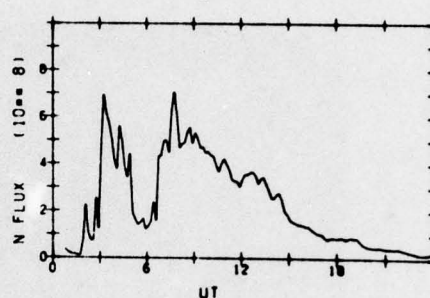
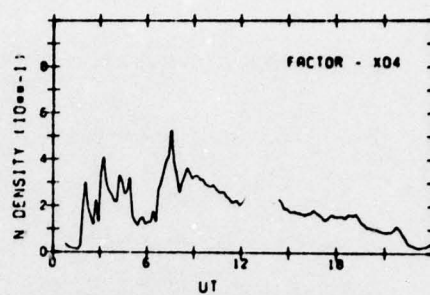


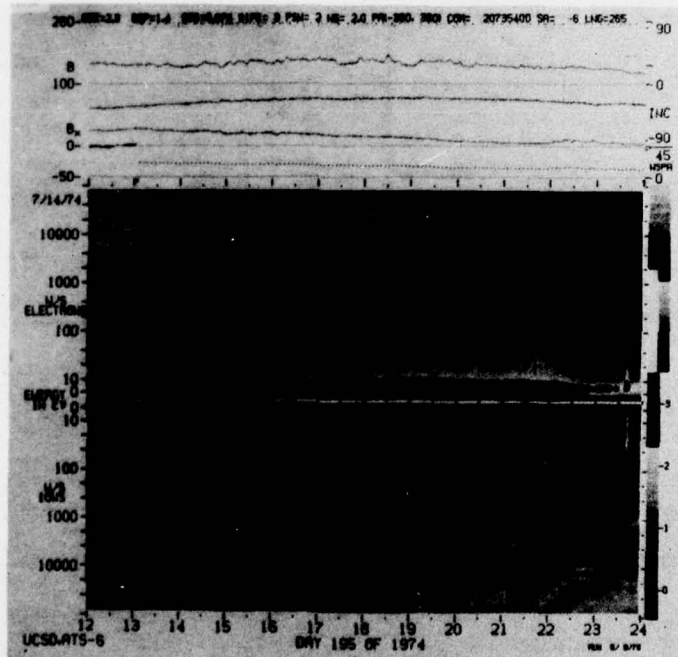
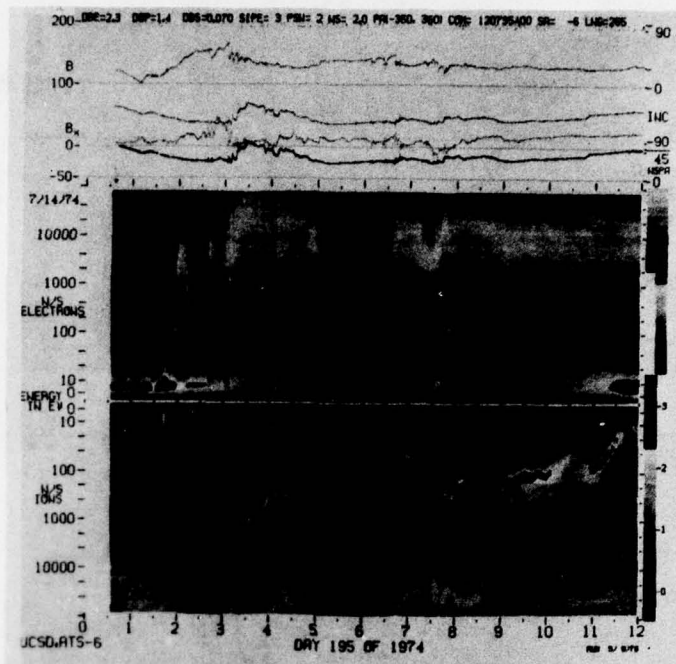
ATS-6 DATA
74/195

IONS



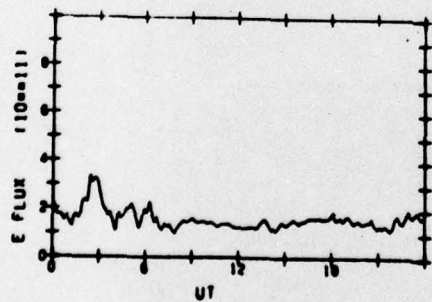
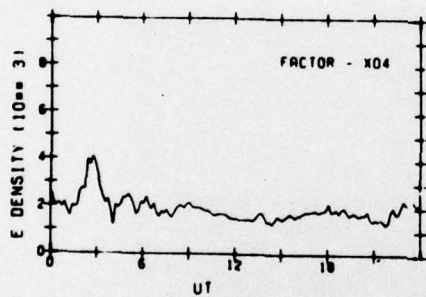
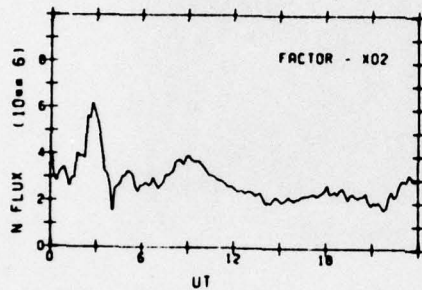
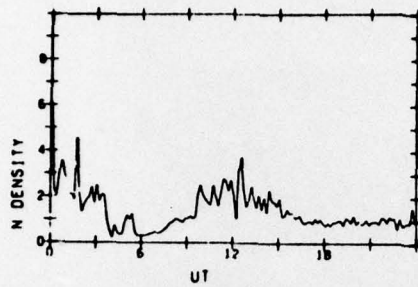
ELECTRONS



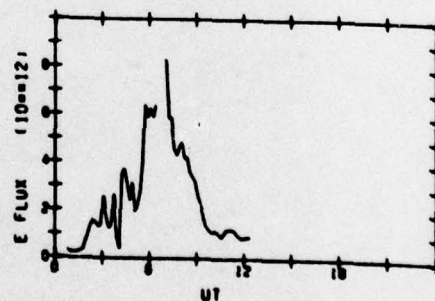
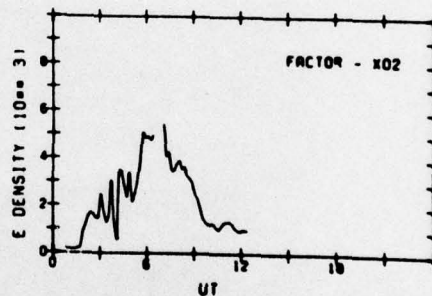
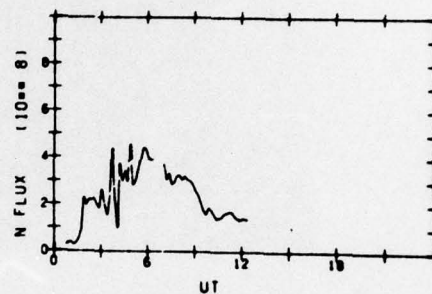
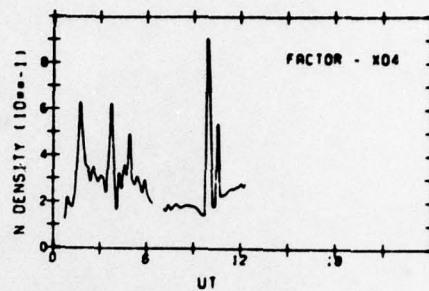


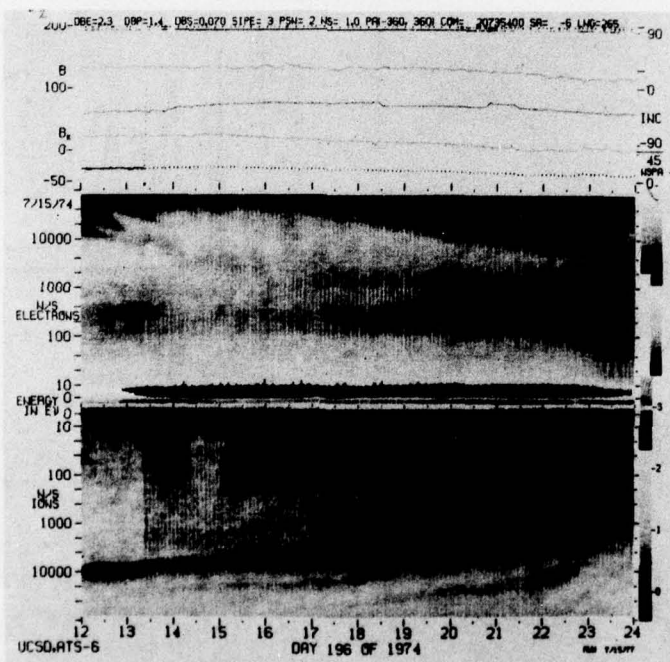
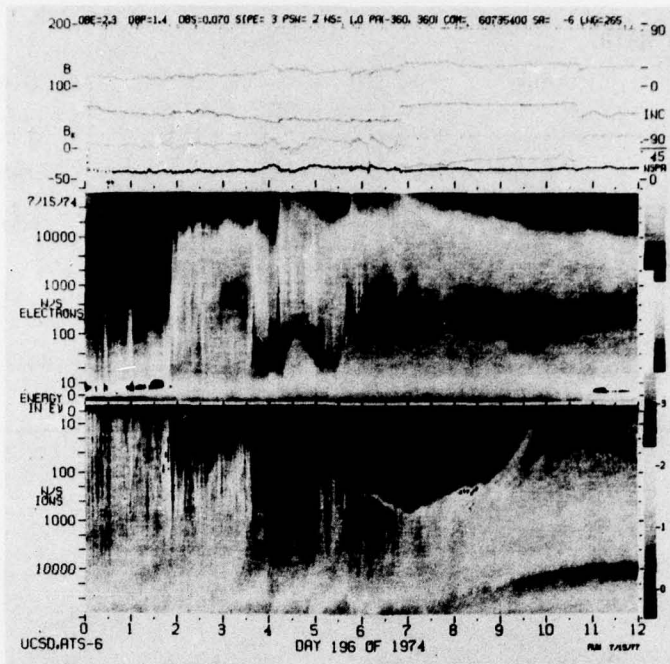
ATS-6 DATA
74/196

IONS



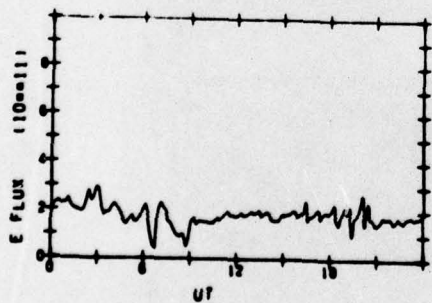
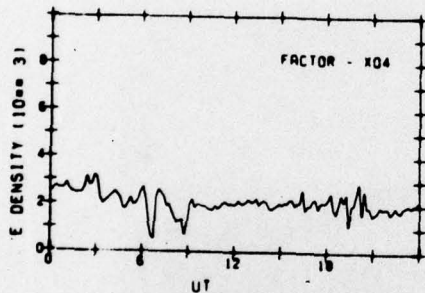
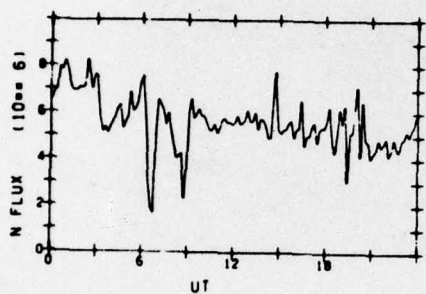
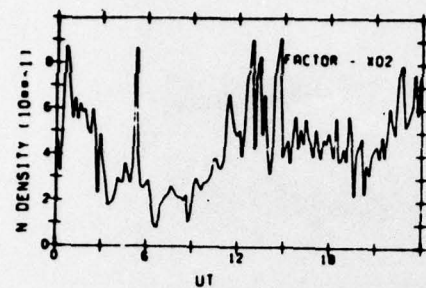
ELECTRONS



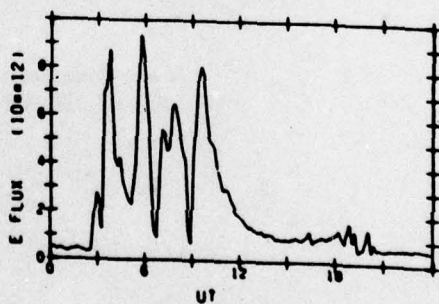
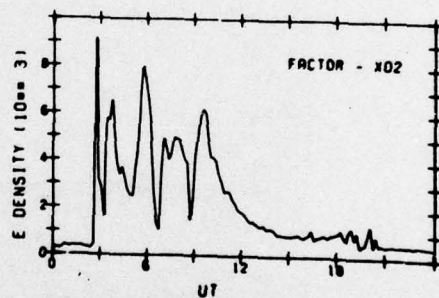
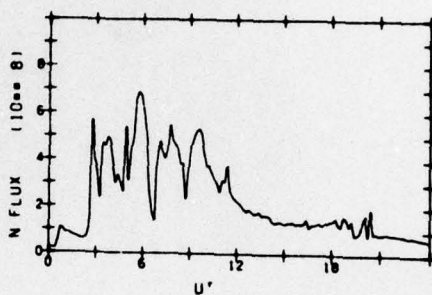
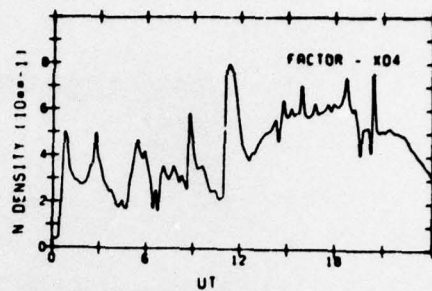


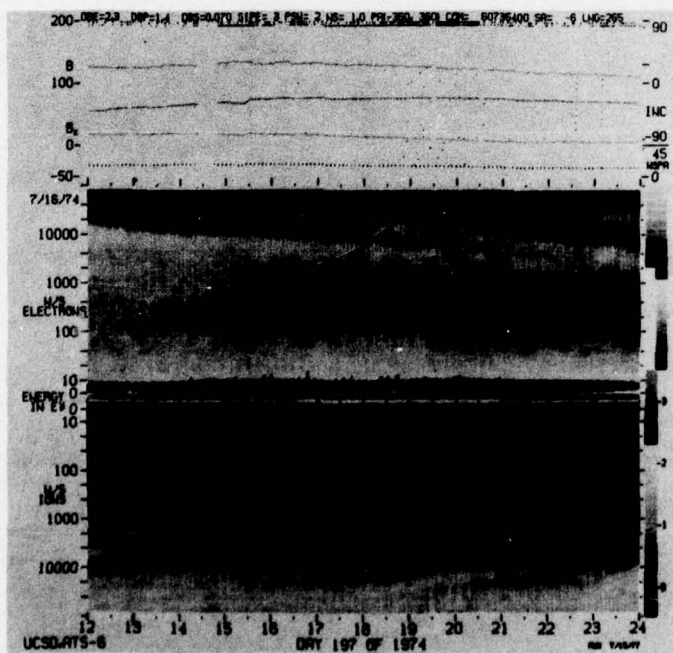
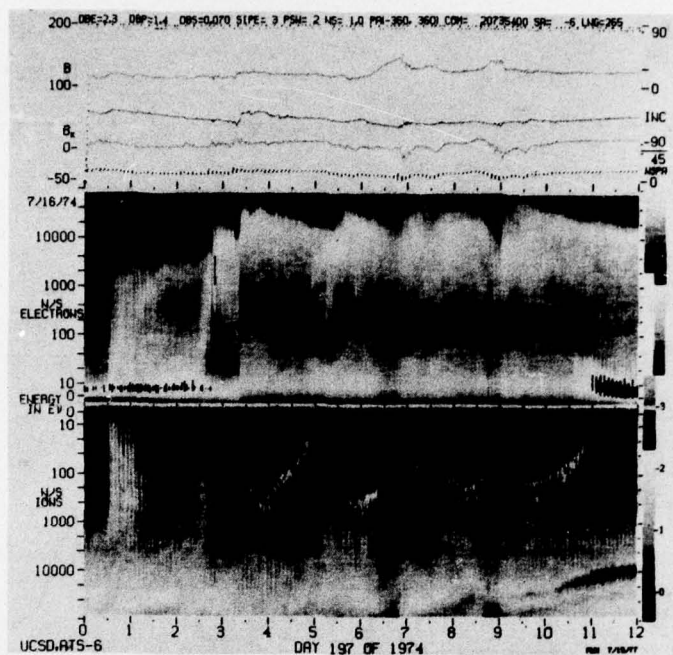
ATS-6 DATA
74/197

IONS



ELECTRONS

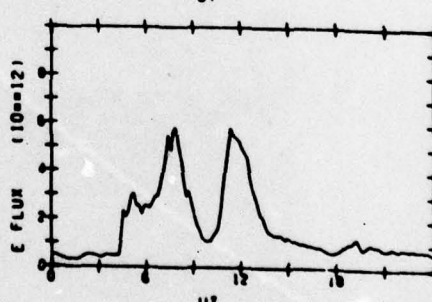
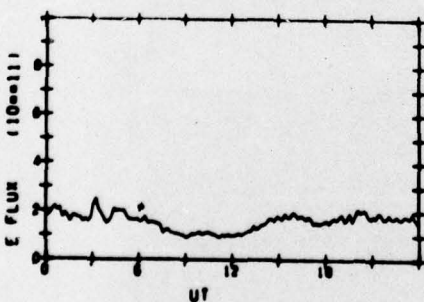
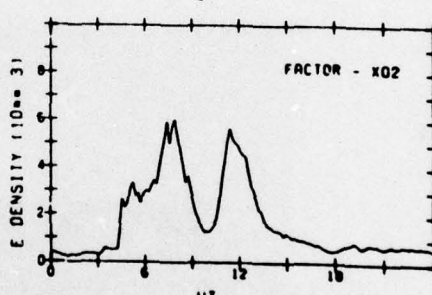
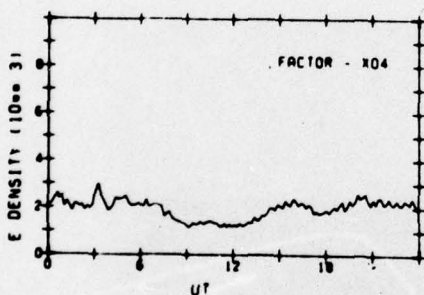
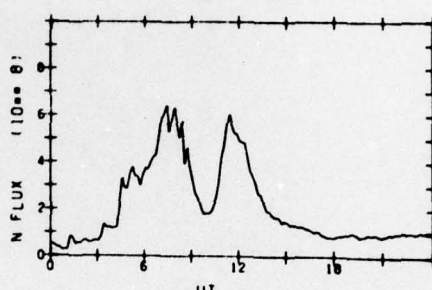
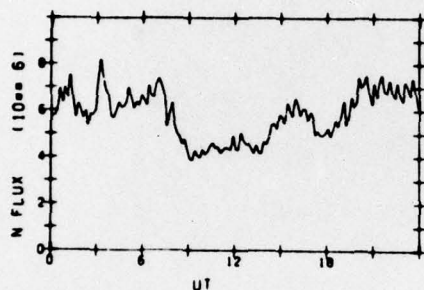
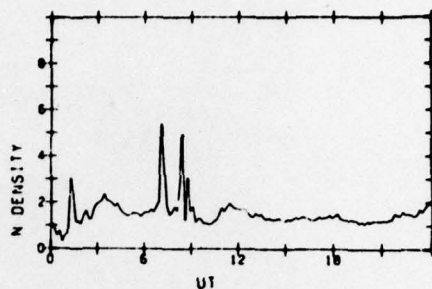
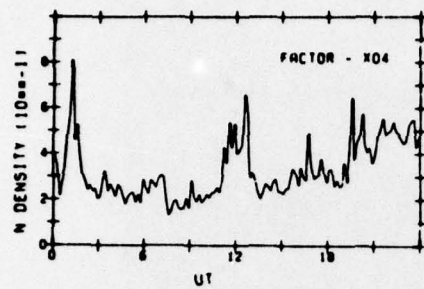


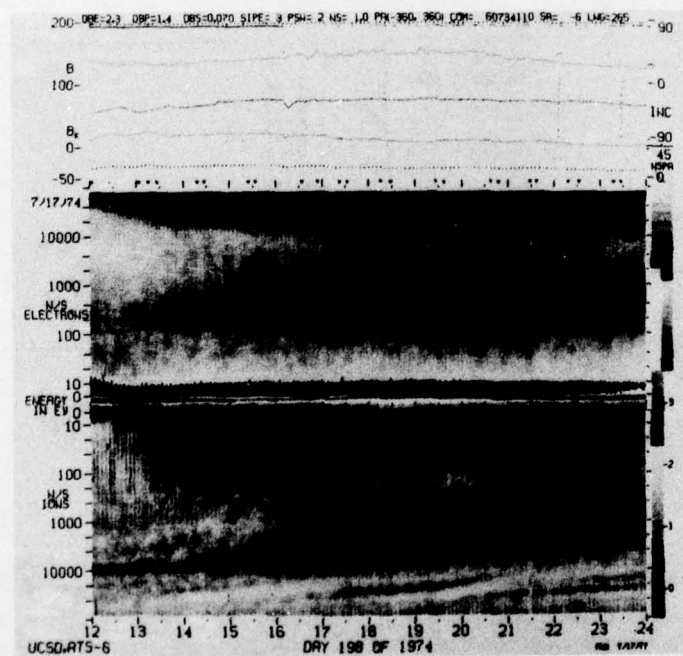
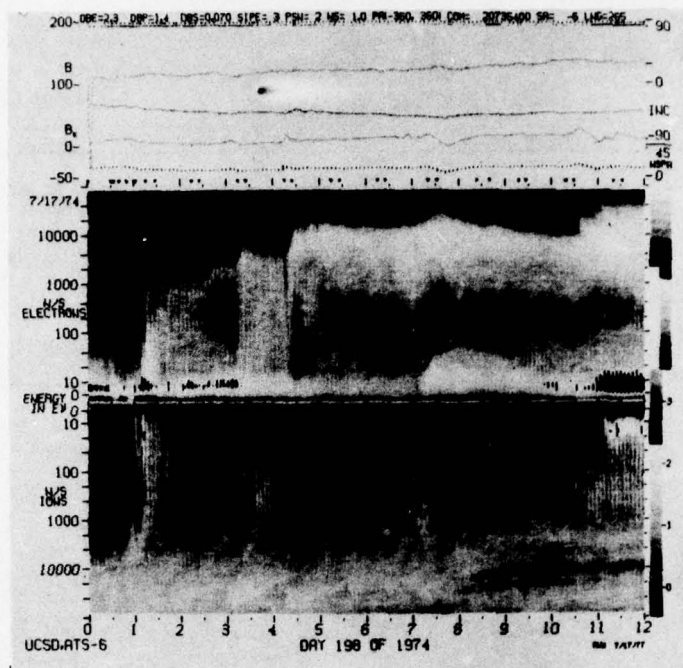


ATS-6 DATA
74/198

IONS

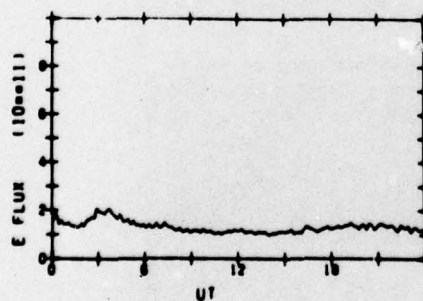
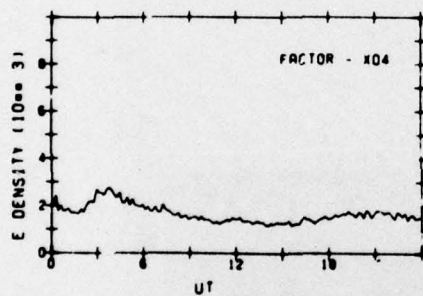
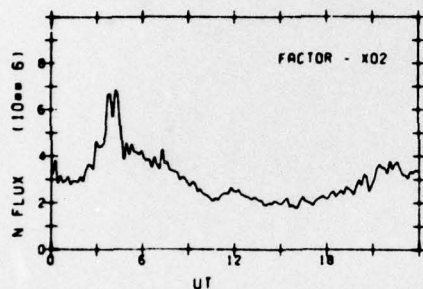
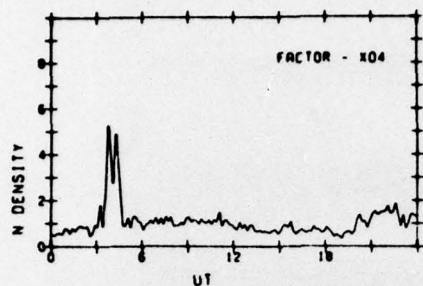
ELECTRONS



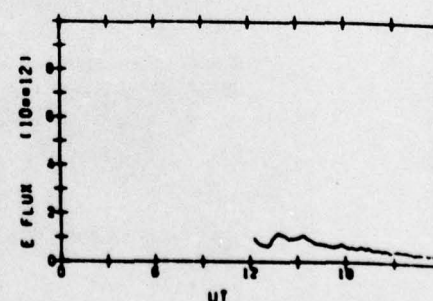
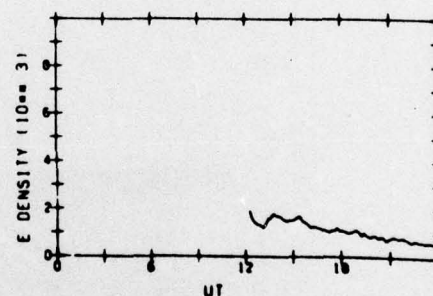
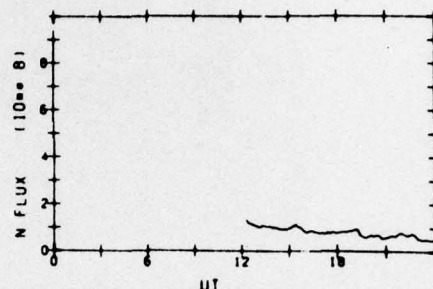
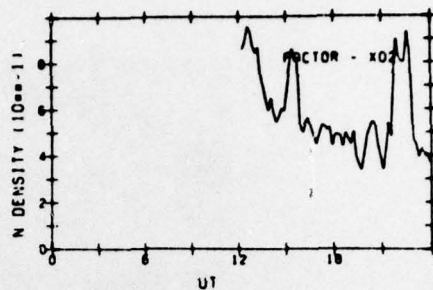


ATS-6 DATA
74/199

IONS

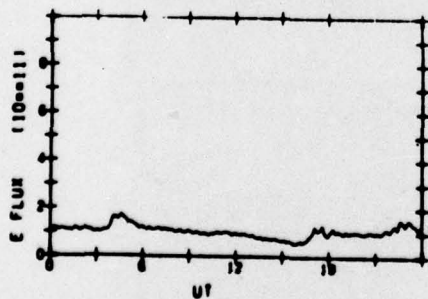
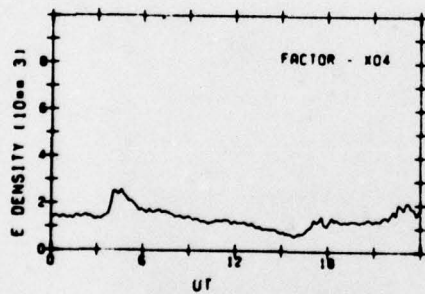
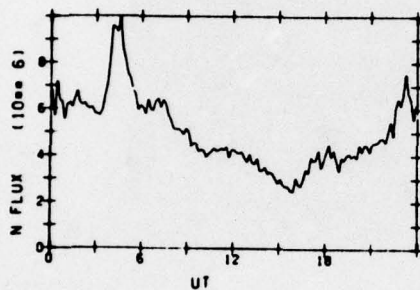
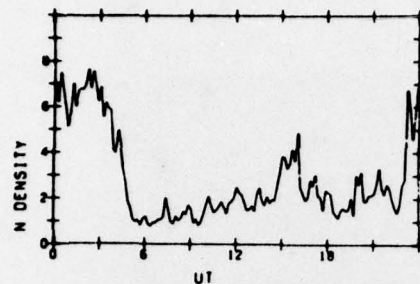


ELECTRONS

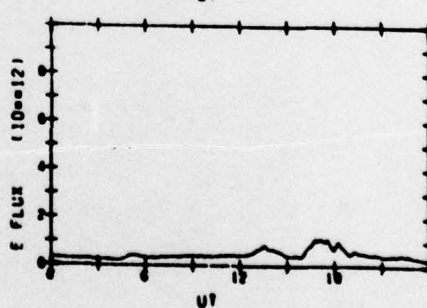
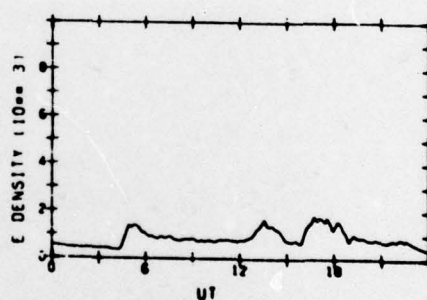
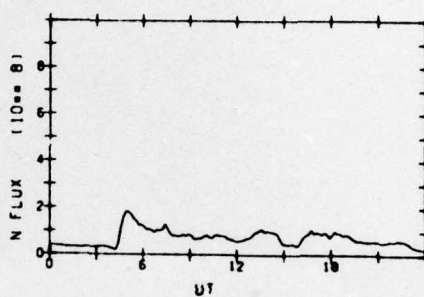
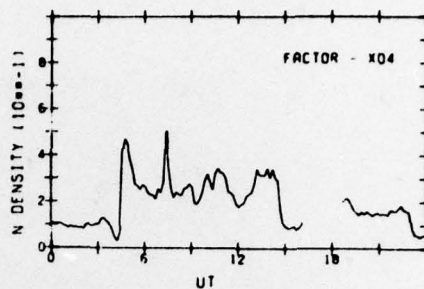


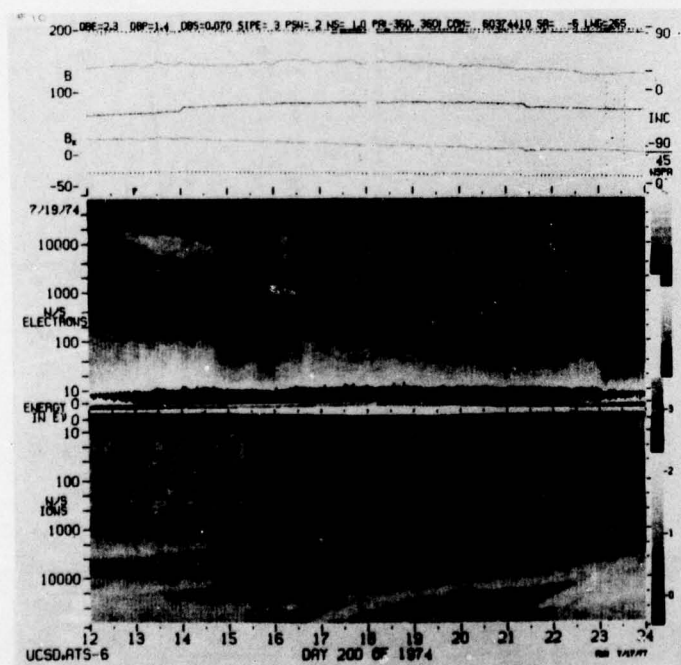
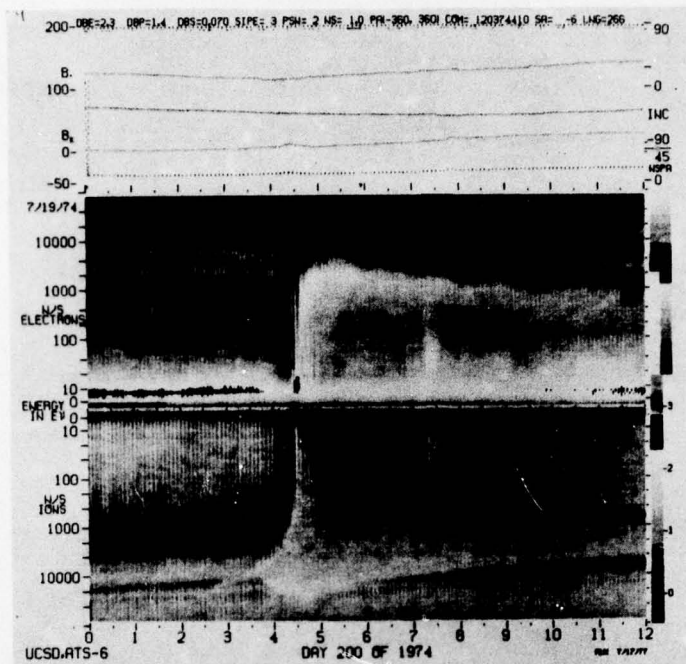
ATS-6 DATA
74/200

IONS



ELECTRONS

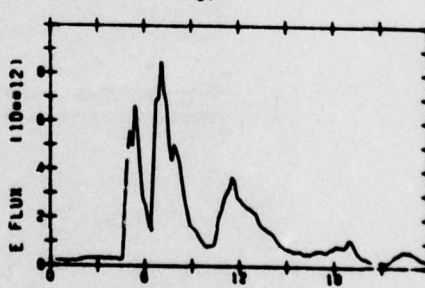
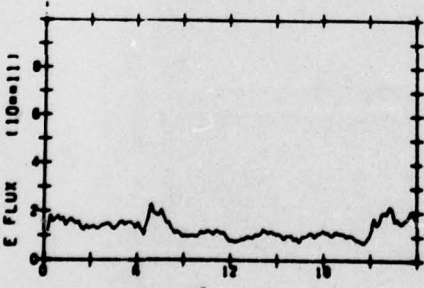
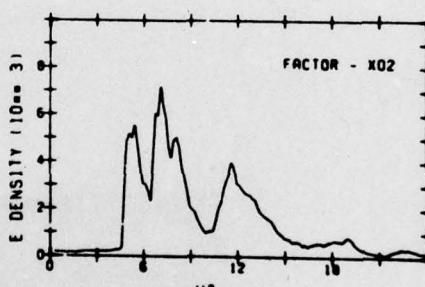
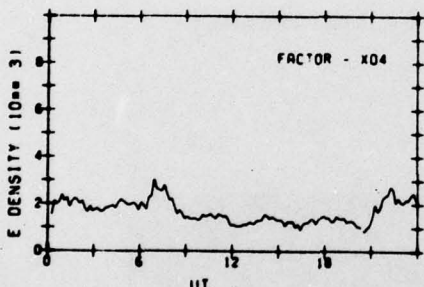
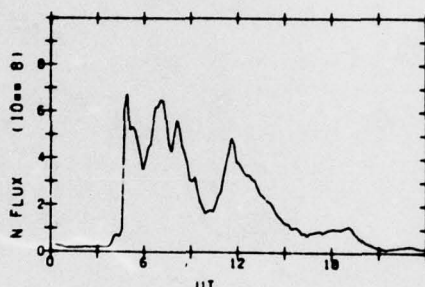
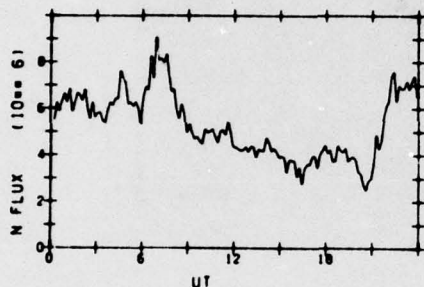
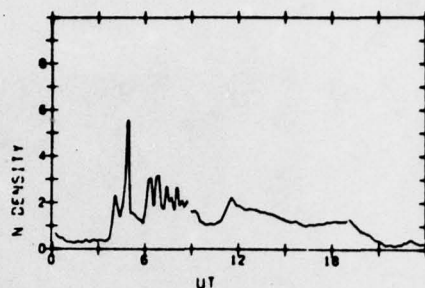
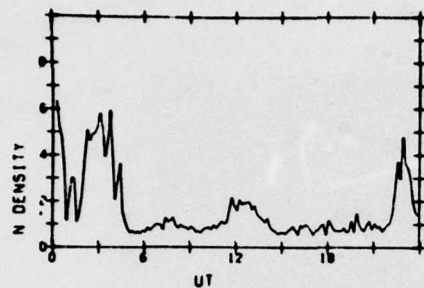




ATS-6 DATA
74/201

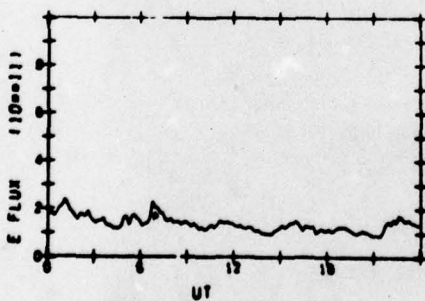
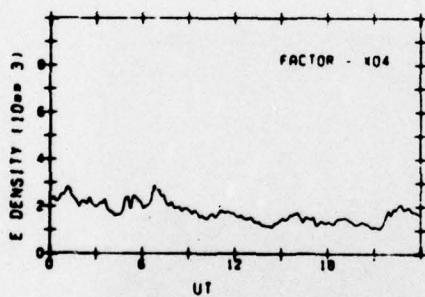
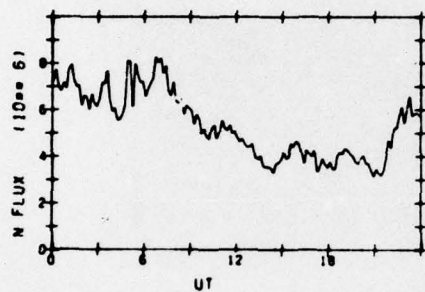
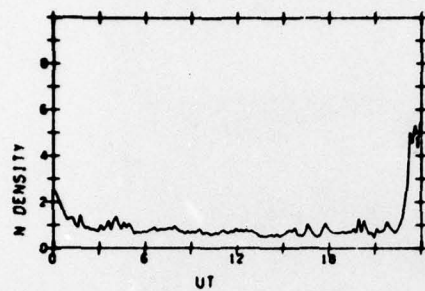
IONS

ELECTRONS

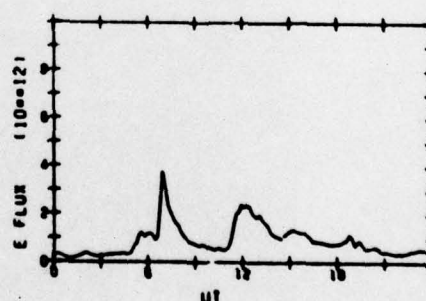
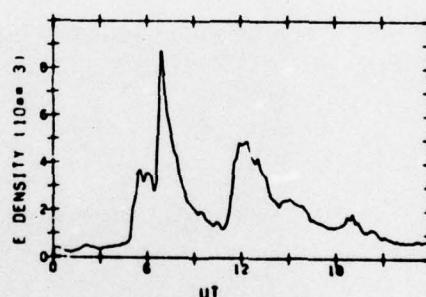
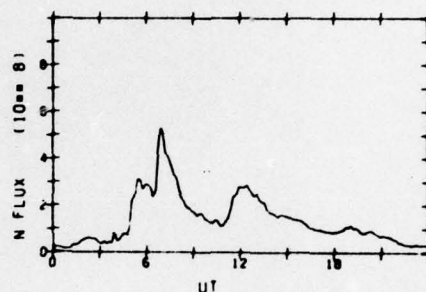
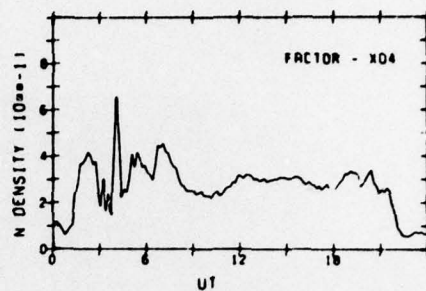


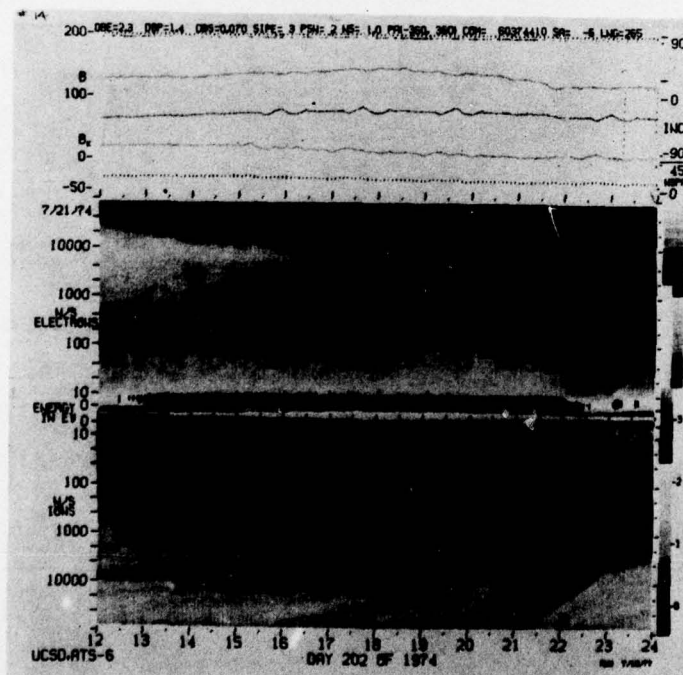
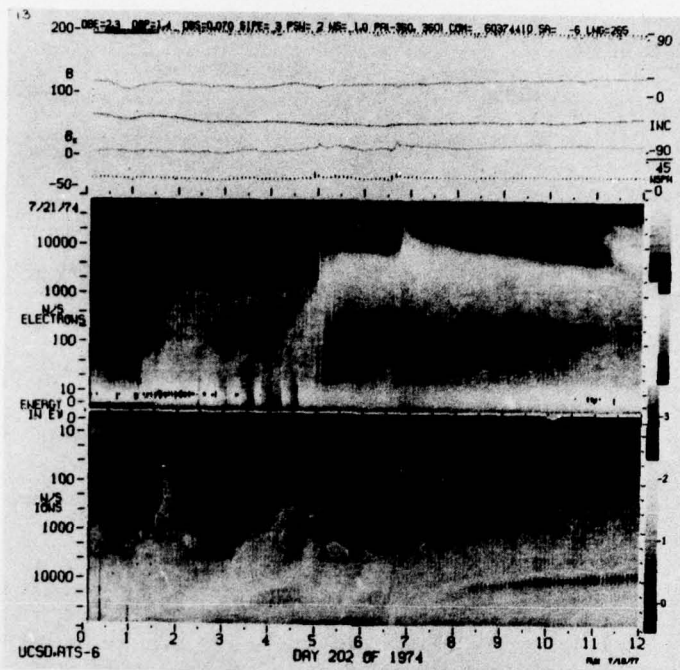
ATS-6 DATA
74/202

IONS



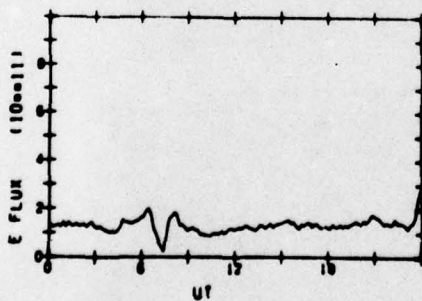
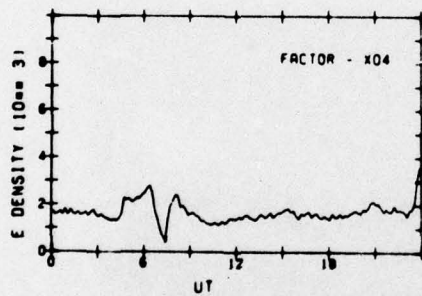
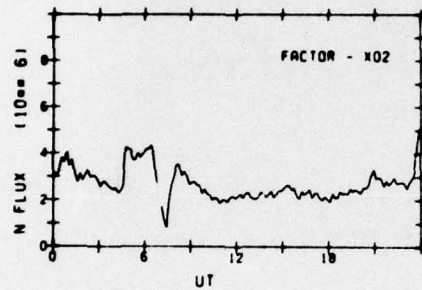
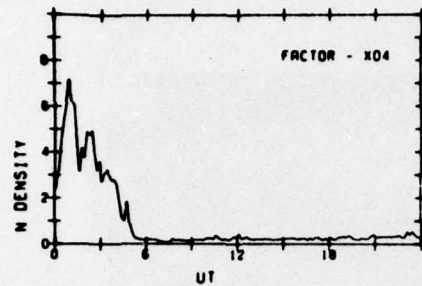
ELECTRONS



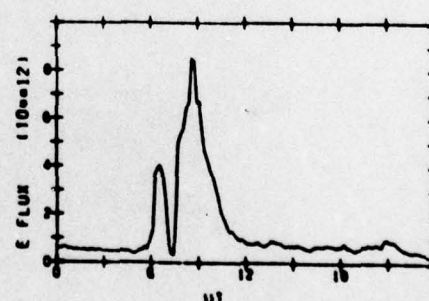
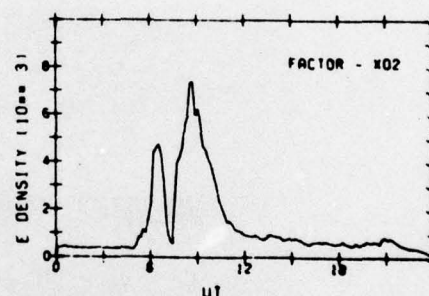
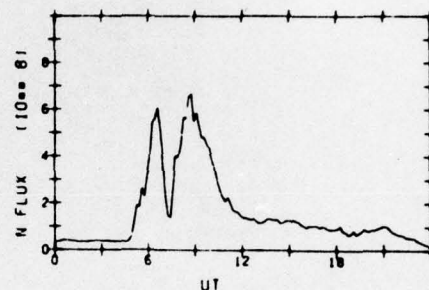
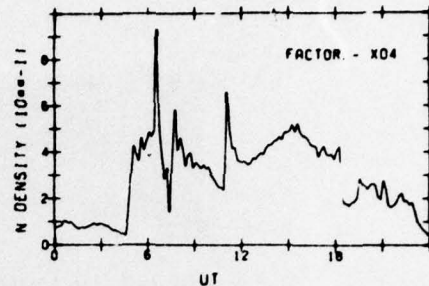


ATS-6 DATA
74/203

IONS

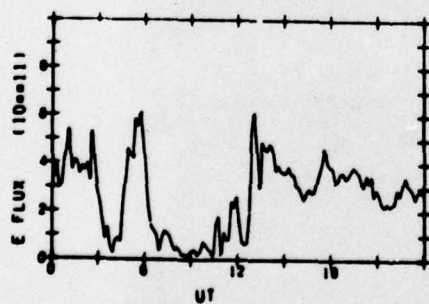
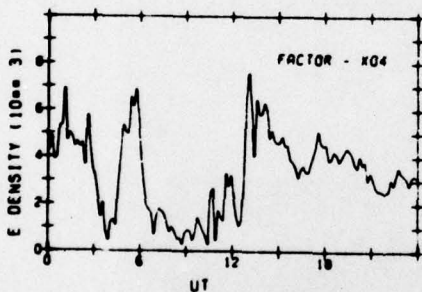
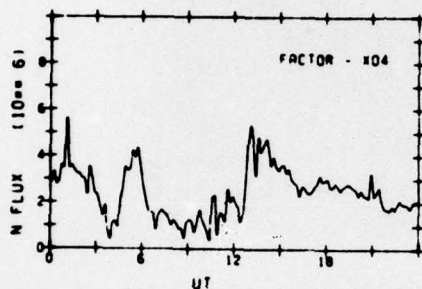
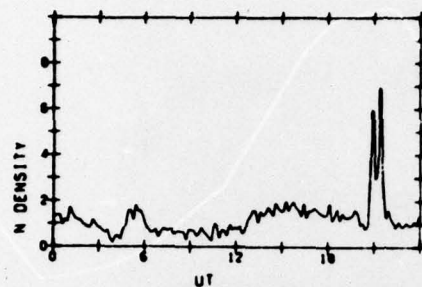


ELECTRONS

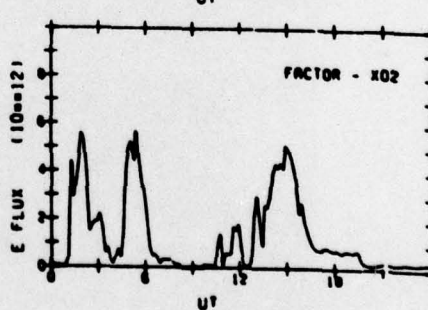
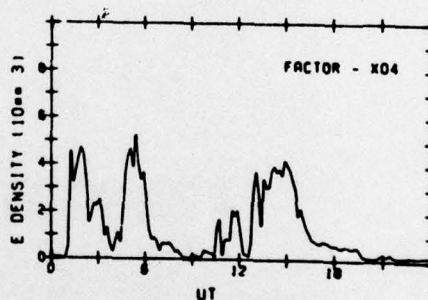
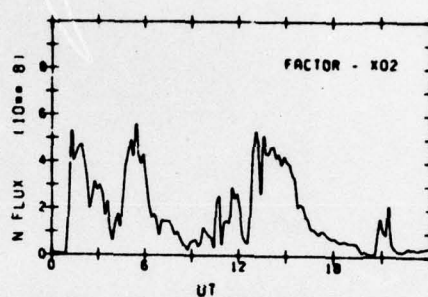
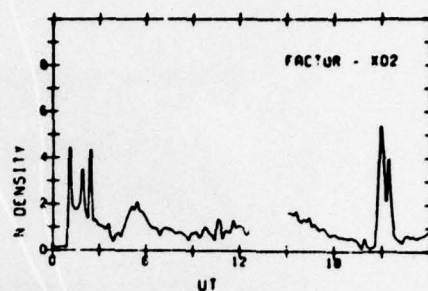


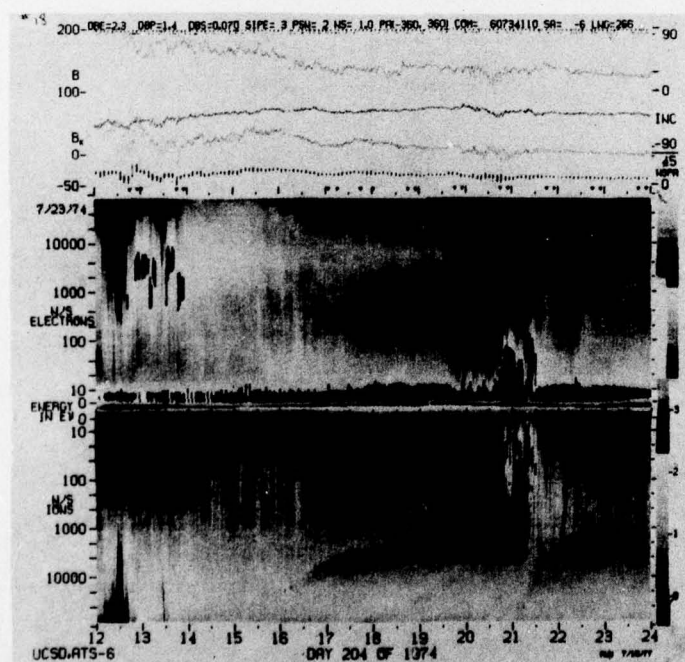
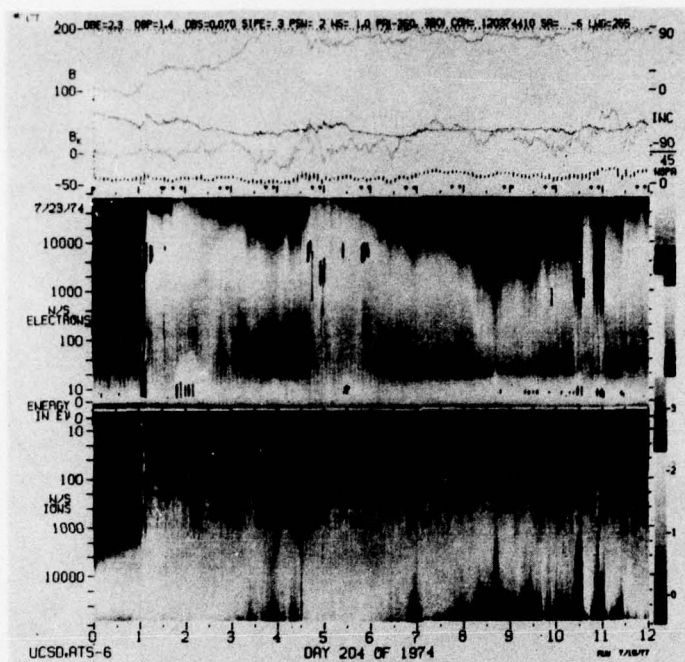
ATS-6 DATA
74/204

IONS



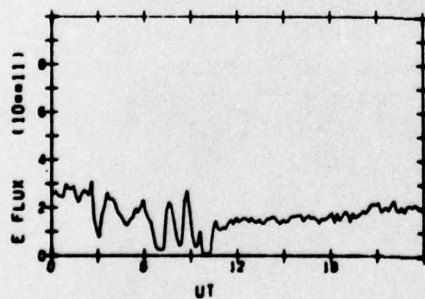
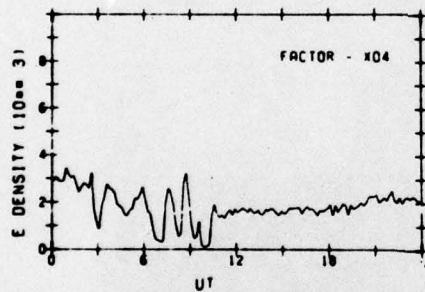
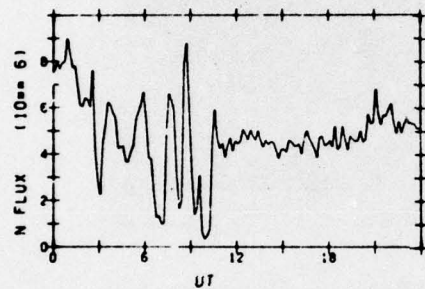
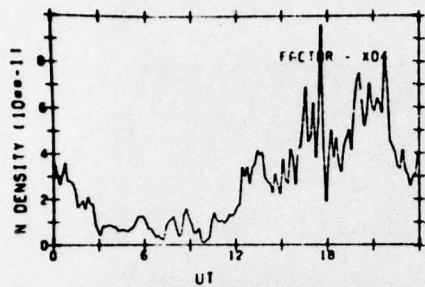
ELECTRONS



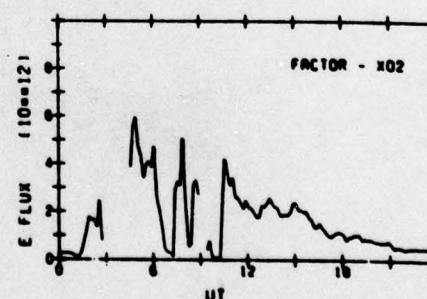
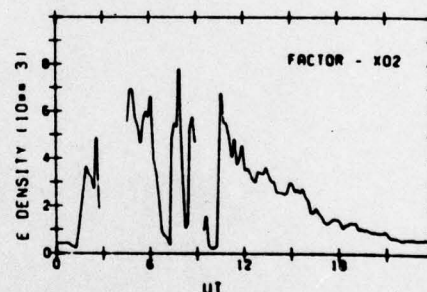
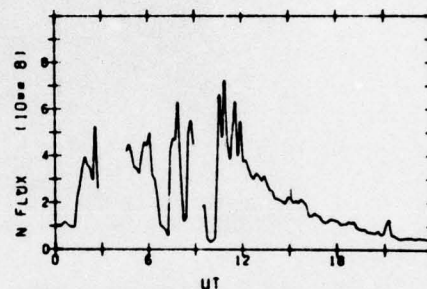
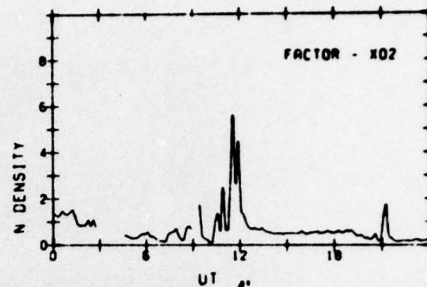


ATS-6 DATA
74/205

IONS

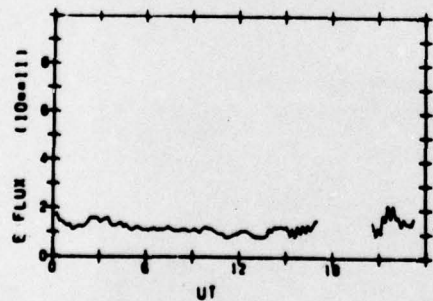
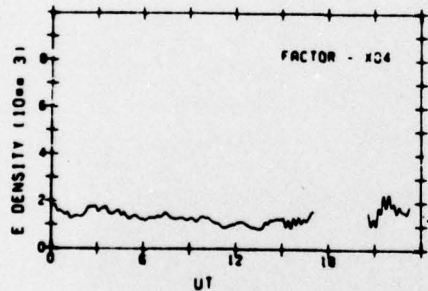
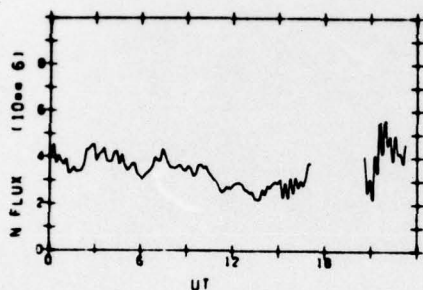
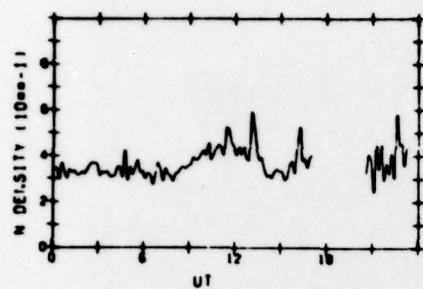


ELECTRONS

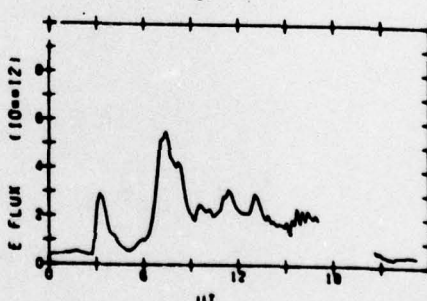
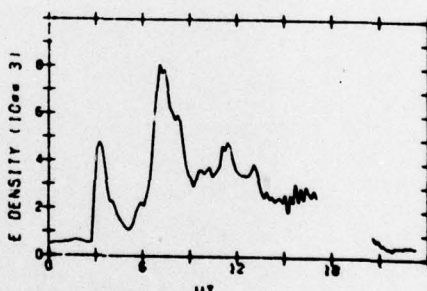
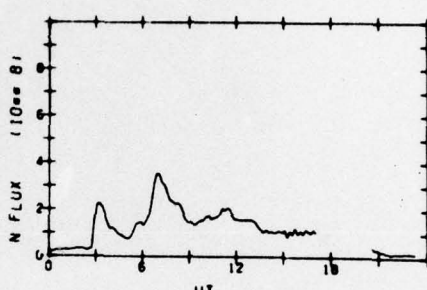
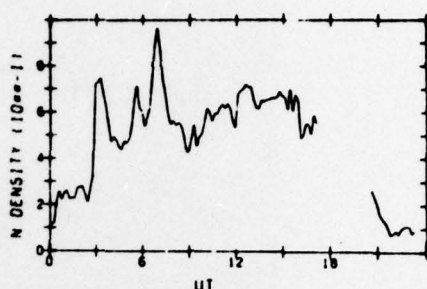


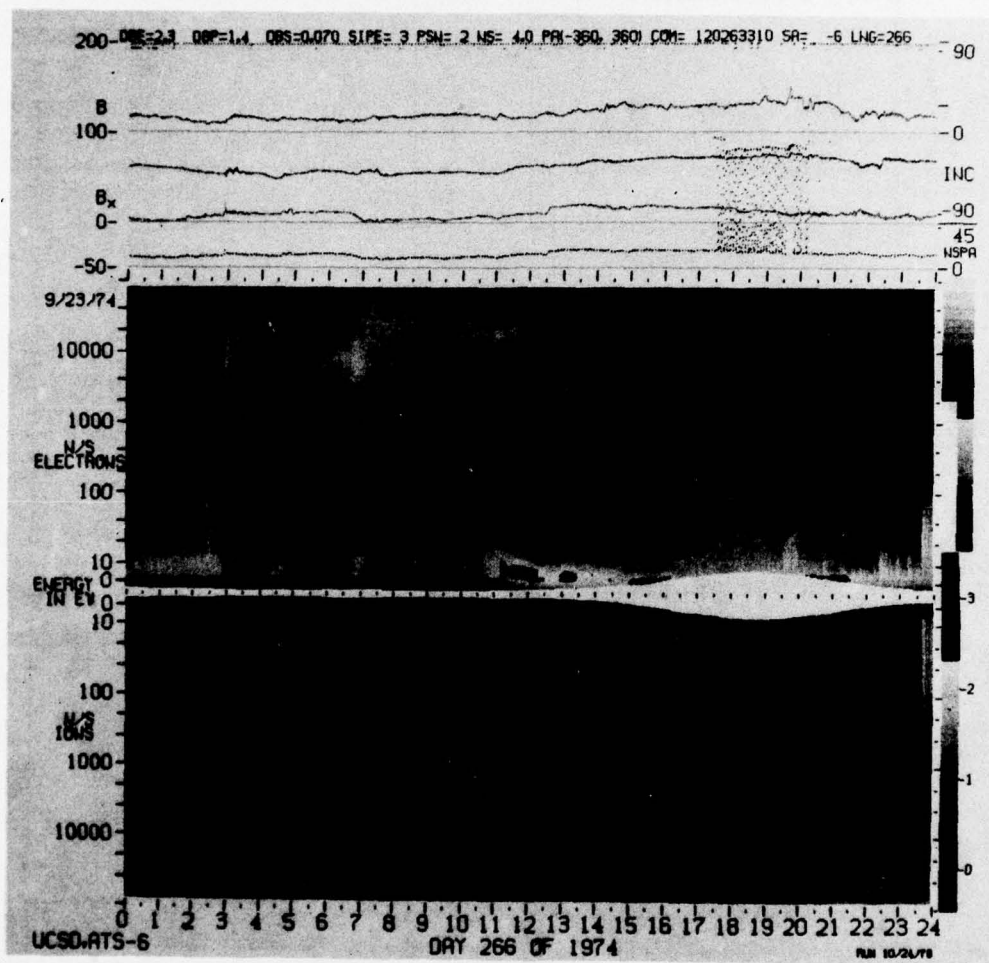
ATS-6 DATA
74/266

IONS



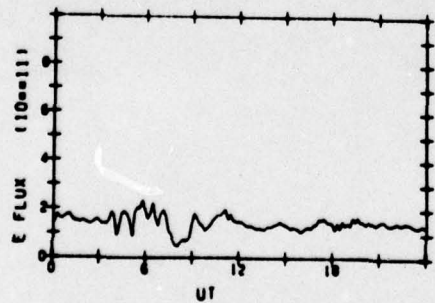
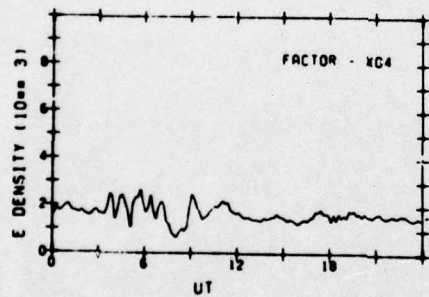
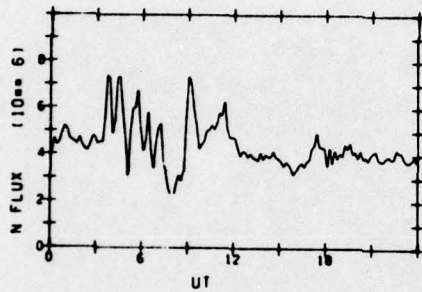
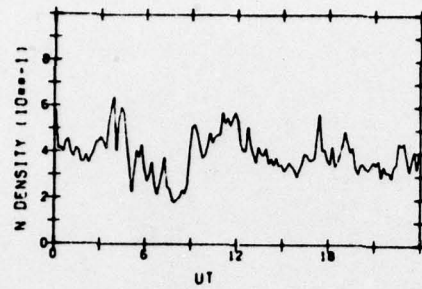
ELECTRONS



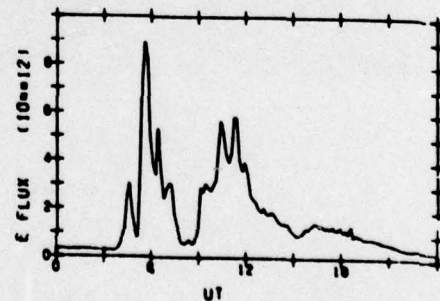
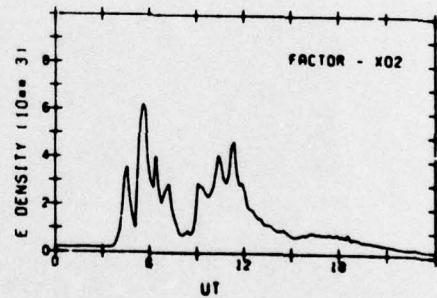
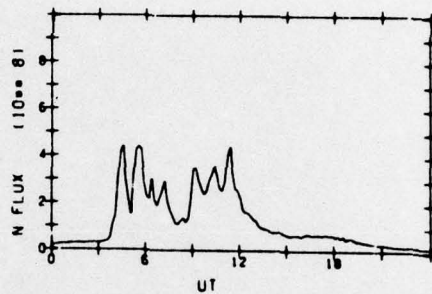
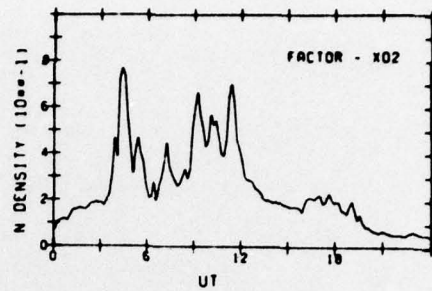


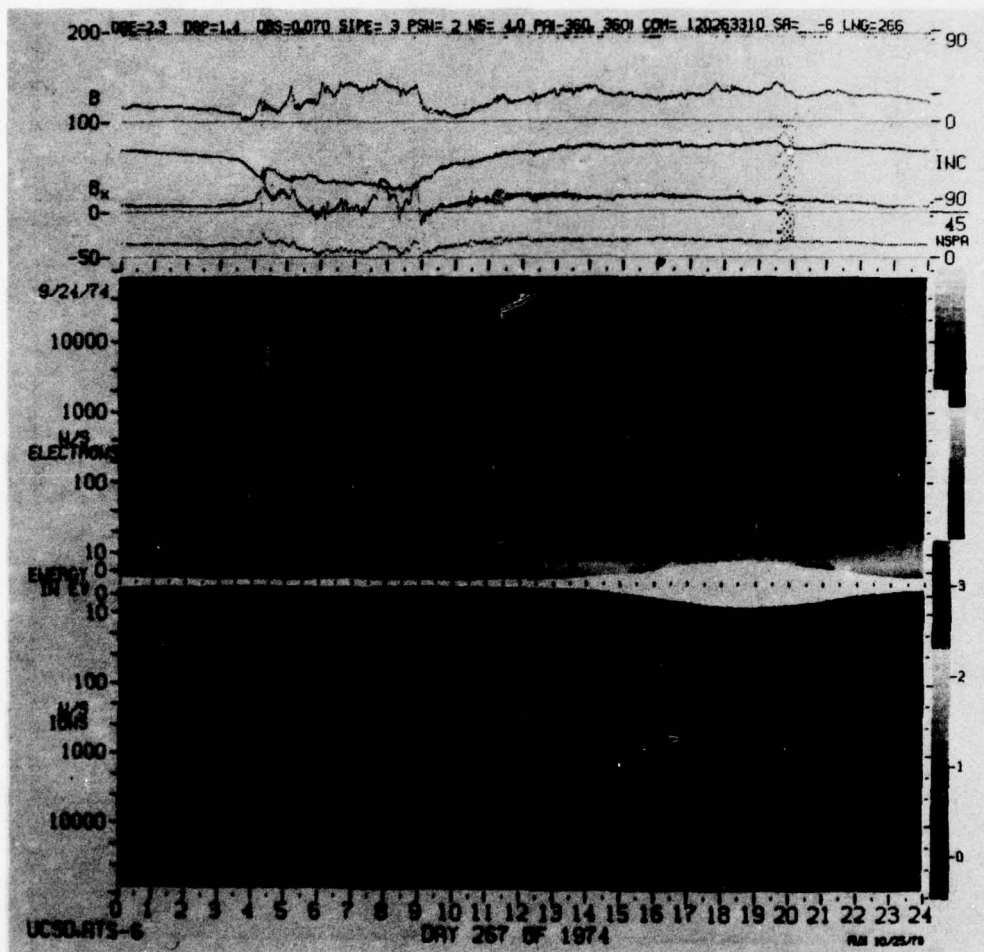
ATS-6 DATA
74/267

IONS



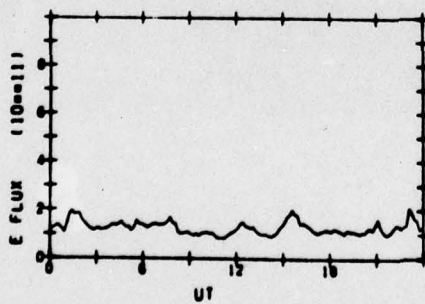
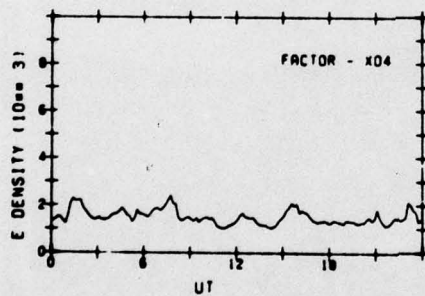
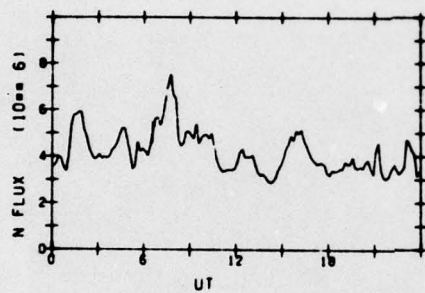
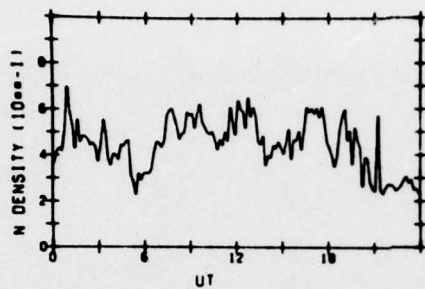
ELECTRONS



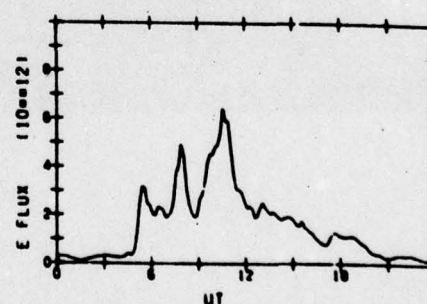
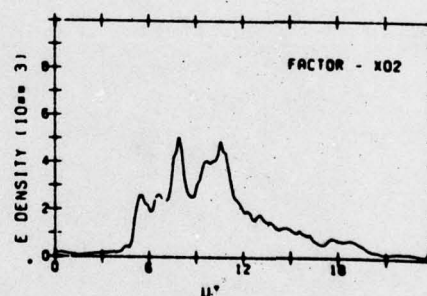
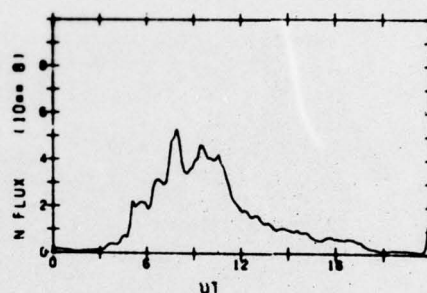
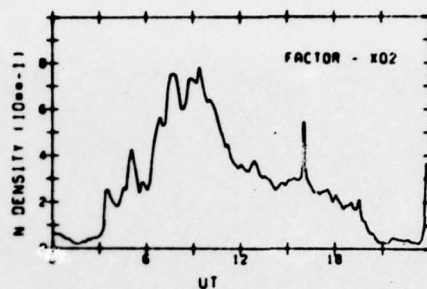


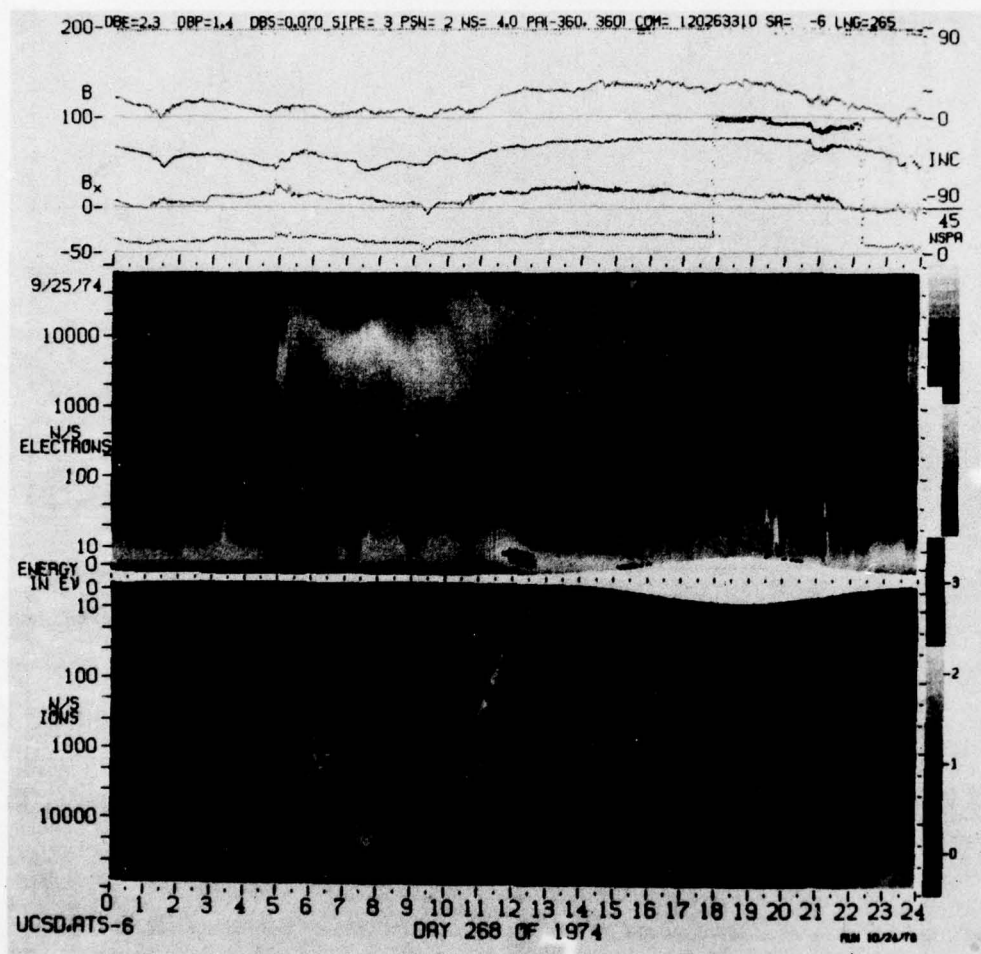
ATS-6 DATA
74/268

IONS



ELECTRONS

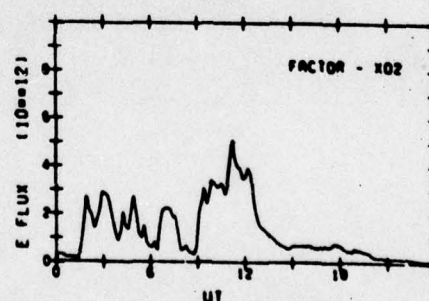
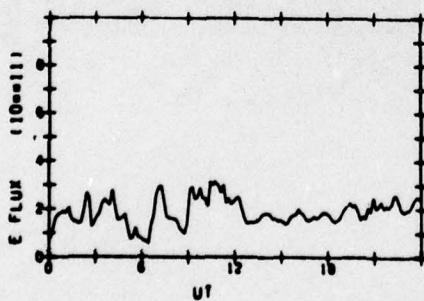
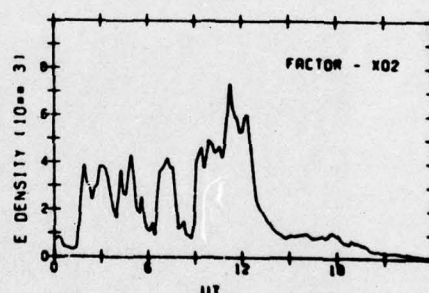
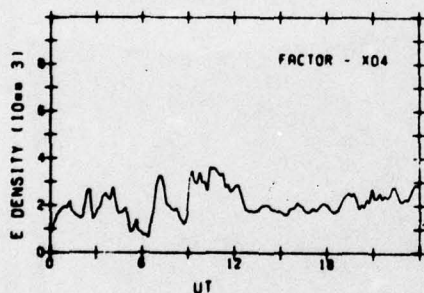
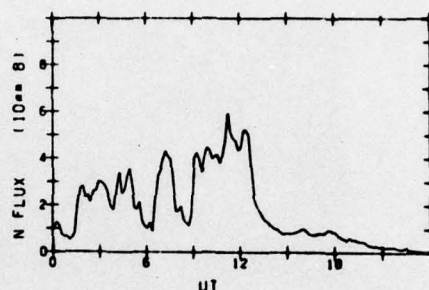
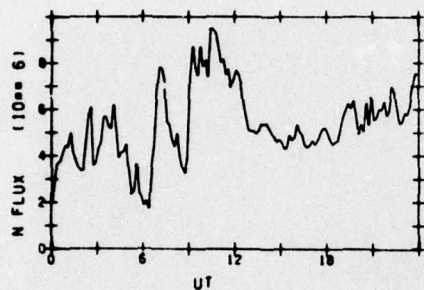
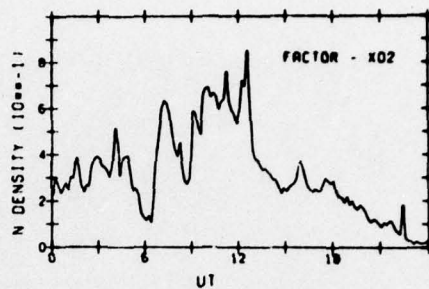
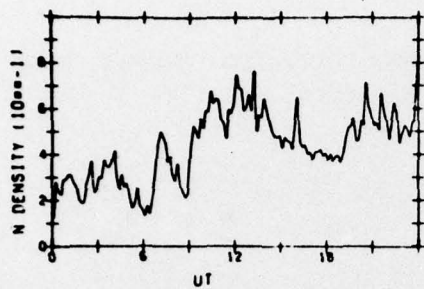


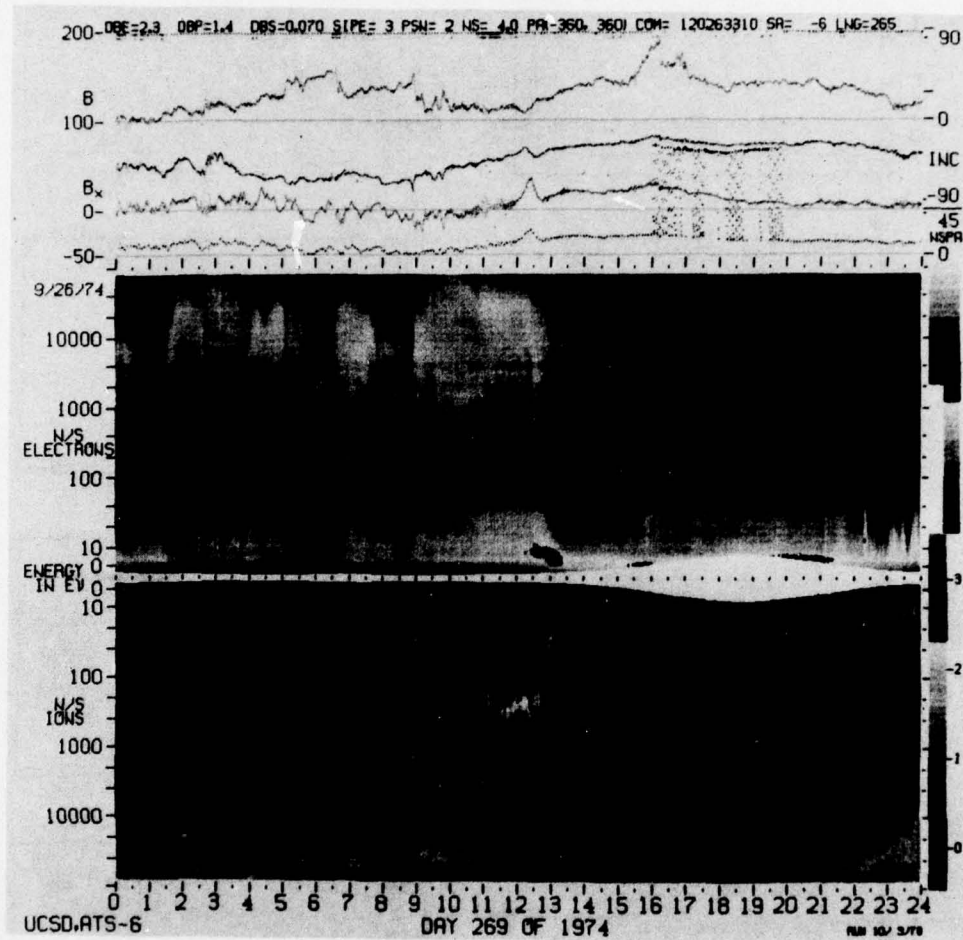


ATS-6 DATA
74/269

IONS

ELECTRONS

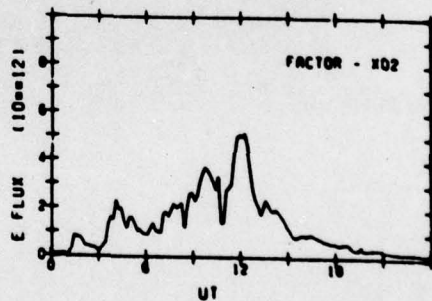
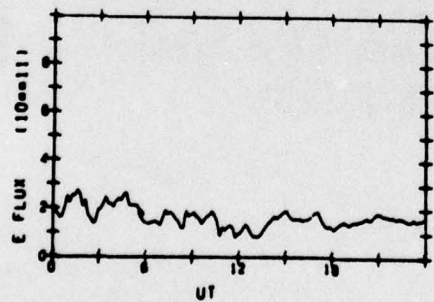
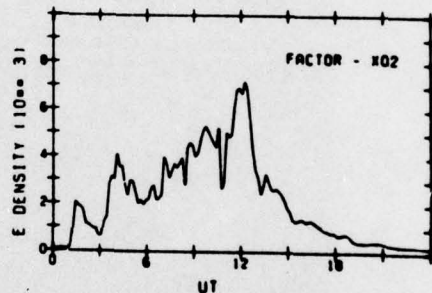
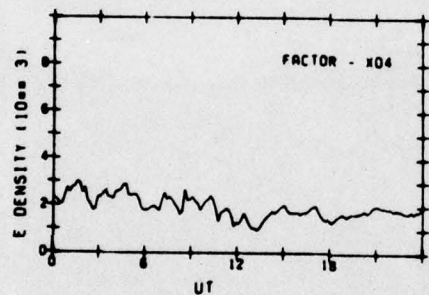
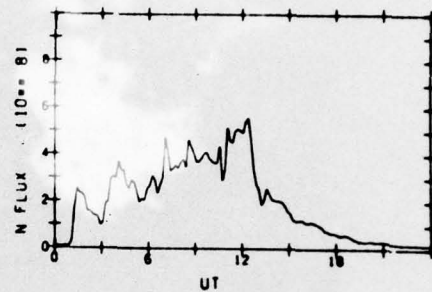
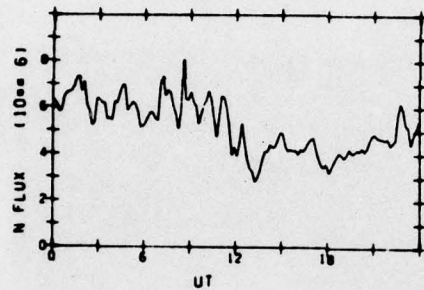
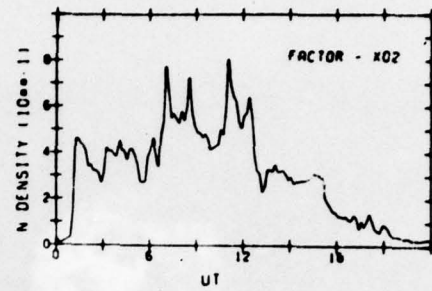
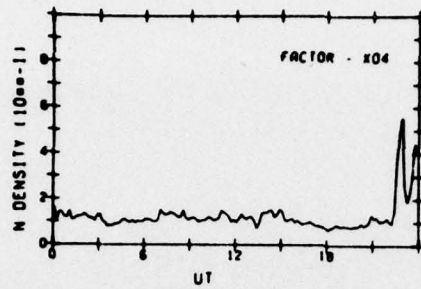


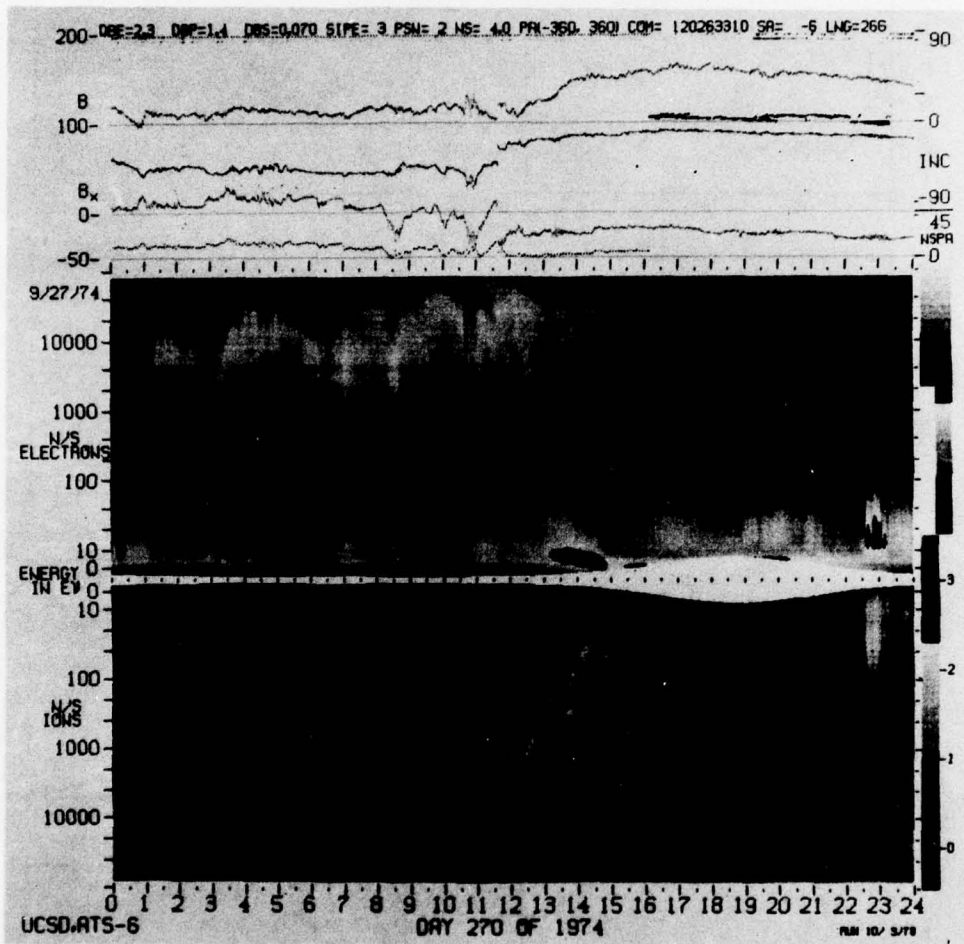


ATS-6 DATA
74/270

IONS

ELECTRONS

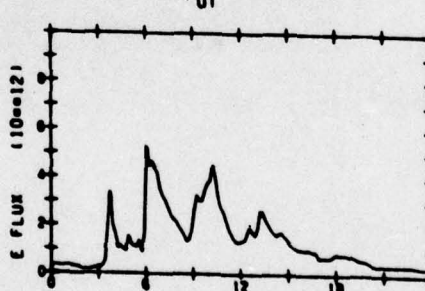
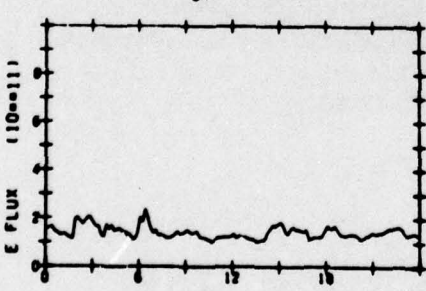
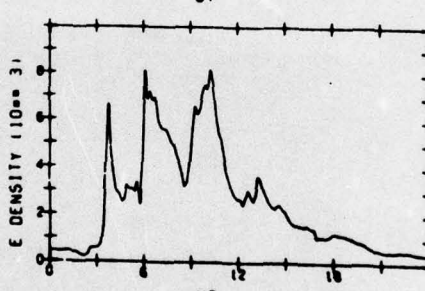
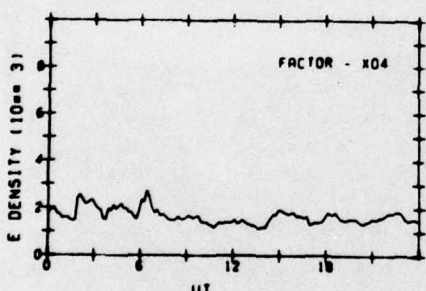
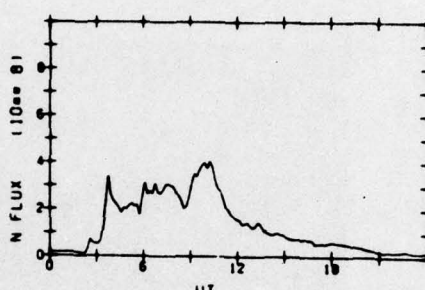
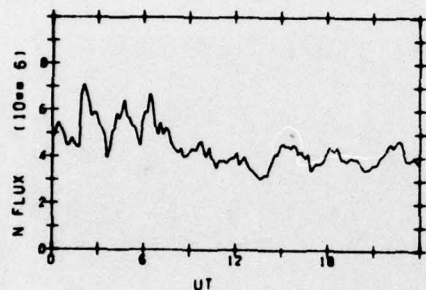
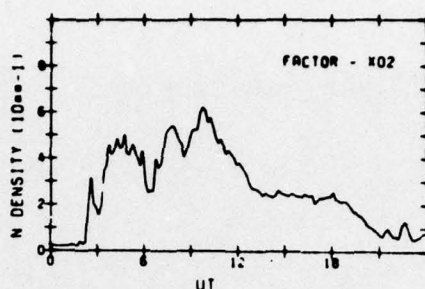
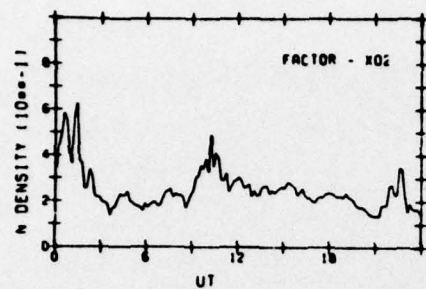


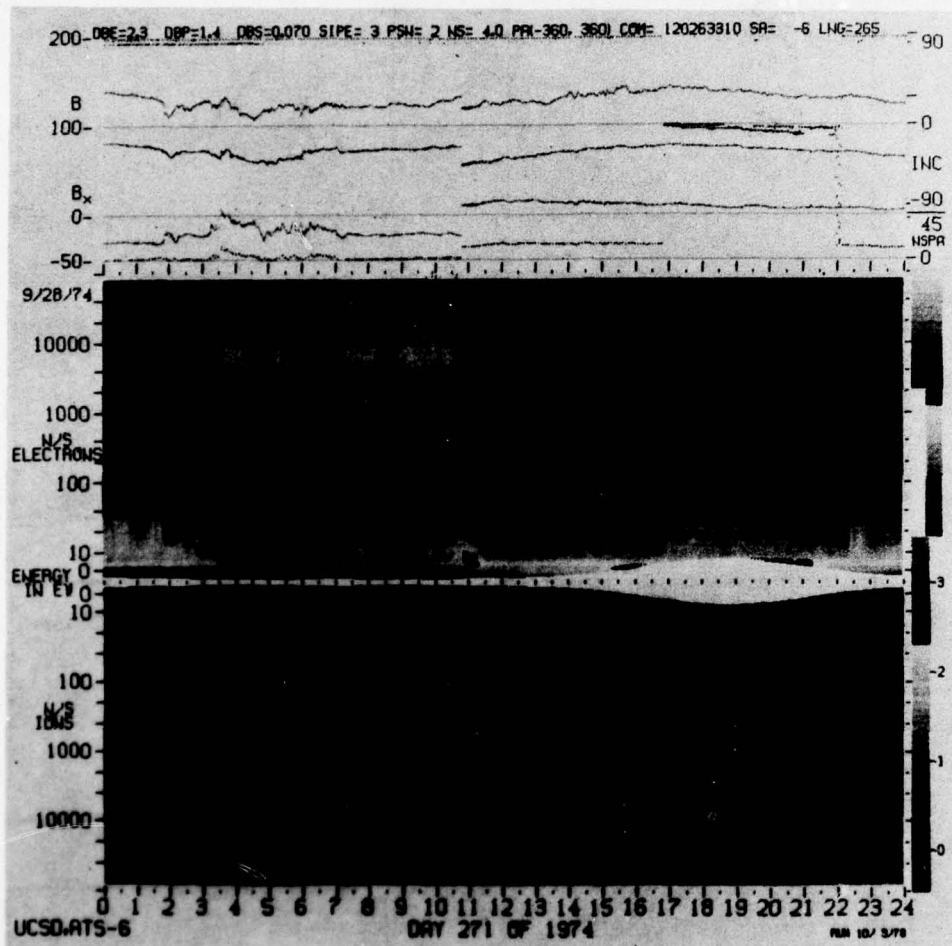


ATS-6 DATA
74/271

IONS

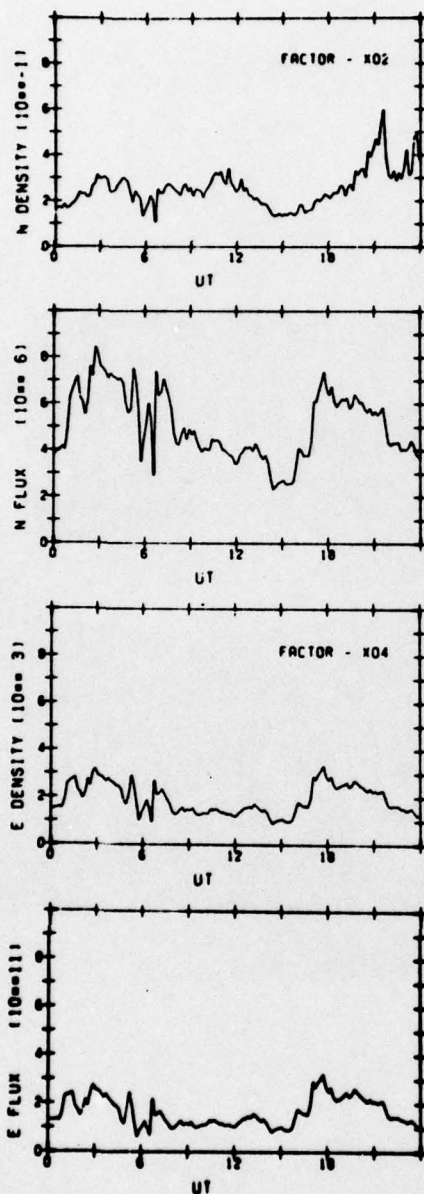
ELECTRONS



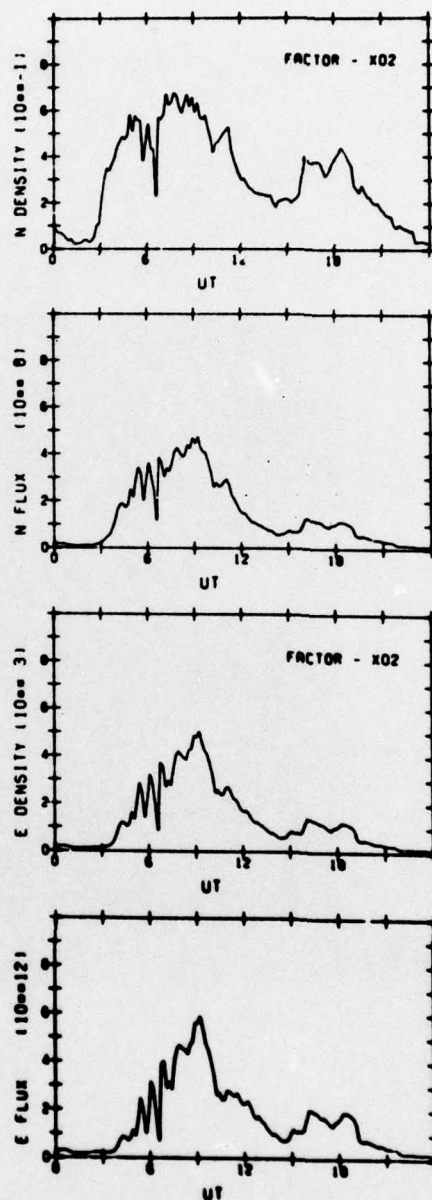


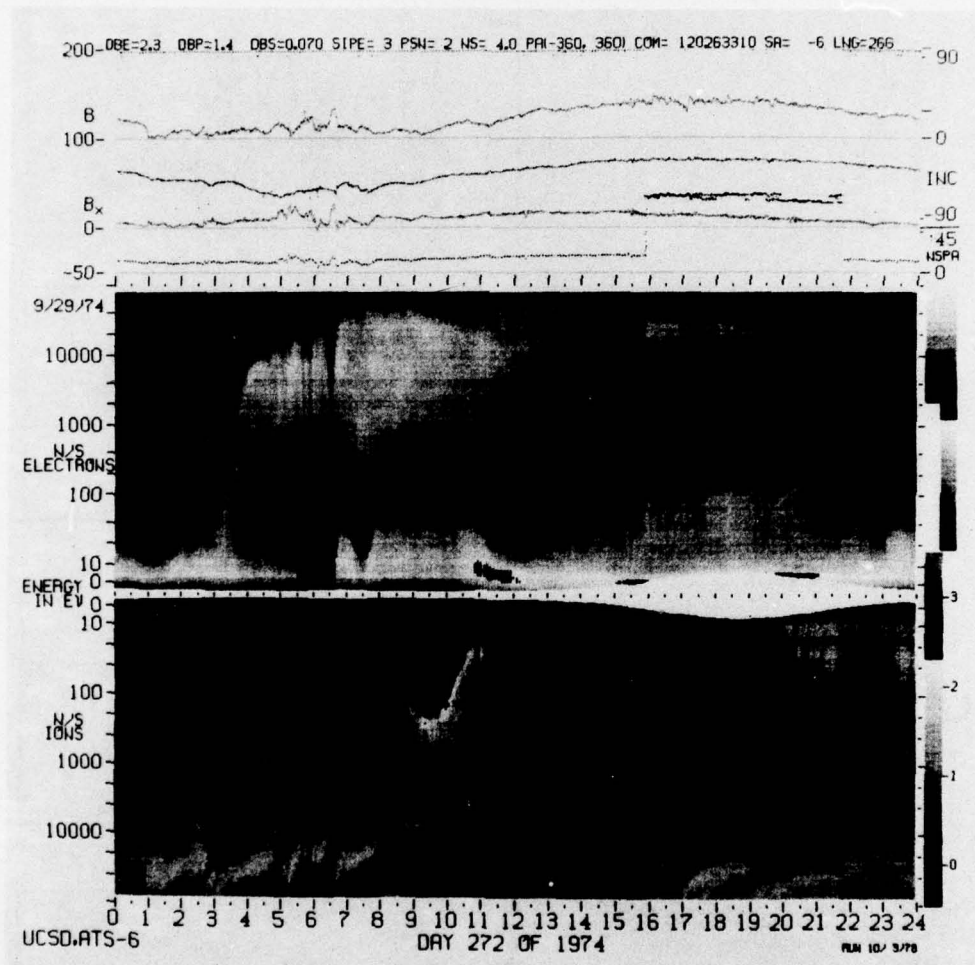
ATS-6 DATA
74/272

IONS



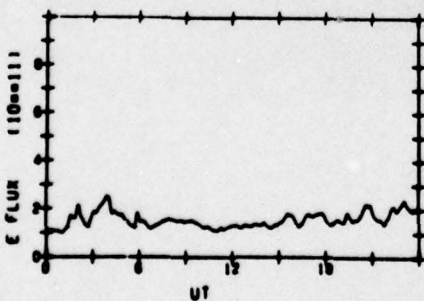
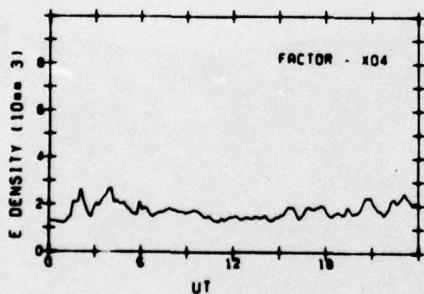
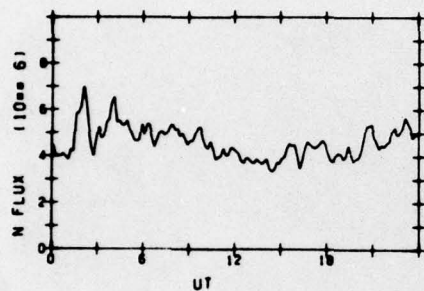
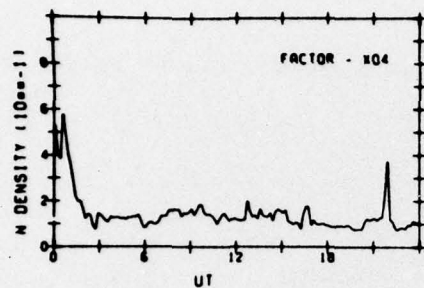
ELECTRONS



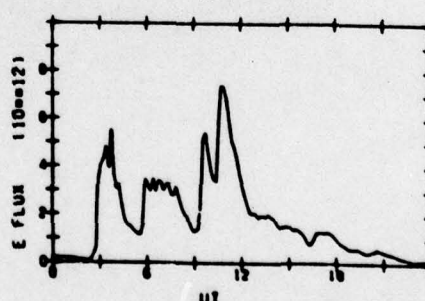
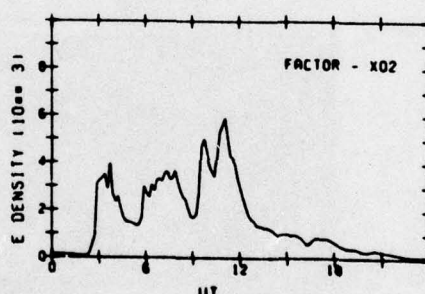
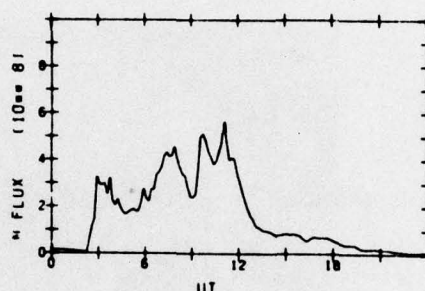
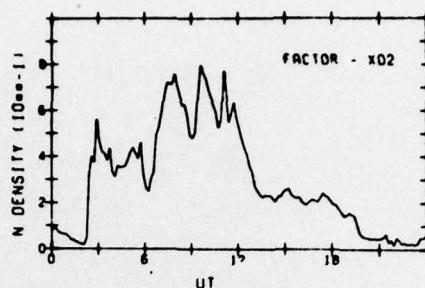


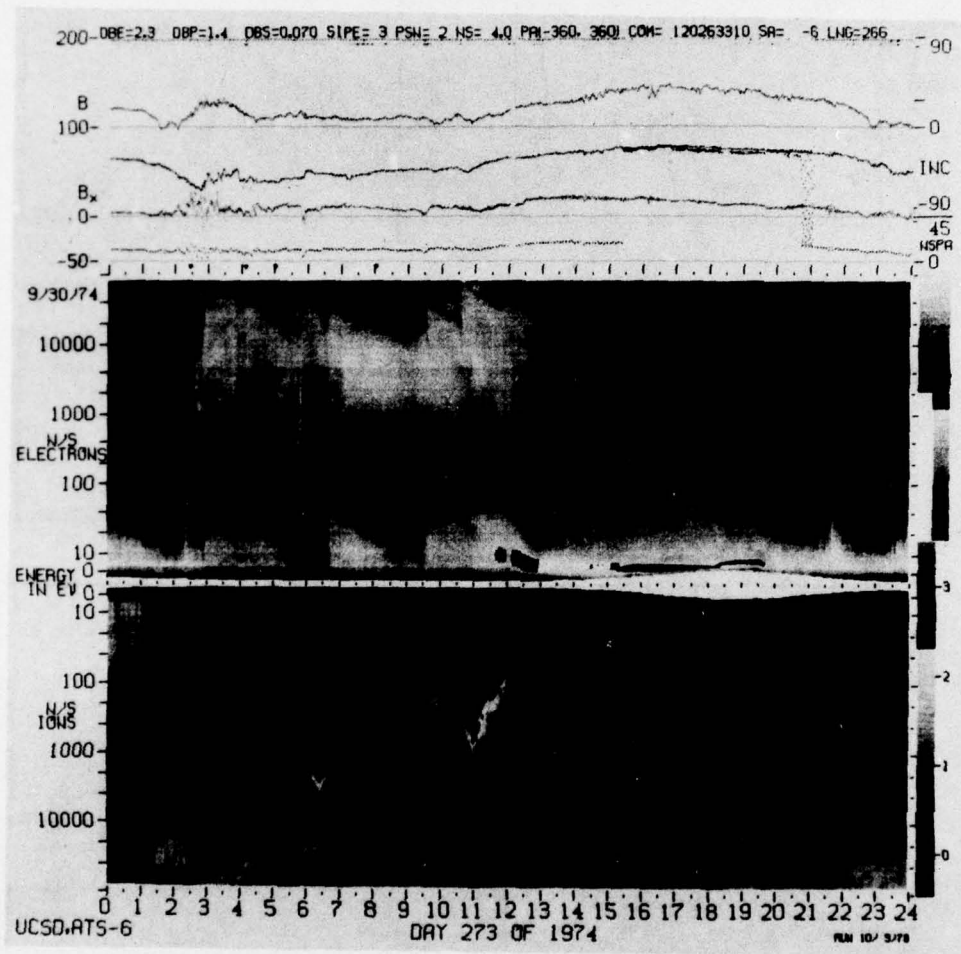
ATS-6 DATA
74/273

IONS



ELECTRONS

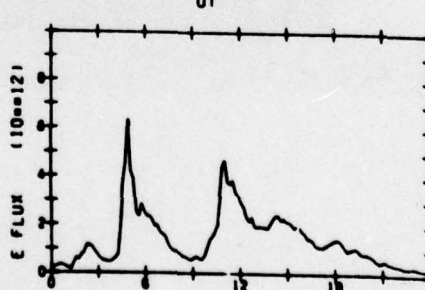
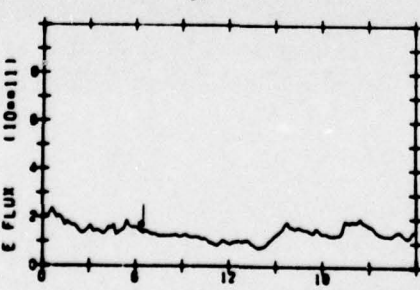
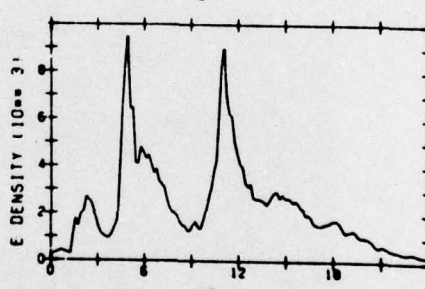
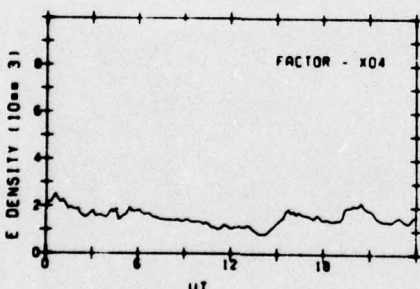
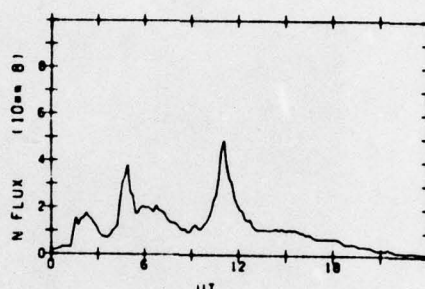
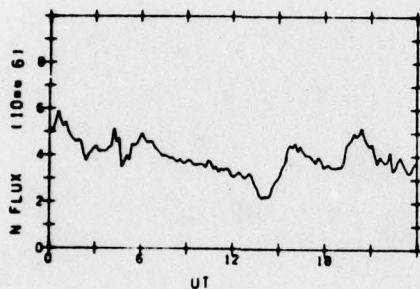
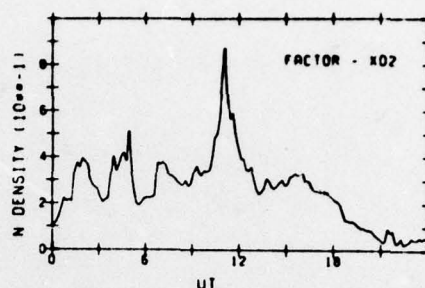
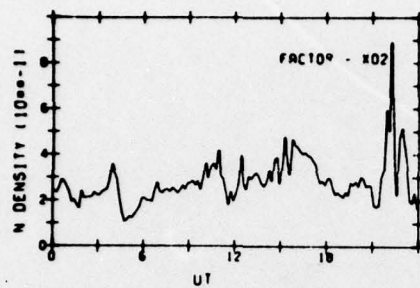


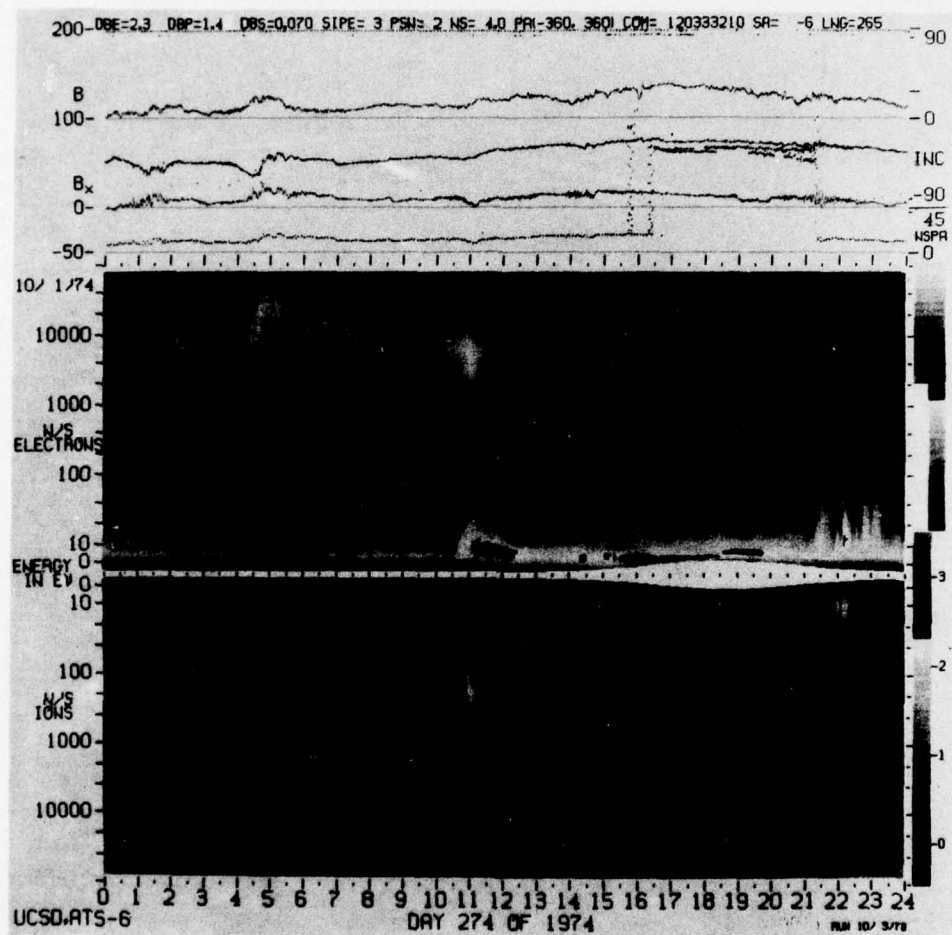


ATS-6 DATA
74/274

IONS

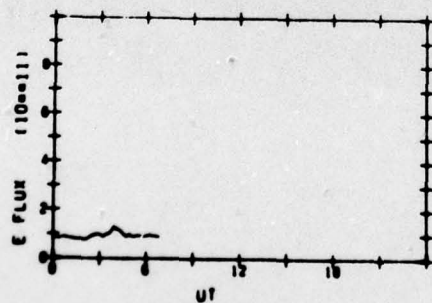
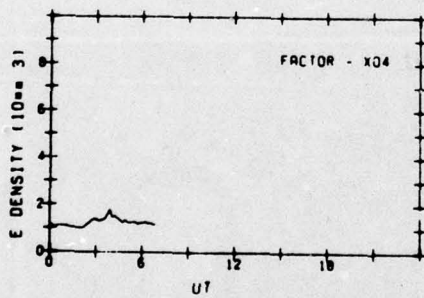
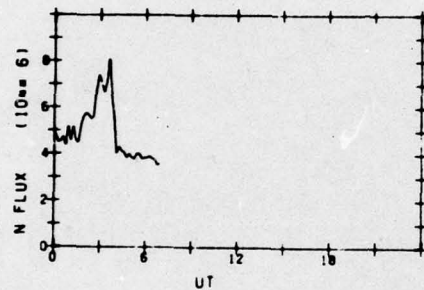
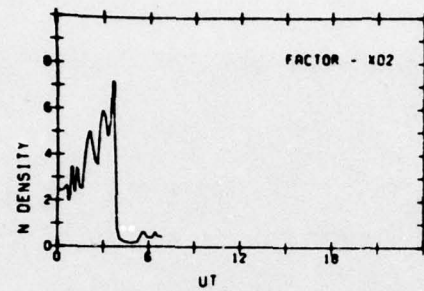
ELECTRONS



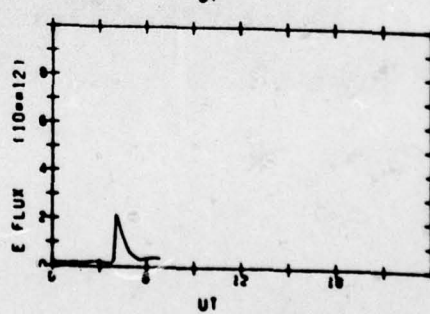
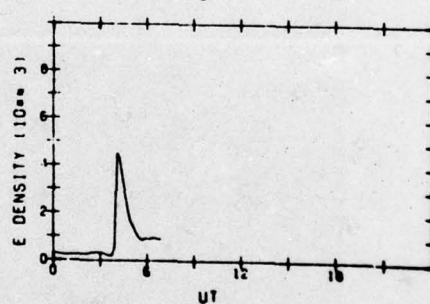
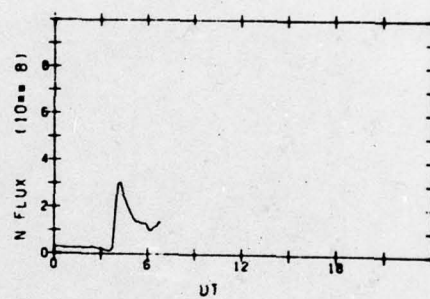
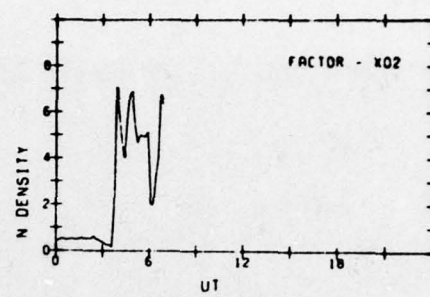


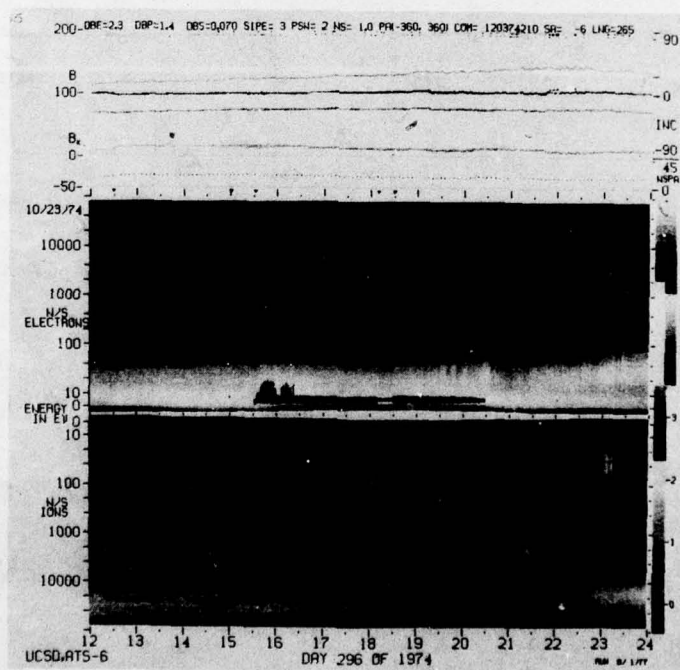
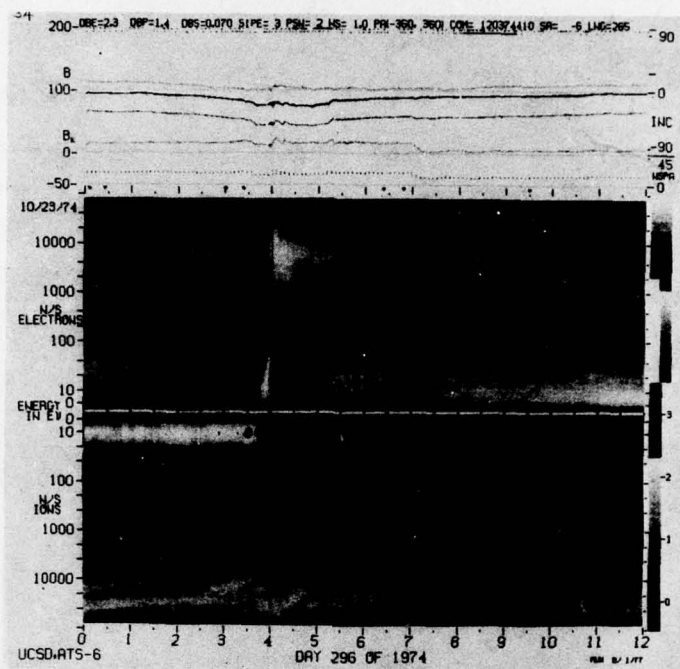
ATS-6 DATA
74/296

IONS



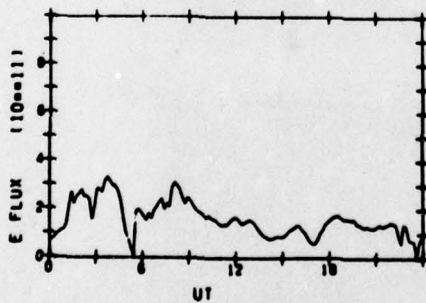
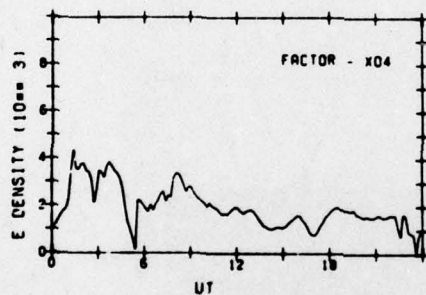
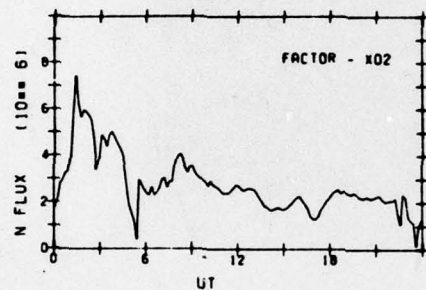
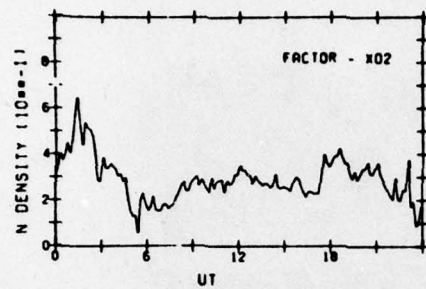
ELECTRONS



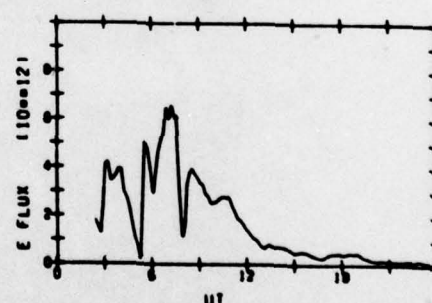
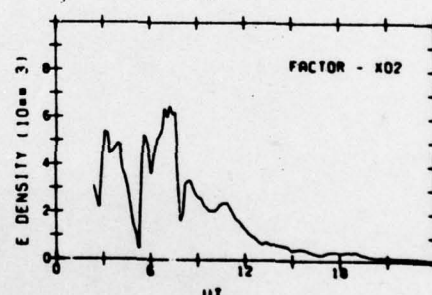
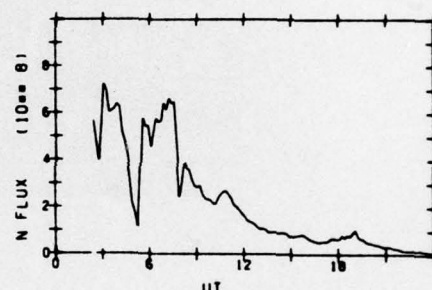
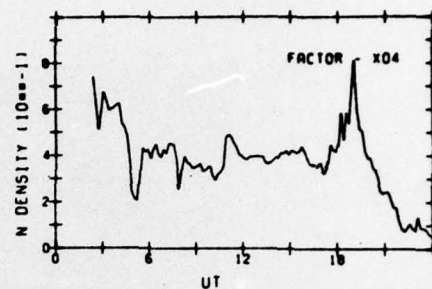


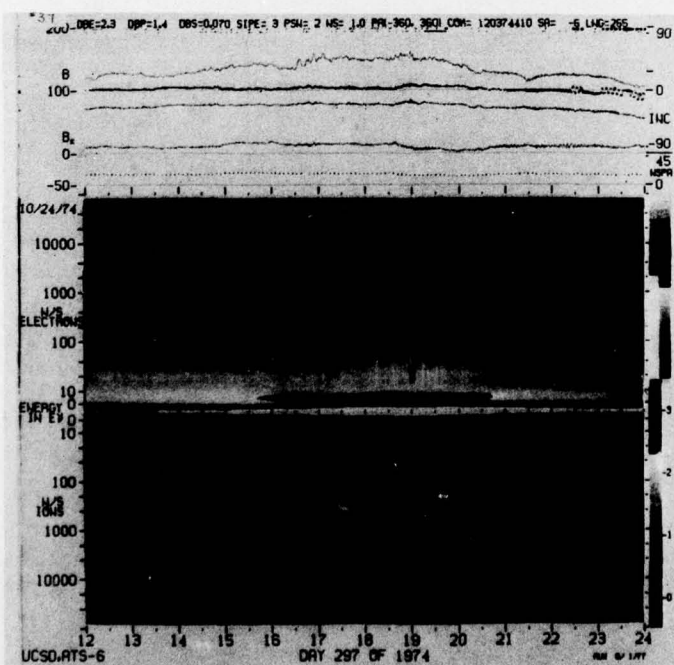
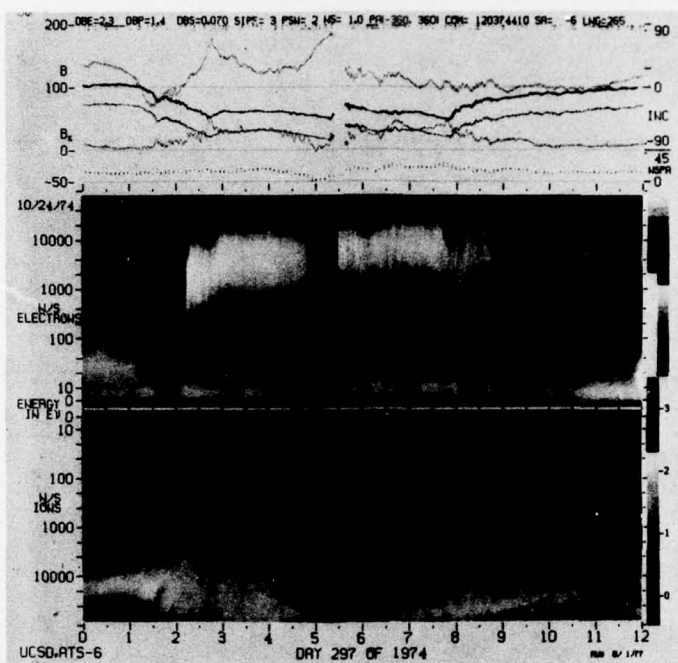
ATS-6 DATA
74/297

IONS



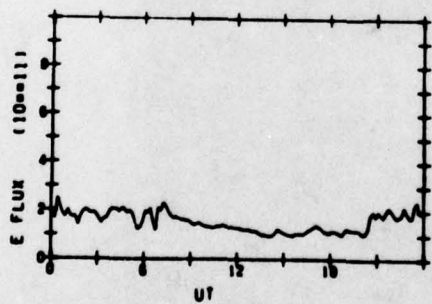
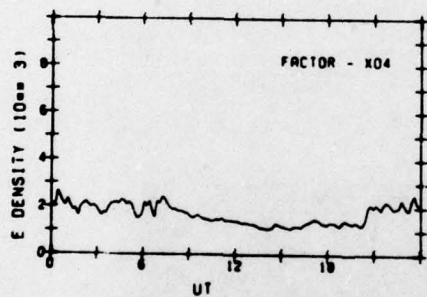
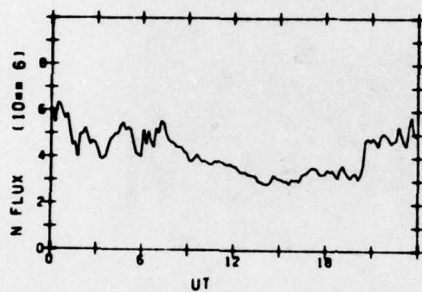
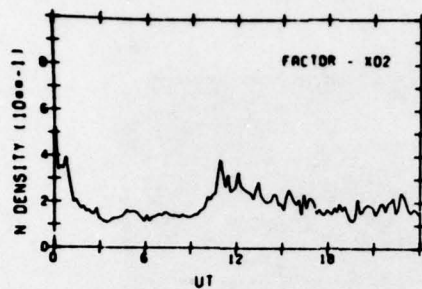
ELECTRONS



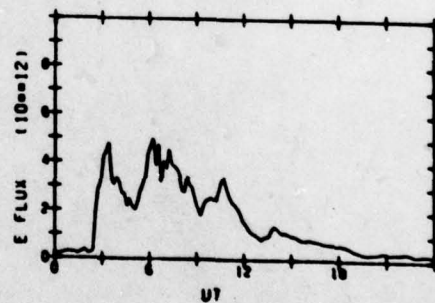
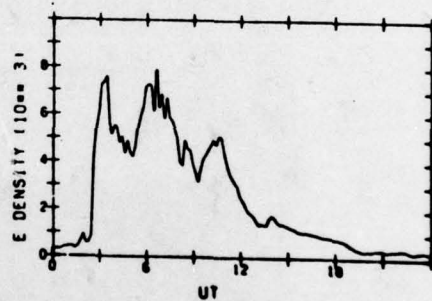
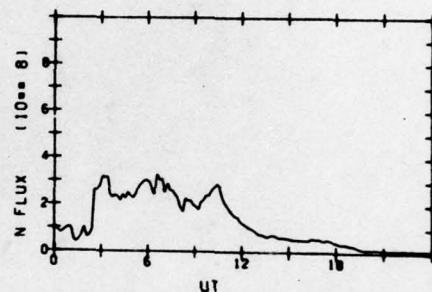
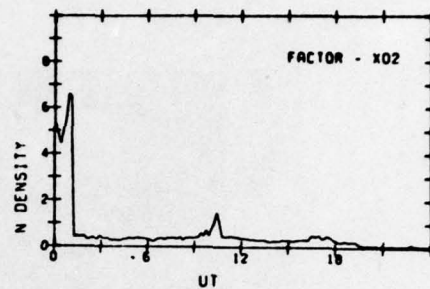


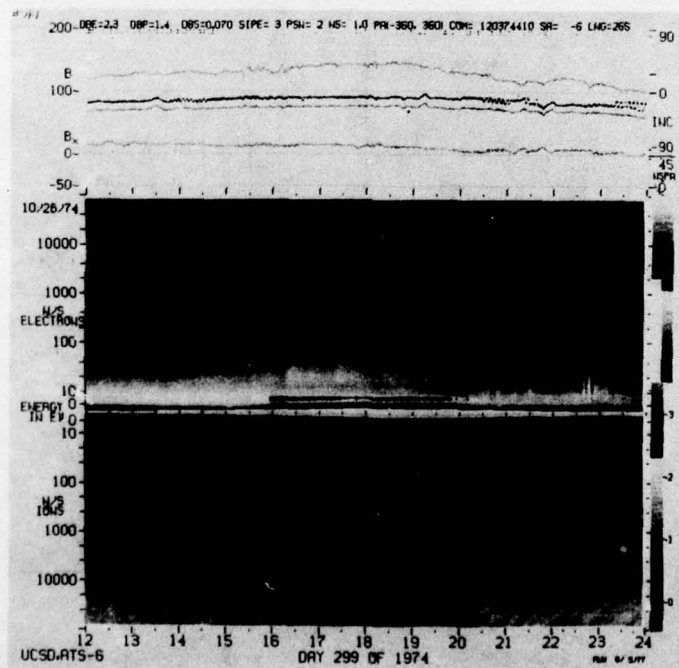
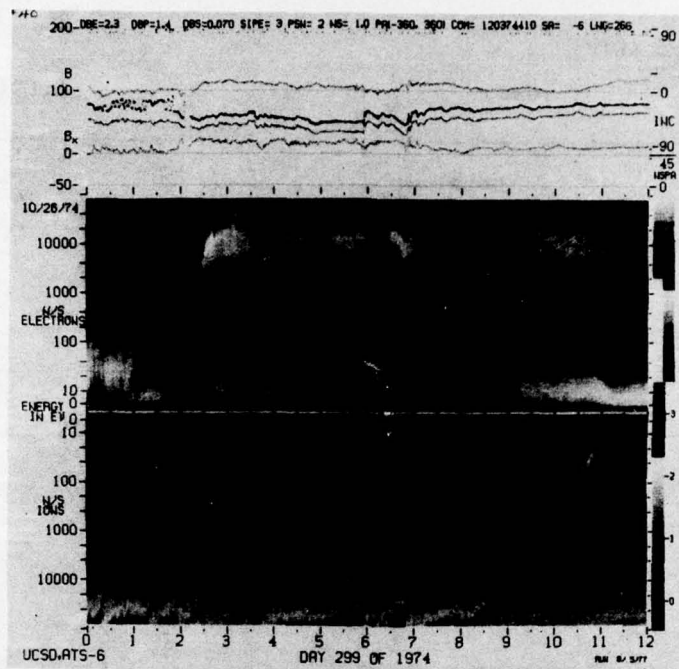
ATS-6 DATA
74/299

IONS



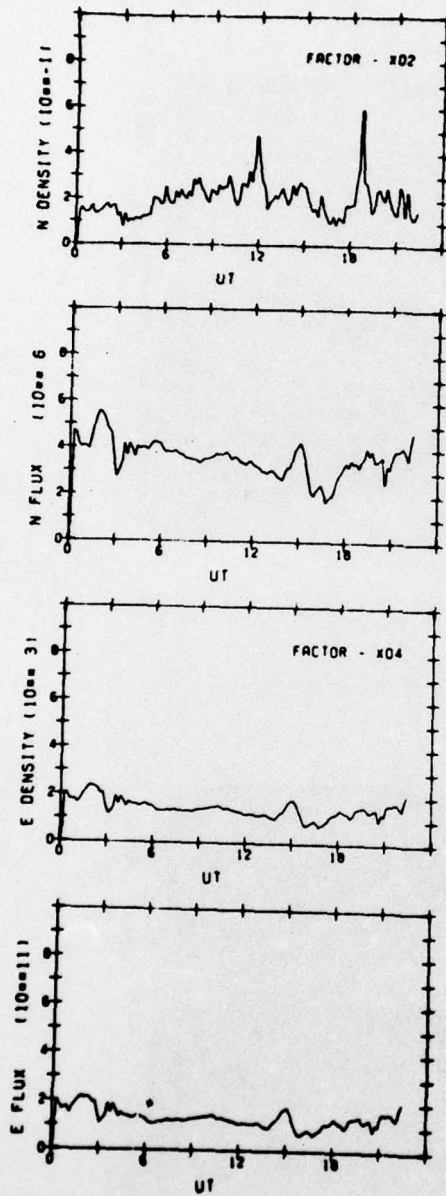
ELECTRONS



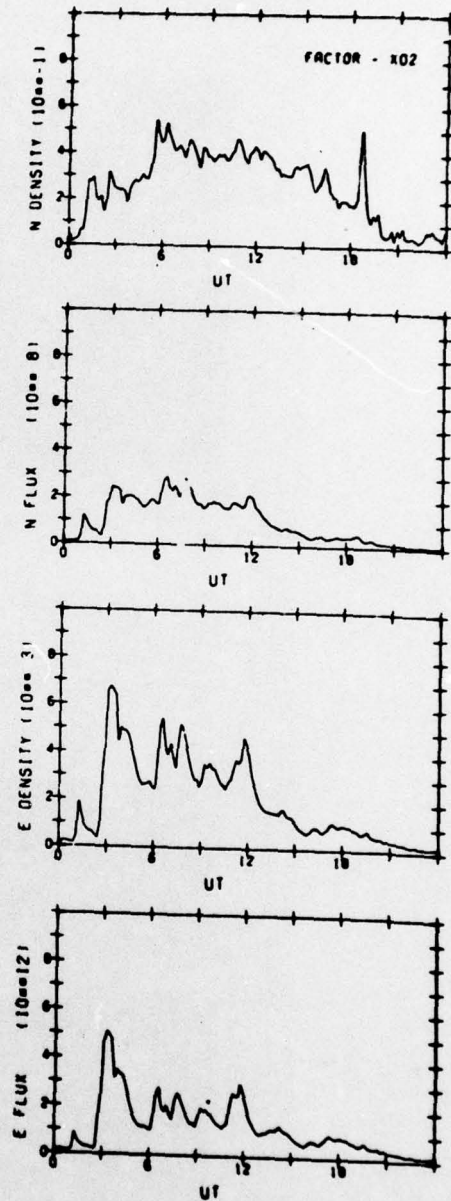


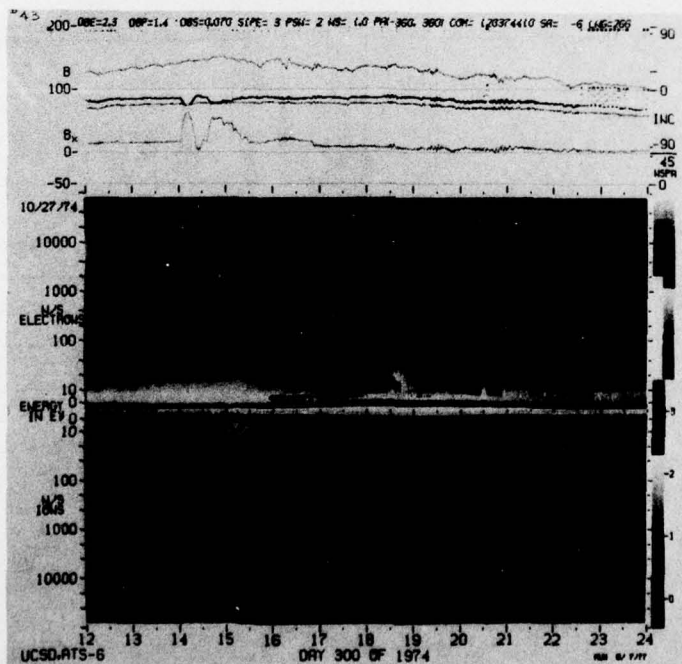
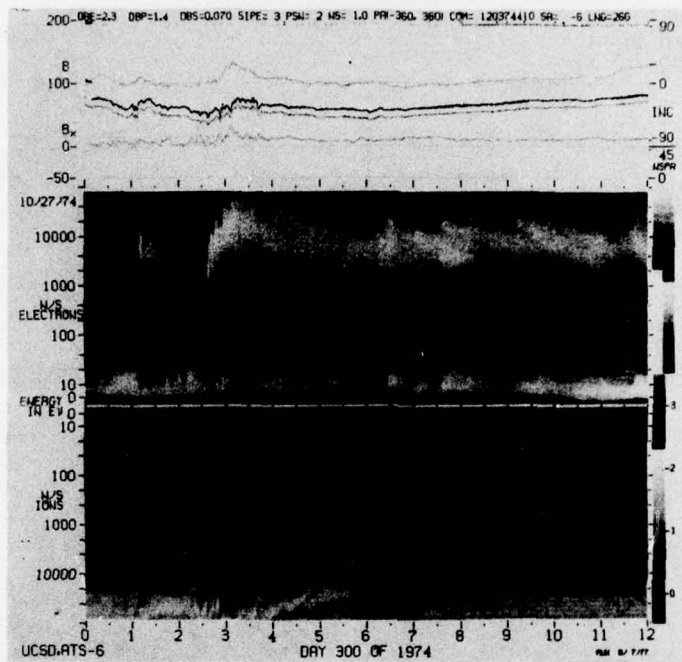
ATS-6 DATA
74/300

IONS



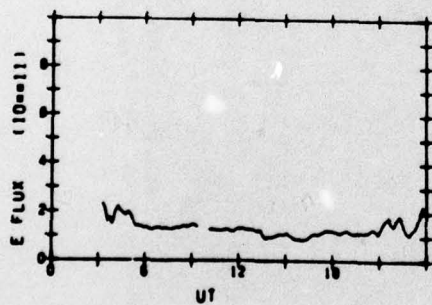
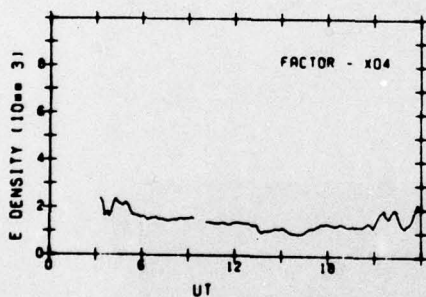
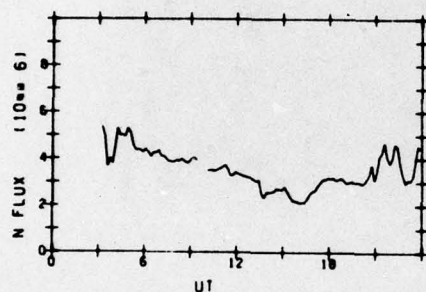
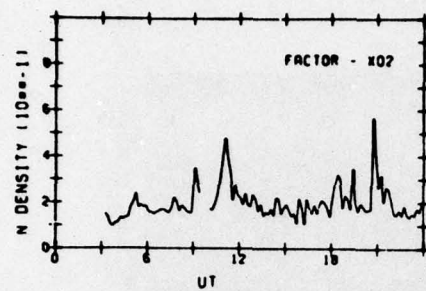
ELECTRONS



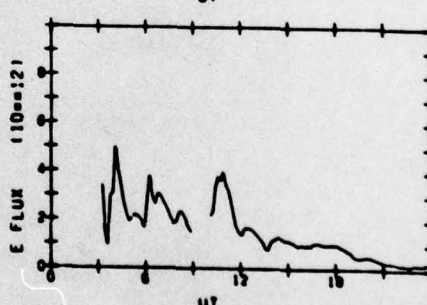
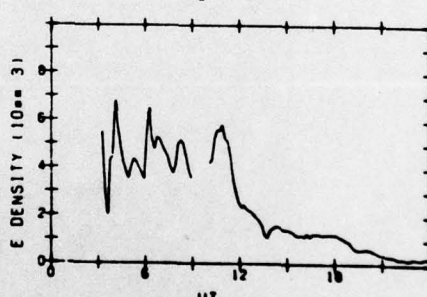
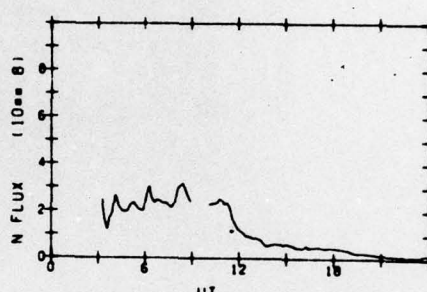
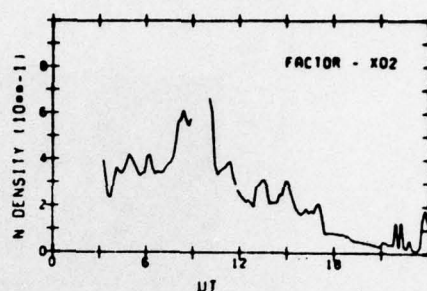


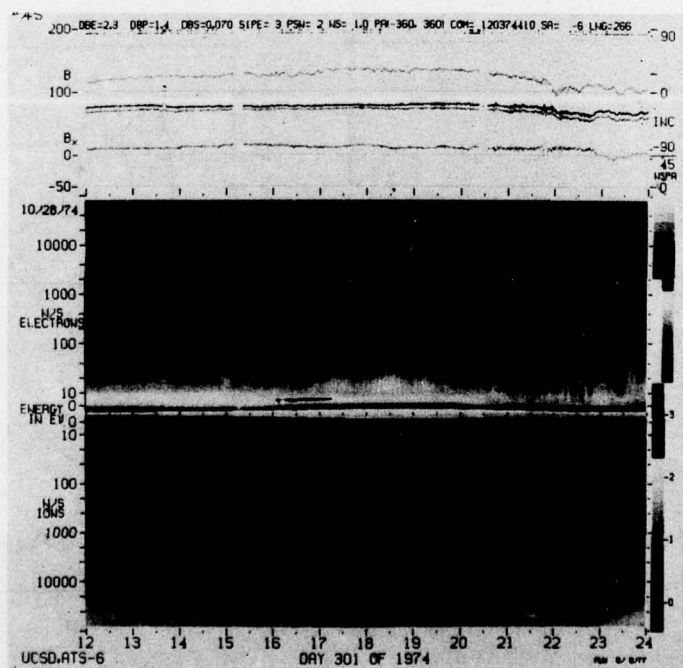
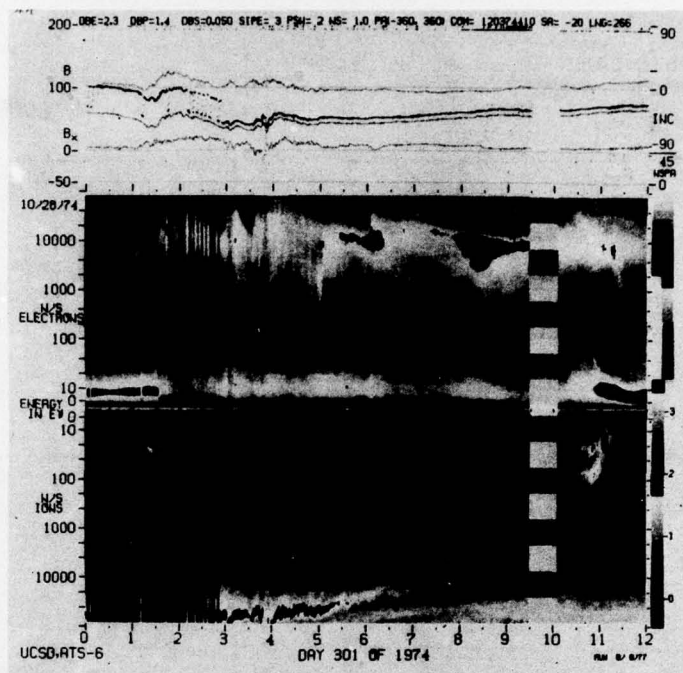
ATS-6 DATA
74/301

IONS



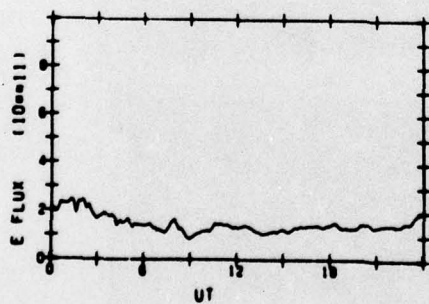
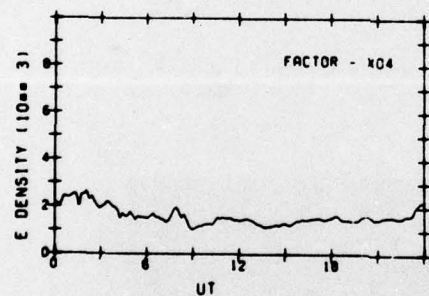
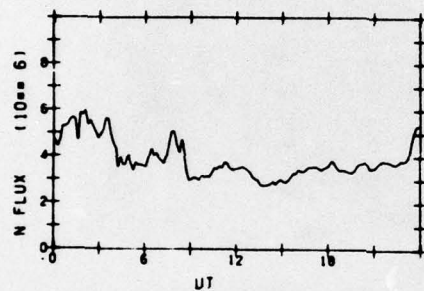
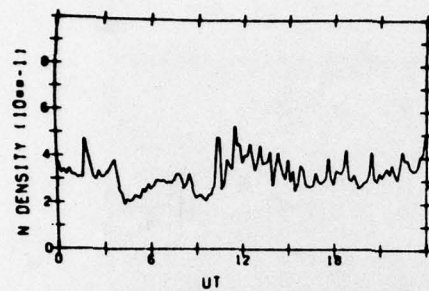
ELECTRONS



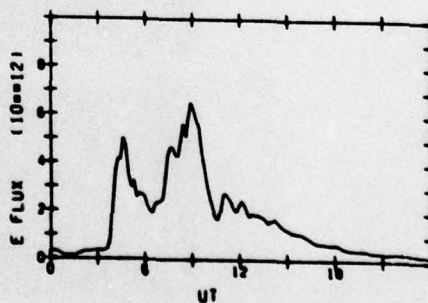
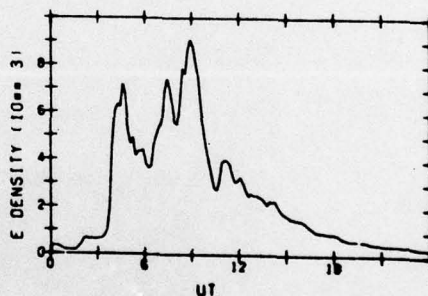
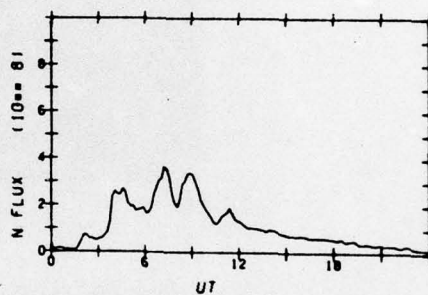
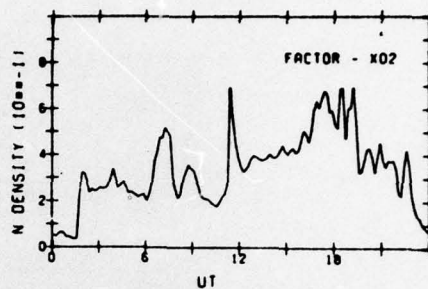


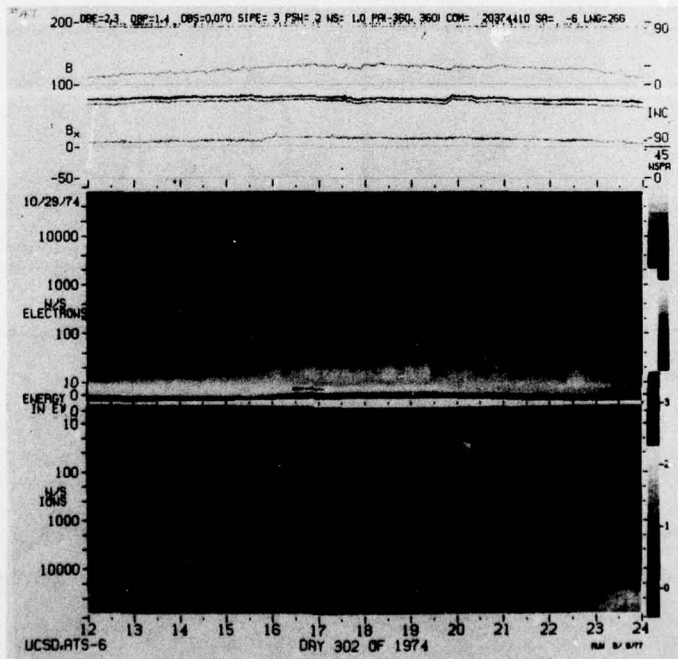
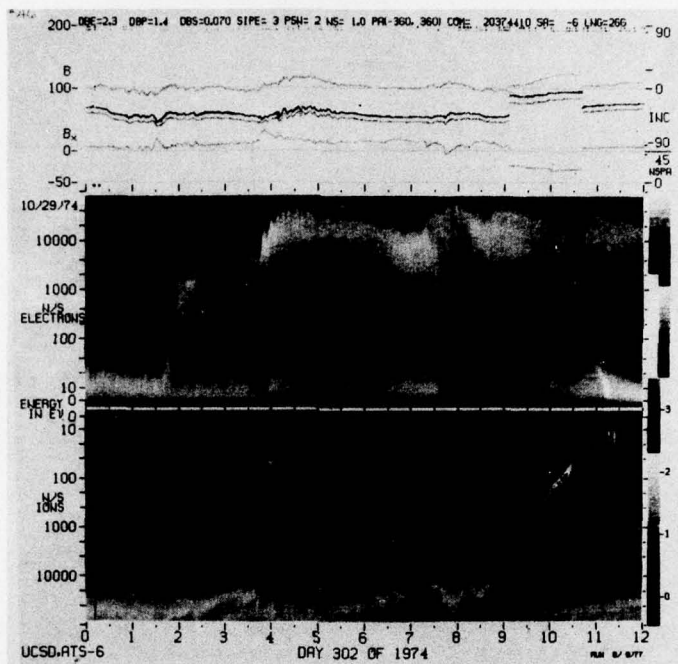
ATS-6 DATA
74/302

IONS



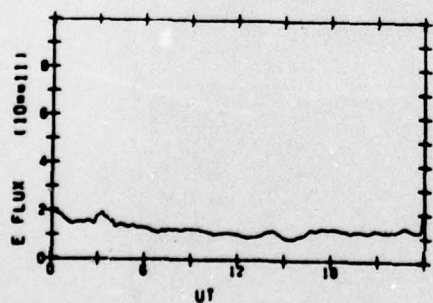
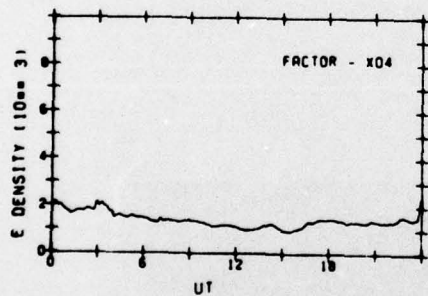
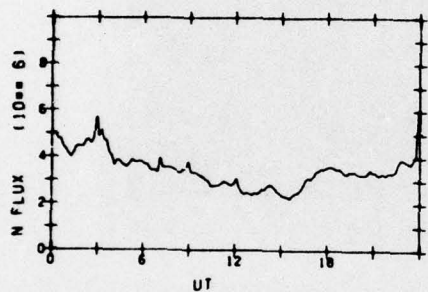
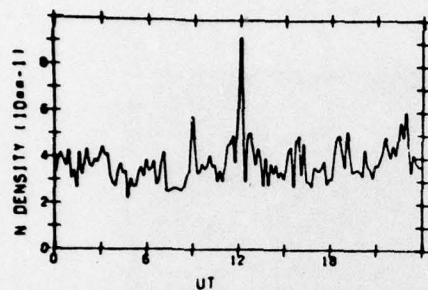
ELECTRONS



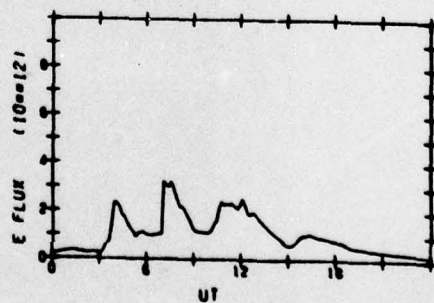
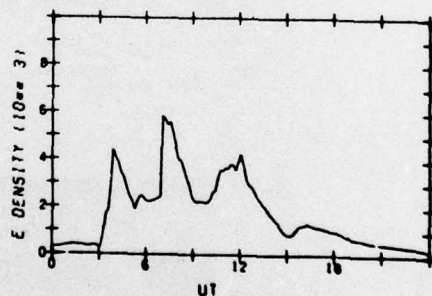
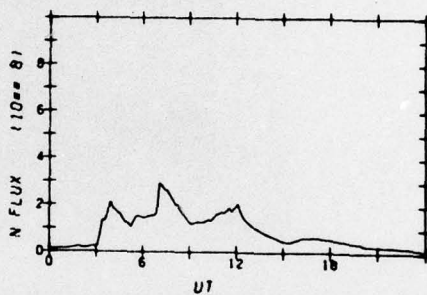
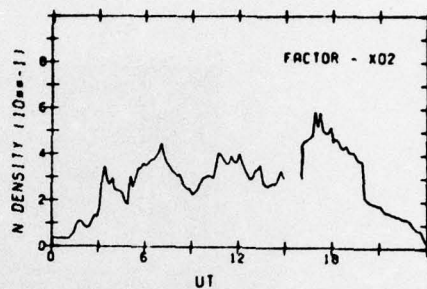


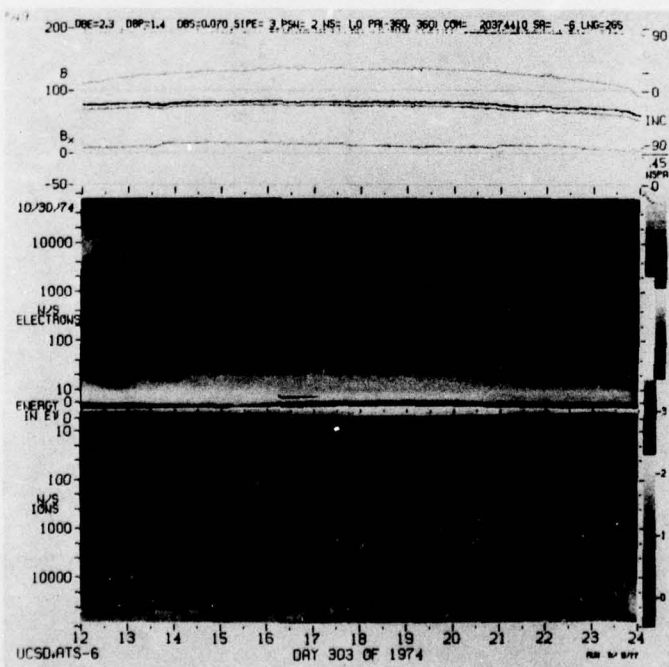
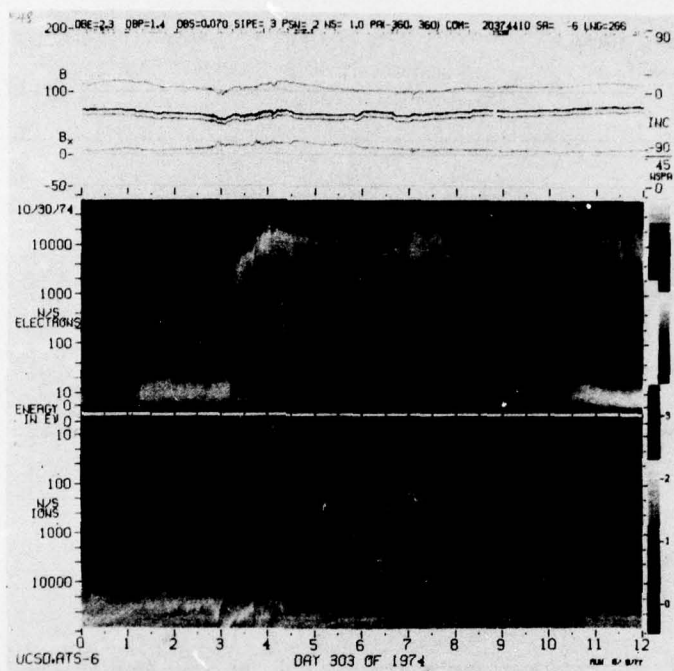
ATS-6 DATA
74/303

IONS



ELECTRONS





AD-A067 843

AIR FORCE GEOPHYSICS LAB HANSCOM AFB MASS

F/G 4/1

MODELING OF THE GEOSYNCHRONOUS ORBIT PLASMA ENVIRONMENT. PART 3--ETC(U)

JAN 79 H B GARRETT, R E MCINERNEY

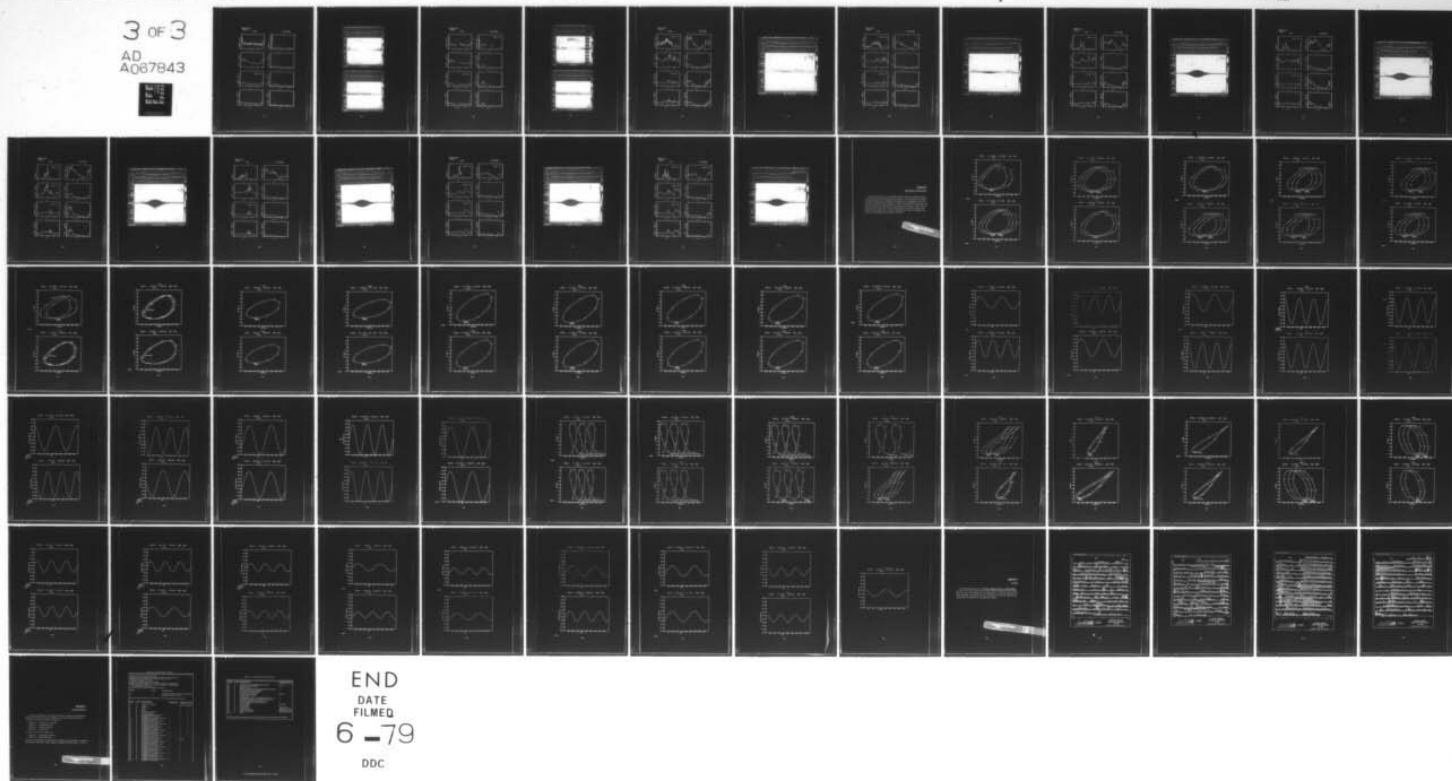
UNCLASSIFIED

AFOL-TR-79-0015

NL

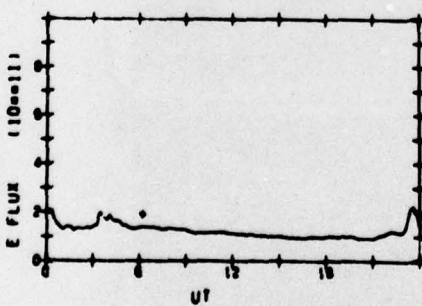
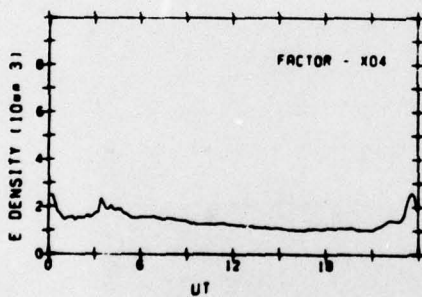
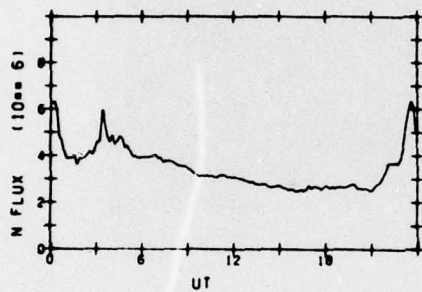
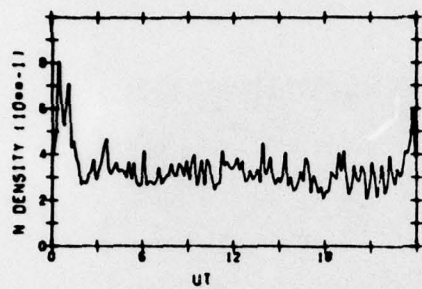
3 OF 3

AD
A067843

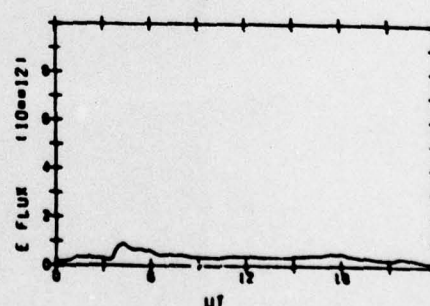
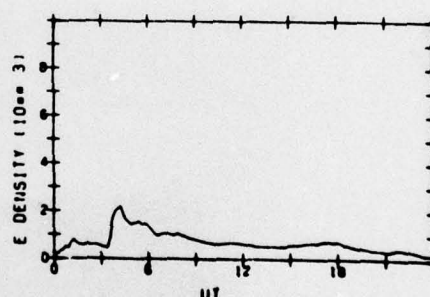
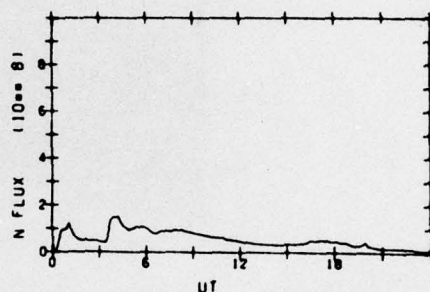
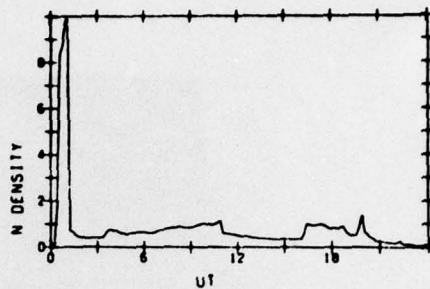


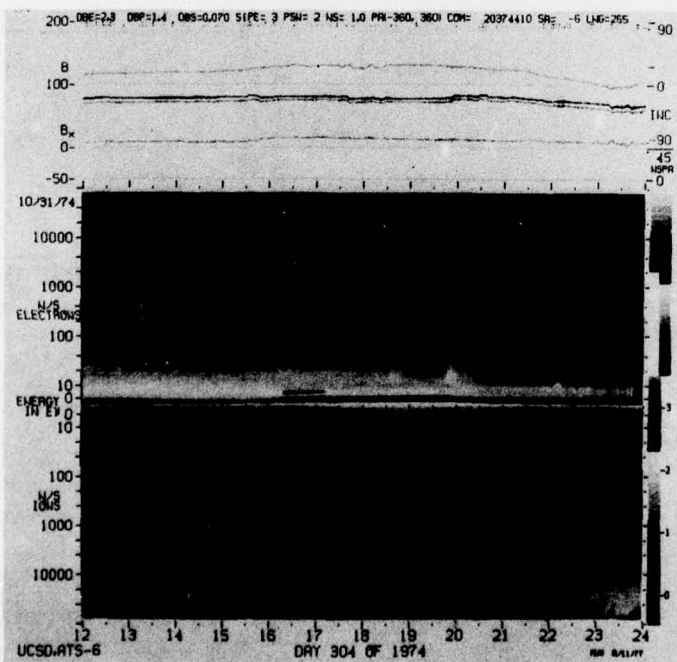
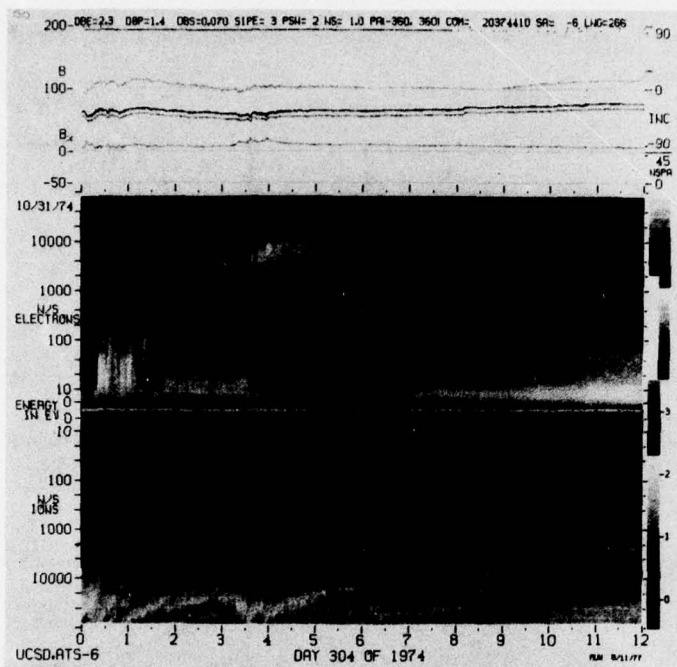
ATS-6 DATA
74/304

IONS



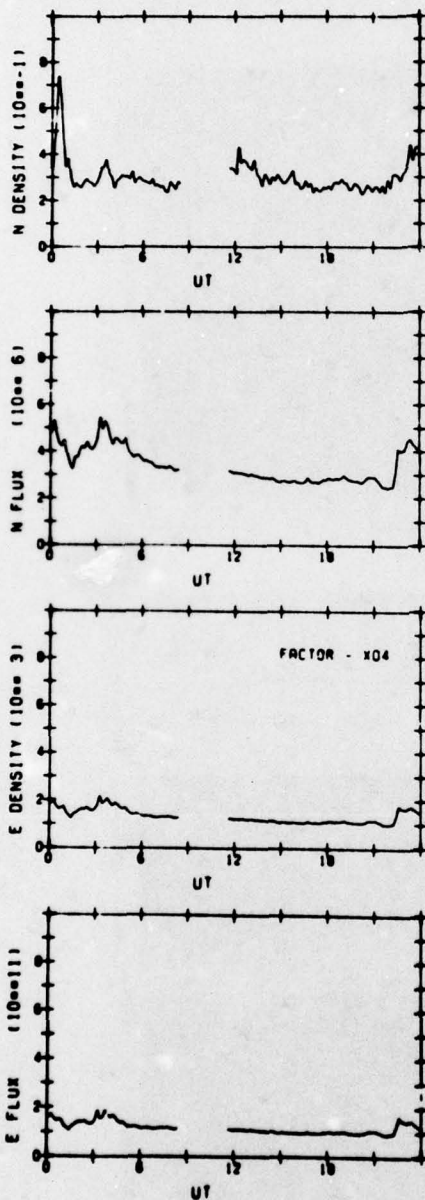
ELECTRONS



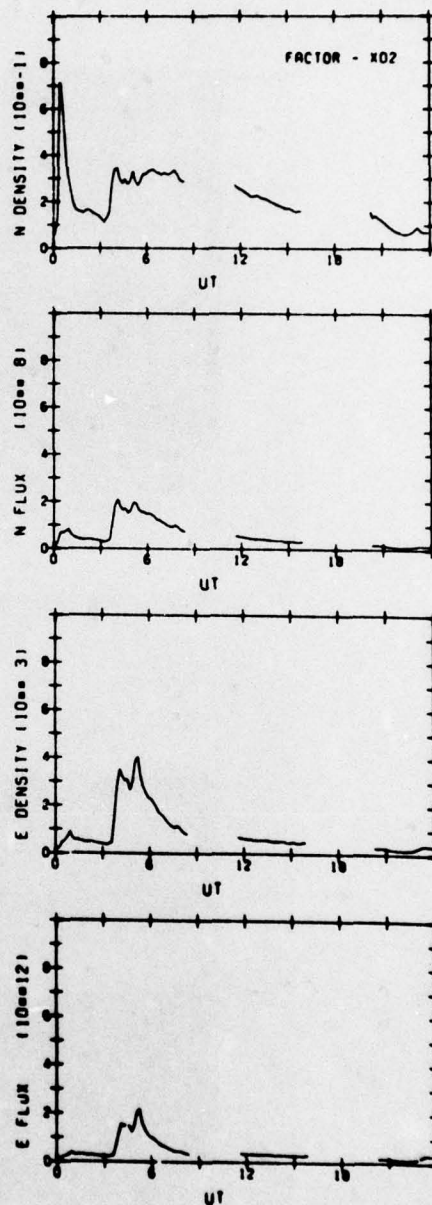


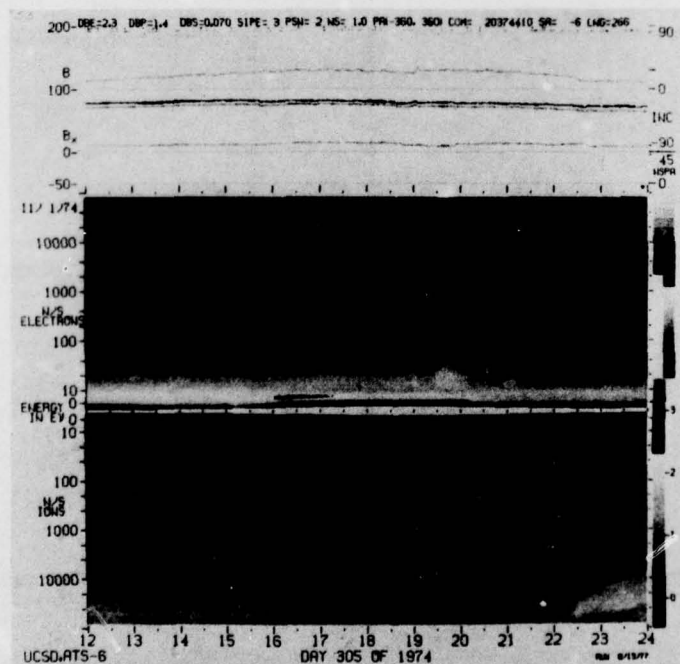
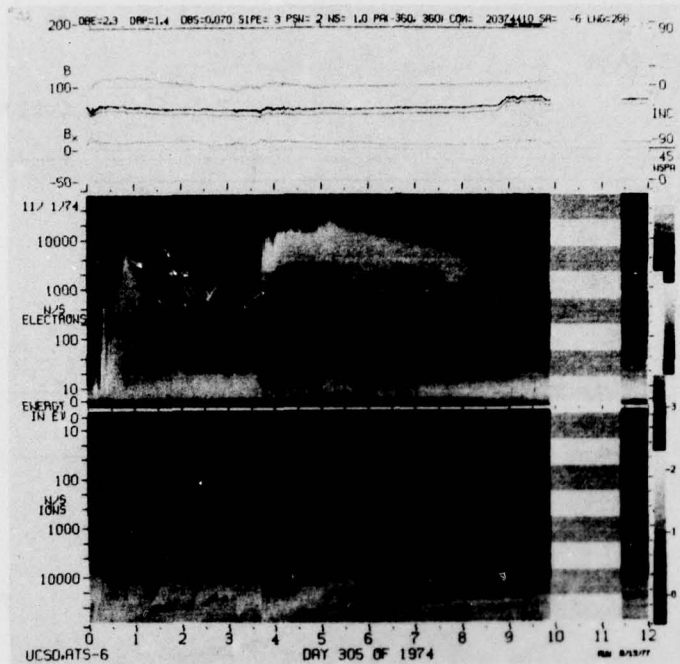
ATS-6 DATA
74/305

IONS



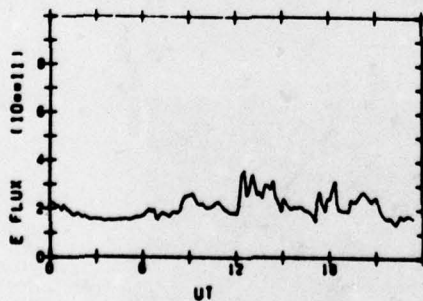
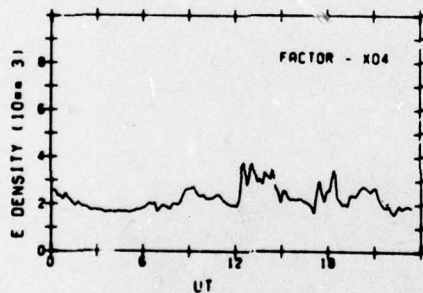
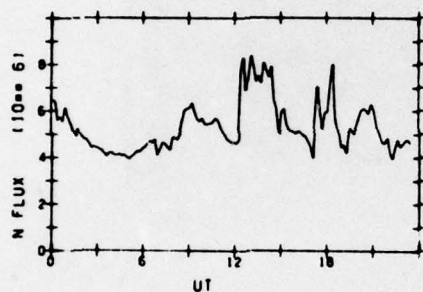
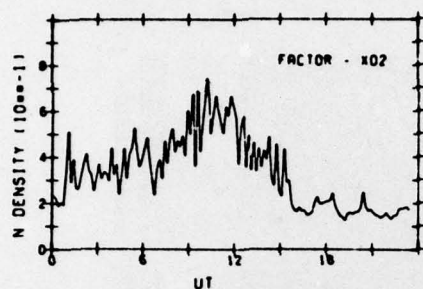
ELECTRONS



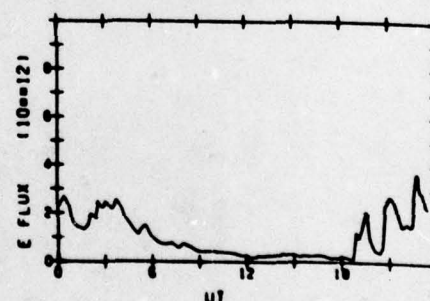
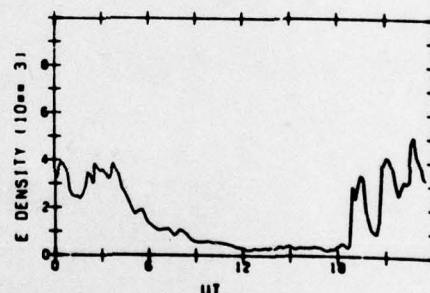
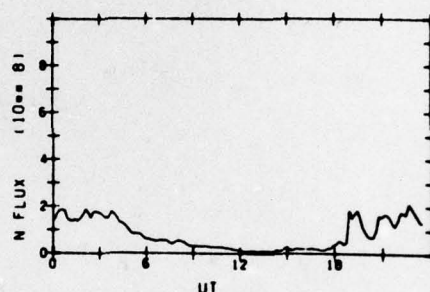
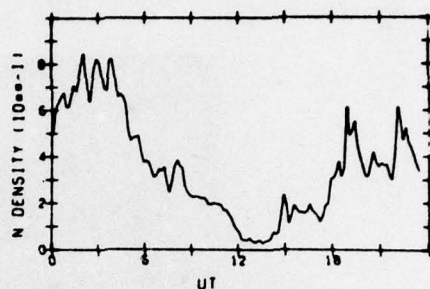


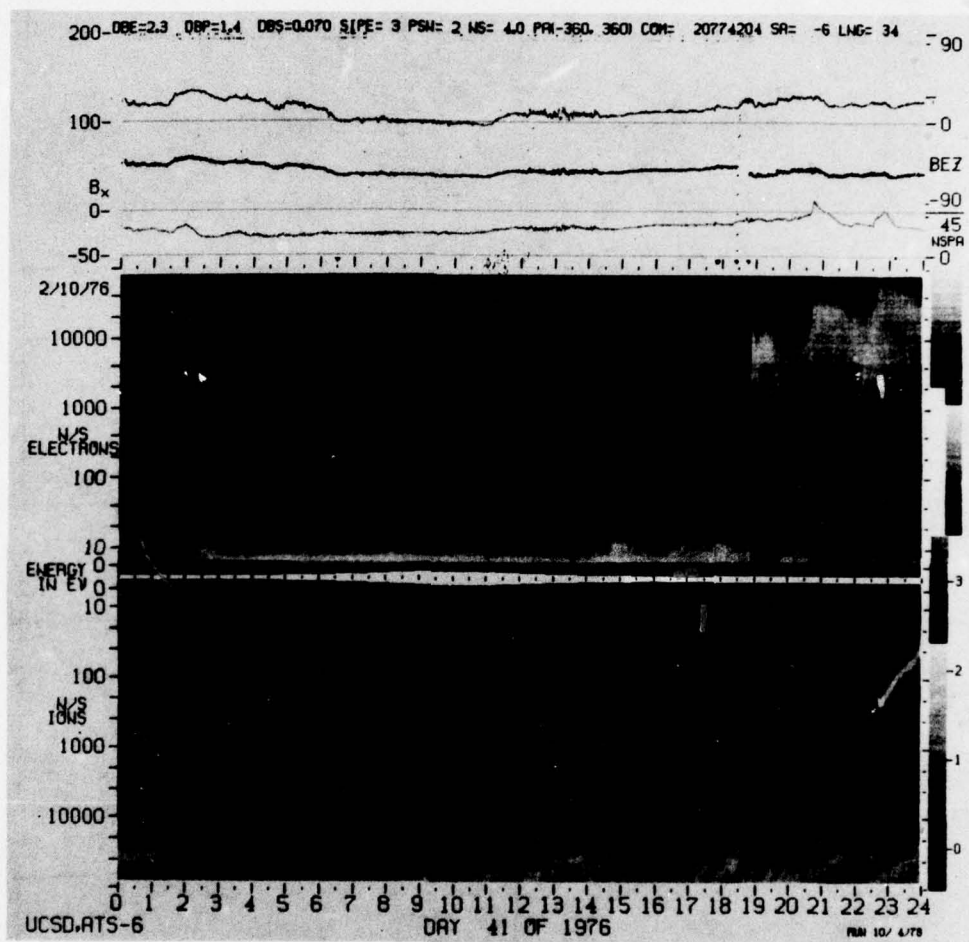
ATS-6 DATA
76/041

IONS



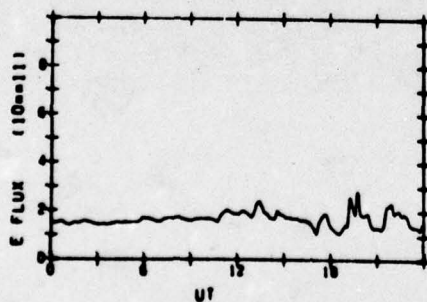
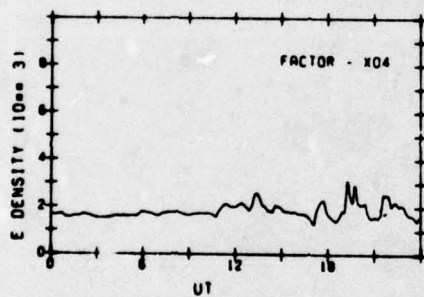
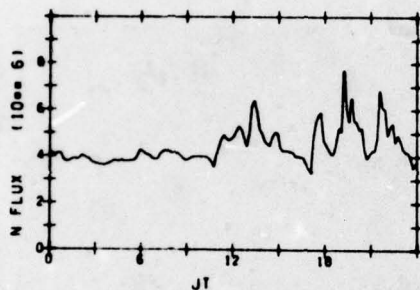
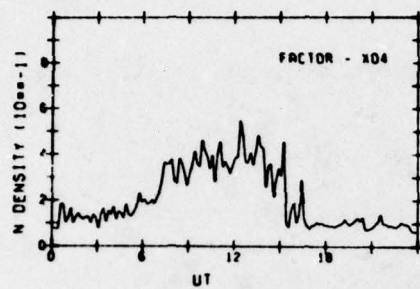
ELECTRONS



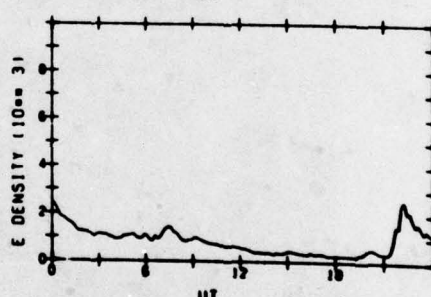
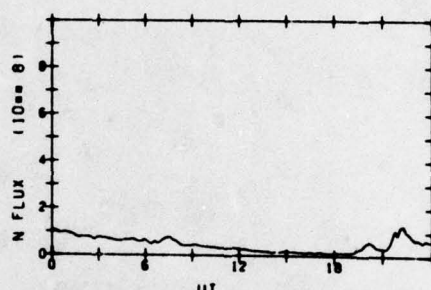
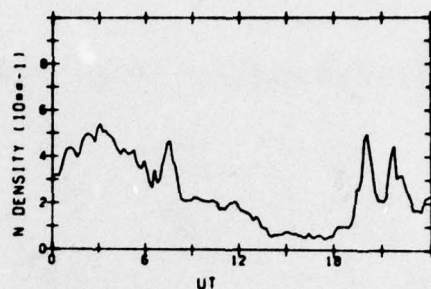


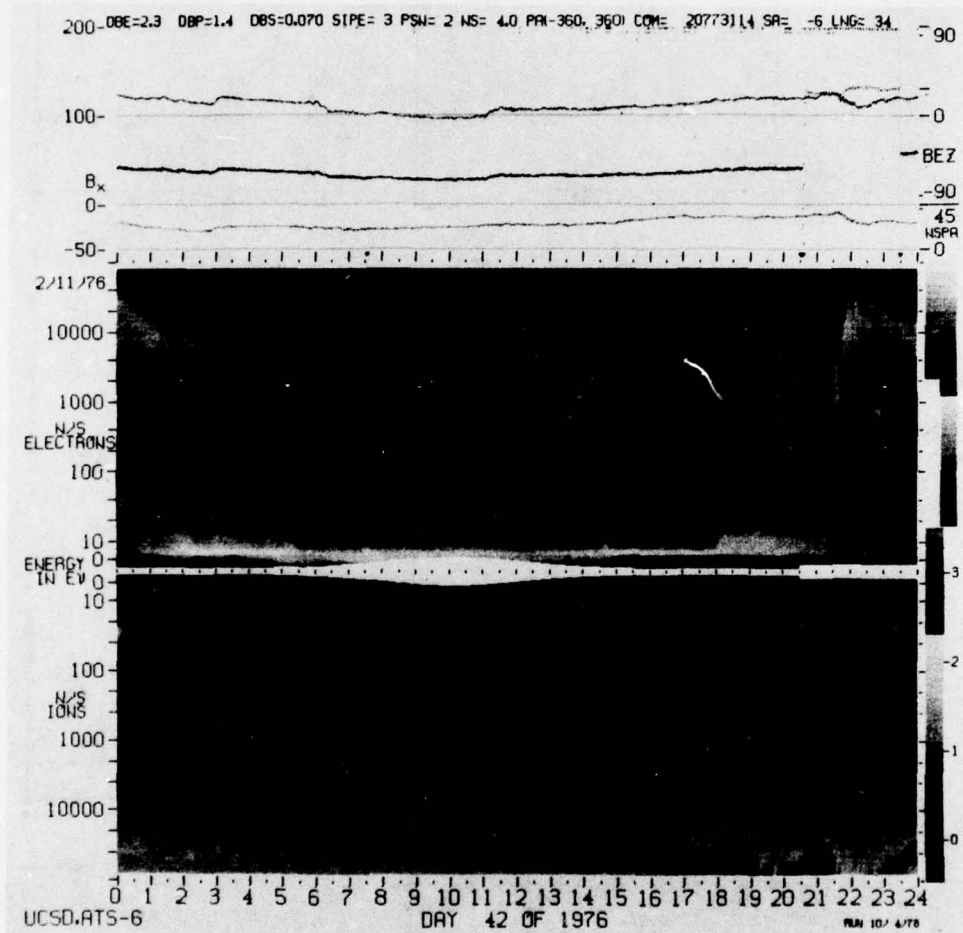
ATS-6 DATA
76/042

IONS



ELECTRONS

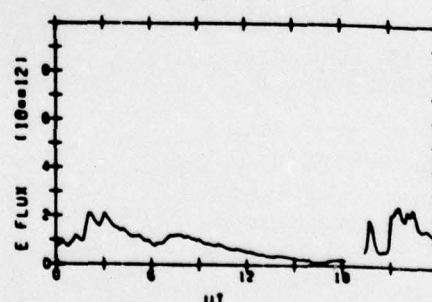
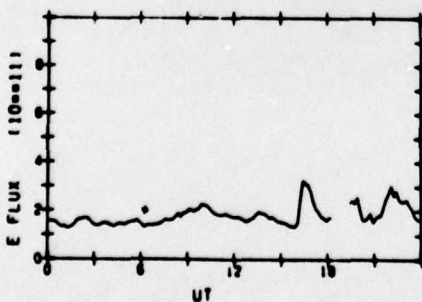
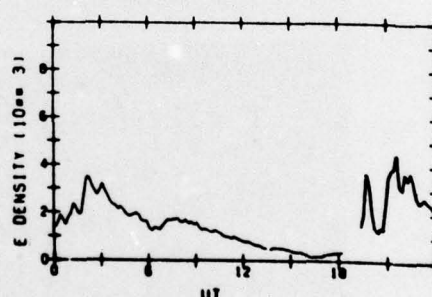
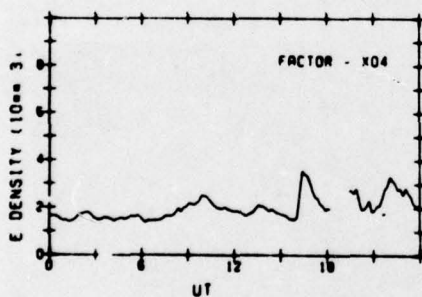
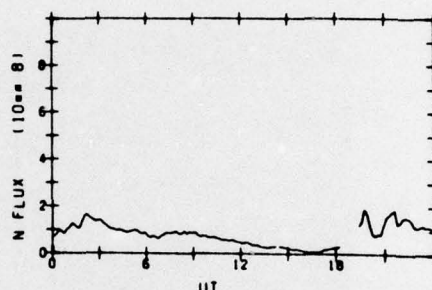
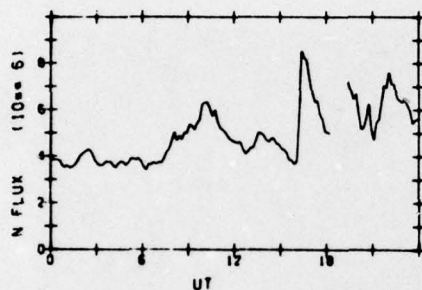
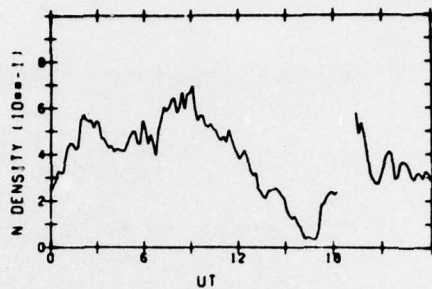
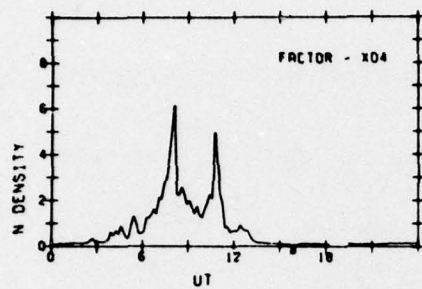


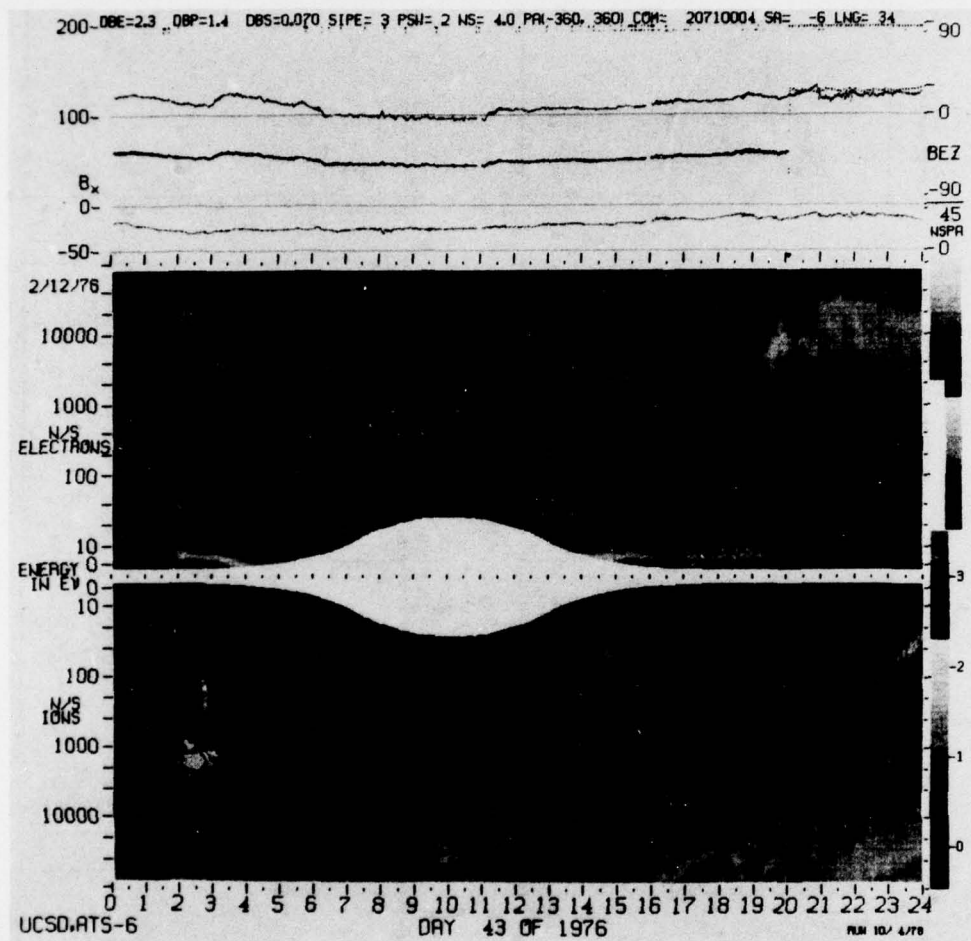


ATS-6 DATA
76/043

IONS

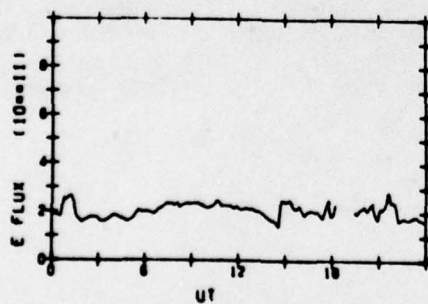
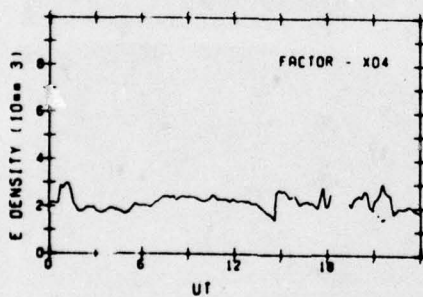
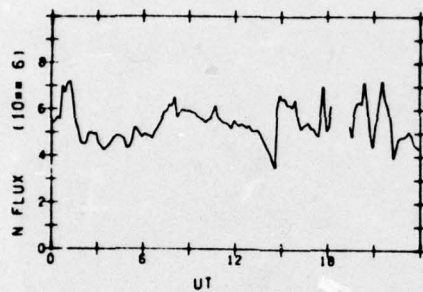
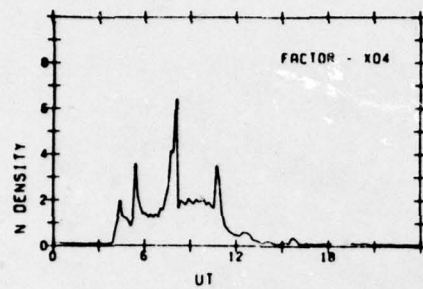
ELECTRONS



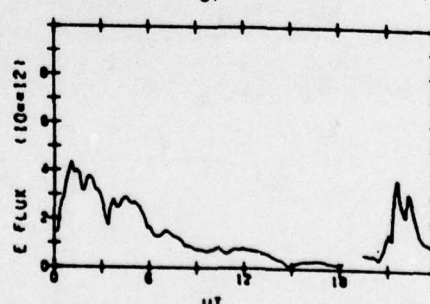
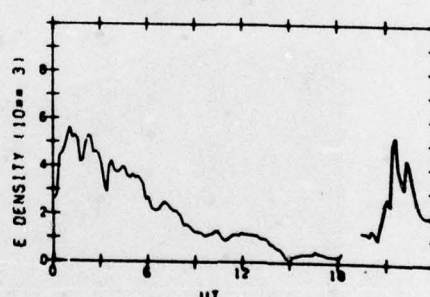
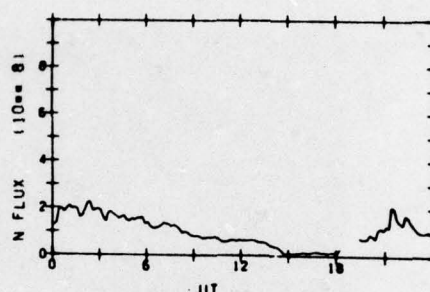
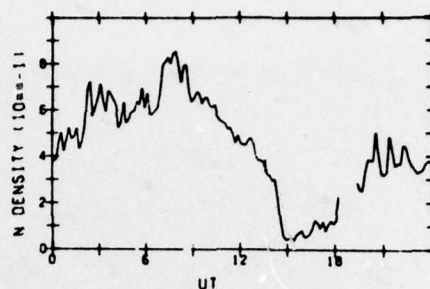


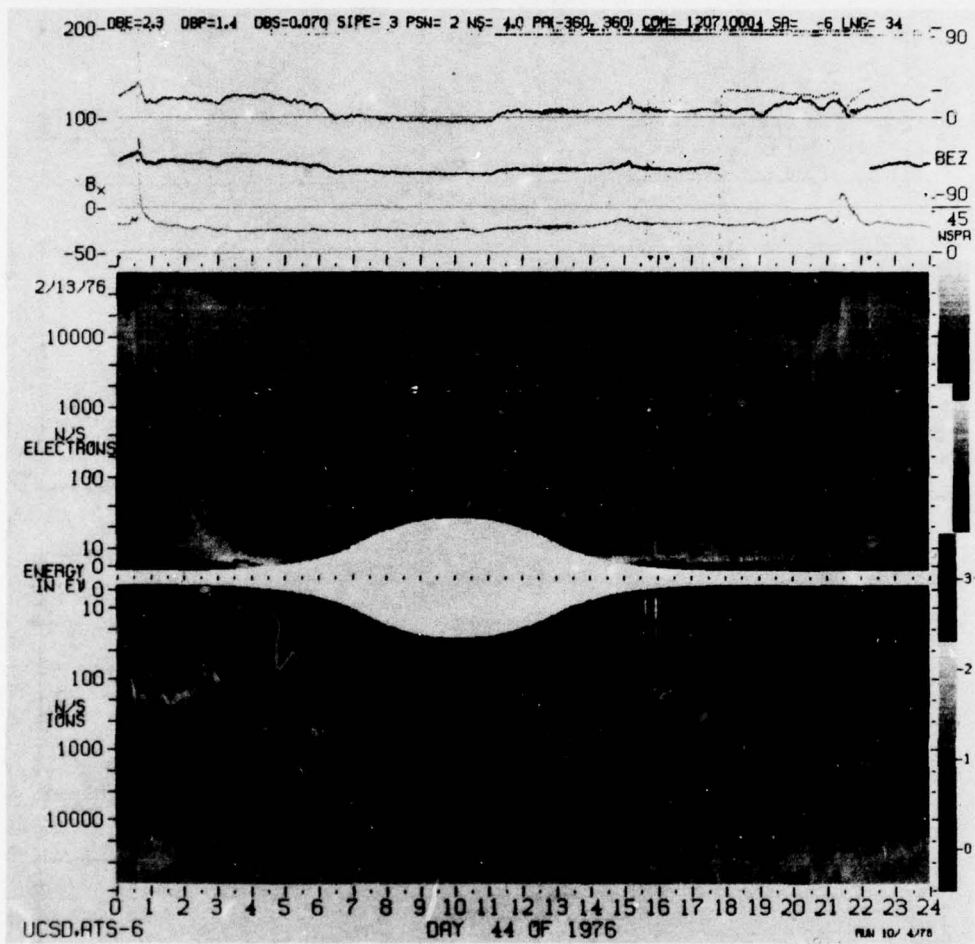
ATS-6 DATA
76/044

IONS



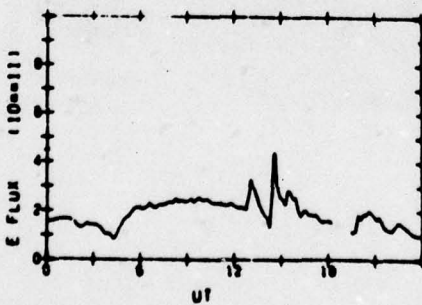
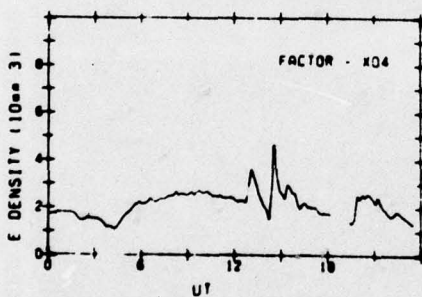
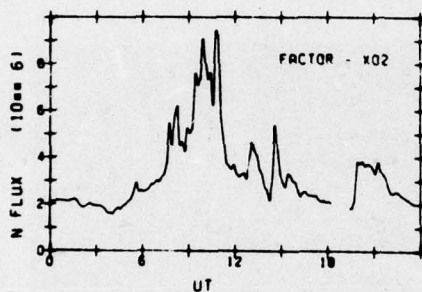
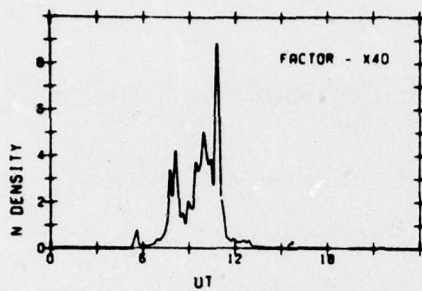
ELECTRONS



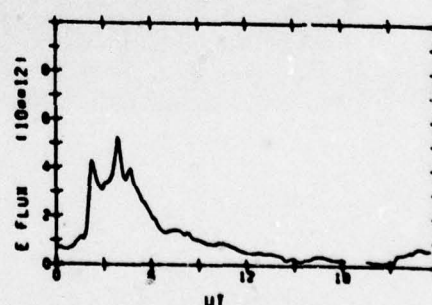
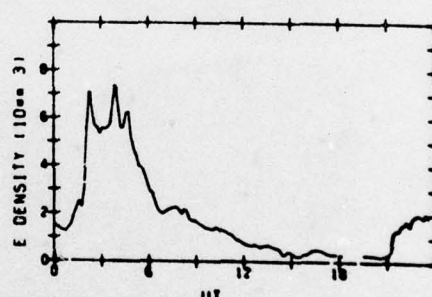
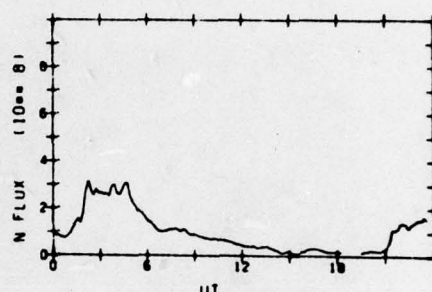
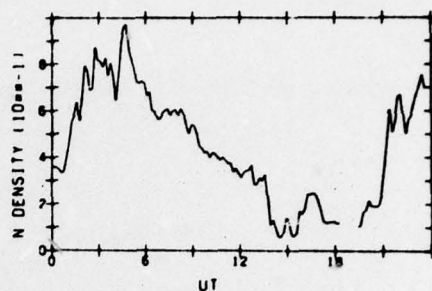


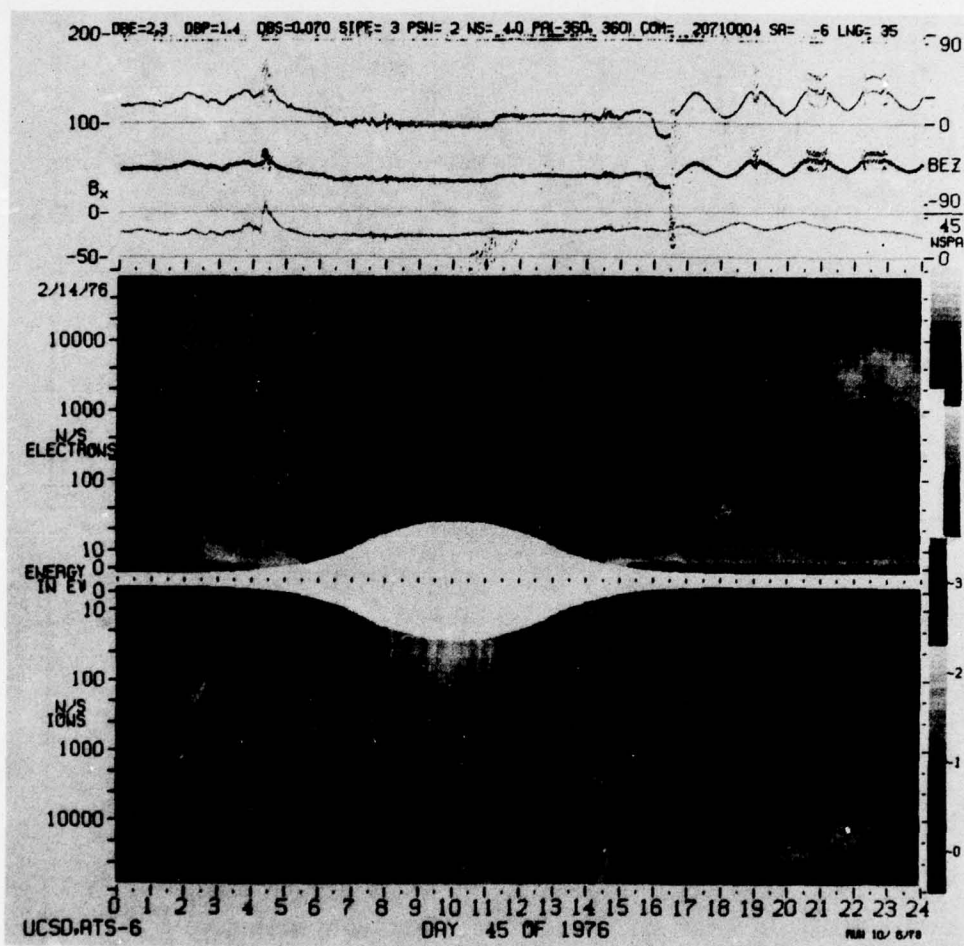
ATS-6 DATA
76/045

IONS



ELECTRONS

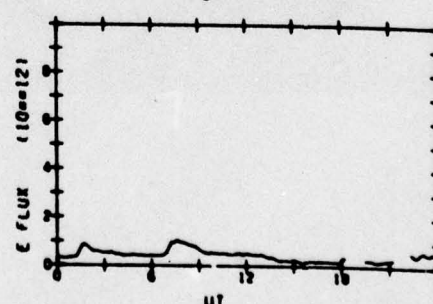
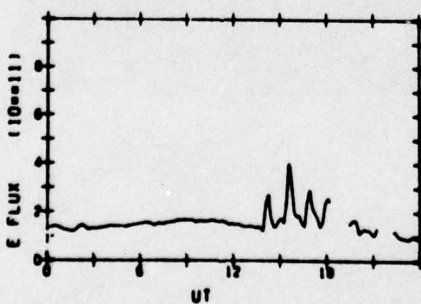
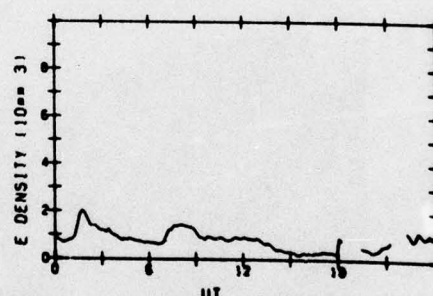
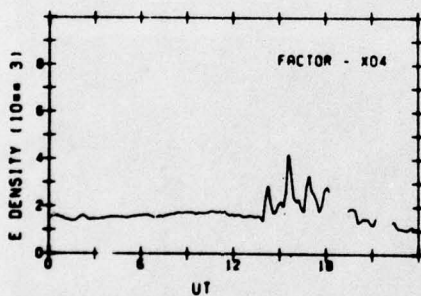
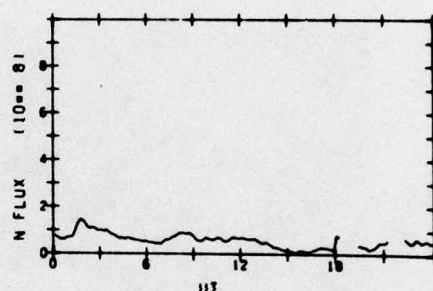
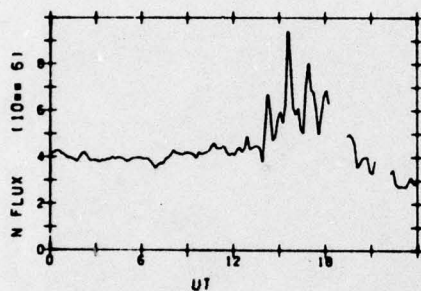
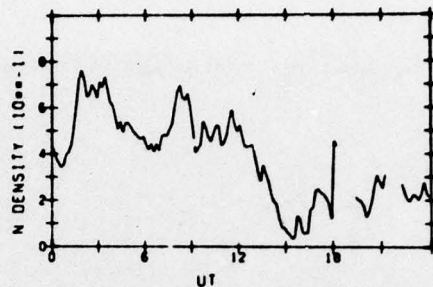
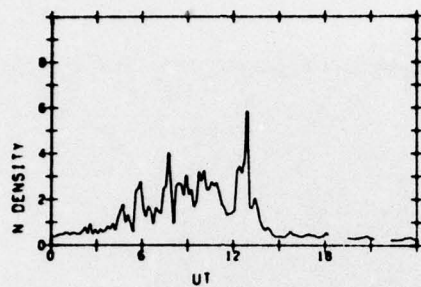


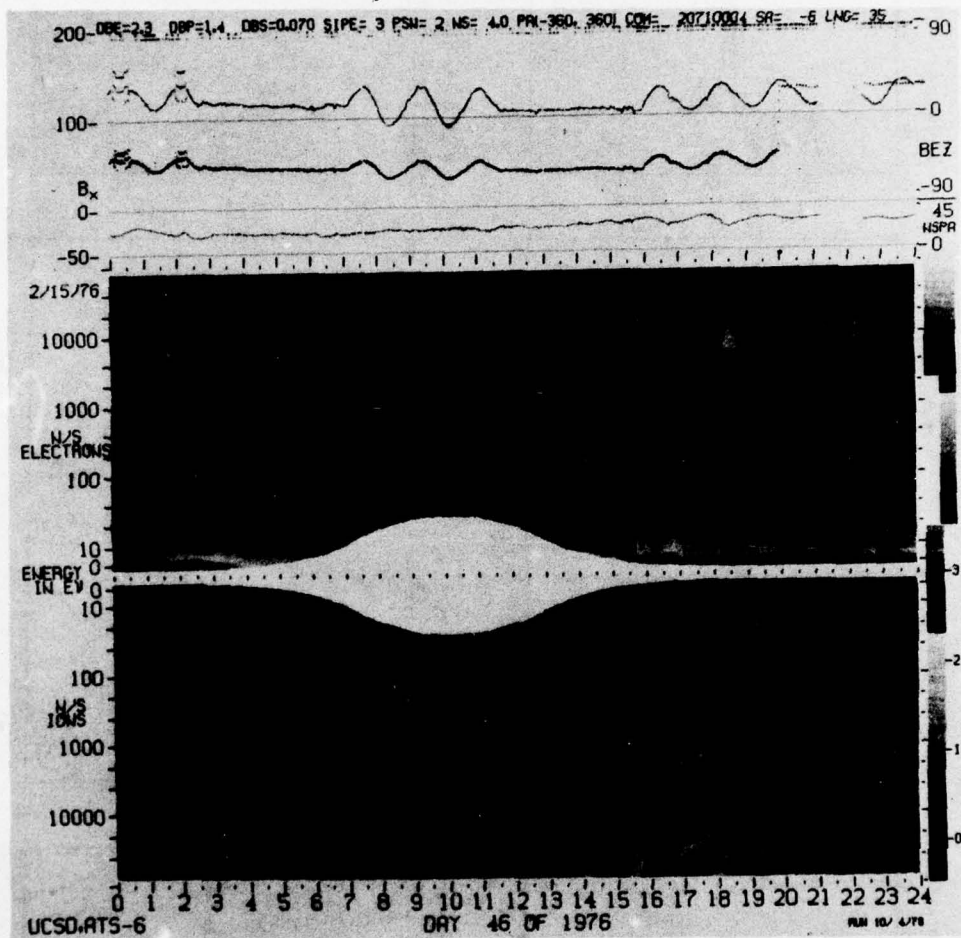


ATS-6 DATA
76/046

IONS

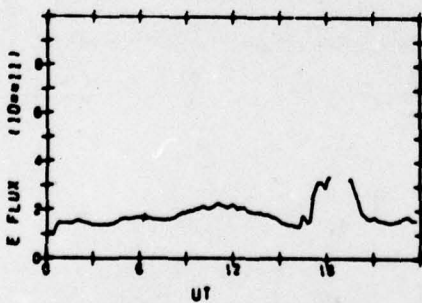
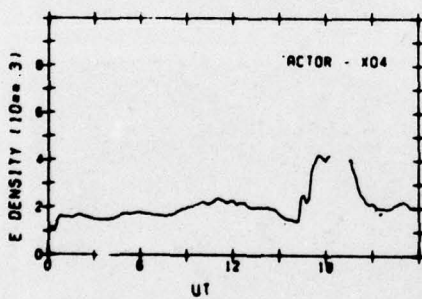
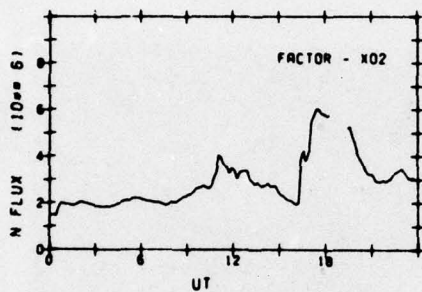
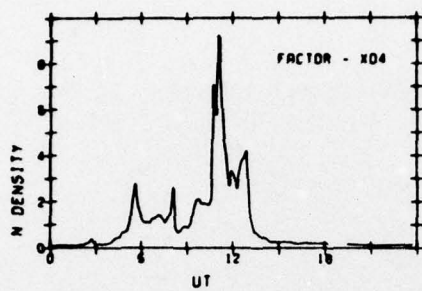
ELECTRONS



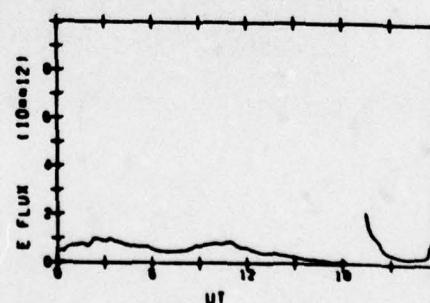
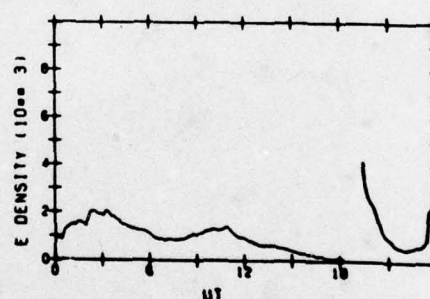
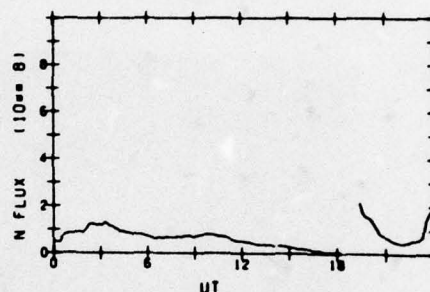
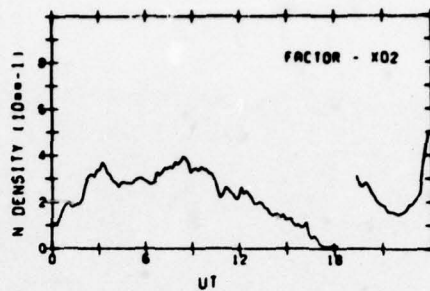


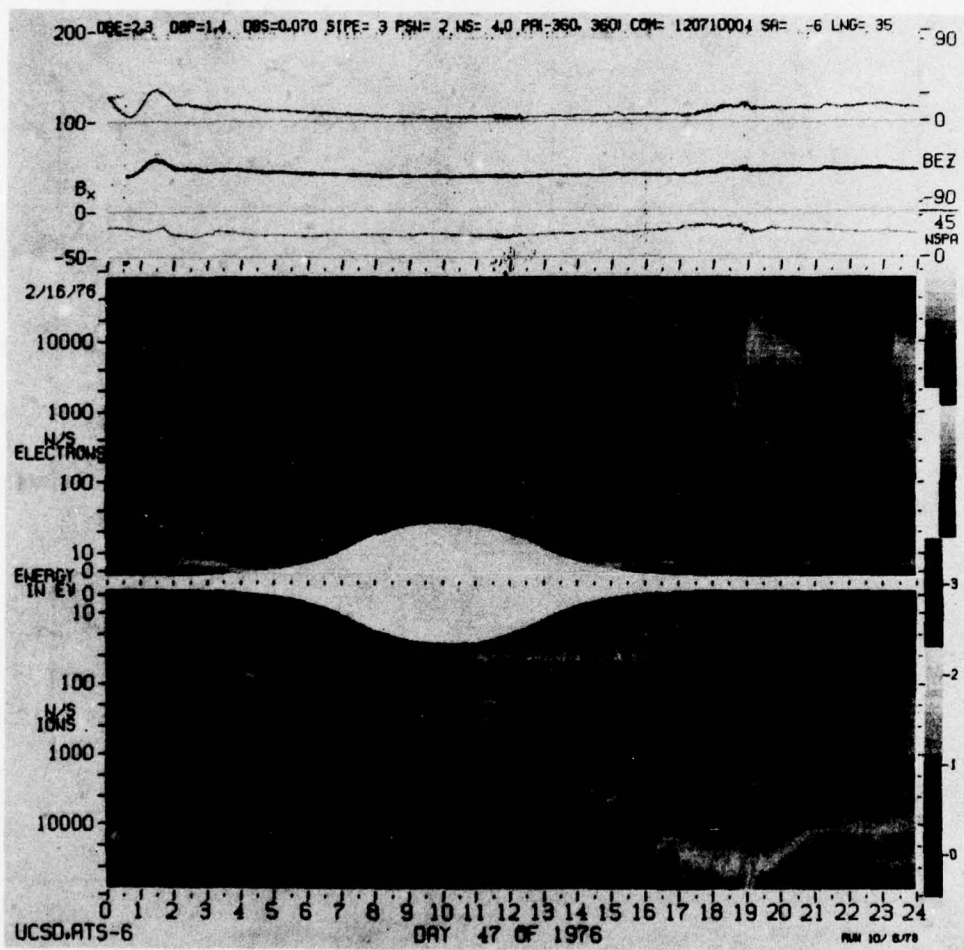
ATS-6 DATA
76/047

IONS



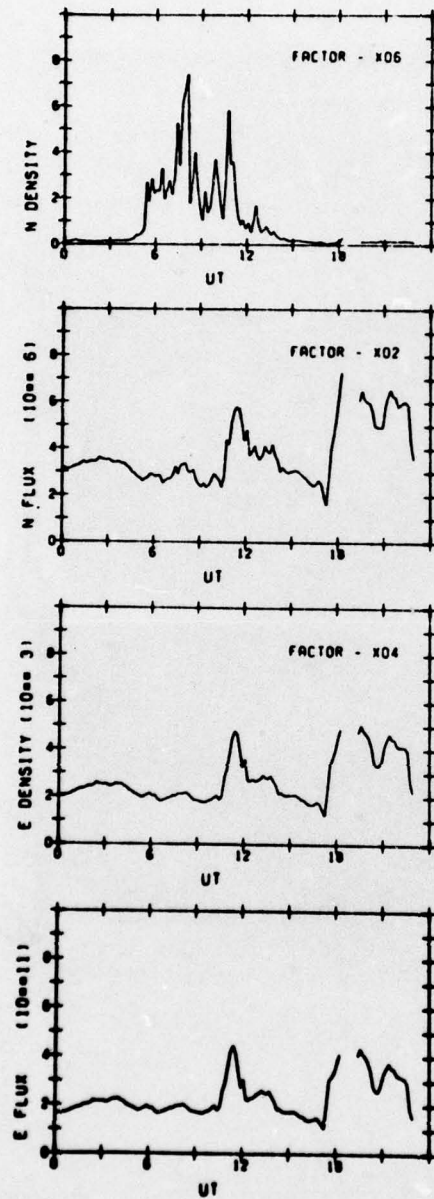
ELECTRONS



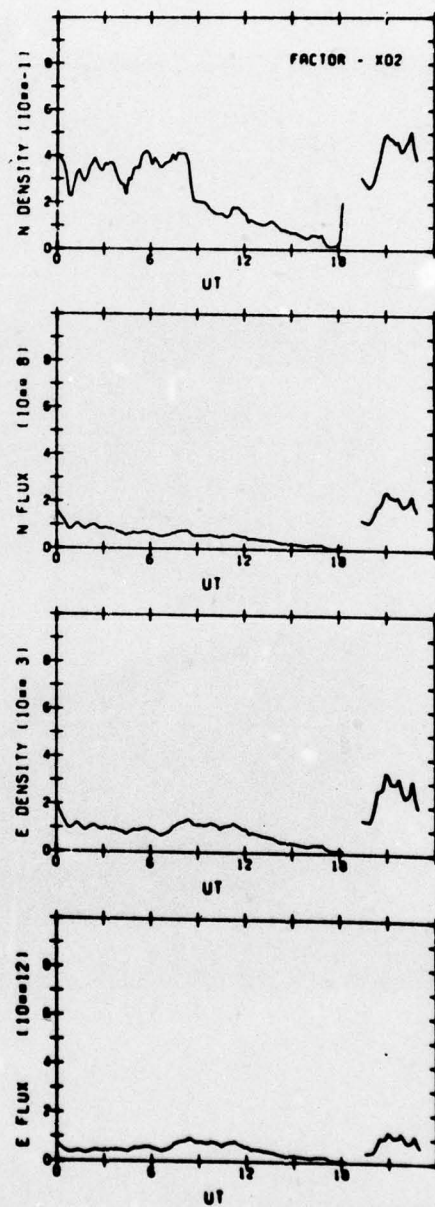


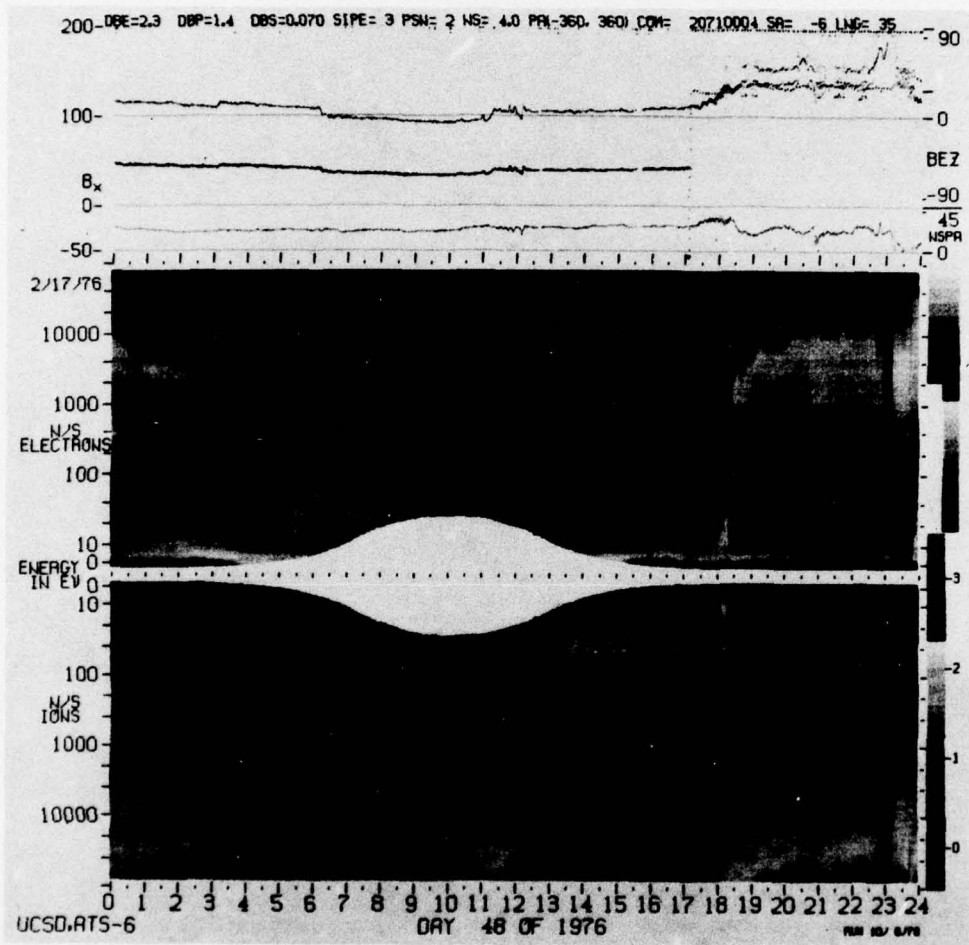
ATS-6 DATA
76/048

IONS



ELECTRONS



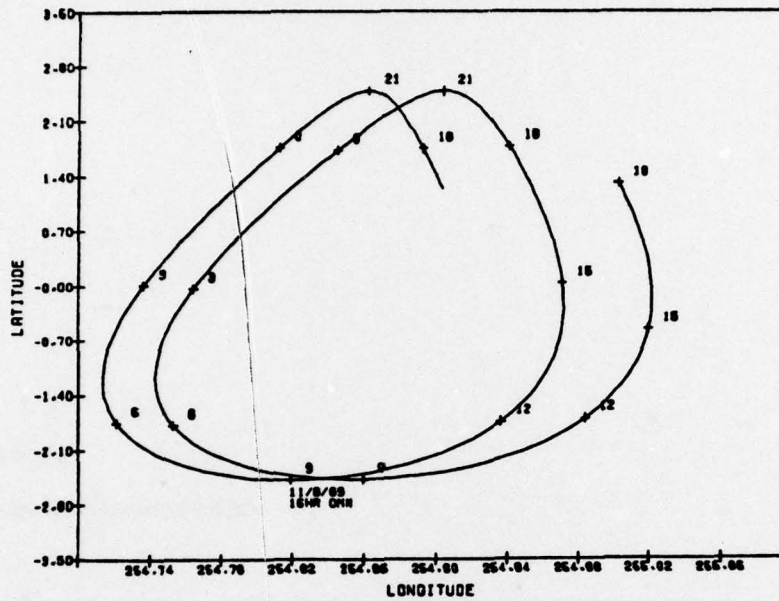


Appendix B

Orbital Elements of ATS-5 and ATS-6

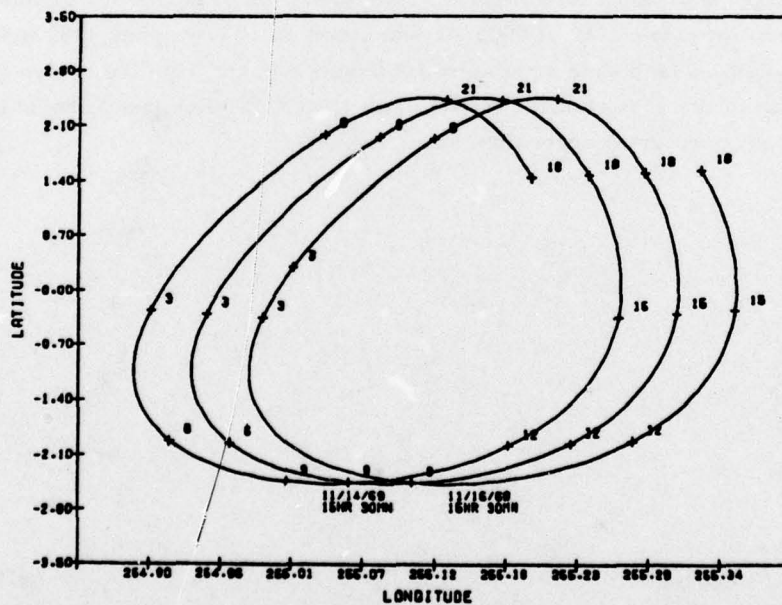
As discussed in the text, this appendix contains plots of the orbital elements for ATS-5 and ATS-6 for the days listed in Table 1. For each satellite the latitude vs longitude in geographic coordinates are shown first. The dates at the top indicate the start and stop times (that is, 11/8/69-11/10/69 0HR 0MN means the plot started on 8 November 1969 at 0000 UT and ended on 10 November 1969 at 0000 UT). The second set in each case are the radial distance in km from the center of the earth vs day of the year (Jan 1 - Day 1). AFGL/SUA (E. Robinson) should be consulted for any questions concerning these elements.

ATS-5 11/ 8/69 11/10/69 OHR OMN
ATS-5



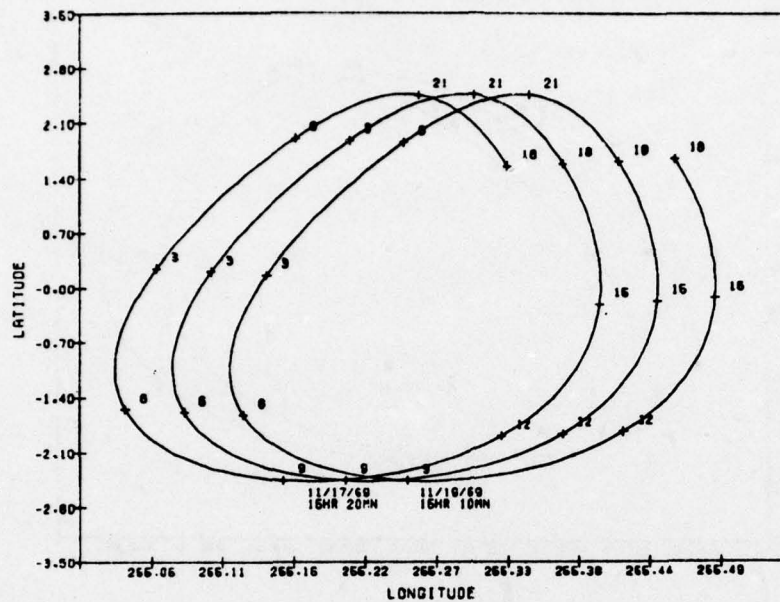
CORWARD-

ATS-5 11/14/69 11/17/69 OHR OMN
ATS-5

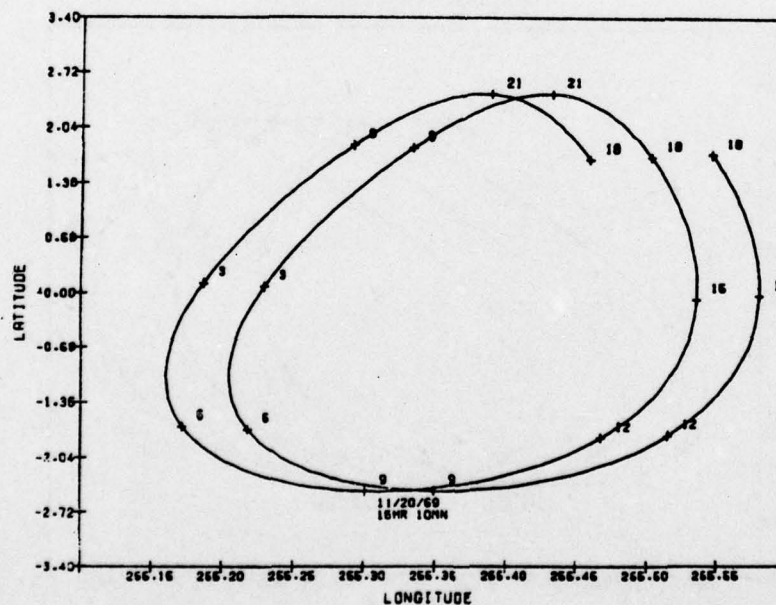


CORWARD-

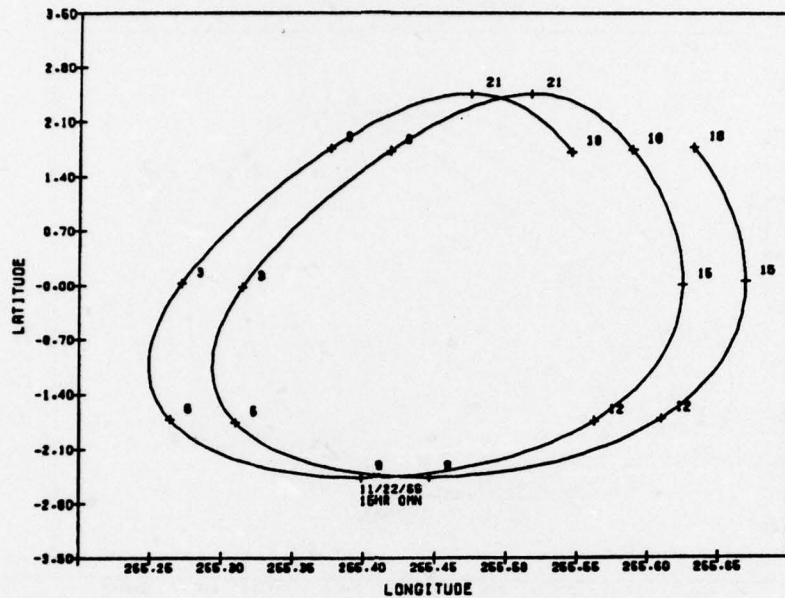
ATS-5 11/17/69 11/20/69 OHR OMN
ATS-5



ATS-5 11/20/69 11/22/69 OHR OMN
ATS-5

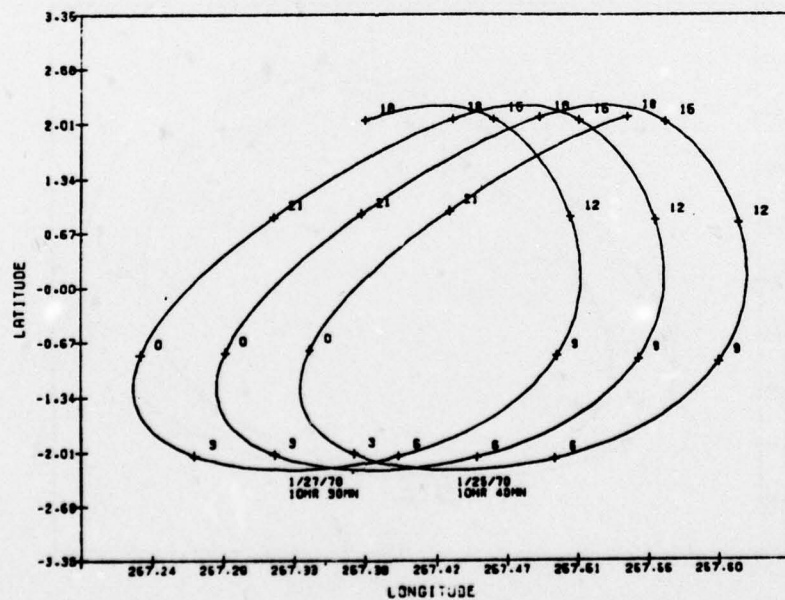


ATS-5 11/22/69 11/24/69 OHR OMN
ATS-5

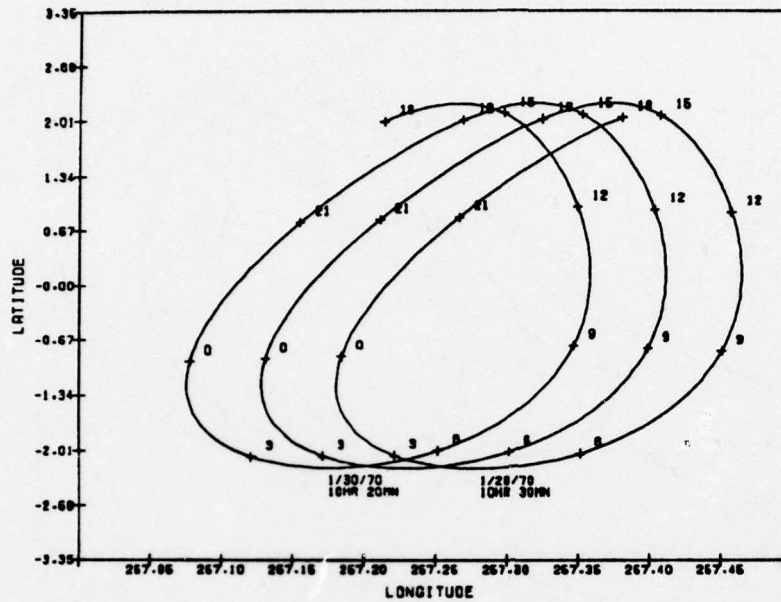


CONTINUED-

ATS-5 1/25/70 1/28/70 OHR OMN
ATS-5

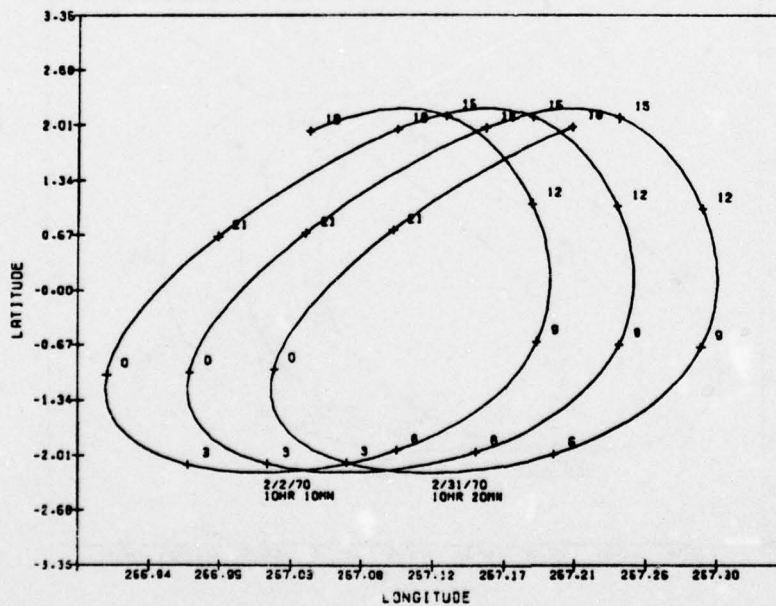


ATS-5 1/28/70 1/31/70 OHR OMN
ATS-5

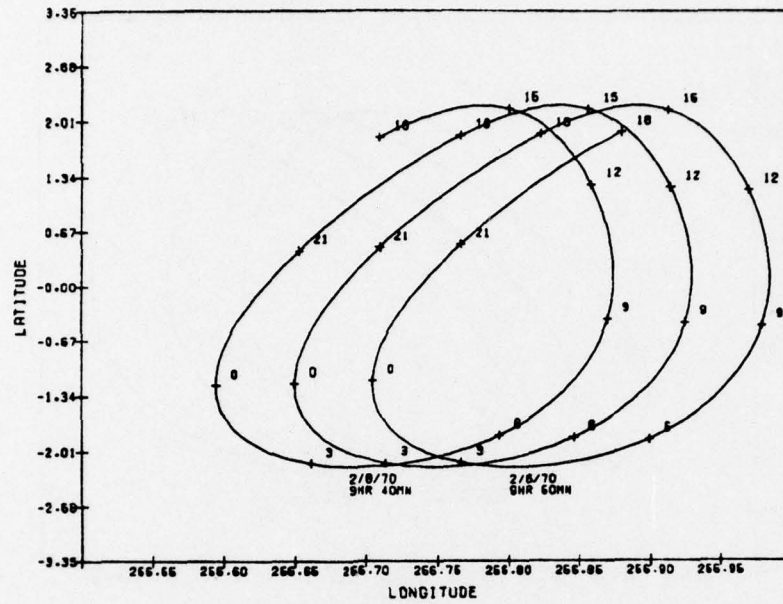


CONTINUED-

ATS-5 1/31/70 2/ 3/70 OHR OMN
ATS-5

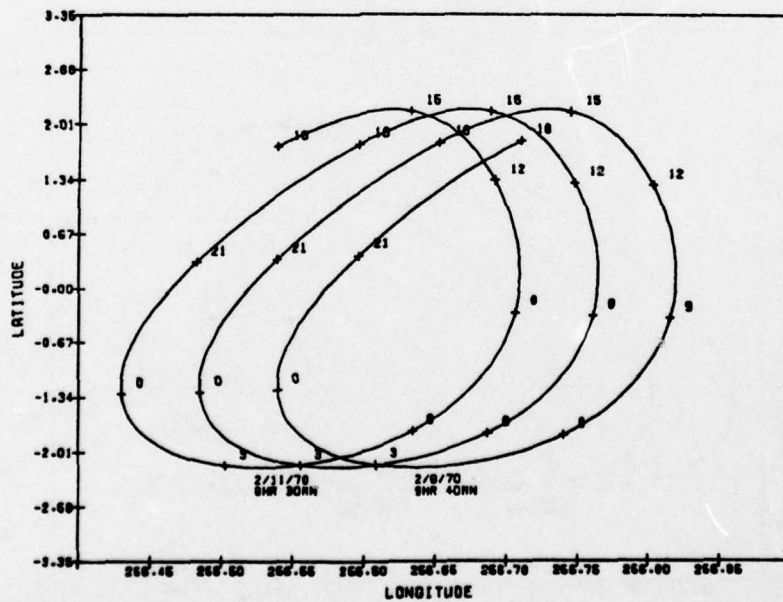


ATS-5 2/ 6/70 2/ 9/70 OHR OMN
 ATS-5



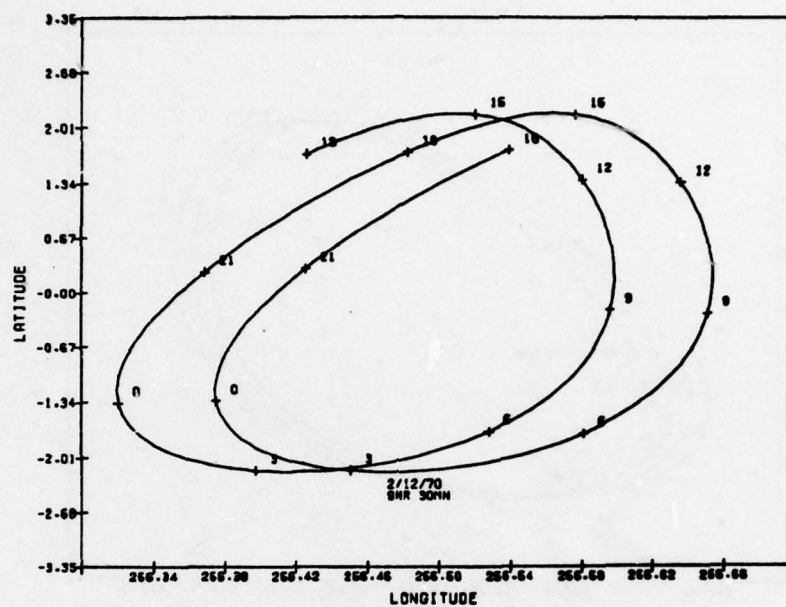
CORRAND-

ATS-5 2/ 9/70 2/12/70 OHR OMN
 ATS-5



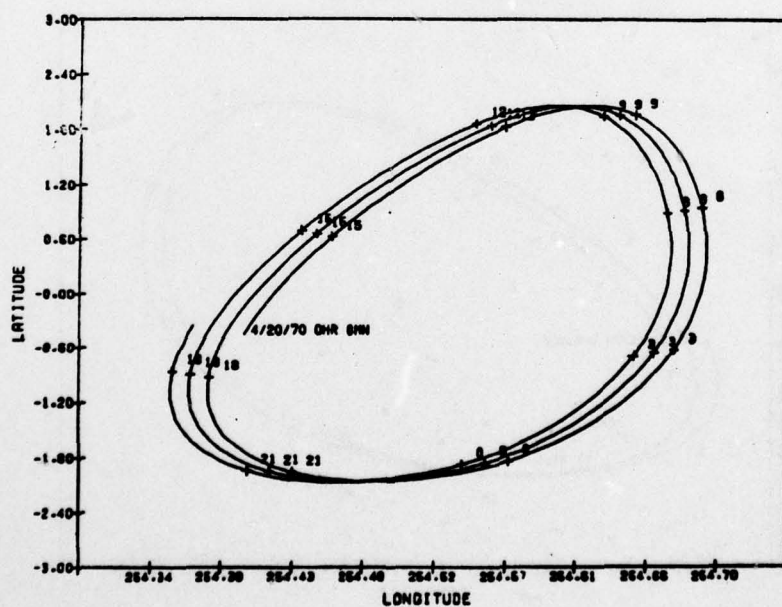
CORRAND-

ATS-5 2/12/70 2/14/70 OHR OMN
ATS-5

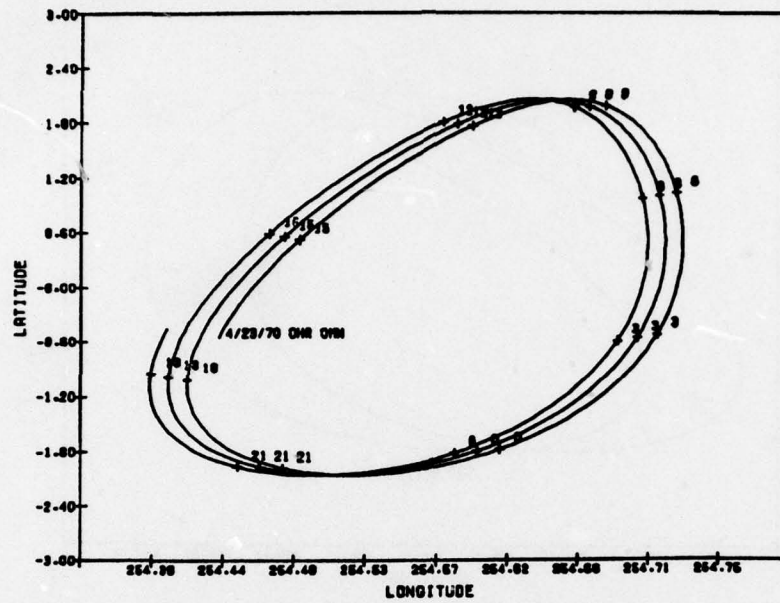


CONRAD-

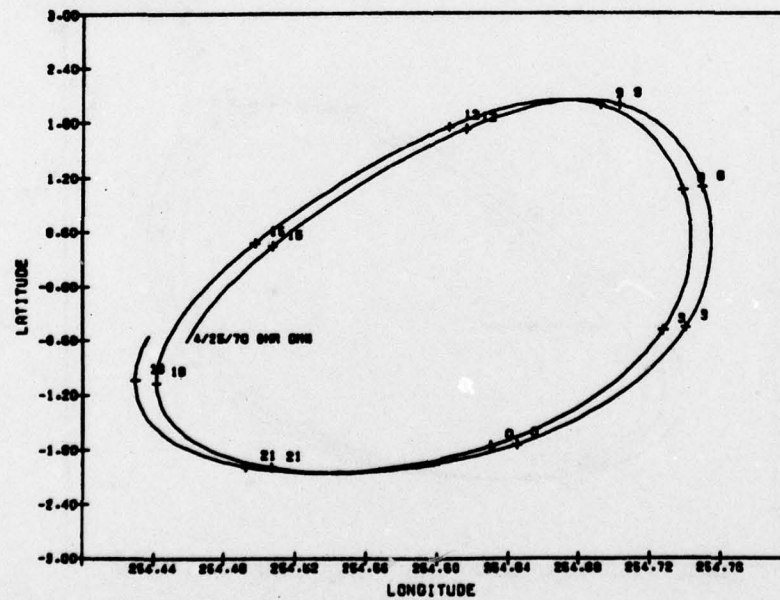
ATS-5 4/17/70 4/20/70 OHR OMN
ATS-5



COMMAND-
 ATS-5 4/20/70 4/23/70 OHR OMN
 ATS-5

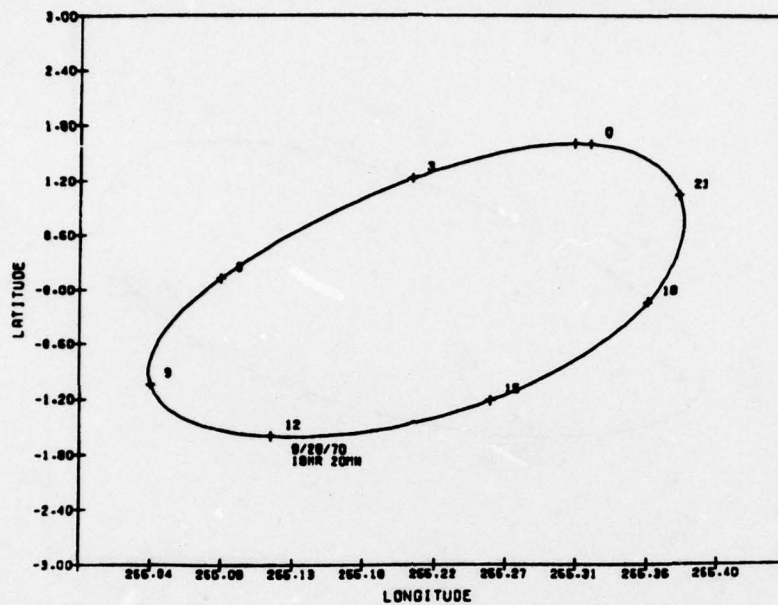


ATS-5 4/23/70 4/25/70 OHR OMN
 ATS-5

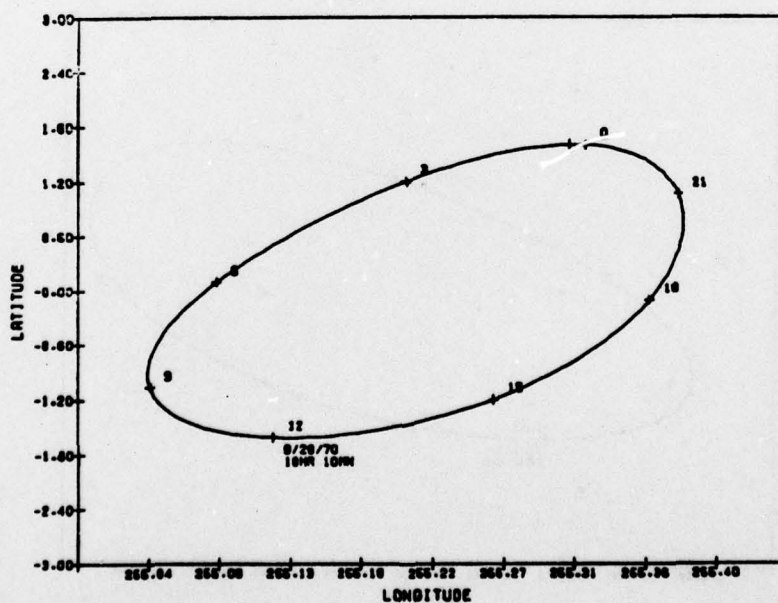


COMMAND-

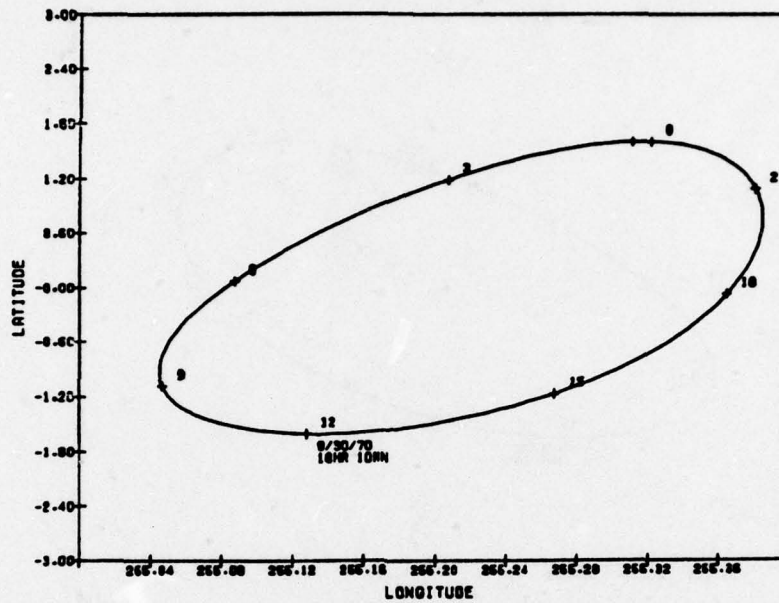
COMMAND-
 ATS-5 9/28/70 9/29/70 OHR OMN
 ATS-5



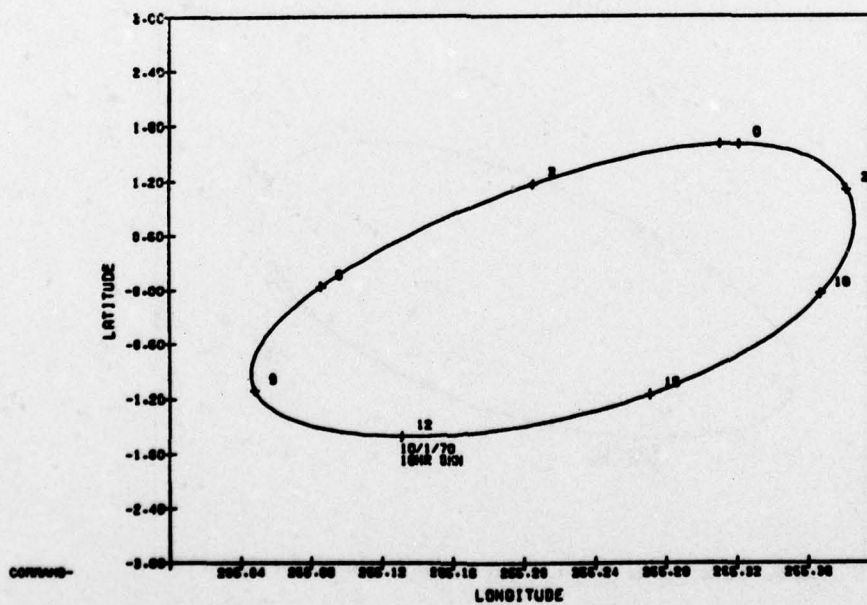
COMMAND-
 ATS-5 9/29/70 9/30/70 OHR OMN
 ATS-5



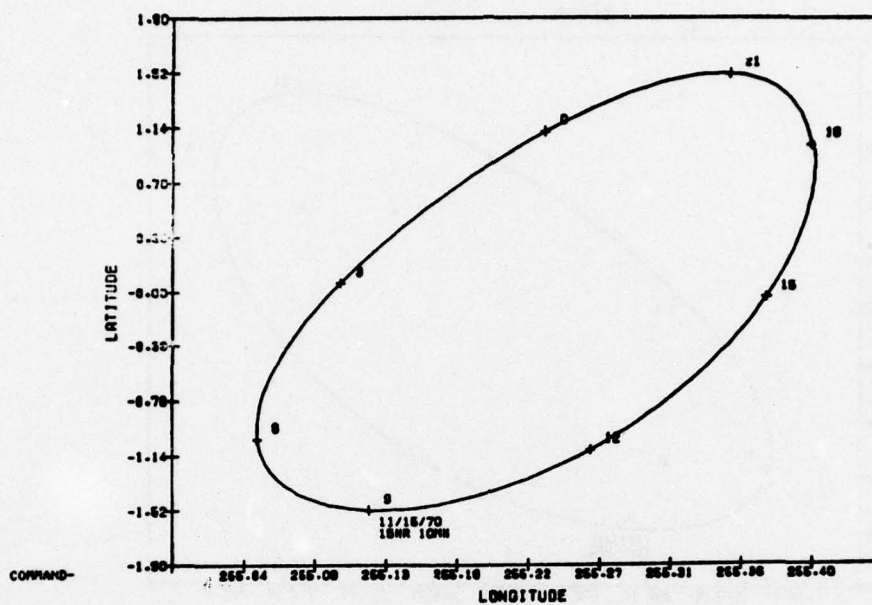
COMMAND-
 ATS-5 9/30/70 10/ 1/70 OHR OMN
 ATS-5



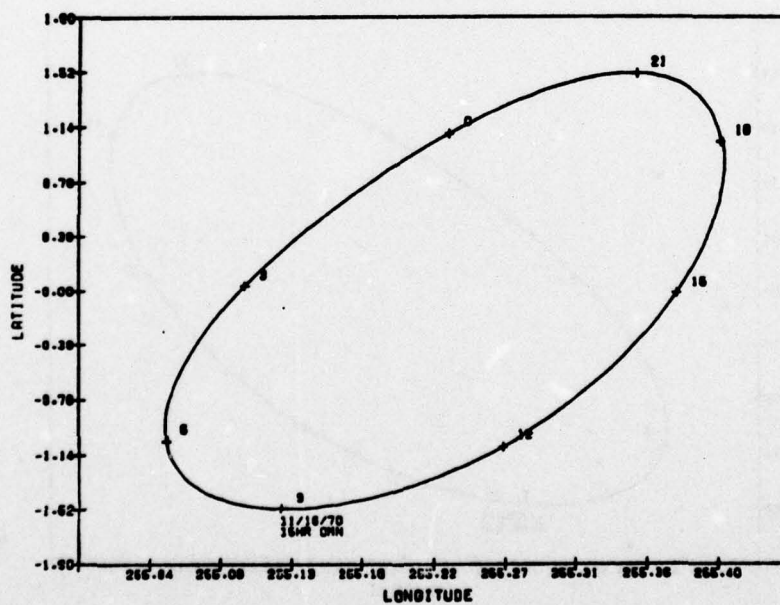
ATS-5 10/ 1/70 10/ 2/70 OHR OMN
 ATS-5



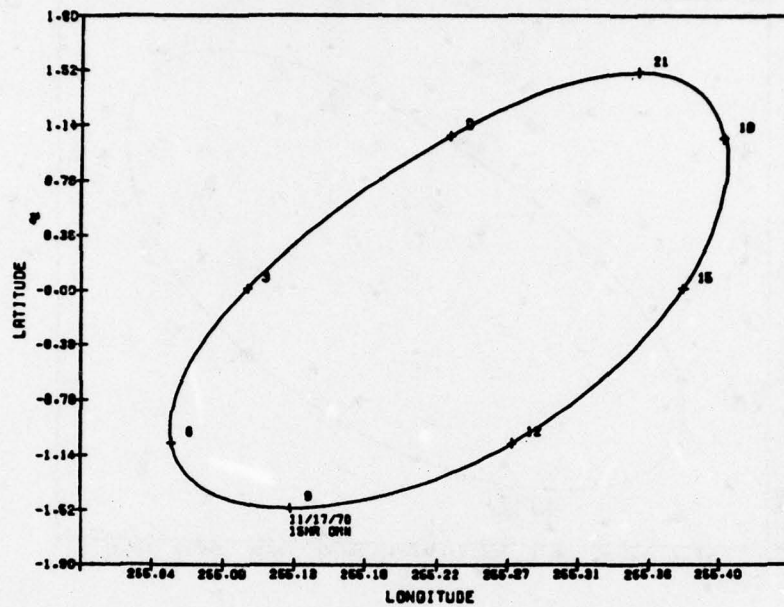
ATS-5 11/15/70 11/16/70 OHR OMN
ATS-5



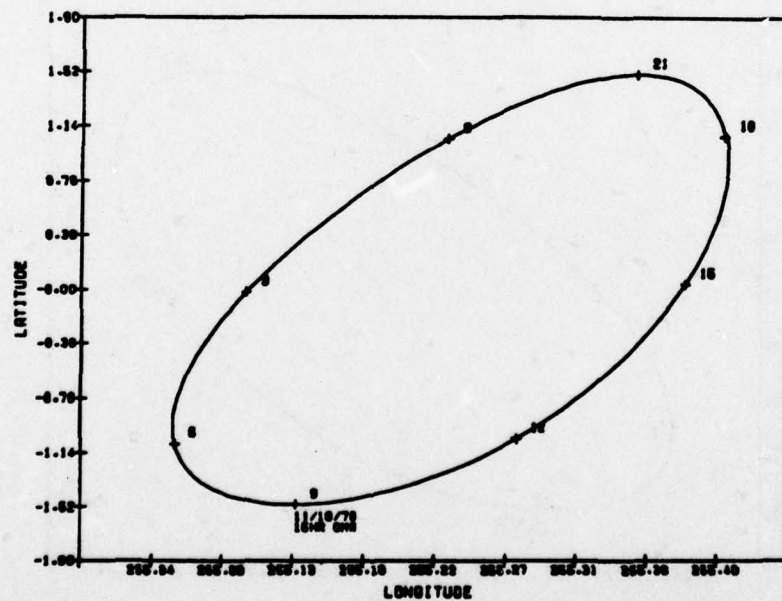
COMMAND-
ATS-5 11/16/70 11/17/70 OHR OMN
ATS-5



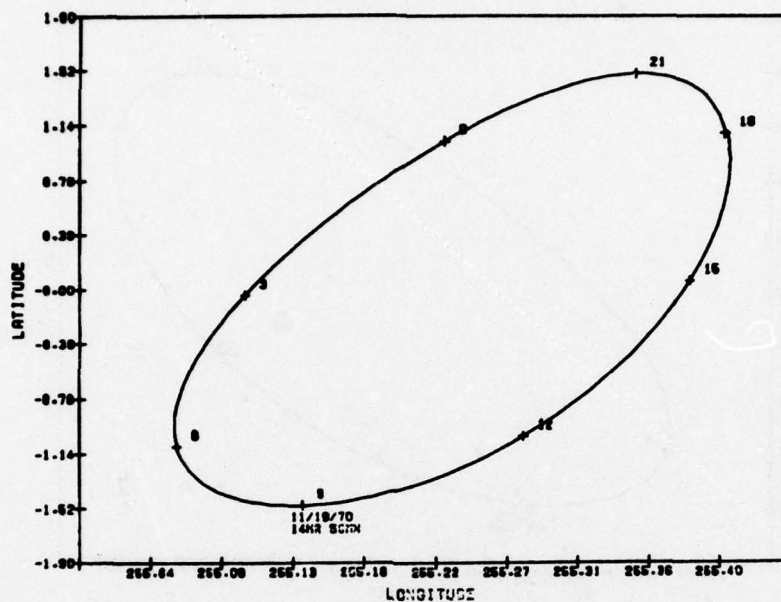
COMMAND-
 ATS-5 11/17/70 11/18/70 OHR OMN
 ATS-5



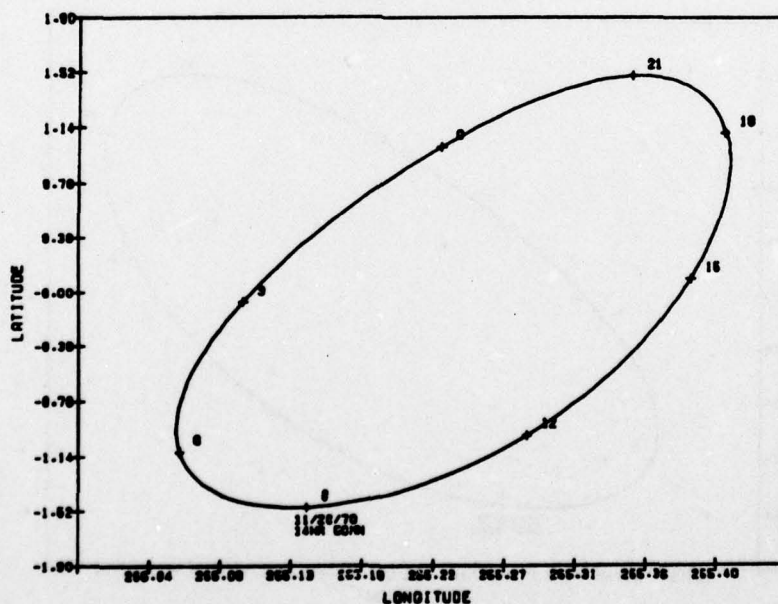
COMMAND-
 ATS-5 11/18/70 11/19/70 OHR OMN
 ATS-5



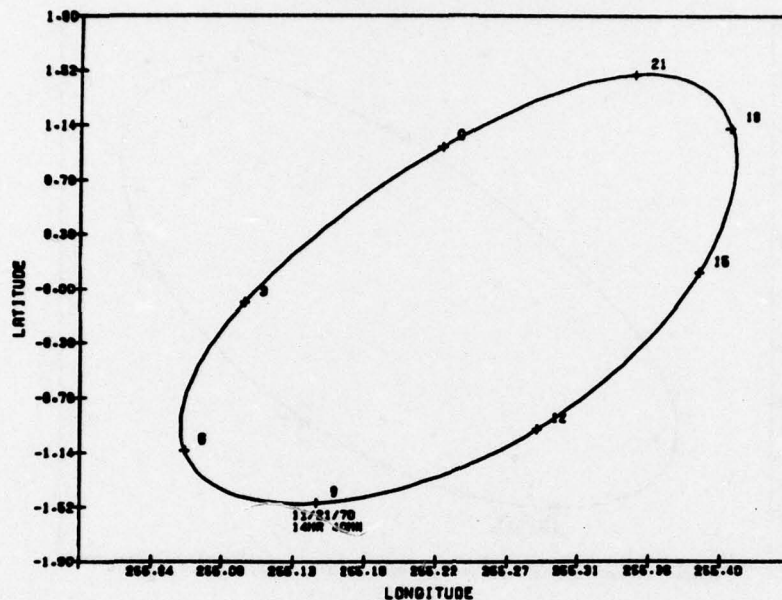
COMMAND-
 ATS-5 11/19/70 11/20/70 OHR OMN
 ATS-5



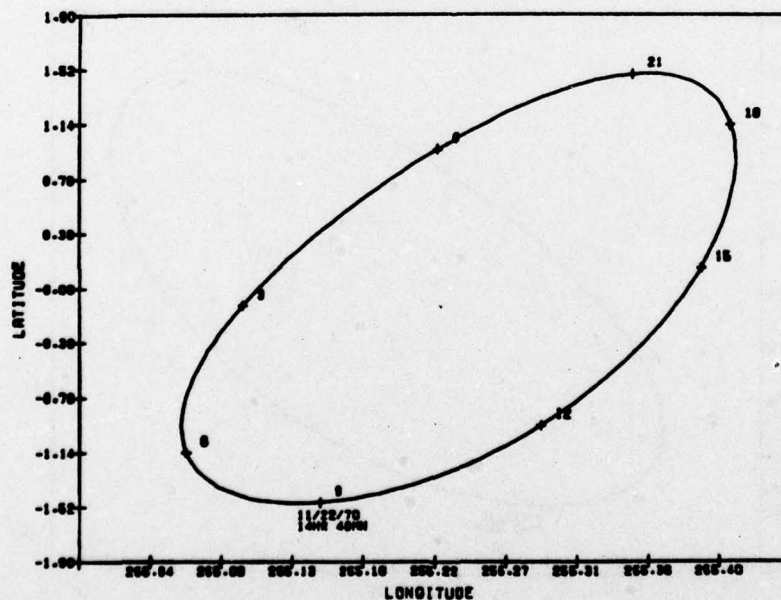
COMMAND-
 ATS-5 11/20/70 11/21/70 OHR OMN
 ATS-5



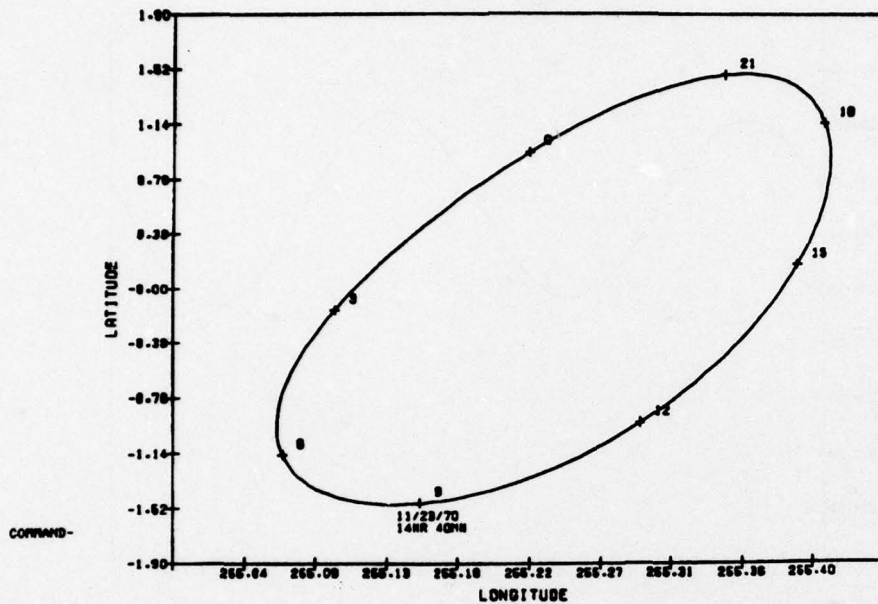
COMMAND-
 ATS-5 11/21/70 11/22/70 OHR OMN
 ATS-5



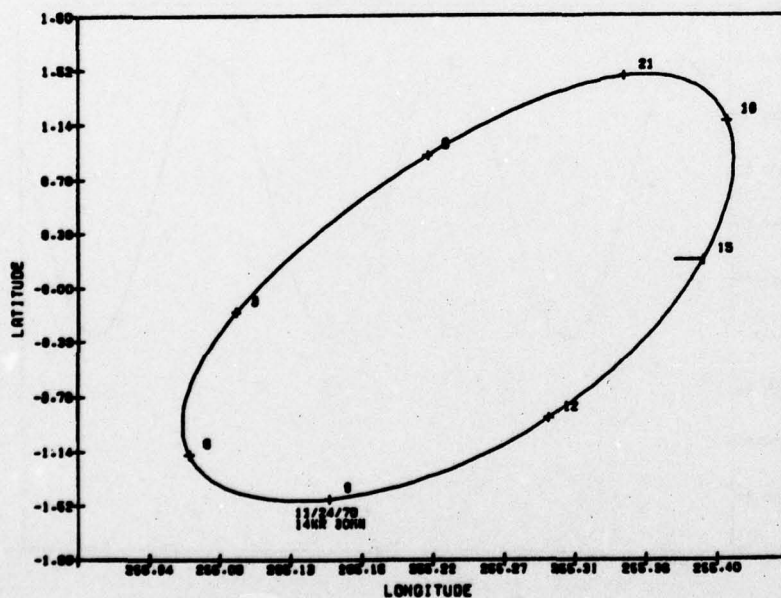
COMMAND-
 ATS-5 11/22/70 11/23/70 OHR OMN
 ATS-5



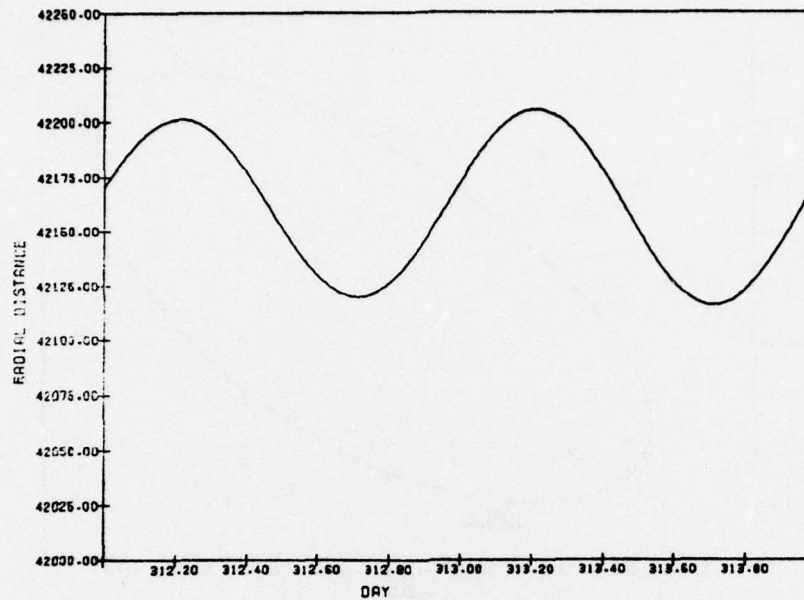
ATS-5 11/23/70 11/24/70 OHR OMN
ATS-5



COMMAND-
ATS-5 11/24/70 11/25/70 OHR OMN
ATS-5

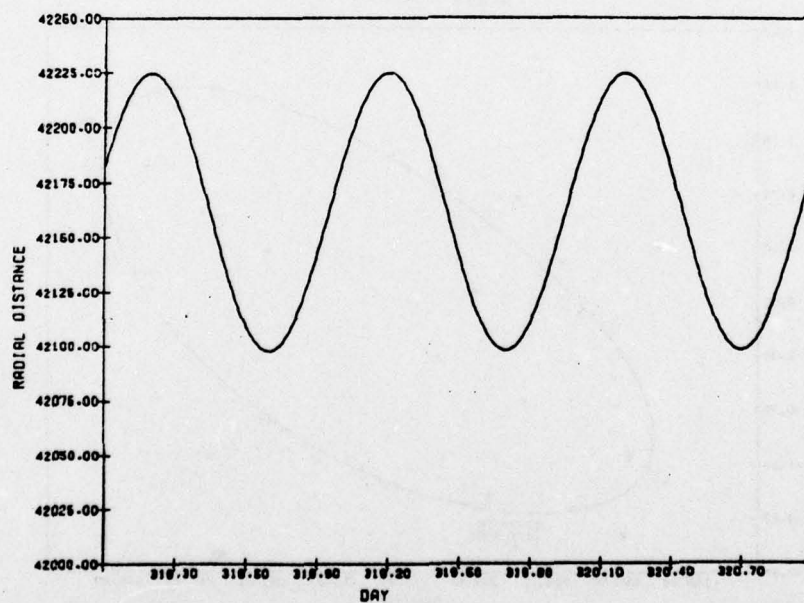


ATS-5 11/ 8/69 11/10/69 OHR OMN
ATS-5



COMMAND-

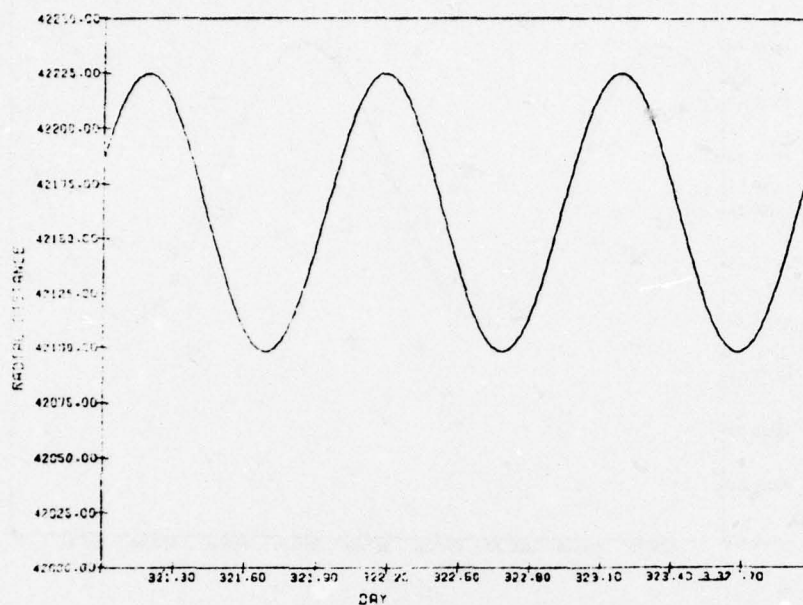
ATS-5 11/14/69 11/17/69 OHR OMN
ATS-5



COMMAND-

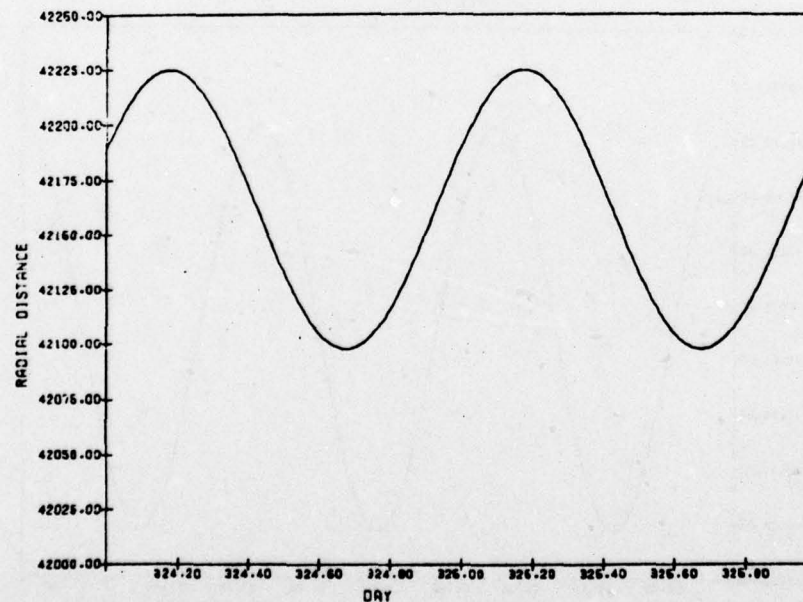
ATS-5 11/17/69 11/20/69 OHR OMN

ATS-5



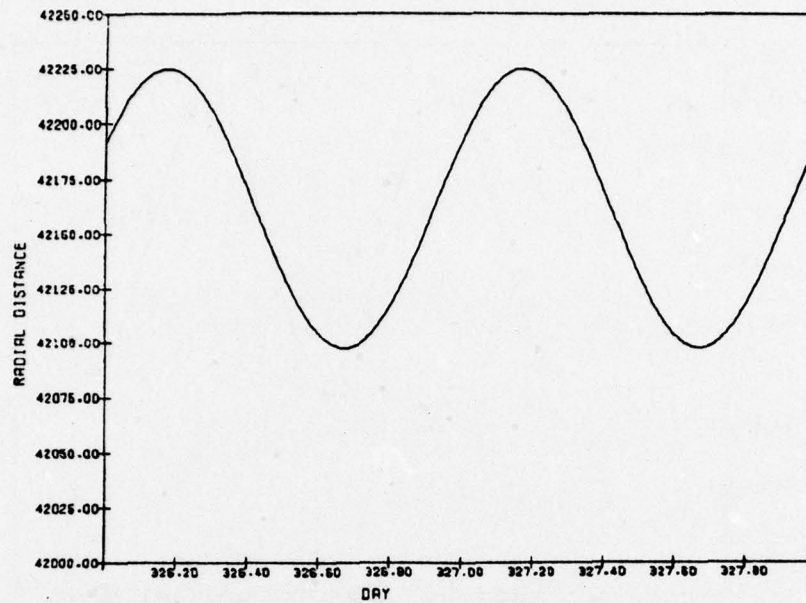
ATS-5 11/20/69 11/22/69 OHR OMN

ATS-5



COPYHARD-

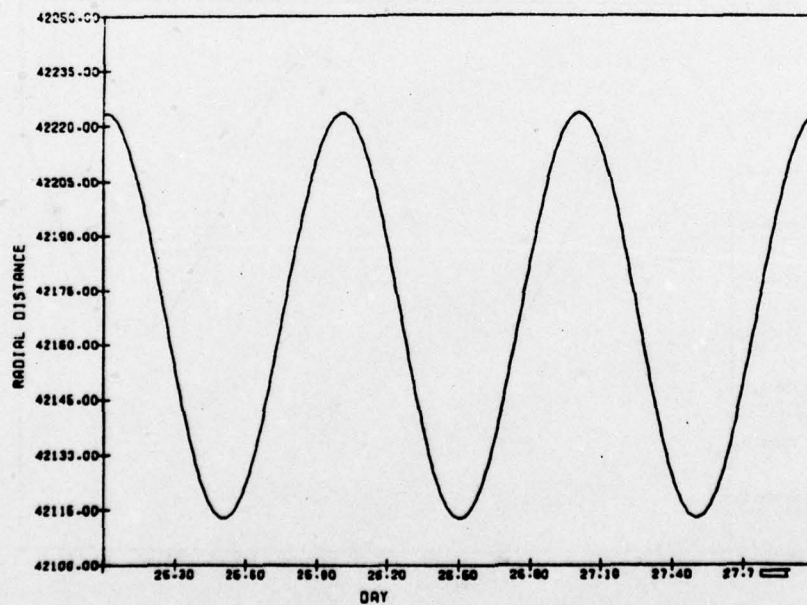
ATS-5 11/22/69 11/24/69 OHR OMN
 ATS-5



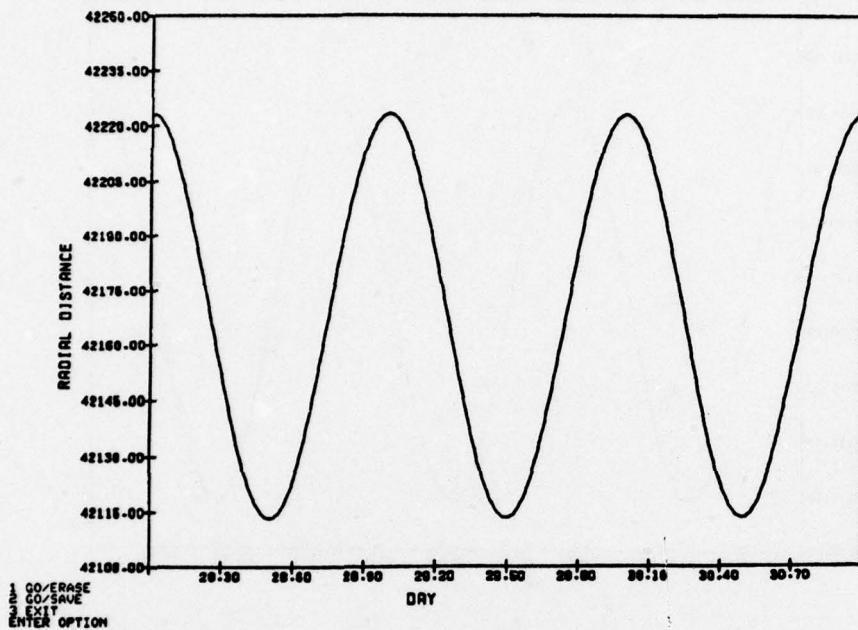
CURRENT-

CURRENT-

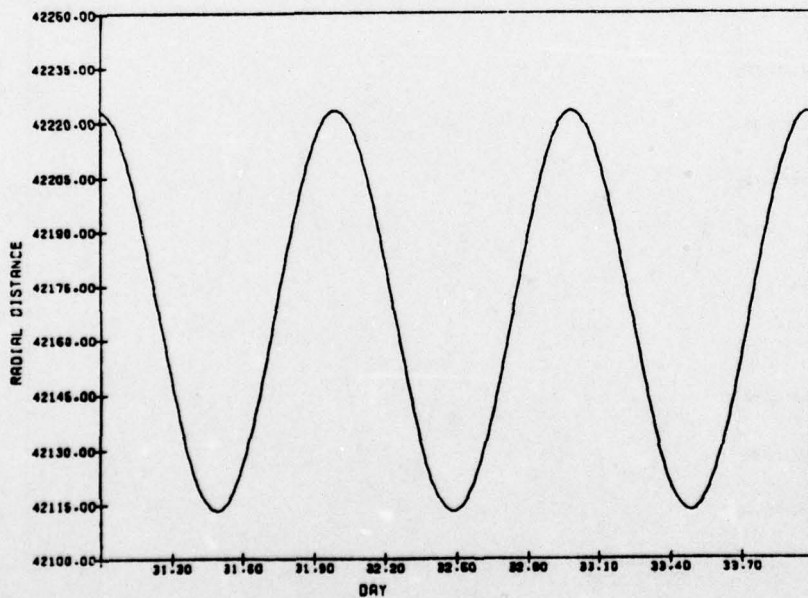
ATS-5 1/25/70 1/28/70 OHR OMN
 ATS-5



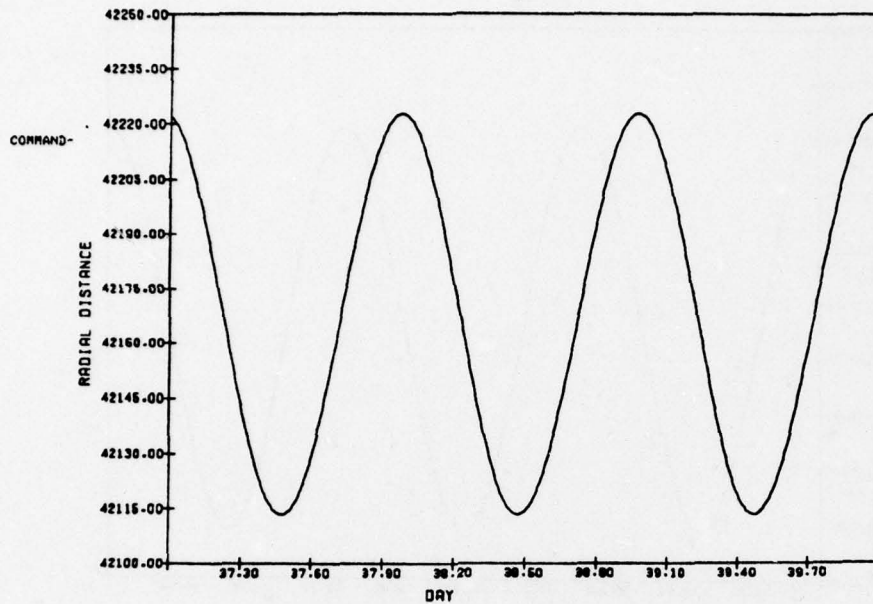
COMMAND-
 ATS-5 1/28/70 1/31/70 OHR OMN
 ATS-5



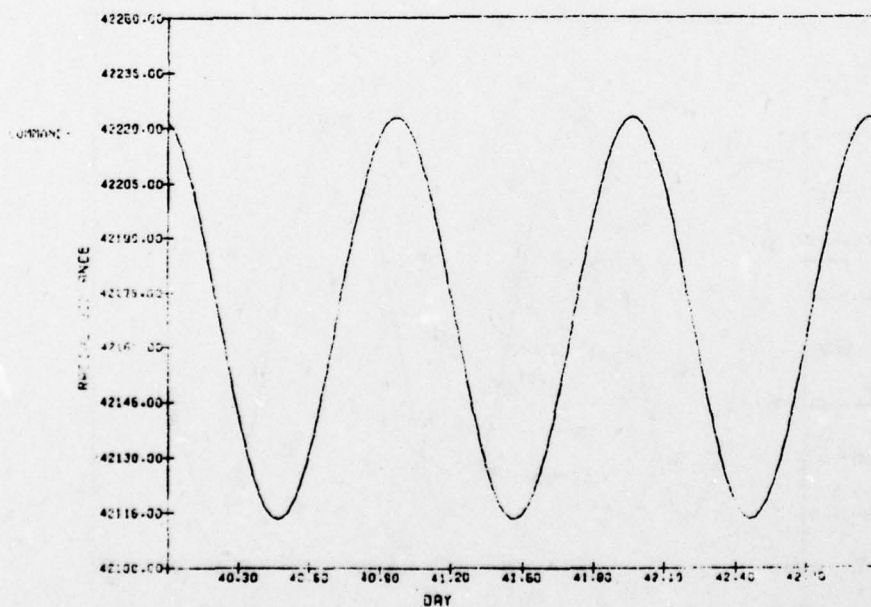
COMMAND-
 ATS-5 1/31/70 2/ 3/70 OHR OMN
 ATS-5



ATS-5 2/ 6/70 2/ 9/70 QHR QMN
ATS-5

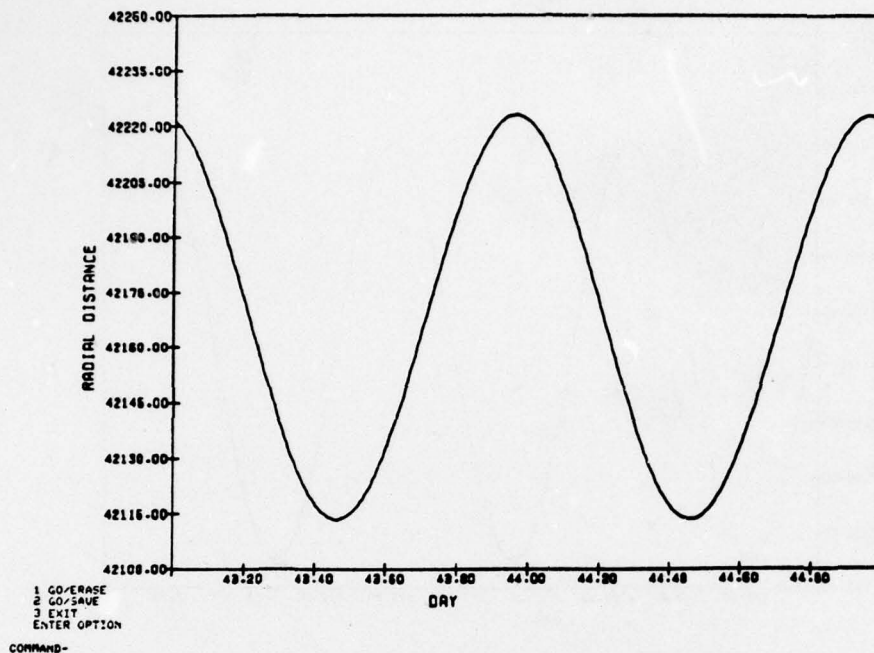


ATS-5 2/ 9/70 2/12/70 QHR QMN
ATS-5



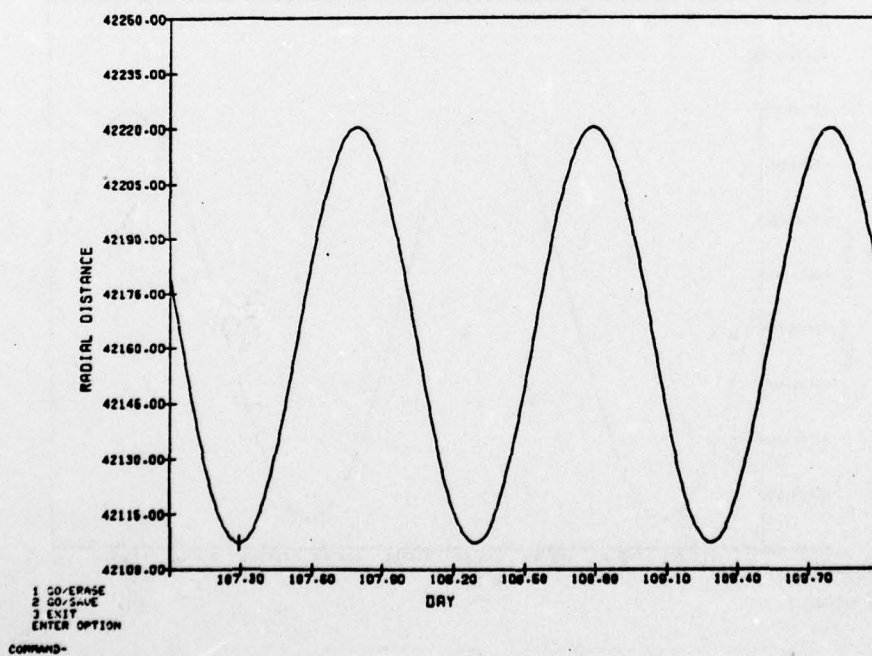
ATS-5 2/12/70 2/14/70 OHR OMN

ATS-5

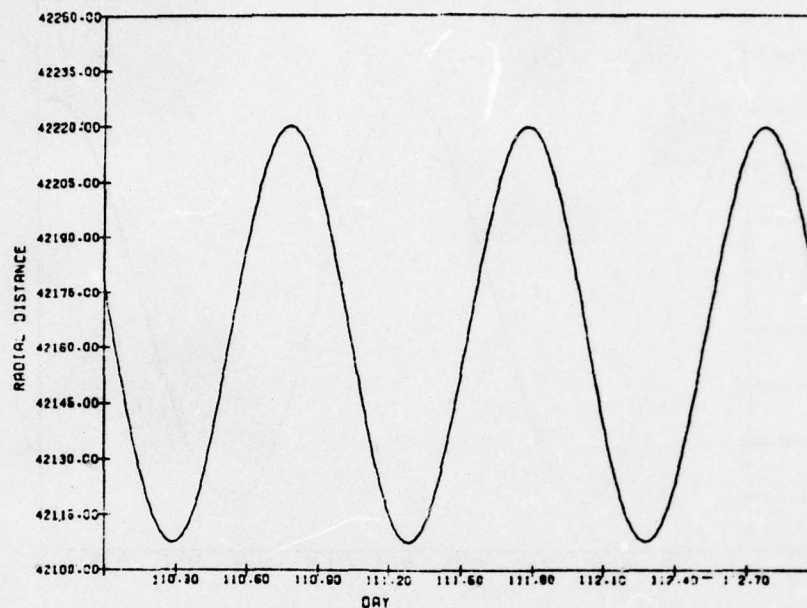


ATS-5 4/17/70 4/20/70 OHR OMN

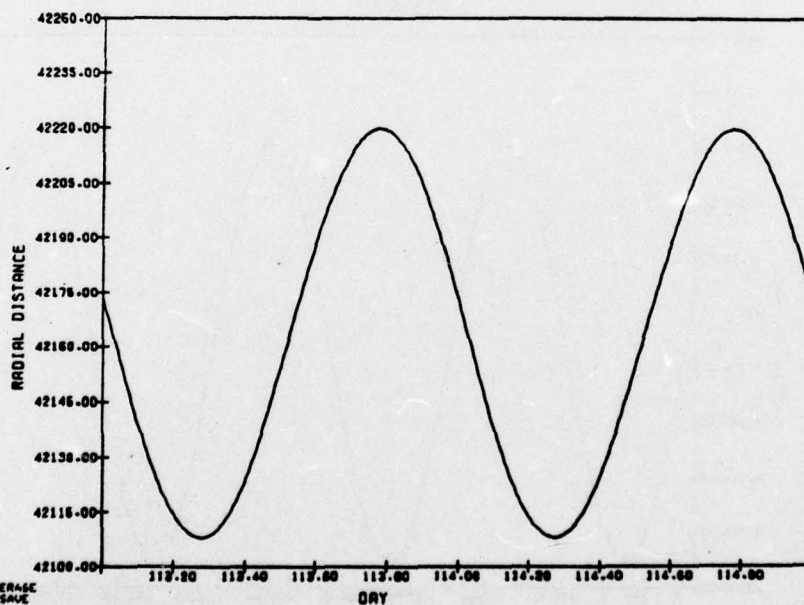
ATS-5



ATS-5 4/20/70 4/23/70 OHR OMN
ATS-5

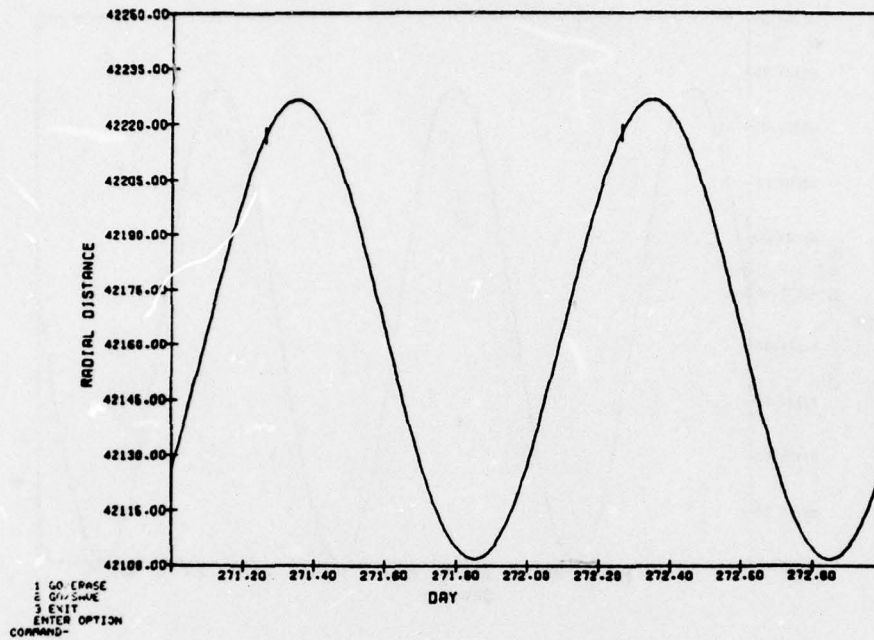


ATS-5 4/23/70 4/25/70 OHR OMN
ATS-5

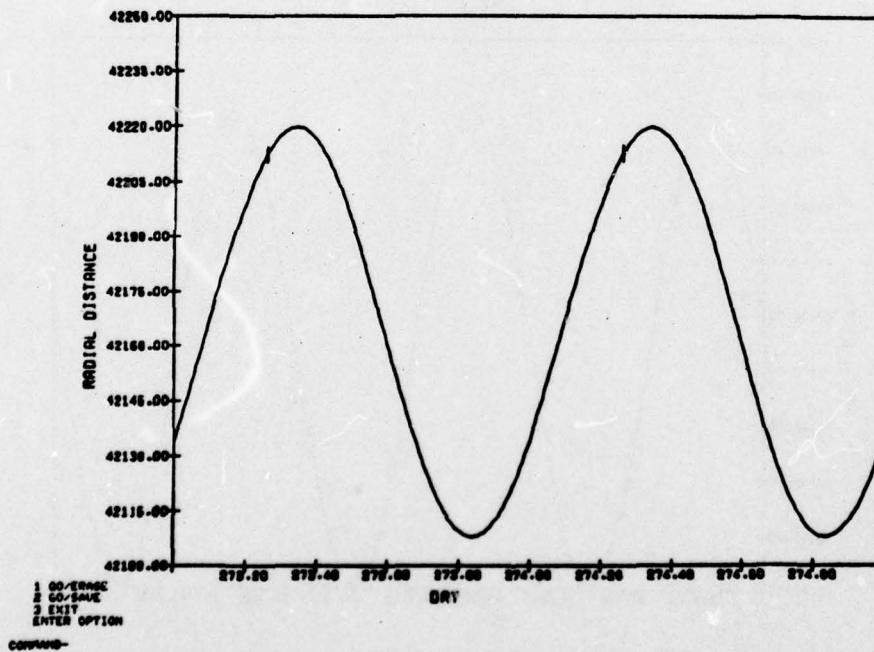


1 COVERAGE
2 GO/SAVE
3 EXIT
ENTER OPTION
COMMAND-

ATS-5 9/28/70 9/30/70 OHR OMN
ATS-5

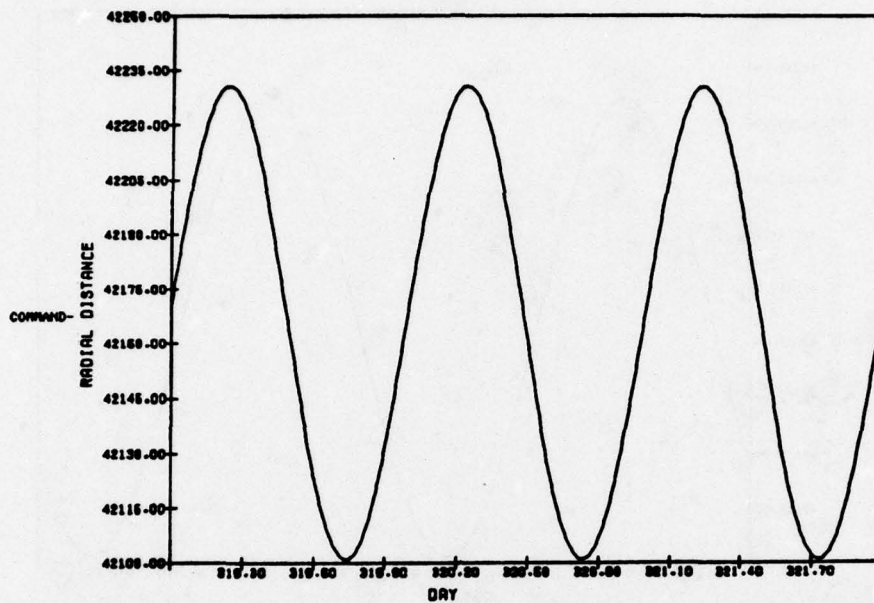


ATS-5 9/30/70 10/ 2/70 OHR OMN
ATS-5



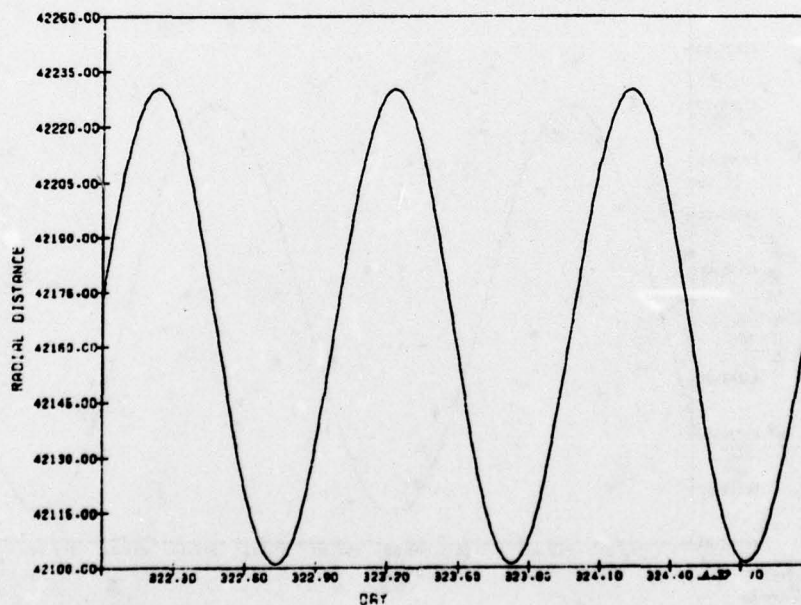
ATS-5 11/15/70 11/18/70 OHR OMN

ATS-5



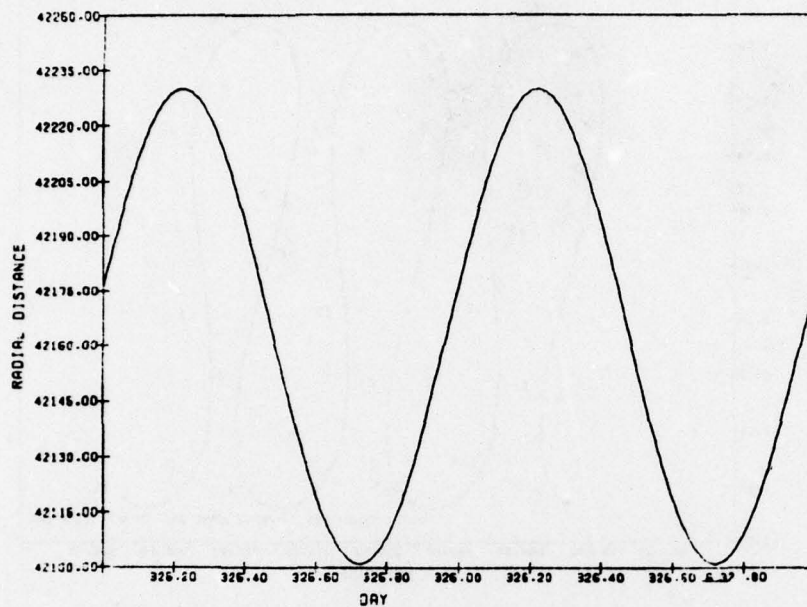
ATS-5 11/18/70 11/21/70 OHR OMN

ATS-5



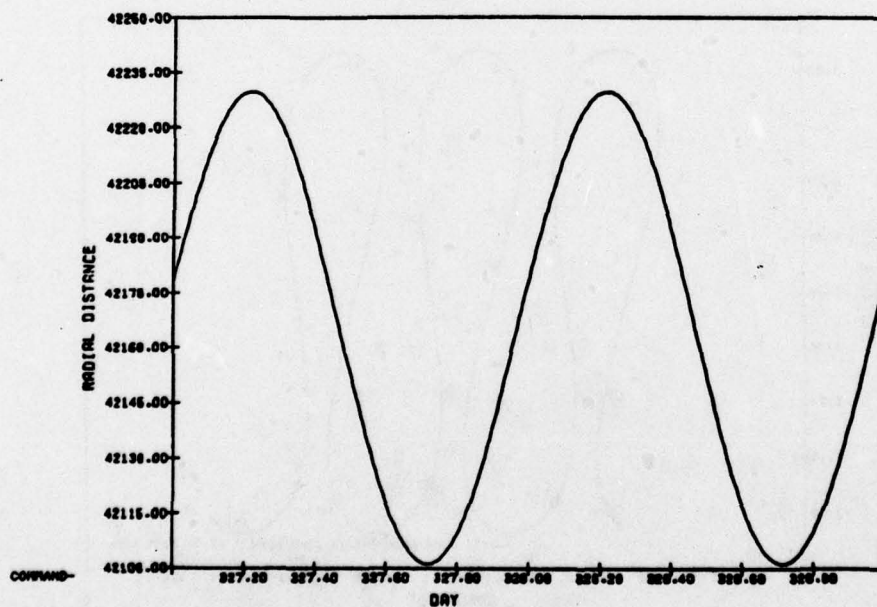
ATS-5 11/21/70 11/23/70 OHR OMN

ATS-5

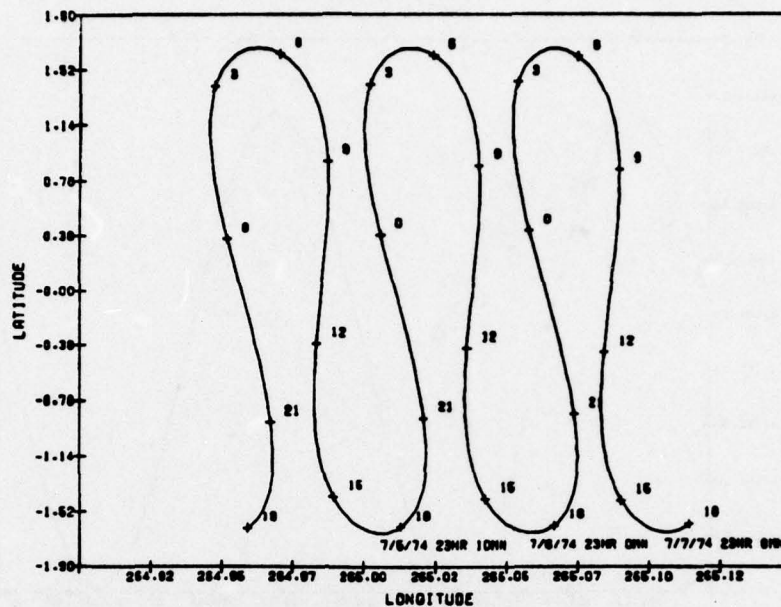


ATS-5 11/23/70 11/25/70 OHR OMN

ATS-5

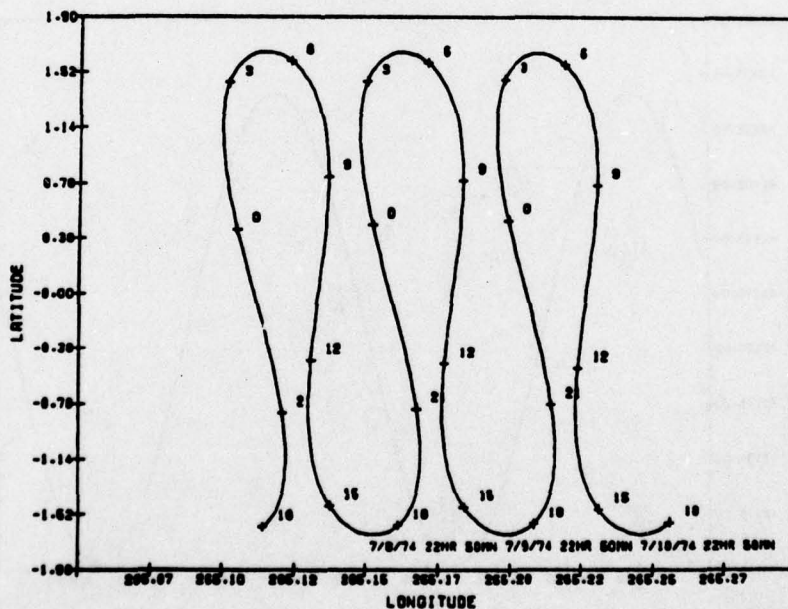


ATS-6 7/ 5/74 7/ 8/74 OHR OMN
ATS-6



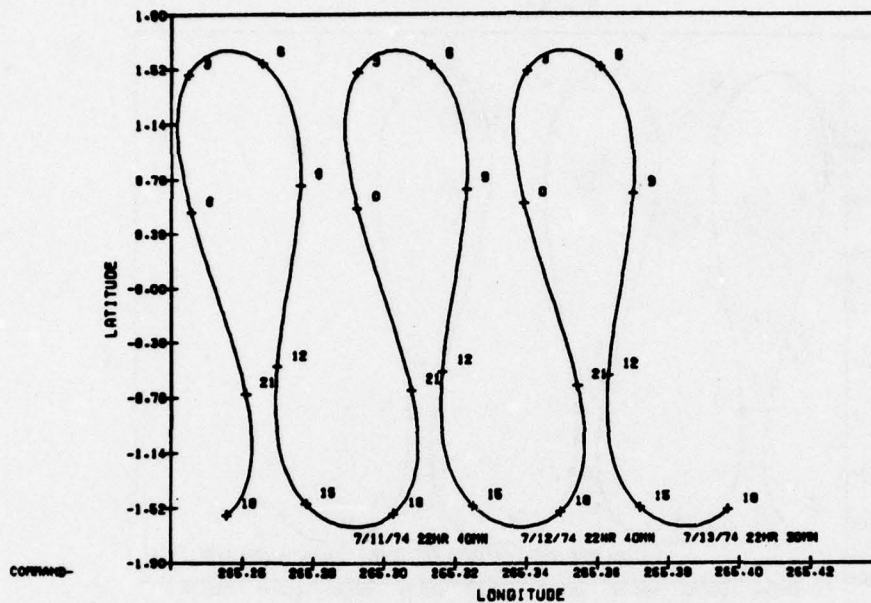
CONTINUED-

ATS-6 7/ 8/74 7/11/74 OHR OMN
ATS-6

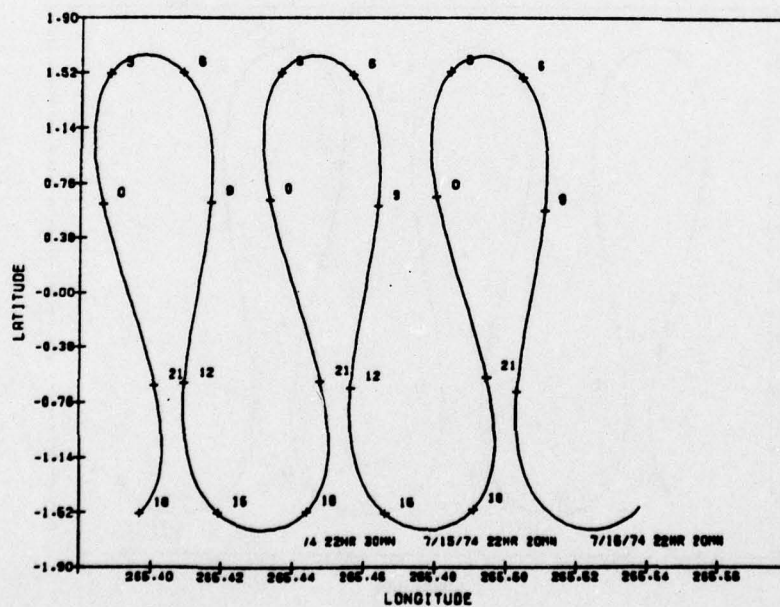


CONTINUED-

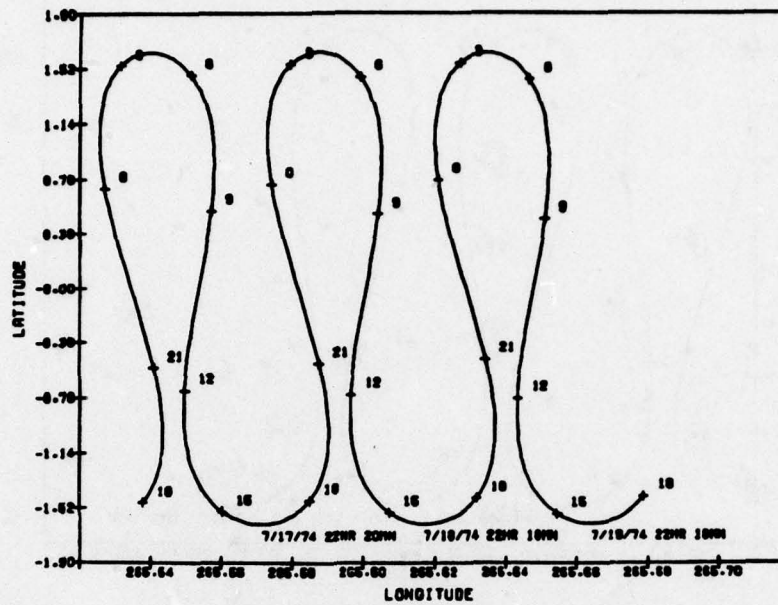
ATS-6 7/11/74 7/14/74 OHR OMN
ATS-6



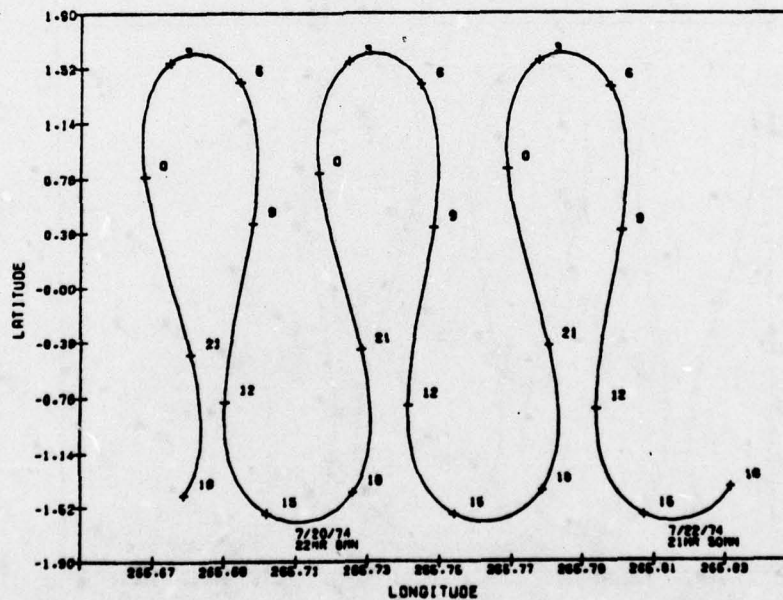
ATS-6 7/14/74 7/17/74 OHR OMN
ATS-6



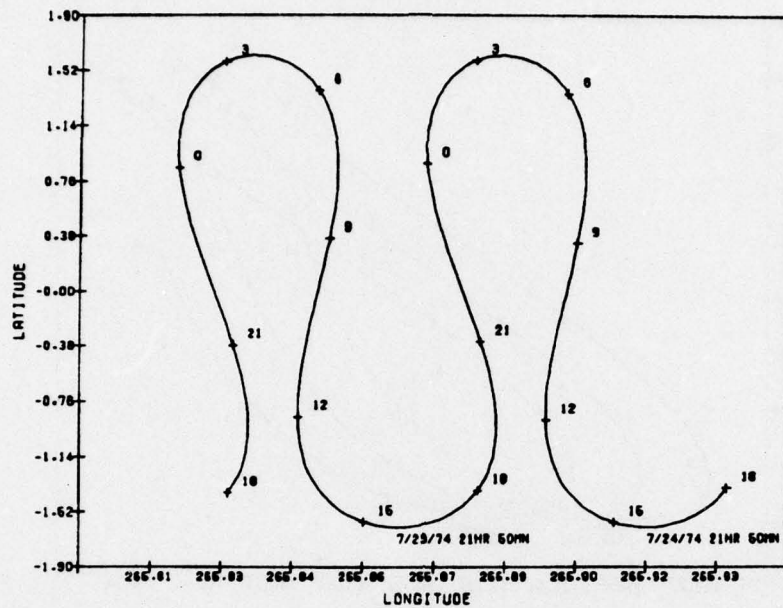
CORPACD-
 ATS-6 7/17/74 7/20/74 OHR OMN
 ATS-8



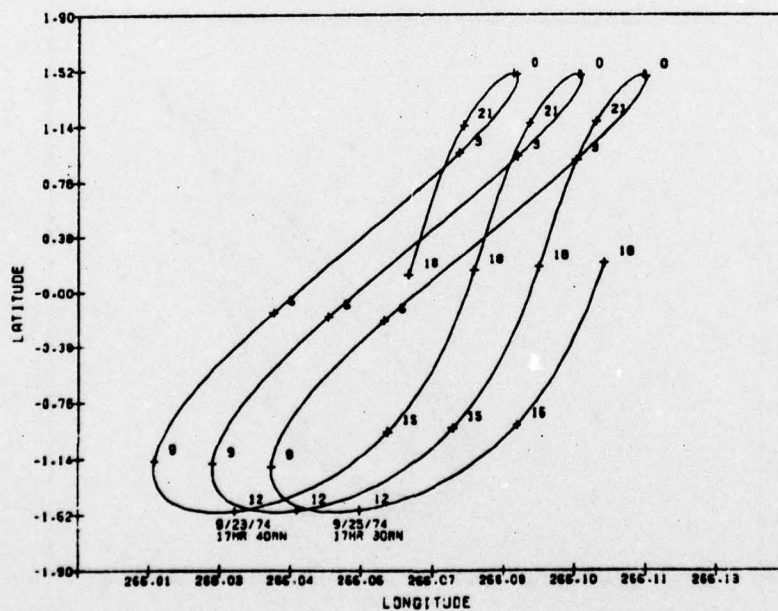
CORPACD-
 ATS-6 7/20/74 7/23/74 OHR OMN
 ATS-6



COMMAND-
 ATS-6 7/23/74 7/25/74 OHR OMN
 ATS-6

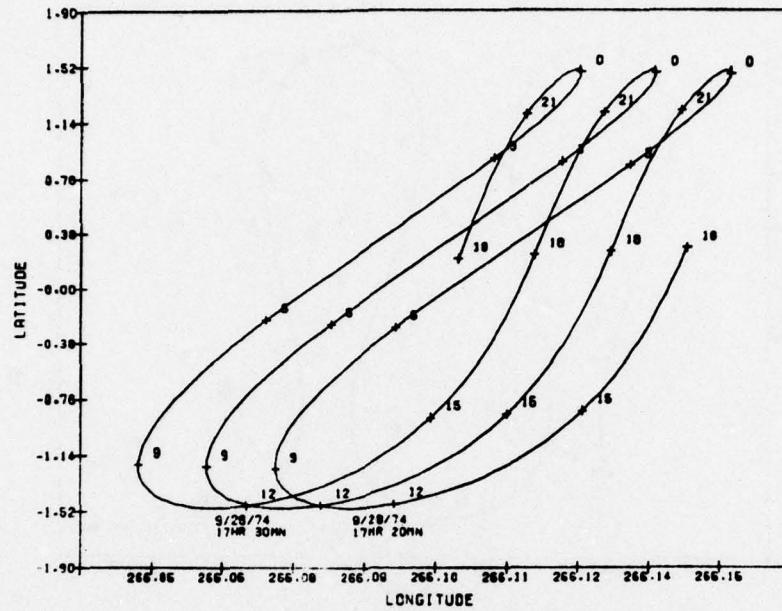


COMMAND-
 ATS-6 9/23/74 9/26/74 OHR OMN
 ATS-6



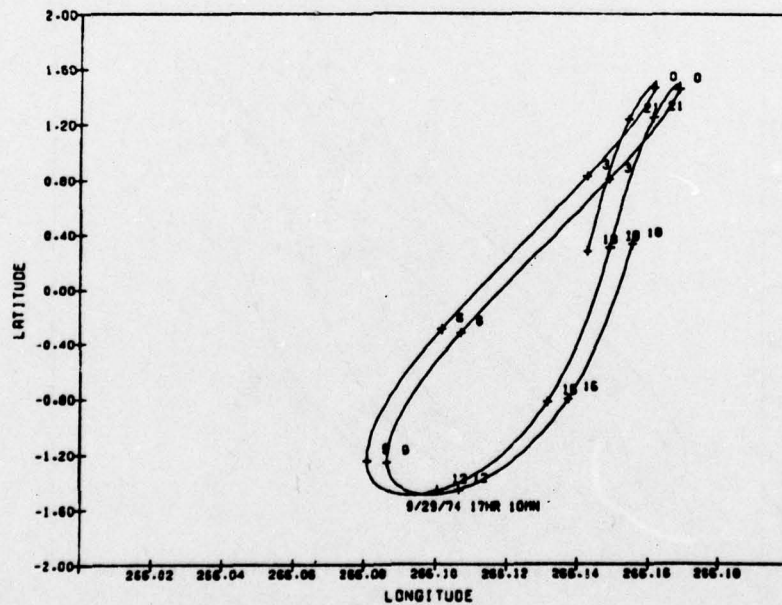
CONTINUED-

ATS-6 9/26/74 9/29/74 OHR OMN
ATS-6

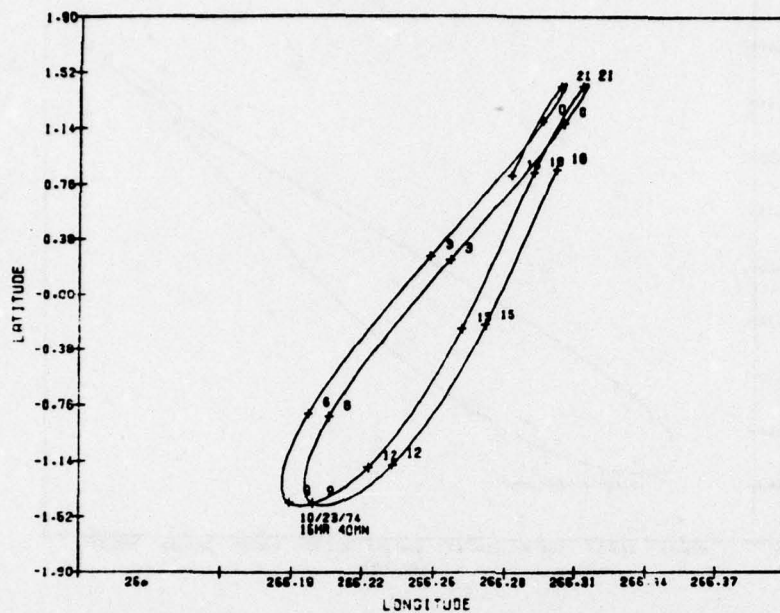


CONTINUED-

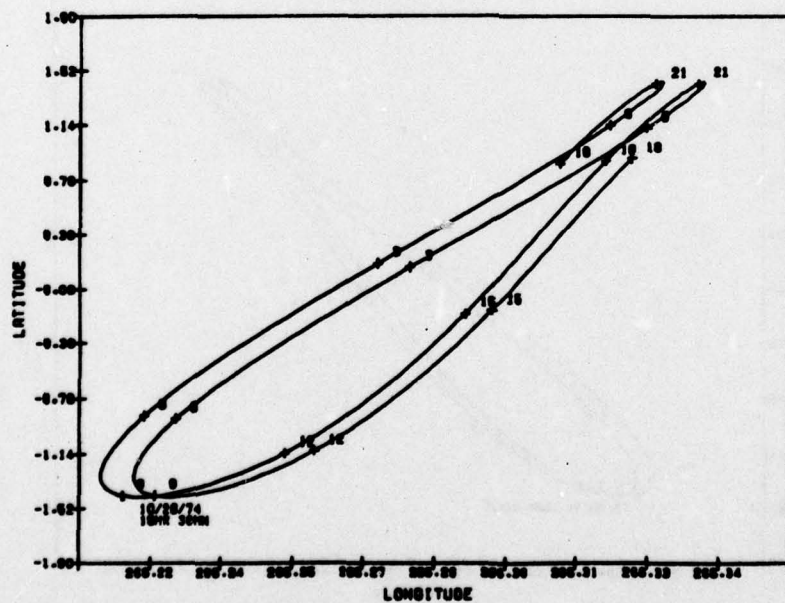
ATS-6 9/29/74 10/ 1/74 OHR OMN
ATS-6



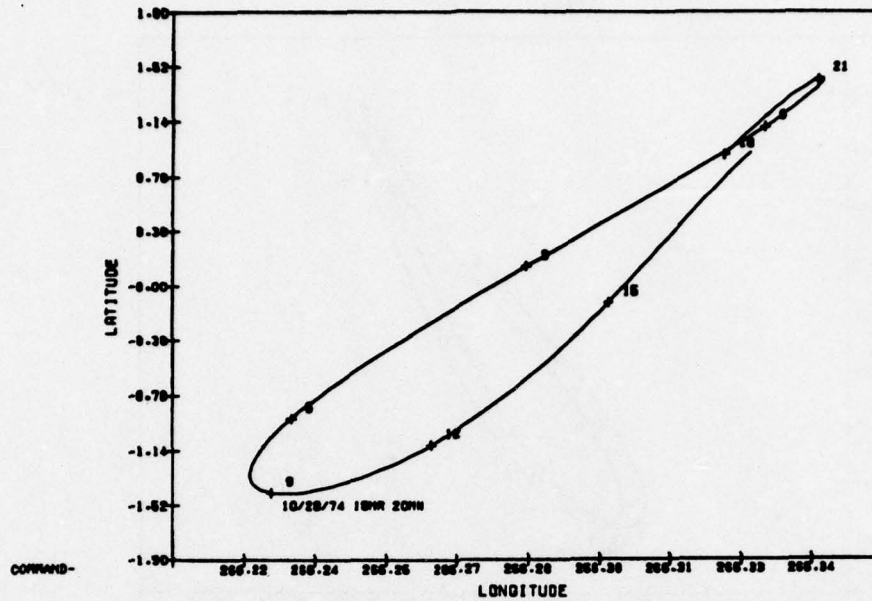
COMMAND-
 ATS-6 10/23/74 10/25/74 OHR OMN
 ATS-6



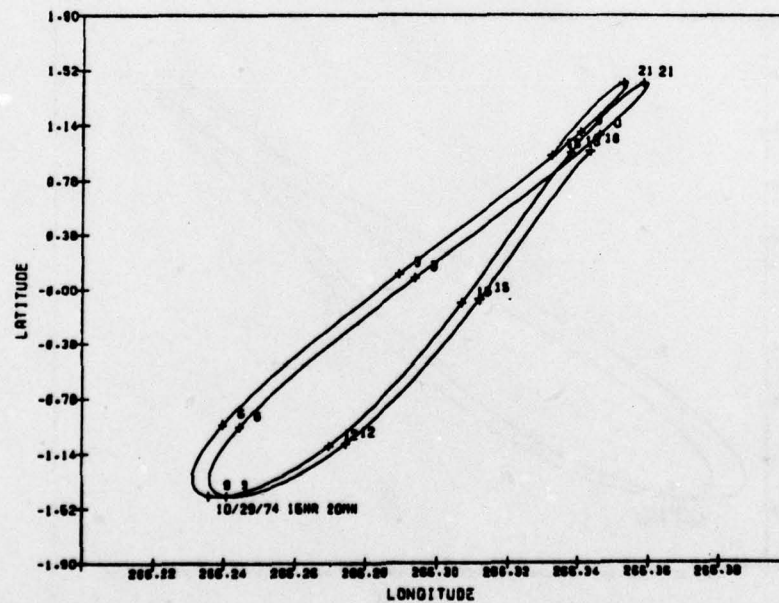
COMMAND-
 ATS-6 10/26/74 10/28/74 OHR OMN
 ATS-6



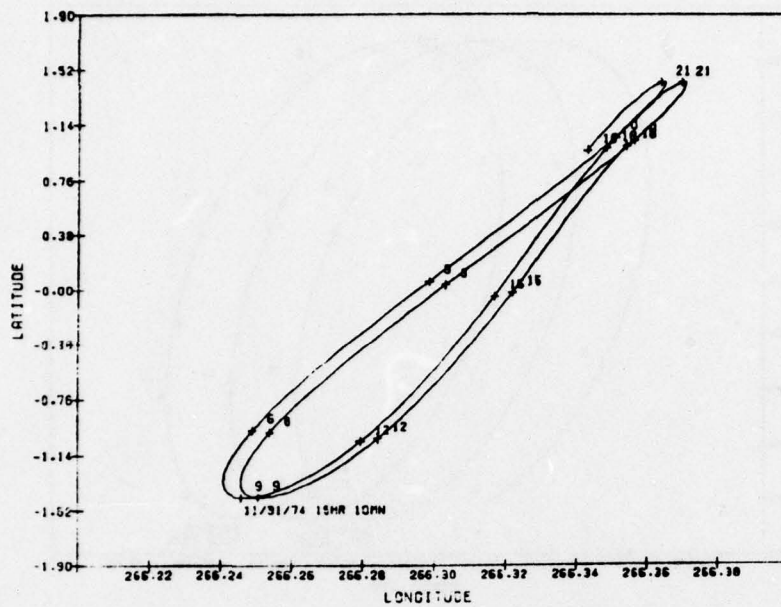
ATS-6 10/28/74 10/29/74 OHR OMN
ATS-6



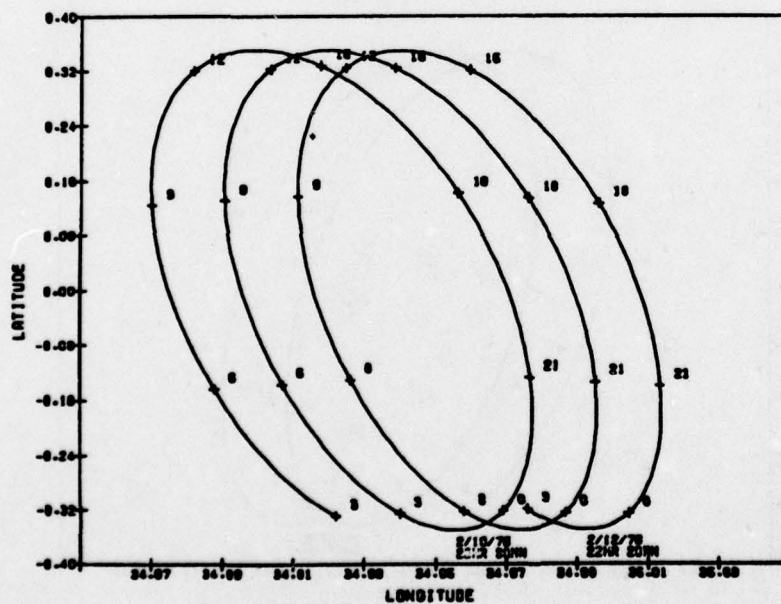
ATS-6 10/29/74 10/31/74 OHR OMN
ATS-6



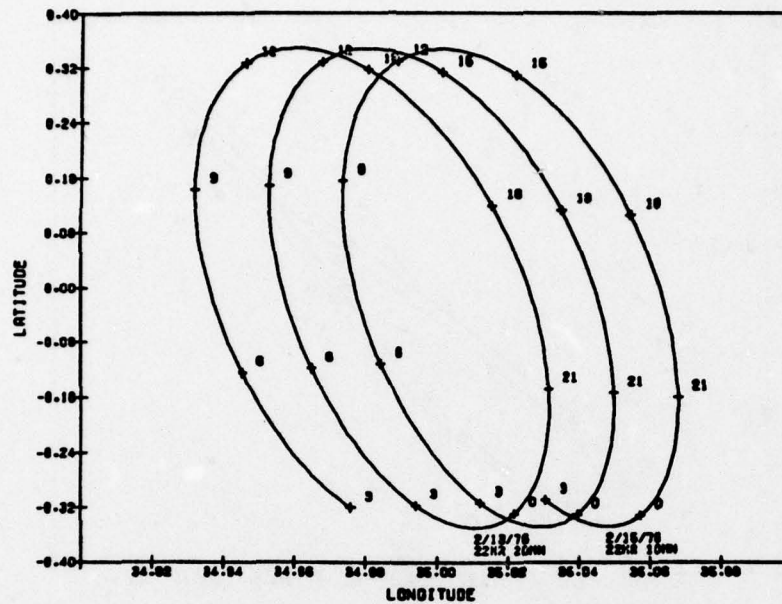
COMMAND-
 ATS-6 10/31/74 11/ 2/74 OHR OMN
 ATS-6



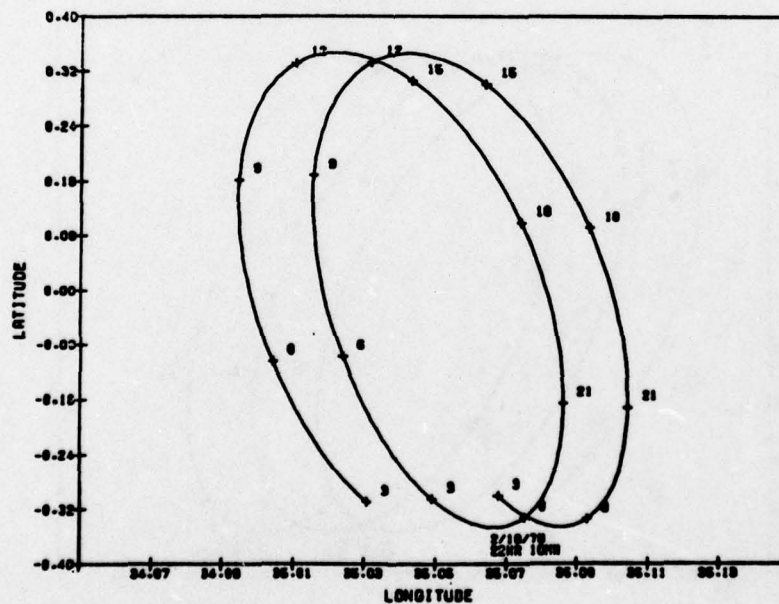
COMMAND-
 ATS-6 2/10/76 2/13/76 OHR OMN
 ATS-6



COMMAND-
 ATS-6 2/13/76 2/16/76 OHR OMN
 ATS-6

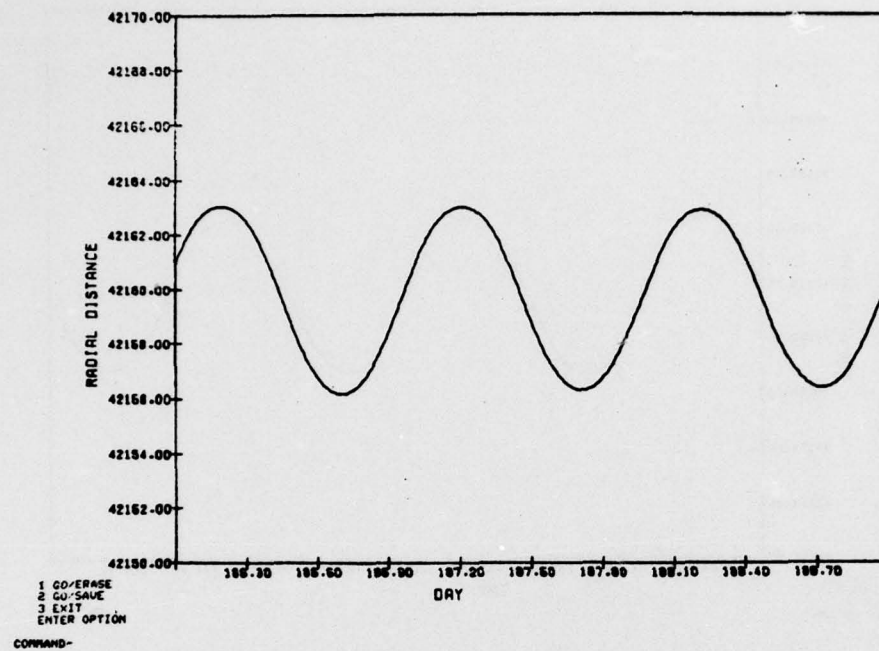


COMMAND-
 ATS-6 2/16/76 2/18/76 OHR OMN
 ATS-6



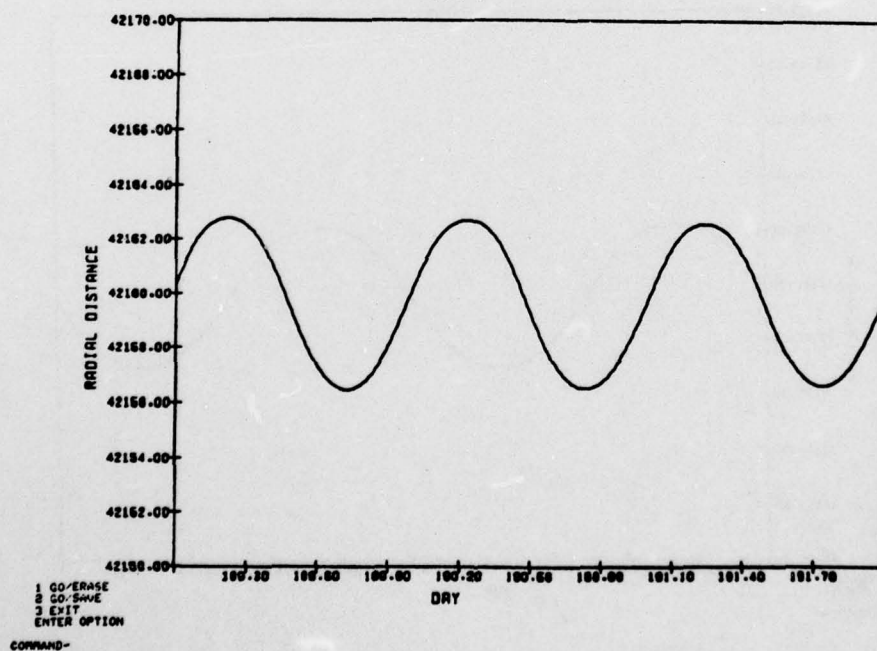
ATS-6 7/ 5/74 7/ 8/74 OHR OMN

ATS-6



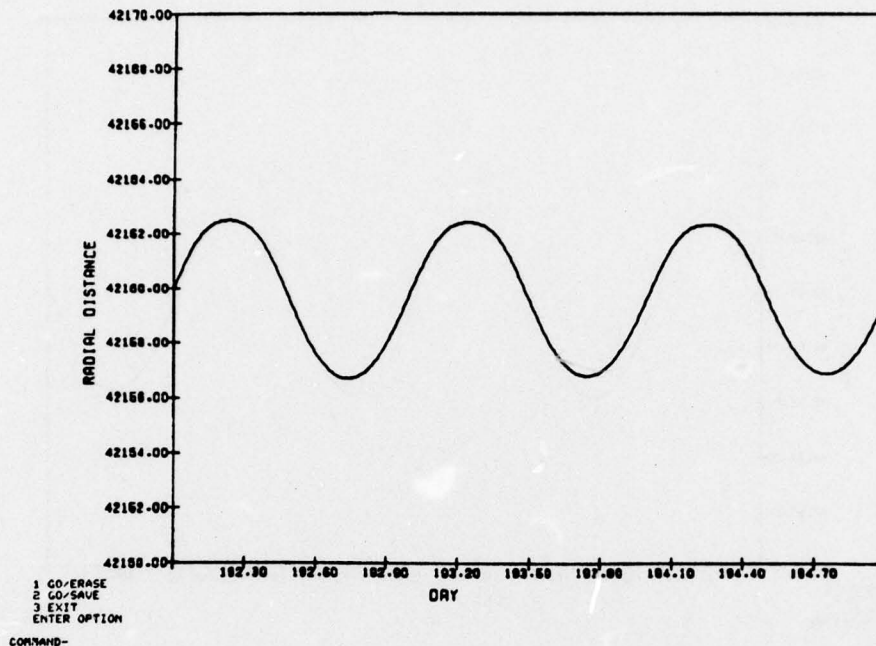
ATS-6 7/ 8/74 7/11/74 OHR OMN

ATS-6



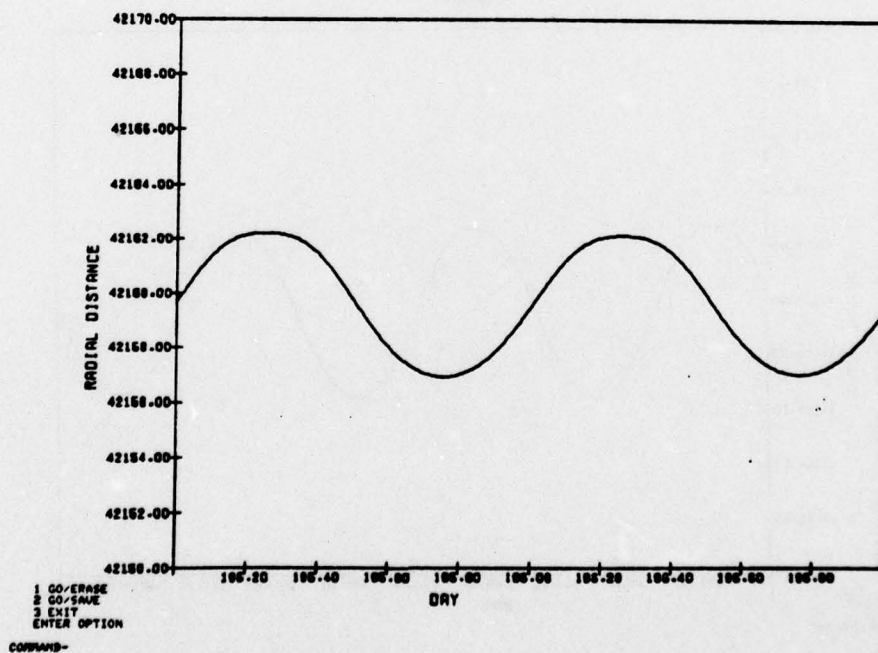
ATS-6 7/11/74 7/14/74 OHR OMN

ATS-6

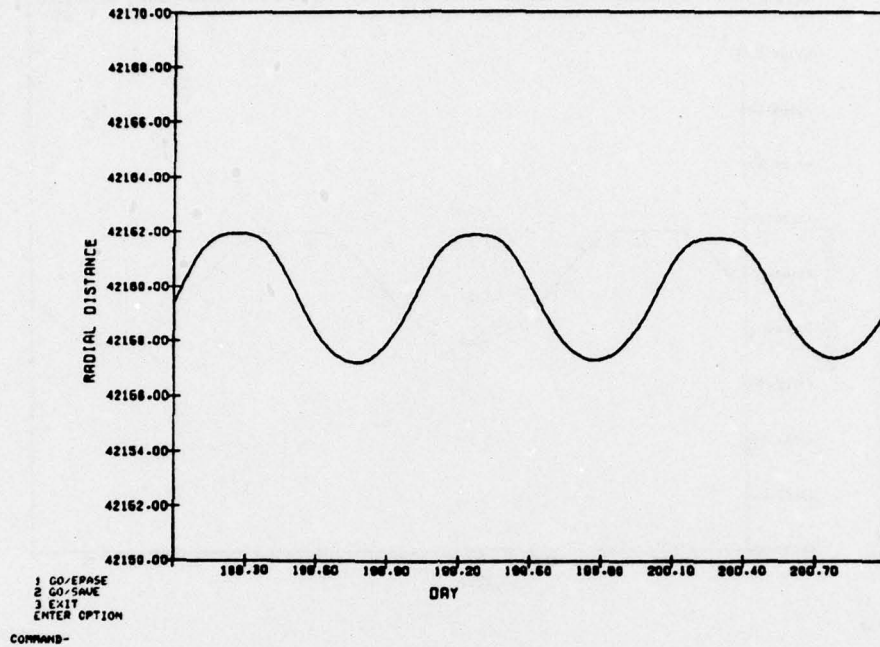


ATS-6 7/14/74 7/17/74 OHR OMN

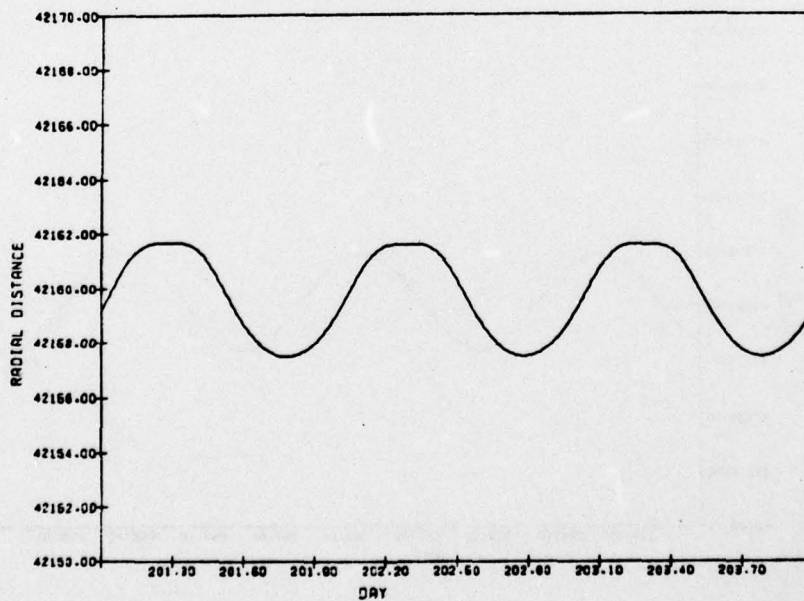
ATS-6



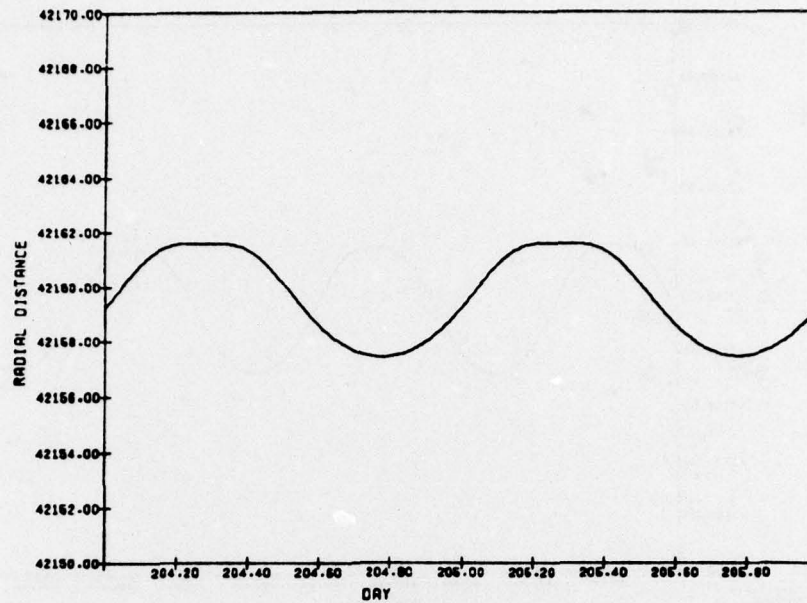
ATS-6 7/17/74 7/20/74 OHR OMN
ATS-6



ATS-6 7/20/74 7/23/74 OHR OMN
ATS-6

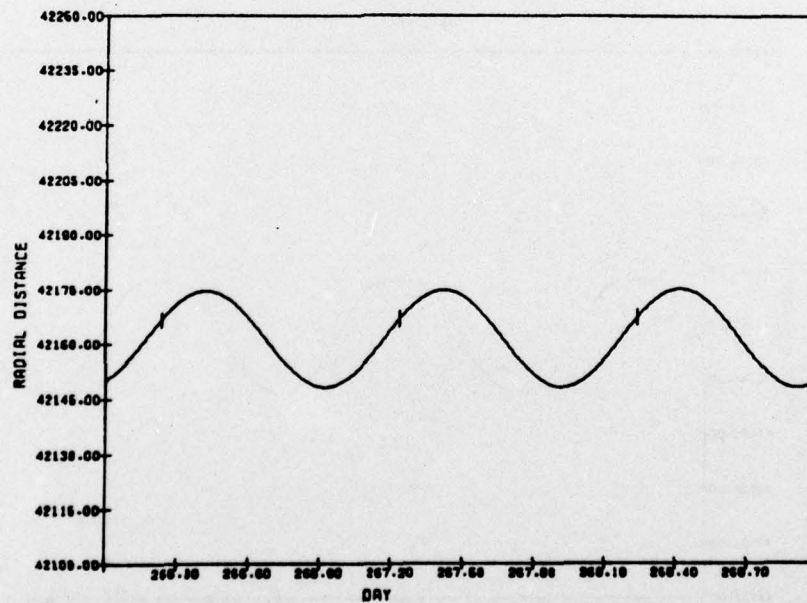


ATS-6 7/23/74 7/25/74 OHR OMN
ATS-6



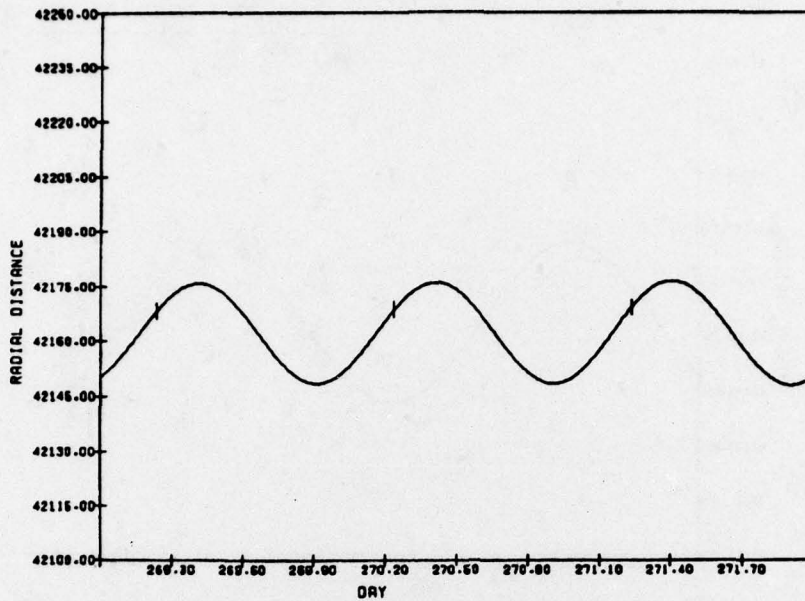
CONTINUED-

ATS-6 9/23/74 9/26/74 OHR OMN
ATS-6



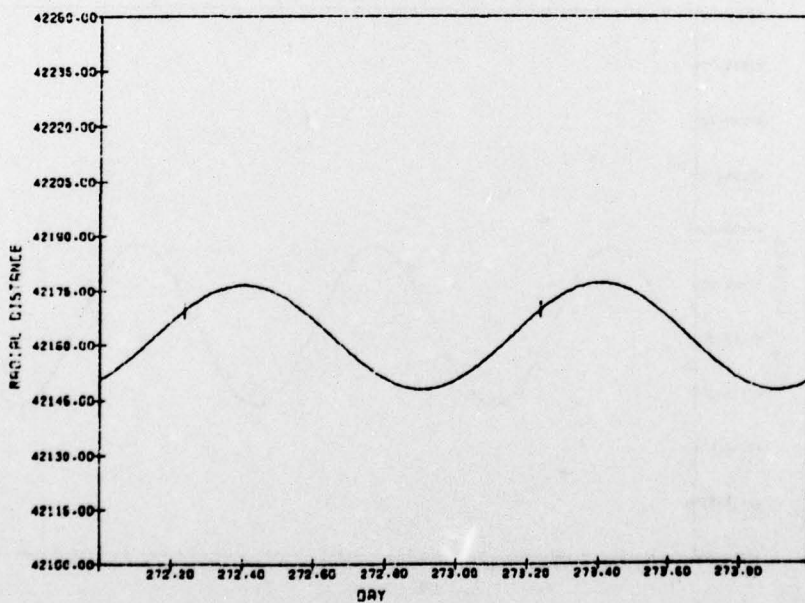
CONTINUED-

ATS-6 9/26/74 9/29/74 OHR OMN
ATS-6

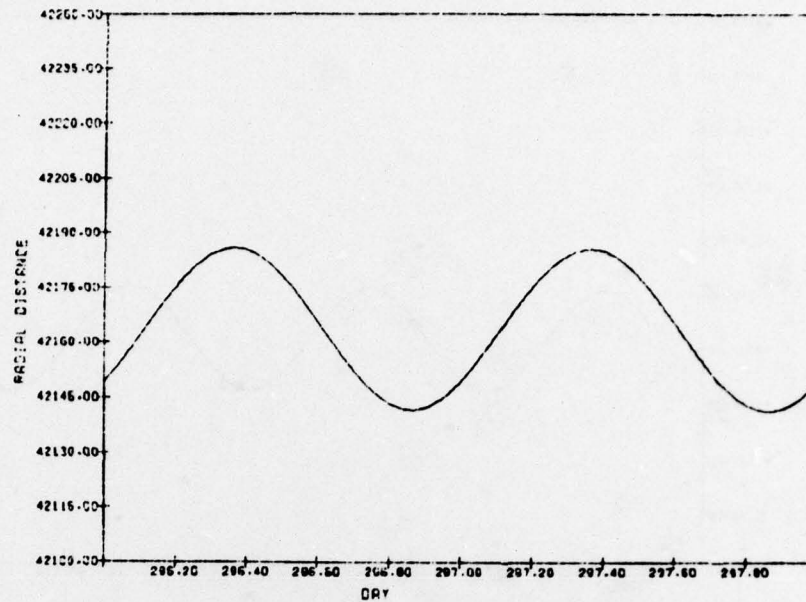


CONTINUED-

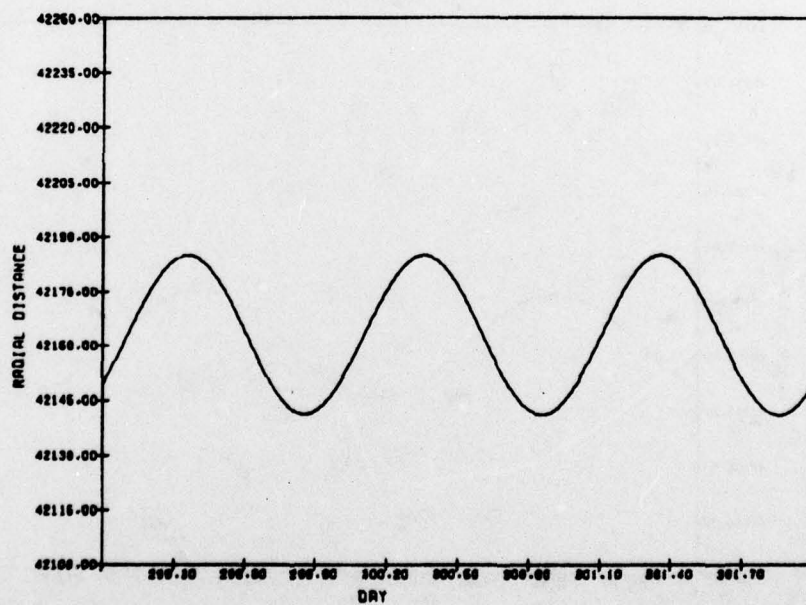
ATS-6 9/29/74 10/ 1/74 OHR OMN
ATS-6



ATS-6 10/23/74 10/25/74 OHR OMN
ATS-6

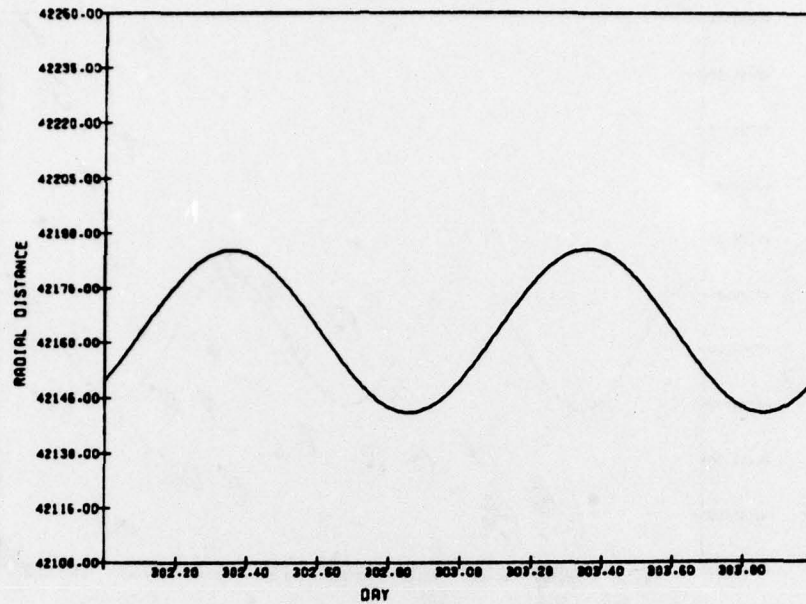


ATS-6 10/26/74 10/29/74 OHR OMN
ATS-6



ATS-6 10/29/74 10/31/74 OHR OMN

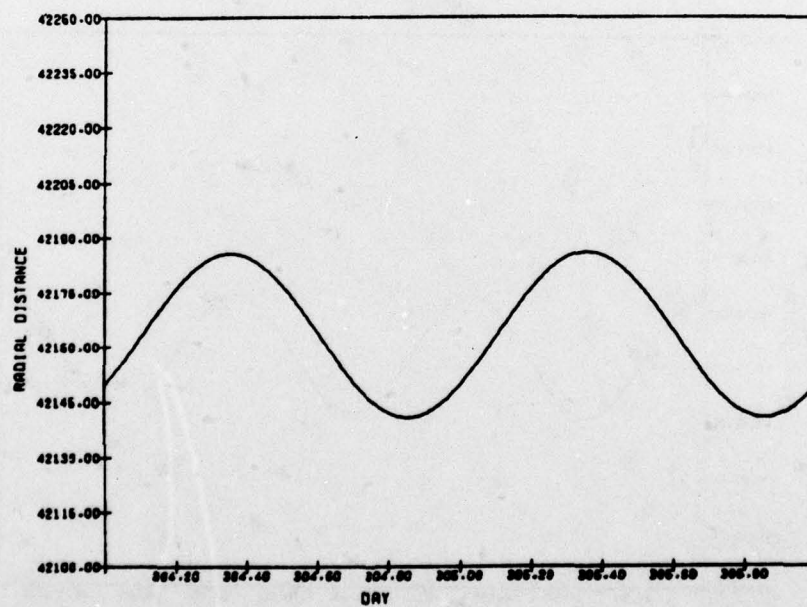
ATS-6



COMMAND-

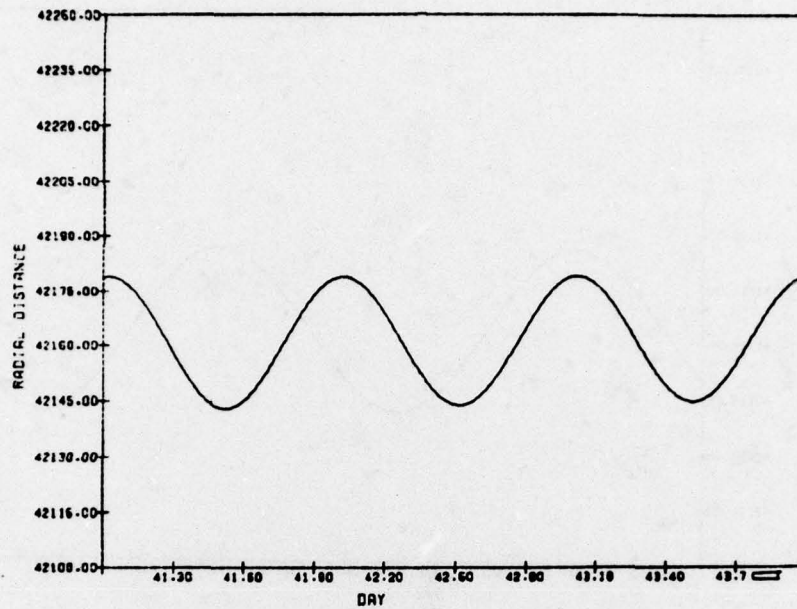
ATS-6 10/31/74 11/ 2/74 OHR OMN

ATS-6

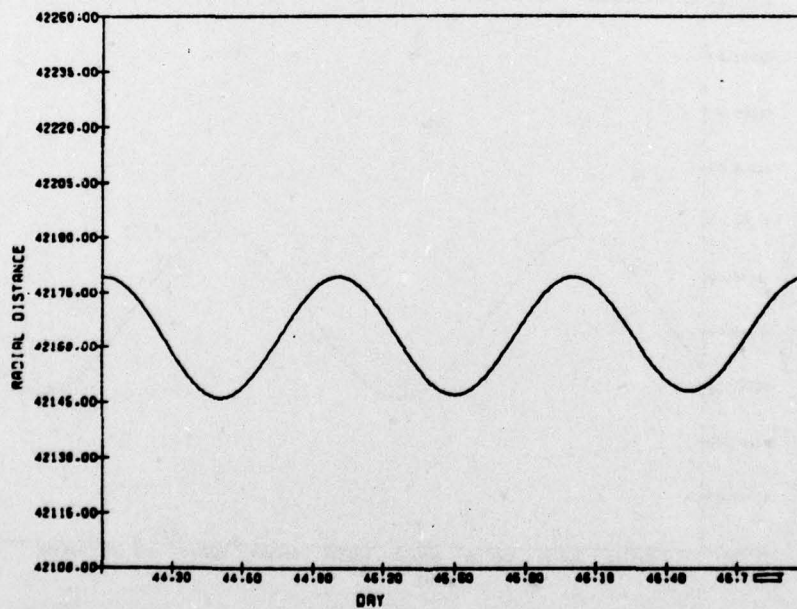


COMMAND-

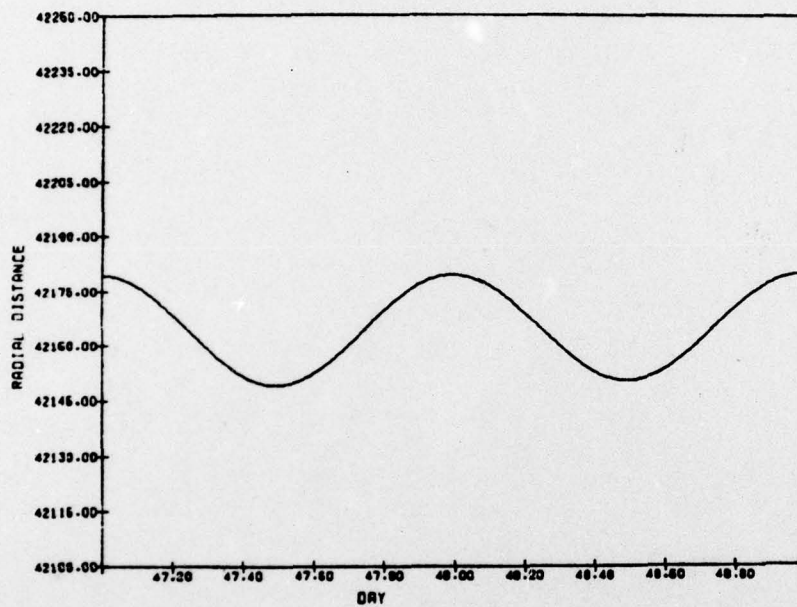
ATS-6 2/10/76 2/13/76 OHR OMN
ATS-6



COFFAND-
ATS-6 2/13/76 2/16/76 OHR OMN
ATS-6



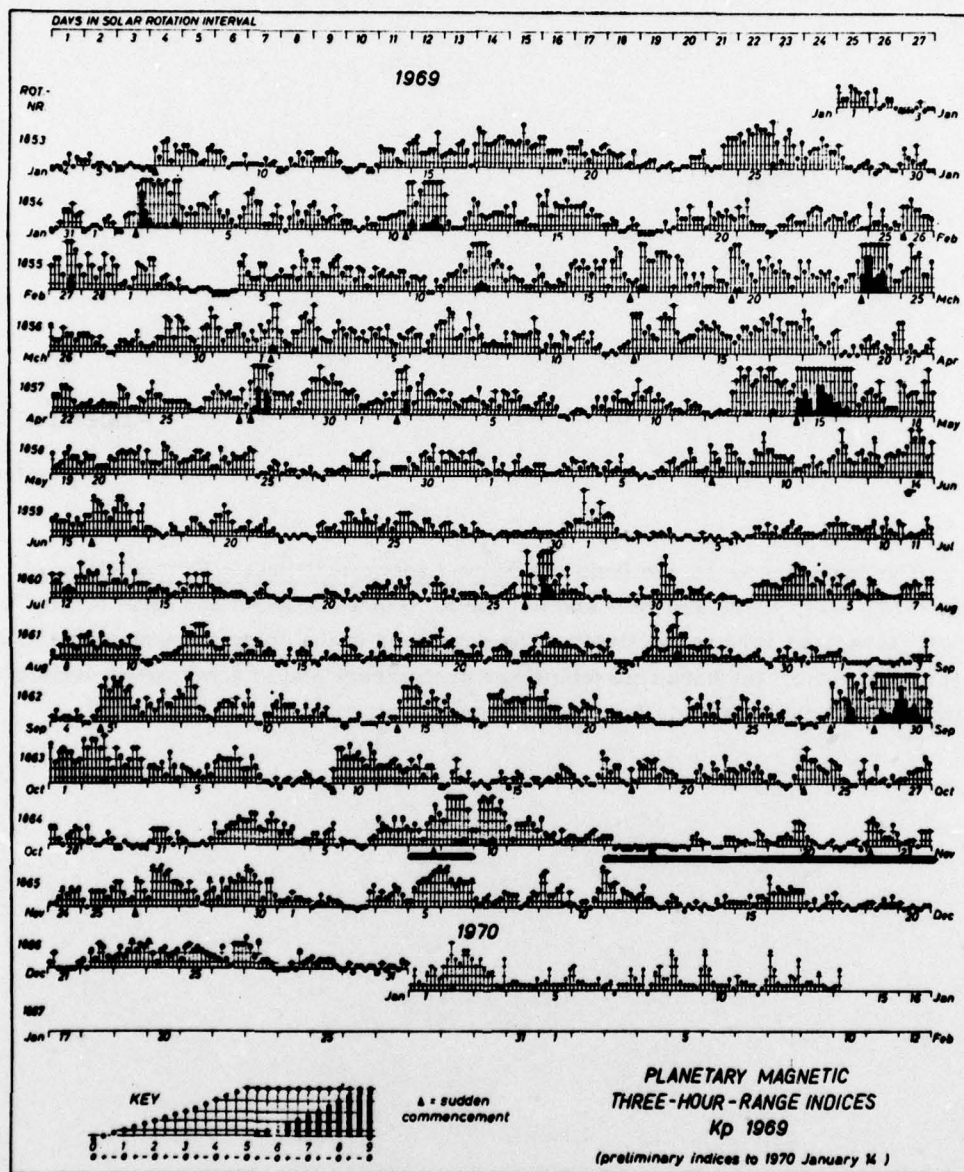
ATS-6 2/16/76 2/18/76 OHR OMN
ATS-6

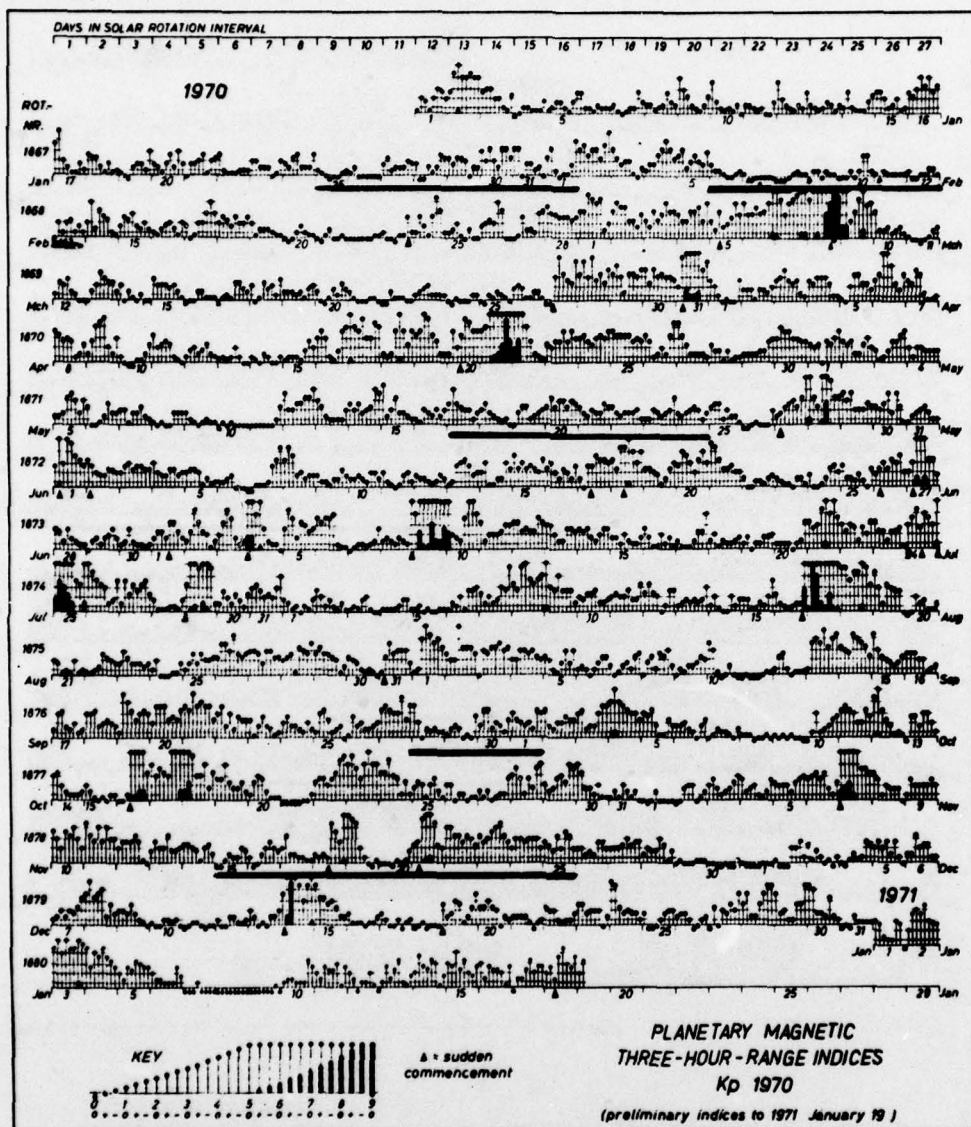


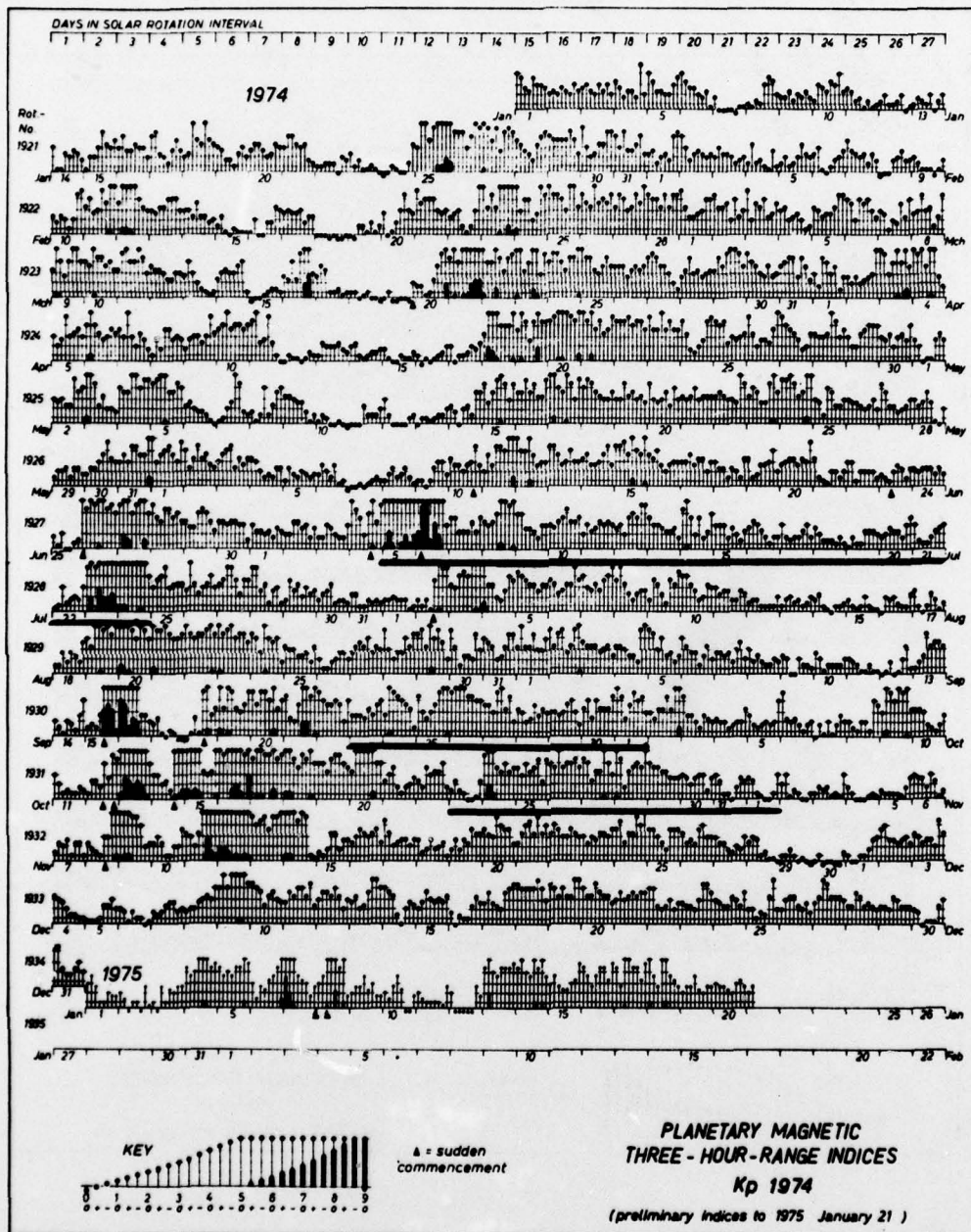
Appendix C

K_p Indices

The following pages are from the Solar-Geophysical Data - Prompt Reports for 1970, 1971, 1975, and 1977 and list the K_p indices in harmonic form for 1969, 1970, 1974, and 1976 respectively. The days used in the study are underlined by a heavy line (note: the harmonic tables are preliminary and in some cases deviate slightly from the WDC data for K_p listed on the tapes).







Appendix D

ATS Data Tape Formats

Two tapes containing 10-min averages of the four moments of the distribution function for ATS-5 and ATS-6 are available in the format described in Table D1. For ATS-5, the detector numbers correspond to

- Detector 1 = perpendicular electrons,
- Detector 2 = perpendicular ions,
- Detector 3 = parallel electrons,
- Detector 4 = parallel ions.

For ATS-6, the detector numbers are

- Detector 1 = North-South electrons,
- Detector 2 = North-South ions.

The tapes are available from AFGL/SUA (R. McInerney) or (preferably) the National Space Science Data Center, NASA Goddard, Greenbelt, MD 20771 (Attn: J. Vette).

Table D1. ATS Data Tape Formats

Data is stored in CDC 60-bit format.
 Standard data set contains data collected during a 10-min interval.
 Standard records contain 1 hr of data, that is, six sets.
 Total record size is 512 words.
 Standard file contains data for one day.
 These are labeled, 800 B.P.I., NOS/BE standard, 7-track tapes
 Record structure, based on CDC words contains two identification words before the data sets.
 Type of word: C, coded; F, floating; I, integer.

WORD	TYPE	DESCRIPTION
1	I	number of words in data set (usually 85)
2	I	presently unused, set to 0

There are six data sets for 1 hr of data or 510 words, based on CDC words.

WORD	TYPE	DESCRIPTION	DETECTOR	ORIGIN OF DATA
1	C	"ATS 5" or "ATS 6"		ATS-5 & ATS-6
2	F	YEAR		" "
3	F	MONTH		" "
4	F	DAY		" "
5	F	HOUR		" "
6	F	AVERAGE MINUTE		" "
7	F	DAY OF YEAR		" "
8	F	NUMBER DENSITY (N/cm^3)	1	" "
9	F	NUMBER OF VALUES		" "
10	F	NUMBER FLUX ($N/cm^2/sec/sr$)	1	" "
11	F	NUMBER OF VALUES		" "
12	F	ENERGY DENSITY (eV/cm^3)	1	" "
13	F	NUMBER OF VALUES		" "
14	F	ENERGY FLUX ($eV/cm^2/sec/sr$)	1	" "
15	F	NUMBER OF VALUES		" "
16	F	NUMBER DENSITY (N/cm^3)	2	" "
17	F	NUMBER OF VALUES		" "
18	F	NUMBER FLUX ($N/cm^2/sec/sr$)	2	" "
19	F	NUMBER OF VALUES		" "
20	F	ENERGY DENSITY (eV/cm^3)	2	" "
21	F	NUMBER OF VALUES		" "
22	F	ENERGY FLUX ($eV/cm^2/sec/sr$)	2	" "
23	F	NUMBER OF VALUES		" "
24	F	NUMBER DENSITY (N/cm^3)	3	ATS 5
25	F	NUMBER OF VALUES		" "
26	F	NUMBER FLUX ($N/cm^2/sec/sr$)	3	" "
27	F	NUMBER OF VALUES		" "
28	F	ENERGY DENSITY (eV/cm^3)	3	" "
29	F	NUMBER OF VALUES		" "
30	F	ENERGY FLUX ($eV/cm^2/sec/sr$)	3	" "
31	F	NUMBER OF VALUES		" "
32	F	NUMBER DENSITY (N/cm^3)	4	" "
33	F	NUMBER OF VALUES		" "
34	F	NUMBER FLUX ($N/cm^2/sec/sr$)	4	" "
35	F	NUMBER OF VALUES		" "
36	F	ENERGY DENSITY (eV/cm^3)	4	" "
37	F	NUMBER OF VALUES		" "
38	F	ENERGY FLUX ($eV/cm^2/sec/sr$)	4	" "
39	F	NUMBER OF VALUES		" "

Table D1. ATS Data Tape Format (Cont)

WORD	TYPE	DESCRIPTION	ORIGIN OF DATA
40	F	TEMPERATURE CORRECTION COEFF.	ATS 6
41	F	ANGLE N-S DETECTOR	"
42	F	PITCH ANGLE	"
43	F	ENERGY STEP OF PHOTOELECTRON CUTOFF	"
44	F	ELECTRON CUTOFF ENERGY	"
45	F	SPACECRAFT POTENTIAL	"
46	F	COLATITUDE (Degrees)	ATS 5
47	F	LONGITUDE (Degrees)	"
48	F	RADIUS (Re)	"
49	F	\perp MAGNETIC FIELD COMPONENT (B_{\perp} in γ)	"
50	F	MAGNETIC FIELD IN Z DIRECTION (B_z in γ)	"
51	F	TOTAL MAGNETIC FIELD (B in γ)	"
52	F	INCLINATION OF SATELLITE TO B	"
53	F	AE AVERAGE	AE Tape
54	F	AE MAXIMUM	"
55	F	KP VALUES	Data Cards
56	F	RADIUS (Km)	Ephemeris Tape
57	F	LATITUDE (Deg.)	Ephemeris Tape
58	F	LONGITUDE (Deg.)	Ephemeris Tape
59-85	F	FILL	

The initial fill value, deleted data, and erroneous data are indicated by -999999.